General Disclaimer

One or more of the Following Statements may affect this Document

- This document has been reproduced from the best copy furnished by the organizational source. It is being released in the interest of making available as much information as possible.

- This document may contain data, which exceeds the sheet parameters. It was furnished in this condition by the organizational source and is the best copy available.

- This document may contain tone-on-tone or color graphs, charts and/or pictures, which have been reproduced in black and white.

- This document is paginated as submitted by the original source.

- Portions of this document are not fully legible due to the historical nature of some of the material. However, it is the best reproduction available from the original submission.

Produced by the NASA Center for Aerospace Information (CASI)

CR-151109

Development of a Self Contained Heat Rejection Module

Phase II and III Final Report

REPORT NO. T211-RP-032

DEC 1976
RECEIVED
NASA STI FACILITY
INPUT BRANCH

Submitted to:

The National Aeronautics and Space Administration
Johnson Space Center
Houston, Texas

by

◉ VOUGHT CORPORATION
systems division

an LTV Company

DEVELOPMENT OF A SELF CONTAINED HEAT REJECTION MODULE

PHASE II AND III FINAL REPORT

REPORT NO. T211-RP-032

17 August 1976

Submitted to:

THE NATIONAL AERONAUTICS AND SPACE ADMINISTRATION
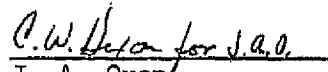JOHNSON SPACE CENTER
HOUSTON, TEXAS

by

VOUGHT CORPORATION
SYSTEMS DIVISION
DALLAS, TEXAS

PREPARED BY:

M. L. Fleming

REVIEWED BY:

J. A. Oren
Environmental Control
Systems

J. C. Utterback-Supervisor
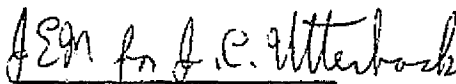Thermal and Environmental
Systems

APPROVED BY:

R. L. Cox
Technical R&D

TABLE OF CONTENTS

LIST OF FIGURES

LIST OF TABLES

1.0 INTRODUCTION AND SUMMARY

This is the final report for Phases II and III of the Development of a Self Contained Heat Rejection Module Program conducted under NASA contract NAS9-14408. The objective of this program was to perform detail design and construct a prototype test article Self Contained Heat Rejection Module (SHRM). Also to install this test article in the NASA/JSC Space Environment Simulation Laboratory Chamber A and conduct thermal vacuum demonstration and performance testing. The end product of this contract was the prototype hardware, the test article and the test results.

The SHRM is an auxiliary heat rejection system designed to provide cooling for advanced spacecraft. The SHRM is to be developed, fabricated and qualified separately from the parent vehicles, but is to be compatible with Shuttle Orbiter payloads, free flying experiment modules launched from the Shuttle or by a dedicated launch vehicle. Phase I of this program involved extensive conceptual design, analysis and design, fabrication and testing of a laboratory prototype SHRM. In addition a preliminary design of a flight prototype SHRM was developed. This effort was reported in the Phase I Final Report, Reference (1).

As a result of the Phase I work a SHRM system was selected which consisted of radiator panels which are deployable by means of scissor type linkage mechanism and the flow equipment necessary to reject heat from these panels. Conceptually there would be two types of systems, one to provide heat load control with low return temperatures (40°F or below) and one at higher temperatures (approximately 100°F). The first type would include a dual mode system which would have the capability of operating as either a pumped liquid radiator or a vapor compression refrigeration system using the radiator panels as the condenser. Condensing radiators have been studied in a previous program documented in Reference (2). Addition of the vapor compression system allows the return of conditioned heat transport fluid at low temperatures under severe environments which limit the return temperature of a pumped liquid system. The second type would be a pure pumped liquid radiator system. The heat load could then be partitioned between the two systems or passed through the systems sequentially with the conventional radiator system providing for high return temperature heat rejection and the dual mode

1

system the low return temperatures. The dual mode system was designed to use the vapor compression refrigeration only when necessary due to higher power requirements. The pumped liquid part of the dual mode system would be used whenever the heat loads and environments are such that the requirements can be met by conventional radiators.

The Phase II and III program was to design, fabricate and test a SHRM system of the dual mode type. In the Phase I study the scissors mechanism was selected and it was found to be quite similar to the device used to deploy solar panels from the Apollo Telescope Mount (ATM) on the Skylab program. Since the ATM deployment device was flight qualified, a successful effort was made to obtain a spare for use on the SHRM program. Radiator panels were sized and designed to fit on four of the five panel locations on the ATM frame. Fluid swivels developed in Phase I were used to provide for fluid transfer across the movable joints. The panels were installed on the ATM frame and a simulated zero-gravity deployment test was successfully conducted at the Marshall Spaceflight Center facility in Huntsville, Alabama.

A prototype flow module was designed to provide dual mode flow equipment in a package approximately the size necessary to fit into the ATM pallet. The components used in the flow module were prototype in that they were selected to be operationally similar to the flight components but not necessarily flight weight or qualified. This allowed considerable cost savings in the purchase of refrigeration components since many off-the-shelf items could be used. It would have been desirable to use R-21 as the transport fluid since this is the substance being used in the Shuttle Orbiter and payload heat rejection systems; however, due to the lack of available R-21 refrigeration hardware, R-12 was selected for use in the flight prototype program.

Two weeks of thermal vacuum testing of the prototype SHRM was conducted in NASA-Johnson Space Center, Chamber A. The two weeks of testing occurred on 20-24 October and 4-7 November 1975. A week was scheduled between the tests since a holiday fell in that week and also to allow equipment refurbishment and changes. A total of 152 hours testing was conducted, 95 in the first week and 57 in the second. The objectives of the test were to demonstrate and map the performance of the deployable dual mode system and to evaluate the radiator and refrigeration components and to obtain the

2

characteristics of the dual mode system in switching operation between the two modes. The test plan to accomplish this included 44 test points, (18 radiator/17 refrigeration) and 9 dual mode tests. Due to various test difficulties and test plan revisions based on real time evaluation of results, 22 radiator, 17 refrigeration and 3 dual mode points were actually taken.

Problems were encountered with the panels, pump, solenoid valves, compressor and one fluid swivel during the testing. The problems were all resolved during the testing except that concerning the swivel. The swivel between the second and third panels would not rotate during a cold retraction and the result was the flex line which connected the swivel to the panels twisted and ruptured. A post test investigation revealed the cause of this anomaly to be frozen refrigerant oil deposited in a close tolerance area between the swivel body and rotating shaft outside the swivel seal. The oil apparently accumulated there as a result of R-12 leaks across the seal due to side load on the swivel during GSE operations. The swivel design is judged to be acceptable for pumped liquid applications but should be redesigned for systems containing oil.

Maps of the heat rejection capacity in both modes were generated for three different return temperatures, 35, -10 and +10°F. These maps indicated distinct operation ranges for the two modes as a function of heat load and thermal environment. Limited low load data was taken due to premature test termination in the second week as a result of the severe leak in the flex line. Component evaluations indicated adequate performance from the pumps, compressor and accumulator. During the first week of testing the contact heat exchanger did not achieve the expected performance level. Between the two weeks of the test the heat exchanger was repacked with GE641 Insulgrease replacing the DC380 thermal grease originally installed between the contact surfaces. The GE641 had indicated superior performance in element tests. In addition the heat load source R-21 flow rate was adjusted to equalize the heat capacities on both sides of the heat exchanger. The second

week's test results indicated greatly improved performance (0.89 effectiveness) and demonstrated the concept is valid and the contact heat exchanger device is suitable for use in the SHRM or other devices with similar requirements.

2.0 HARDWARE DESIGN AND DESCRIPTION

This section discusses the SHRM flight system design and the component design and selection. The test hardware, installation and instrumentation are also described.

2.1 Flight System Design

During the early portion of the SHRM Phase I effort a set of design requirements were formulated. These design requirements are summarized in Table 1. Extensive trade studies were subsequently conducted in Phase I to define an efficient flight system design which would meet these design requirements.

A schematic of the resulting final system is shown in Figure 1. The system contains four arrays of deployable radiator panels arranged into two separate and somewhat different types of systems. The first is a conventional pumped liquid radiator which consists of two of the panel arrays and a liquid pump. An accumulator is included to maintain system pressure above vapor pressure and to provide the volume to allow for changes in liquid volume due to thermal expansion. A bypass valve provides heat load control to maintain a constant return from the heat rejection system to the intercooler. The bypass val.e (radiator control valve) routes part of the liquid flow around the radiators then mixes this relatively hot liquid with the cold liquid returning from the radiators to achieve the desired mixed return temperature. An automatic controller senses the mixed return temperature, compares it with a desired set point and adjusts the valve position accordingly. A heat exchanger is used to transfer heat from the spacecraft thermal control system into the SHRM heat rejection system. The two arrays of radiator panels are connected in parallel, however, the four panels in each array are series flow connected. Such an arrangement maintains equal flow through each panel which is sufficiently high to effect efficient forced convection heat transfer from the fluid to the radiator tubes but does not result in excessive pressure drop through the panels.

The second type of system, illustrated on the right side of Figure 1, is a dual mode system which can operate as either a pumped liquid or vapor compression heat rejection system. A pumped liquid system is included similar to that already described and in addition a vapor compressor and liquid

TABLE 1 — SHRM DESIGN GUIDELINES AND CONSTRAINTS
- FULL 4 WING SYSTEM -

VEHICLE INTERFACE

	LOW RETURN TEMP	MODERATE RETURN TEMP	HIGH RETURN TEMP
Return Temperature, °C	-18	2	27
Delivery Temperature, °C	93	71	71
Max. Heat Load, kW	23.4	58.6	58.6
Working Fluid	Refrigerant 12	Water	Refrigerant 21
Required Flowrate, kg/s	0.164	0.201	1.234
Application	Manned or unmanned scientific payload with cold storage requirement	Manned Payload	Unmanned Scientific Payload
Heat Load Range	100:1	1000:1	1000:1

Physical Characteristics : Mechanical interface rather than fluid if possible.

On-Orbit Mate-Up : Attachment to and deployment from the Spacelab.

SHRM

Controls : Applicable to any design return temperature

Working Fluid : R-21 for flight system, R-12 is allowable for prototype system.

Envelope : Maximum diameter of 4.6 m for stowage in Shuttle cargo bay.
Use volume above spacelab pallet if possible.

External Environment : Design Conditions:

EARTH ORBIT	TRANSLUNAR	LUNAR ORBIT
370 km full sun orbit	fixed orientation	92.6 km full sun orbit
free-flying or attached to Shuttle	free-flying	free-flying
Radiant interchange with Shuttle: None with other vehicles or solar cells	No radiant exchange with other vehicles or solar cells	No radiant exchange with other vehicles or solar cells

Launch & Re-entry Environment : Inside vehicle, so no aerodynamic heating thermal protection is required.
Use Shuttle orbiter vibroacoustic environment.
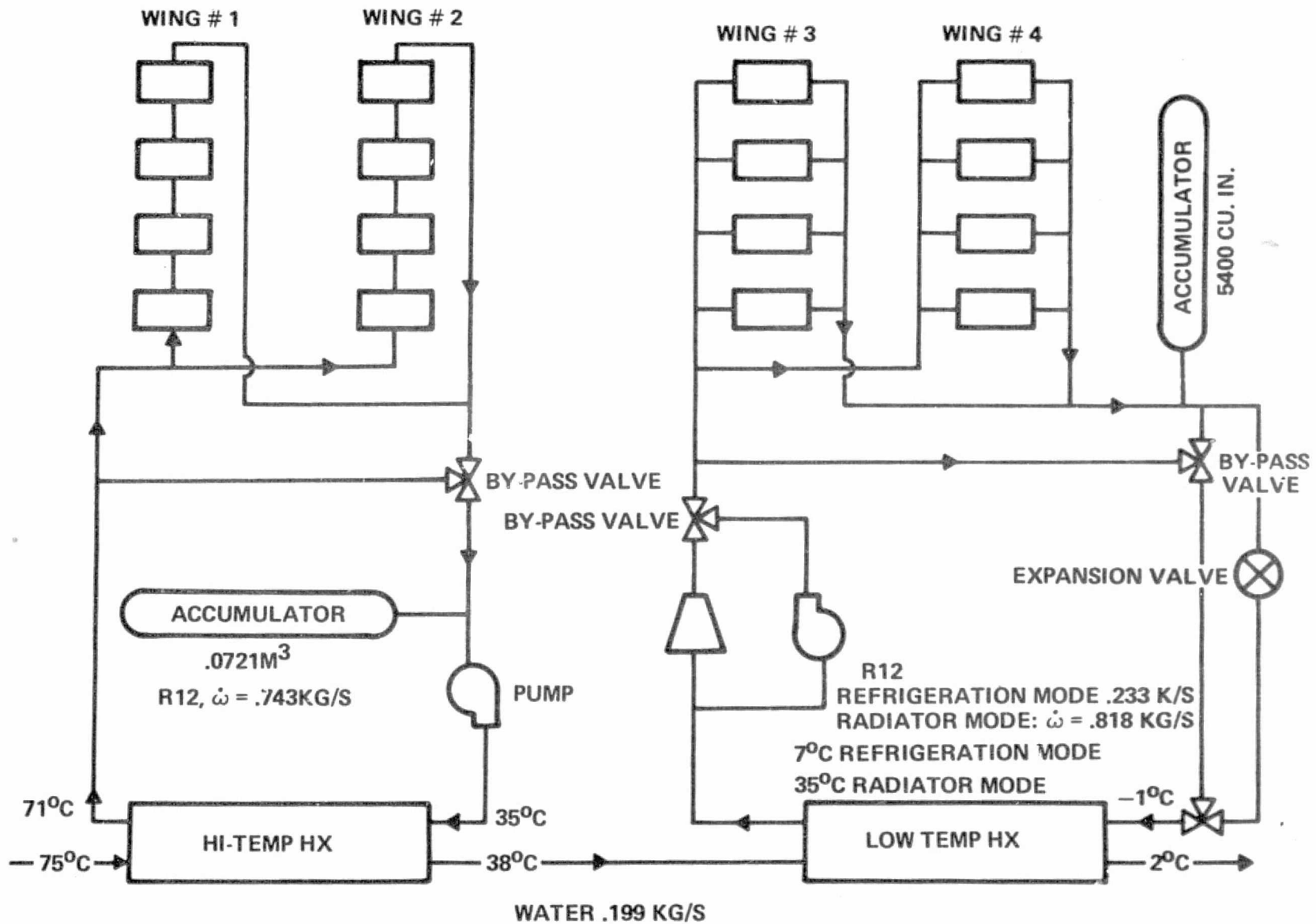
SHRM FLOW SCHEMATIC

FIGURE 1   SHRM FLIGHT DESIGN SCHEMATIC

expansion valve are added. The necessary valves to switch from one mode to the other are included and the accumulator is sized large enough to contain the approximately 2/3 of the liquid volume which must be removed in order to operate the system in the refrigeration mode. The two arrays of radiator panels are connected in parallel as in the other system and the four panels in each array are also connected in parallel. The parallel connection is necessary in order to operate the radiators as both pumped liquid radiators and as condensing radiators in the vapor compression cycle. Significantly higher pressure drops are experienced with condensing panels and therefore the parallel connections are necessary to avoid excessive performance degradation. Parallel connections create a problem in achieving an equal flow split between the panels in both modes since identical flow paths to each panel are difficult with a deployable radiator system. Pressure drop characteristics of flow metering devices such as orifices and venturis differ for vapor and liquid flow and for different flow regimes. Thus, if such devices are used to achieve an equal flow split, the split for pumped liquid will differ from that for the two phase condensing operation. Some compromise is necessary to select a flow distribution which is satisfactory for both modes of operation. The intercooler heat exchanger would also seem to present a similar problem, however, design for liquid to evaporating liquid heat exchange and design for liquid to liquid heat transfer do not result in significantly different designs.

  The two types of systems could best be combined as shown in Figure 1 where the pumped liquid radiator system is used to reject heat at the higher temperatures with control to lower temperature accomplished with the dual mode system. When a combination of high heat load and environment prevents return at the desired temperature the refrigeration system may be used. The power penalty associated with the use of the compressor makes it more efficient to minimize the amount of heat rejected using the vapor compression. This is done, as shown in Figure 1, by rejecting all the heat possible from the pumped liquid system prior to routing the coolant to the dual mode system. In doing this, the heat rejection has been partitioned into a high temperature system and a low temperature system to achieve the desired total heat rejection and return temperature as efficiently as possible. When the

requirements could be met without the use of refrigeration in the low temperature system it would be operated in the pumped liquid mode also, thus saving power. An automatic controller senses when this is the case and selects the proper mode of operation for the dual mode system.

Trade studies to select a deployment mechanism were also conducted in Phase I. The selected type of mechanism is illustrated in Figure 2. The mechanism is of a scissors linkage type design similar to that used in the Skylab program to deploy the Apollo Telescope Mount solar panels. The actual radiator panel design is an optimization considering the higher efficiency with thicker fins and more flow tubes versus the added weight. In general the most weight optimum panel is the one with the thinnest fin, however, this requires more area which increases the weight of the deployment system. In addition there are inherent structural lower limits to the fin thickness which usually defines this parameter rather than radiator efficiency/weight trades. Past studies (References 3 and 4) have indicated that designing for a fin effectiveness of about 0.90 produces a near optimum design. Area sizing was made assuming the panels are coated with silver-Teflon tape with optical properties of solar absorptivity 0.10 and thermal emissivity 0.80.

2.2   Test System Design

The selection of the scissors linkage mechanism for the deployment fixture resulted in an actual Apollo Telescope Mount (ATM) deployment frame being obtained by Johnson Space Center from the Marshall Space Flight Center (MSFC) for use in the SHRM program. The use of this device dictated, to a large extent, the design of the prototype test system. By installing four radiator panels on the ATM frame, one wing of the flight design can be simulated. Since the dual mode system is the most complex, and since it also contains a pumped liquid radiator system similar to that in the high temperature part of the system, a dual mode wing was selected for the flight prototype test. The radiator panels were designed to install on the ATM frame and eight fluid swivels of a design which was developed in Phase I were used to provide fluid transfer across the joints. A sketch of the panel configuration is shown in Figure 3, along with the details of panel design. Complete details of the panel design and installation are given in Reference (5).

9
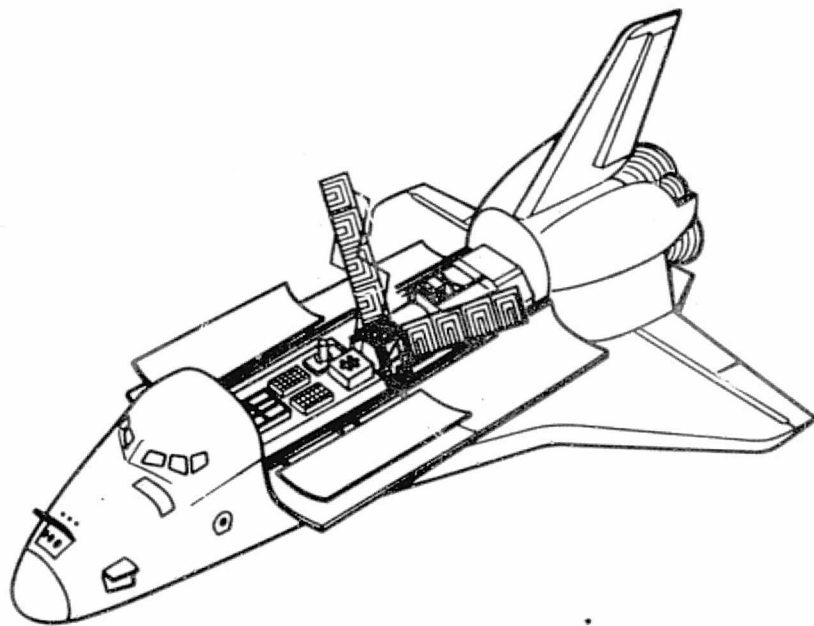
SELF-CONTAINED HEAT REJECTION MODULE (SHRM).
APPLIED TO EXPERIMENT MODULE IN THE SHUTTLE
ORIBTER CARGO BAY

PARTIALLY DEPLOYED
RADIATOR

DEPLOYED
RADIATOR

STOWED
RADIATORS
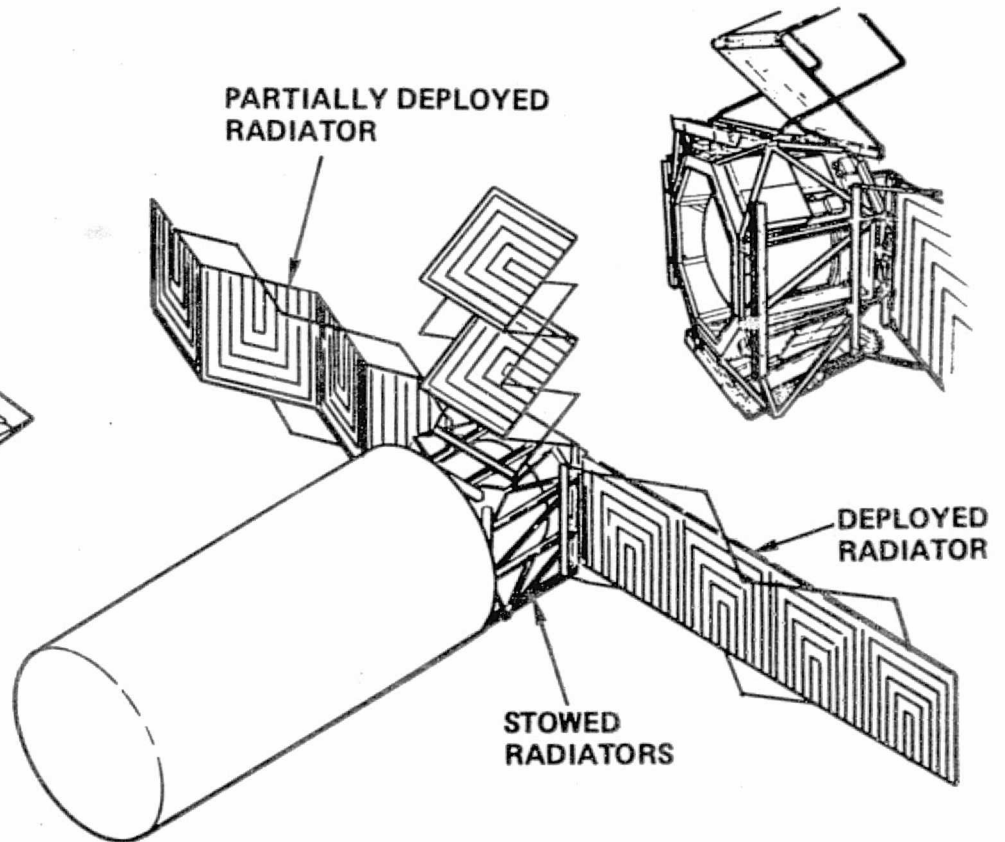
SELF-CONTAINED HEAT REJECTION MODULE APPLIED
TO A FREE-FLYING EXPERIMENT MODULE

FIGURE 2   SELECTED SHRM DEPLOYMENT CONCEPT

OUTLET MANIFOLD (TYP)

RADIATOR PANEL
(ONE OF 4)

RETURN LINE

16 PARALLEL
TUBES (TYP)

INLET MANIFOLD

DELIVERY
LINE

SWIVEL

NOTE: PANEL WIDTH = 101.25"
PANEL LENGTH = 93.25
(TUBE LENGTH = 93.25
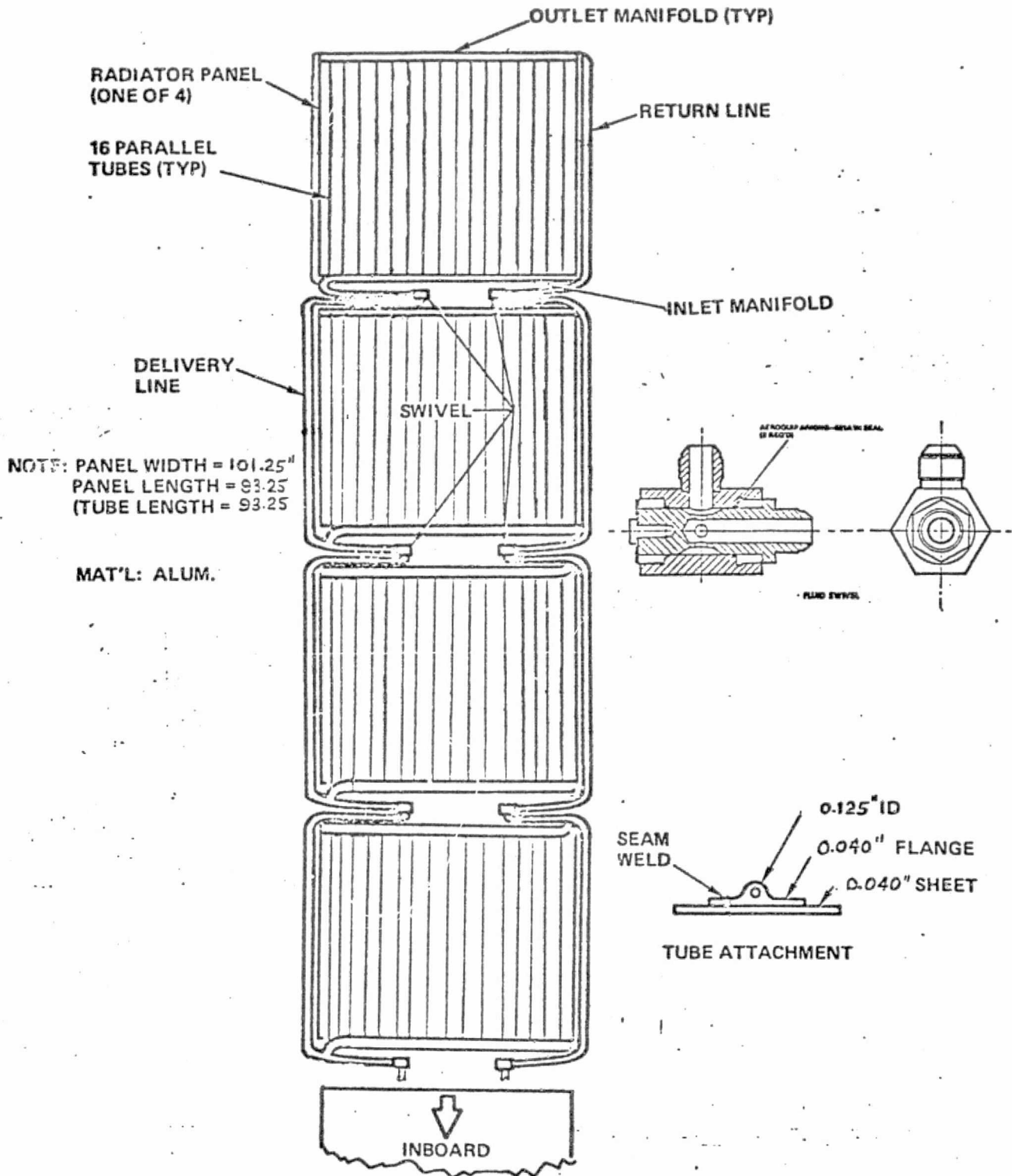
MAT'L: ALUM.

SEAM
WELD

0.125" ID
0.040" FLANGE
0.040" SHEET

TUBE ATTACHMENT

INBOARD

FIGURE 3 SHRM RADIATOR CONFIGURATION

A prototype flow module was designed to be the approximate size to fit into the ATM pallet. A schematic of this flow module is shown in Figure 4. Due to the prototype nature of this hardware the arrangement is somewhat more complicated than the flight system illustrated in Figure 1. The major differences are:

1. Three way latching control valves were not available to perform system selection as shown in Figure 1. It was necessary to use five pneumatically controlled valves to accomplish this function.

2. A selection of two evaporator temperatures during the thermal vacuum test was provided by installing two expansion valves in parallel.

3. The metal bellows accumulators were too small to contain enough R-12 to allow mode switches. An auxiliary accumulator was added to provide the necessary volume.

4. An oil separator, liquid filter dryer, and a suction filter were included to provide for positive lubrication and protect the system from contaminants.

5. Check valves and manual fill valves were added to allow servicing and rework of parts of the system without evacuating the entire SHRM.

Operation can be switched between modes by adjusting the position of the remotely operated valves, solenoid valves 3, 4, 7, 8 and 9 and ball valve 3 and adding or removing R-12. As explained previously, the amount of refrigerant necessary for operating in the two modes differs. A completely full "hard liquid" system is required for pumped liquid operation. It is also necessary to have a system pressure somewhat above the vapor pressure at the hottest point in the system in order to prevent cavitation in the pump. For vapor compression it is necessary to have liquid in the system in an amount equal to about 1/3 of the system volume. A metal bellows accumulator with an electrical quantity readout was provided to accommodate these changes. One side of the bellows in the accumulator was pressurized with regulated GN_2 to allow adjustment of system pressure to the desired value. However, this

SHRM FLOW SCHEMATIC

13

NOMENCLATURE

BV – BALL VALVE
CV – CHECK VALVE
CHX – CONTACT HEAT EXCHANGER
DP – DELTA PRESSURE
EXPV – EXPANSION VALVE
FD – FILTER DRYER
FM – FLOW METER
FV – FILL VALVE
P – PRESSURE TRANDUCER
PR – PRESSURE REGULATOR
RCV – RADIATOR CONTROL VALVE
RV – RELIEF VALVE
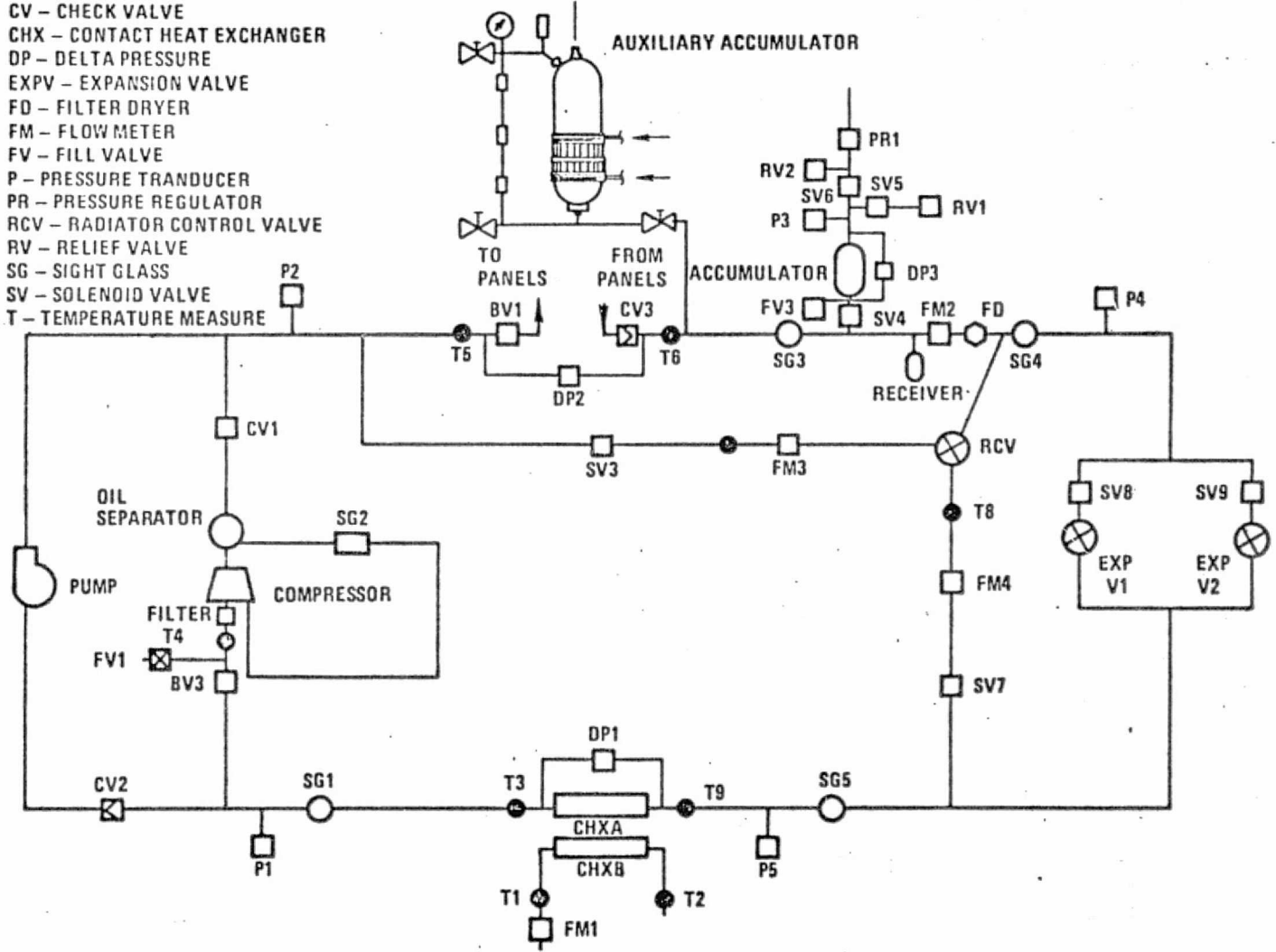SG – SIGHT GLASS
SV – SOLENOID VALVE
T – TEMPERATURE MEASURE

AUXILIARY ACCUMULATOR

PR1
RV2
SV6 SV5
P3 RV1
ACCUMULATOR DP3

TO PANELS
FROM PANELS
BV1
CV3
FV3 SV4 FM2 FD
T5 T6
SG3 SG4
DP2
RECEIVER
P2
P4

CV1
SV3 FM3 RCV
T8

OIL SEPARATOR
SG2
SV8 SV9
PUMP
COMPRESSOR
EXP V1 EXP V2
FILTER
T4
FV1
BV3
FM4

SV7

DP1
CV2 SG1 T3 T9 SG5
CHXA
P1 CHXB P5
T1 T2
FM1

FIGURE 4 PROTOTYPE TEST FLOW MODULE SCHEMATIC AND INSTRUMENTATION

accumulator proved to be too small and it was necessary to add a temperature controlled auxiliary accumulator later. Fluid was transferred out of this accumulator by electrically heating the reservoir. Fluid was returned to the auxiliary accumulator for vapor compression operation by starting the compressor and utilizing it to force the desired amount of liquid into the accumulator. The transfer process was facilitated by liquid nitrogen cooling of the auxiliary accumulator. The amount of liquid in the system and accumulators was monitored by sight glasses on the auxiliary accumulator and an electrical quantity readout signal from the metal bellows accumulator. R-12 return temperature control was accomplished by use of a bypass mixing valve (radiator control valve, RCV in Figure 4) in the radiator mode and by constant pressure expansion valves (EXPV1 and EXPV2) which regulate evaporator pressure (and therefore temperature) to selected values. Choice of two evaporator temperatures during testing was made by selectively opening and closing remotely controlled valves SV8 and SV9.

The selection of the components in the system was made based on both requirements and availability. A Sunstrand centrifugal pump was selected. This device was purchased by JSC according to Vought specifications and furnished to Vought for installation. The compressor, and accumulator were obtained in a similar manner.

The compressor selected was a Fairchild Stratos heli-rotor model with a nominal 10,500 W of cooling rating (3 tons). The accumulator was made by the Metal Bellows Corporation. The remote control, valves and the radiator control valve were purchased under previous contracts and were furnished Vought by JSC. The radiator panels were specifically designed to fit into the ATM frame and were constructed by Vought under the Phase II and III SHRM contract. A uniquely designed contact heat exchanger was selected for the

interface heat exchanger. This device, shown in Photographs of Figures 5 and 6, was designed by Vought and built by United Aircraft Products. The contact heat exchanger provides a mechanical rather than fluid interface between the SHRM and the spacecraft thermal control loop. This will allow the installation and removal of the SHRM from a spacecraft without breaking into either fluid system. These tests represented the first full scale testing of this device.

Figure 5 shows a photograph of an assembled contact heat exchanger and Figure 6 partially assembled. Each half of the heat exchanger was comprised of five flat cold plates of heat exchanger core manifolded together as shown in the photograph. The surfaces were coated with a highly conductive thermal grease, originally Dow Corning 380 and later replaced with General Electric 641. The grease can be seen in Figure 6. The two halves were assembled as shown in Figure 6 and bolted together with 45 bolts to provide the high contact pressure necessary for efficient conduction. The expansion valves selected were constant pressure expansion valves made by the Refrigerating Specialties Company. These valves maintain the evaporator at a constant pressure and therefore temperature regardless of the capacity at which the system is being operated. The remainder of the flow components were commercially available hardware obtained from local suppliers.
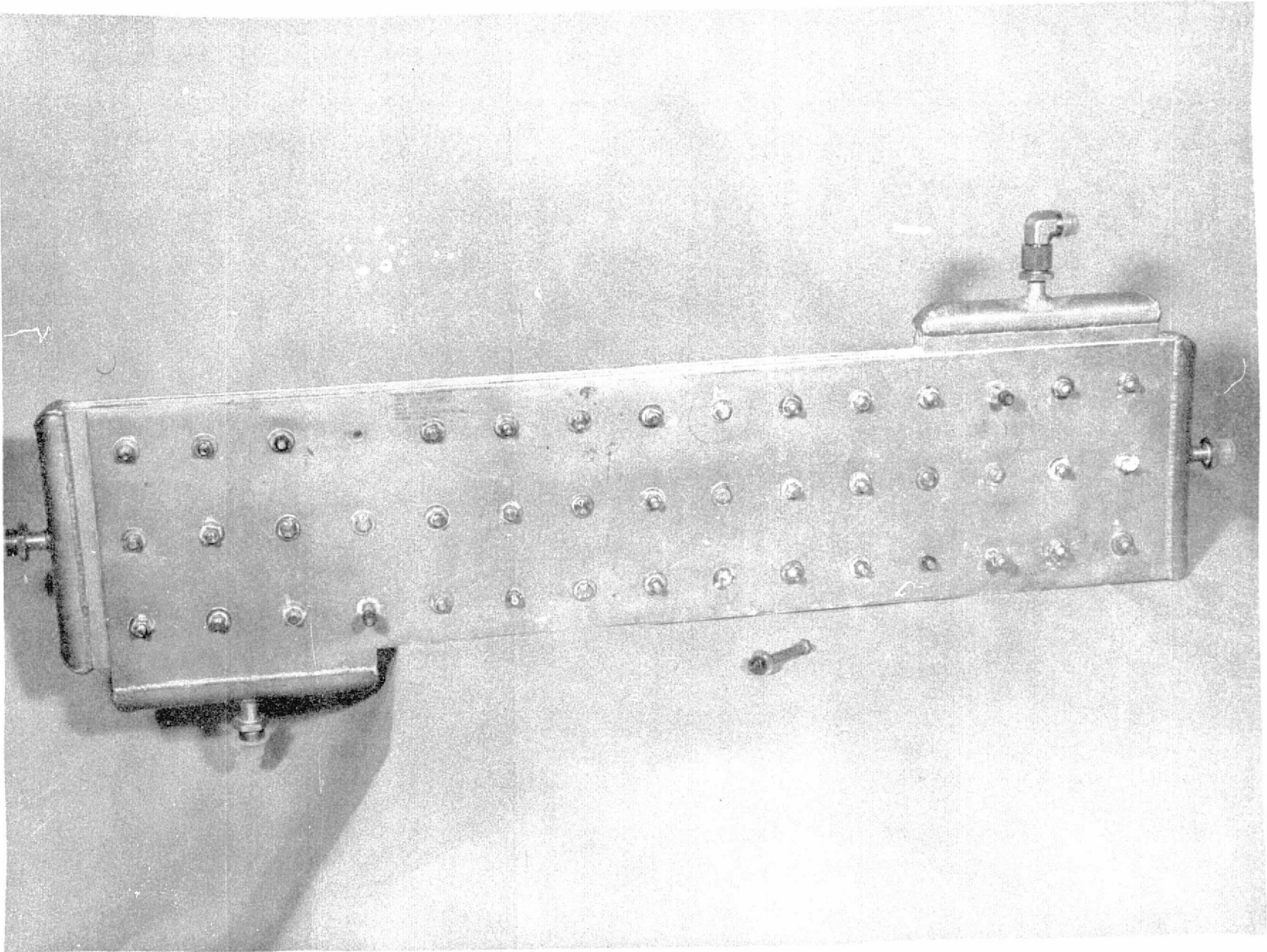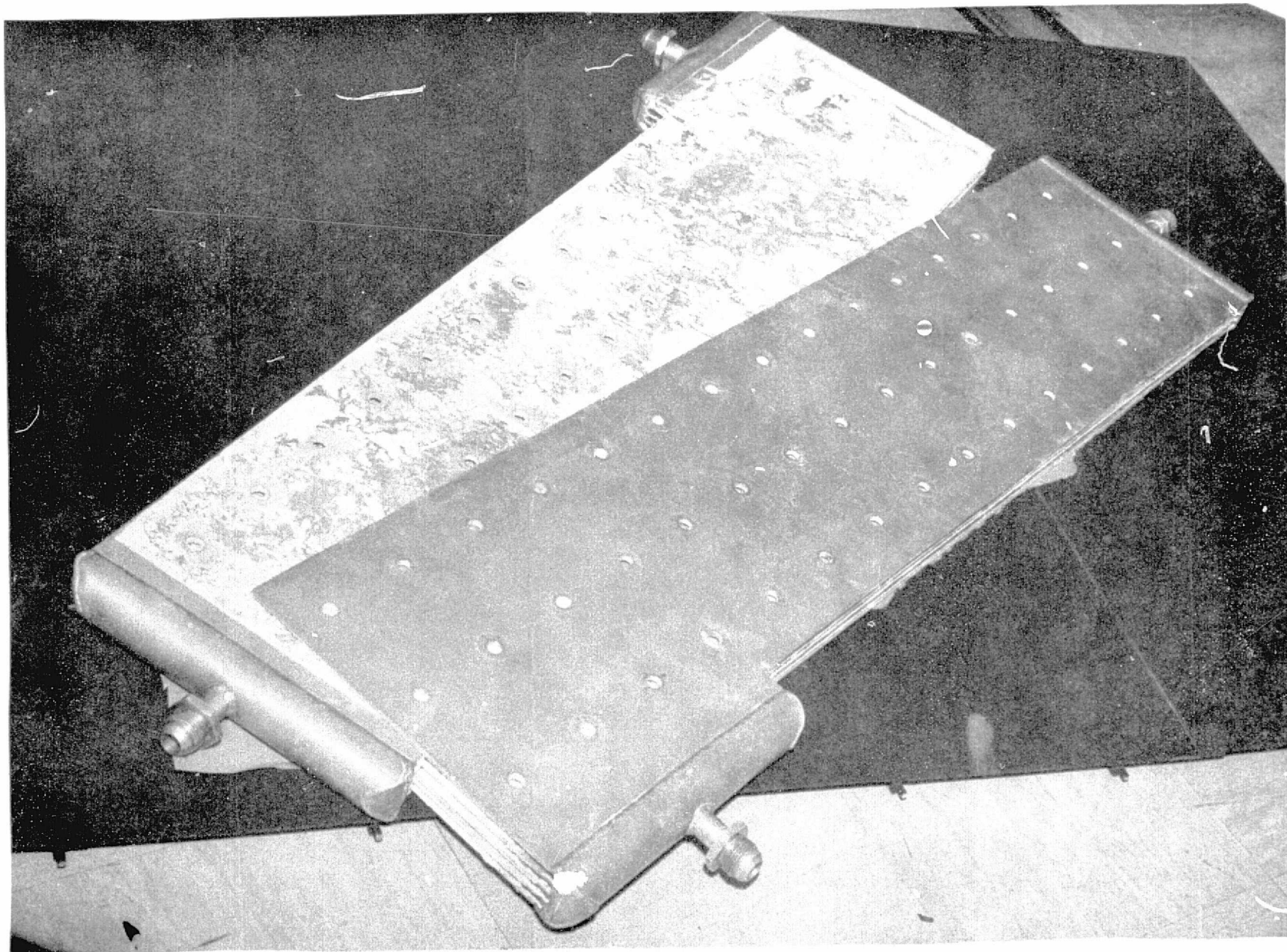
FIGURE 5 CONTACT HEAT EXCHANGER

FIGURE 6   ASSEMBLY OF CONTACT HEAT EXCHANGER

therefore temperature regardless of the capacity at which the system is being operated. The remainder of the flow components were commercially available hardware obtained from local suppliers.

2.3   Test Hardware Installation and Instrumentation

The test hardware used in the subject test consisted of four radiator panels connected with fluid swivels, an ATM deployment mechanism, a deployment fixture to allow deployment and retraction of the ATM mechanism at earth gravity, a flow module containing the compressor, pump and other flow hardware and an electronic controller to provide return temperature and mode selection control. In addition there was a three phase, variable frequency, variable voltage power generator for compressor power and deployable infrared lamps that provided environment simulation. Sufficient instrumentation of the test hardware was included for system monitoring and control and to evaluate the system performance.

The overall test installation is illustrated in the photograph of Figure 7 which was taken from the third level of the chamber. As can be seen in this photograph there were locations for five panels in the ATM frame, however, only four radiator panels were installed. The empty frame represents the end of the deployment mechanism which would be attached to the spacecraft or pallet. The relative locations of the deployment/retraction motor and flow module are also shown in this photograph. A closer view of the radiator panels is shown in Figure 8. The four panels were constructed of aluminum tube extrusions seam welded to 0.00102 meter (0.040 in.) aluminum sheets at 0.16 meter (6.3 in.) intervals. The panel size to fit on the ATM frame was 2.57 (101.25 inches) by 2.37 meters (93.25 inches). These panels provide a total radiating area of 48.7 m^2 (524.5 ft^2) since they radiate from both sides. The panels were coated with a black velvet paint in order to facilitate non-reflective environment simulation with infrared lamps. The eight fluid swivels were located between the panels at the locations illustrated in Figure 8. The radiator panels were heavily instrumented with copper-constantan thermocouples. There were 70 locations on panel 1, 35 on panel 2 and 18 on panels 3 and 4. Locations of these thermocouples are shown in Figure 9. The locations were selected to provide temperature maps of the panels for heat rejection calculations and to evaluate panel performance both as pumped fluid radiators and as

18

FIGURE 7 – SHRM TEST HARDWARE INSTALLATION
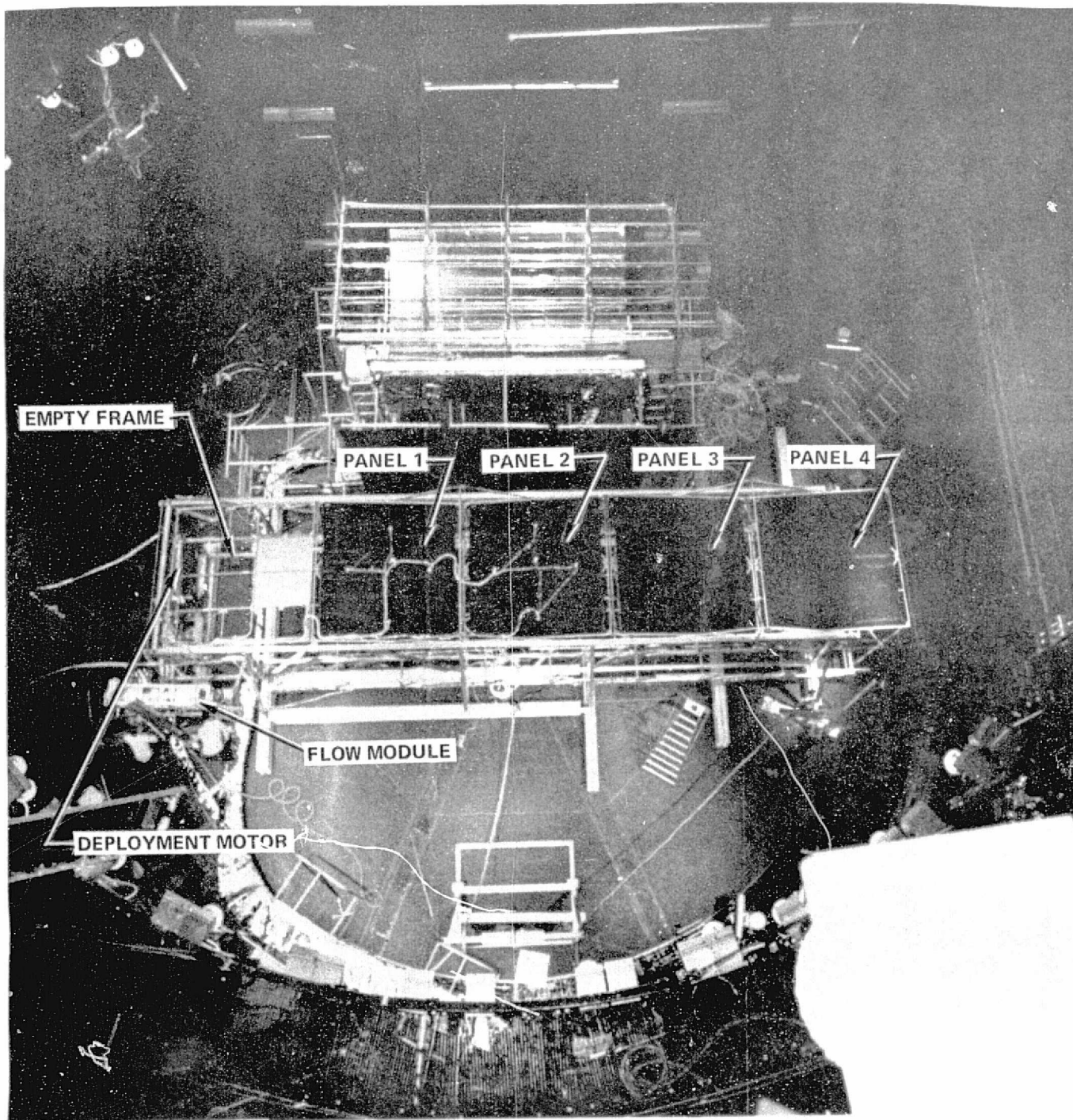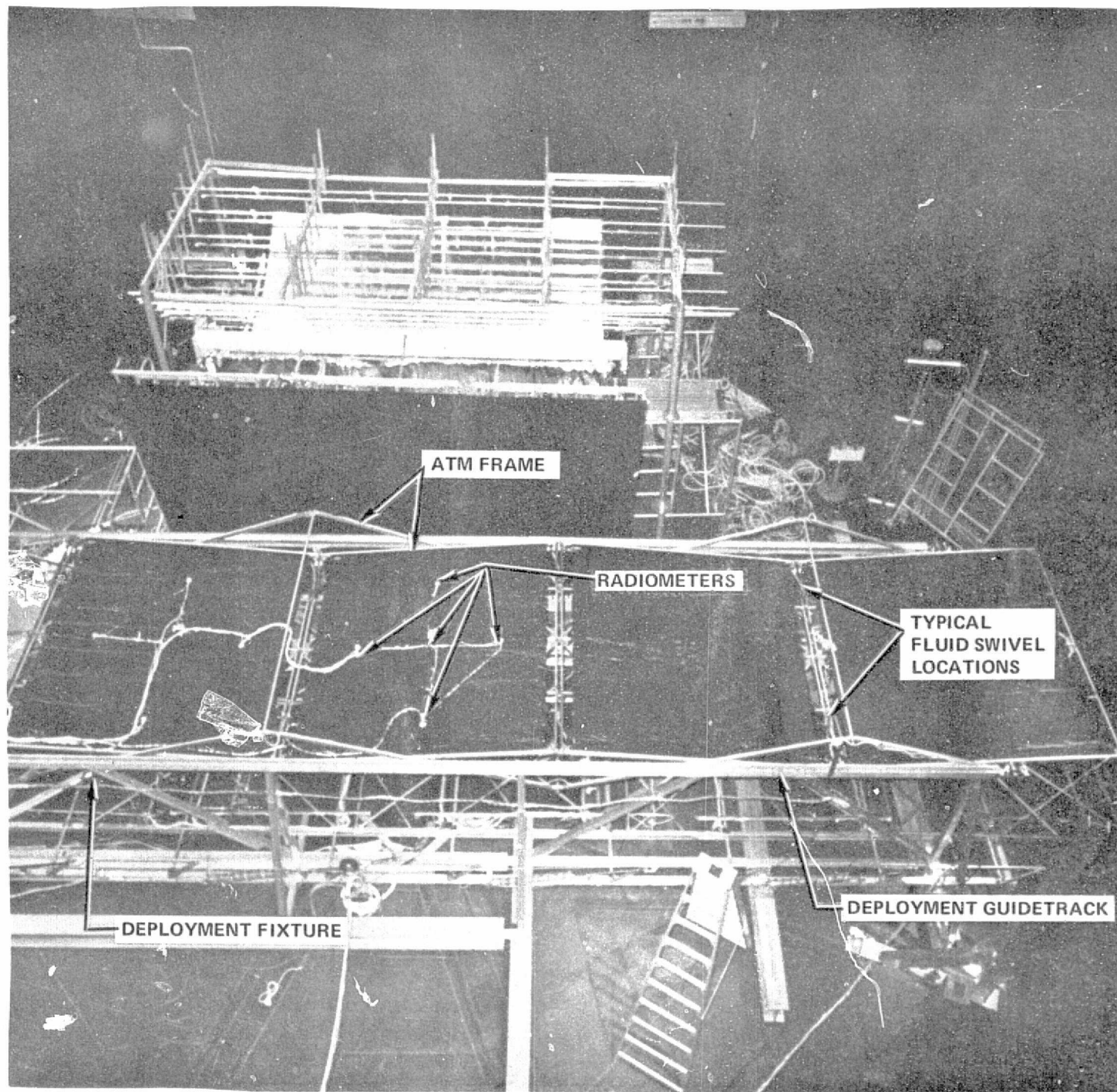
ATM FRAME

RADIOMETERS

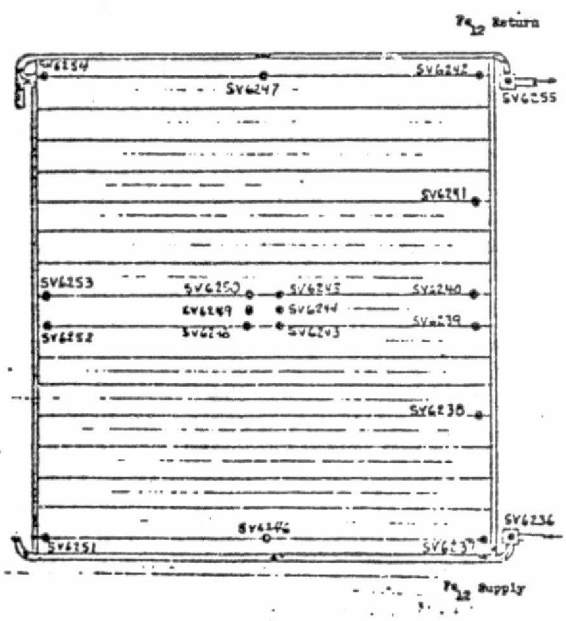TYPICAL
FLUID SWIVEL
LOCATIONS

DEPLOYMENT FIXTURE

DEPLOYMENT GUIDETRACK

FIGURE 8 — SHRM PANELS AND DEPLOYMENT FIXTURE

PANEL 2

PANEL 1

PANEL 4

PANEL 3

FIGURE 9   PANEL INSTRUMENTATION

21

condensing radiator panels. In addition, a thermocouple was located on each of the eight fluid swivels. The first two panels were instrumented with five radiometers to measure absorbed flux from the environment simulator. The locations are shown on Figure 8.

The ATM frame on which the panels are mounted is also shown in Figures 7 and 8 This scissors-linkage type mechanism ordinarily deploys by placing a force on the ends of the linkage and causing an accordion like outward projection. For this test, however, a chain drive mechanism and a guide track were used to pull the linkage mechanism in and out in a horizontal plane. The guiding track can be seen in Figure 8. A large electric motor located at the end of the mechanism was used to provide the deployment and retraction force and load cells on each side of the frame were used to measure the force.

A prototype of the flow module is shown in Figure 10. This module contains the flow equipment which was illustrated in Figure 4. The flow module was instrumented with immersion thermocouples, pressure transducers and flow meters at key locations in the system. These instrumentation locations are shown in the schematic of Figure 4.

The simulated heat load was provided by an external R-21 fluid system which could deliver a wide range of flowrates and temperatures to the payload thermal control system side of the contact heat exchanger.

An electric controller provided return temperature control and mode selection. It provided for temperature and therefore heat rejection control in the pumped liquid mode by variation of radiator flowrate based on a comparison of T8 (see Figure 4) with the desired value. Capability of two different control set points was included. Capacity control in the refrigeration mode was accomplished by manual adjustment of compressor speed by power frequency variations to the compressor's three phase, 400 cycle motor. The controller had the capability to automatically initiate a switch from the radiator to the refrigeration mode when either the heat load or environment prevented coolant return (T2 on Figure 4) at the desired control temperature. Return to radiator mode could be manually initiated from a control console. In both cases the controller set the proper valve positions, allowed time delays for the transfer of fluid in or out of the system, and started the compressor or pump. The control console shown in Figure 11 also provided read-

FLEX LINE TO PANELS

EXPANSION VALVES

REMOTE CONTROL VALVE

CONTACT HEAT EXCHANGE

RADIATOR CONTROL
VALVE

REMOTE CONTROL BALL VALVE

COMPRESSOR

SUCTION FILTER

METAL BELLOWS ACCUMULATOR
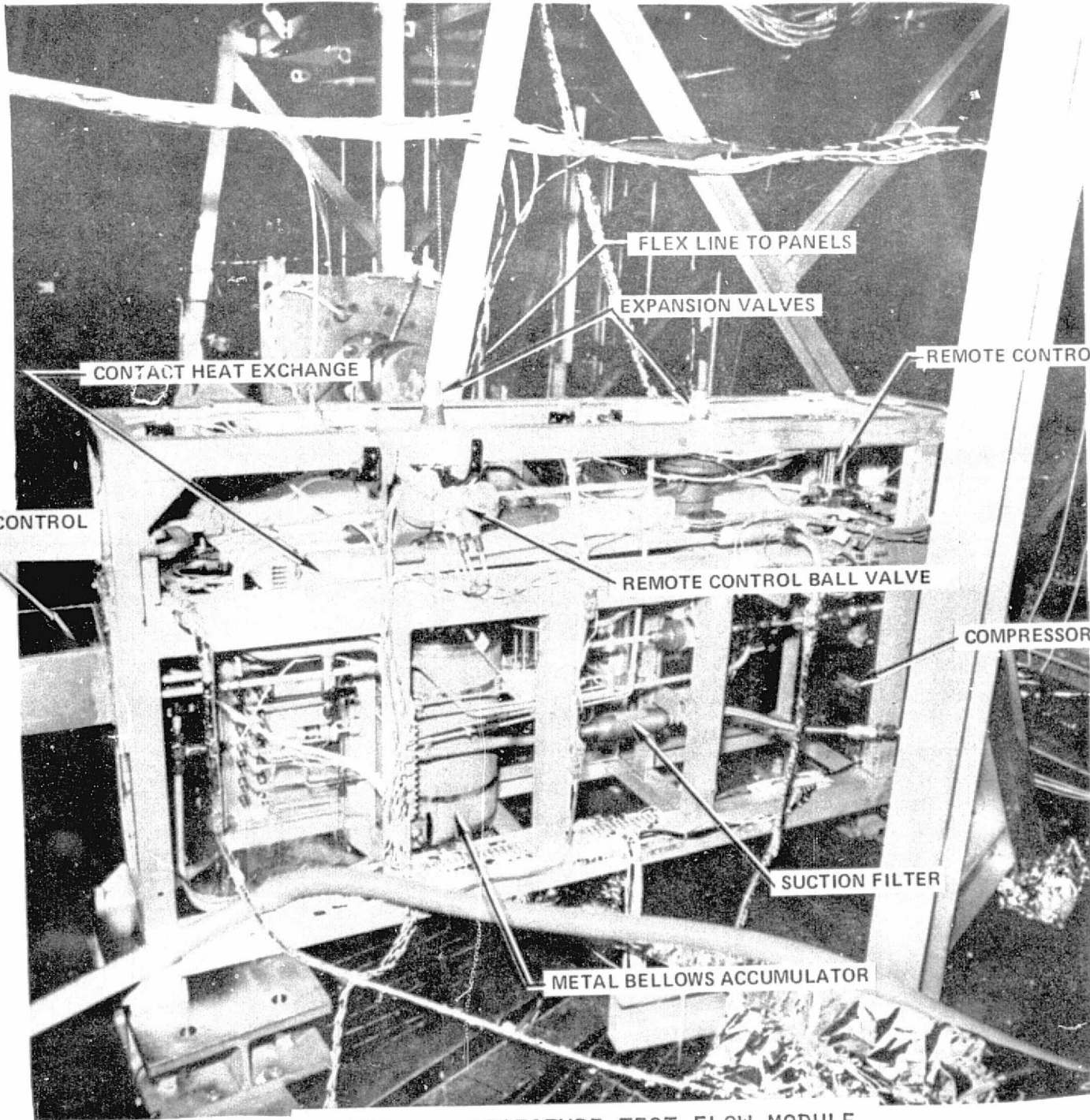
FIGURE 10   PROTOTYPE TEST FLOW MODULE

COMPRESSOR POWER
WATTS

VALVE POSITION INDICATOR

REF
REF
AUTO
RAD
MODE SELECTION
RAD
TEMPERATURE ERROR METER

COMP
AUTO
OFF

PUMP
AUTO
OFF

1   3   4   5   OPEN
CLOSED
ON OFF
SV4 CONTROL
AUTO
OFF
SV5 CONTROL

ERROR
ON
OFF
ERROR AUDIO SIGNAL

6   7   8   9   OPEN
CLOSED

COMPRESSOR INPUT FREQUENCY CONTROL
STPT 0°/38°
SV6 CONTROL
AUTO
ON

SHRM CONTROL CONSOLE

COMPRESSOR POWER FREQ.

PUMP POWER CIRCUIT BREAKER

AMPS 0 50
AMPS 0 50
AMPS 0 50

VOLTS 0 300
VOLTS 0 300
VOLTS 0 300

PHASE A
PHASE B
PHASE C

COMPRESSOR ELECTRICAL MEASUREMENTS

0   100
TEMPERATURE °F

50   0   50
TEMP. ERROR °F
−5°F TO +5°F

50   0   50
VALVE POSITION
−0.05 TO +0.05 IN.

AUTO
MAN
OPERATION MODE
AUTO MODE

35°F
−5°F
TEMP. CONTROL

FAST
SLOW
PULSE RATE

+
−
DIREC.

SINGLE STEP
NORMAL OPERATION
SINGLE STEP
SINGLE PULSE

MANUAL MODE

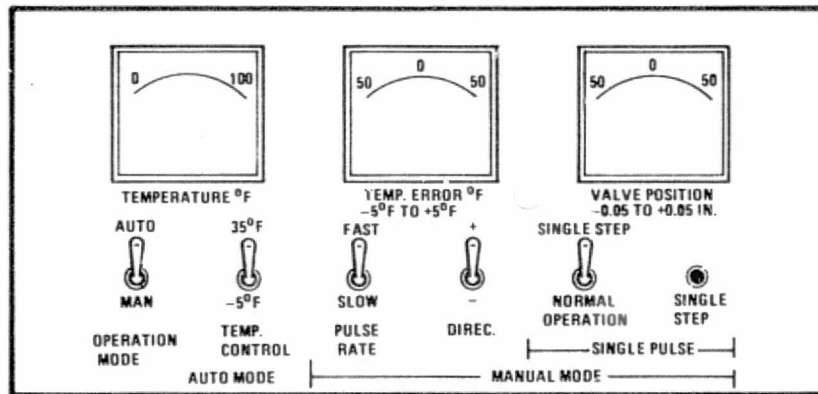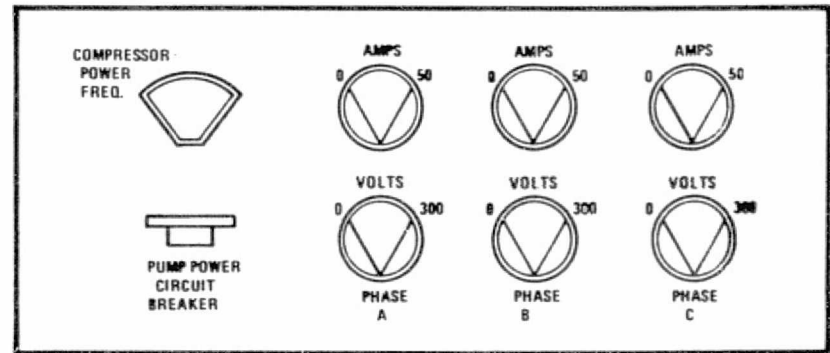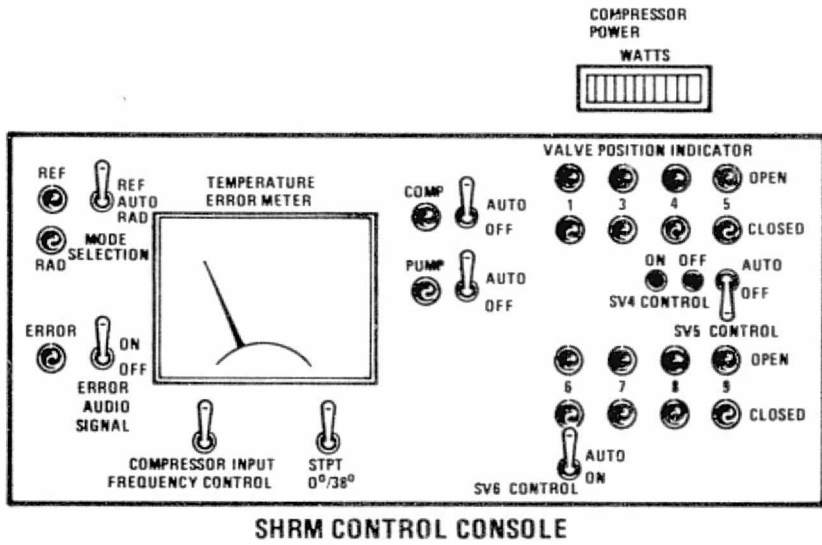**FLOW VALVE CONTROL CONSOLE**

FIGURE 11   SHRM CONTROL CONSOLES

24

outs of key signals such as valve positions, temperature error, compressor electrical measurements and contained manual overrides of key valve positions.

Power to the compressor was provided by a rotary, three phase generator. The generators' voltage regulator was modified to cause a linearly decreasing voltage as frequency is reduced from 400 cycles per second, 208 volts (rated power input to the compressor). This is necessary to optimize the power consumption at reduced compressor speeds. Frequency was controlled by speed control of the generator's drive motor.

Environment simulation was provided by arrays of deployable infrared lamps as shown in the photograph of Figure 12. The arrays are shown in the retracted position. Position adjustment of the lamps was necessary to allow deployment and retraction of the radiator panels during the test. The lamps could be deployed upward to just below the panels when the panels were in a deployed (flat) position by use of the pneumatic actuators shown in Figure 12. Flux from the lamps was monitored by the panel radiometers and adjusted to the desired values. All environment simulation flux was incident on the lower panel surface with the upper surface exposed to chamber simulation of deep space environment.
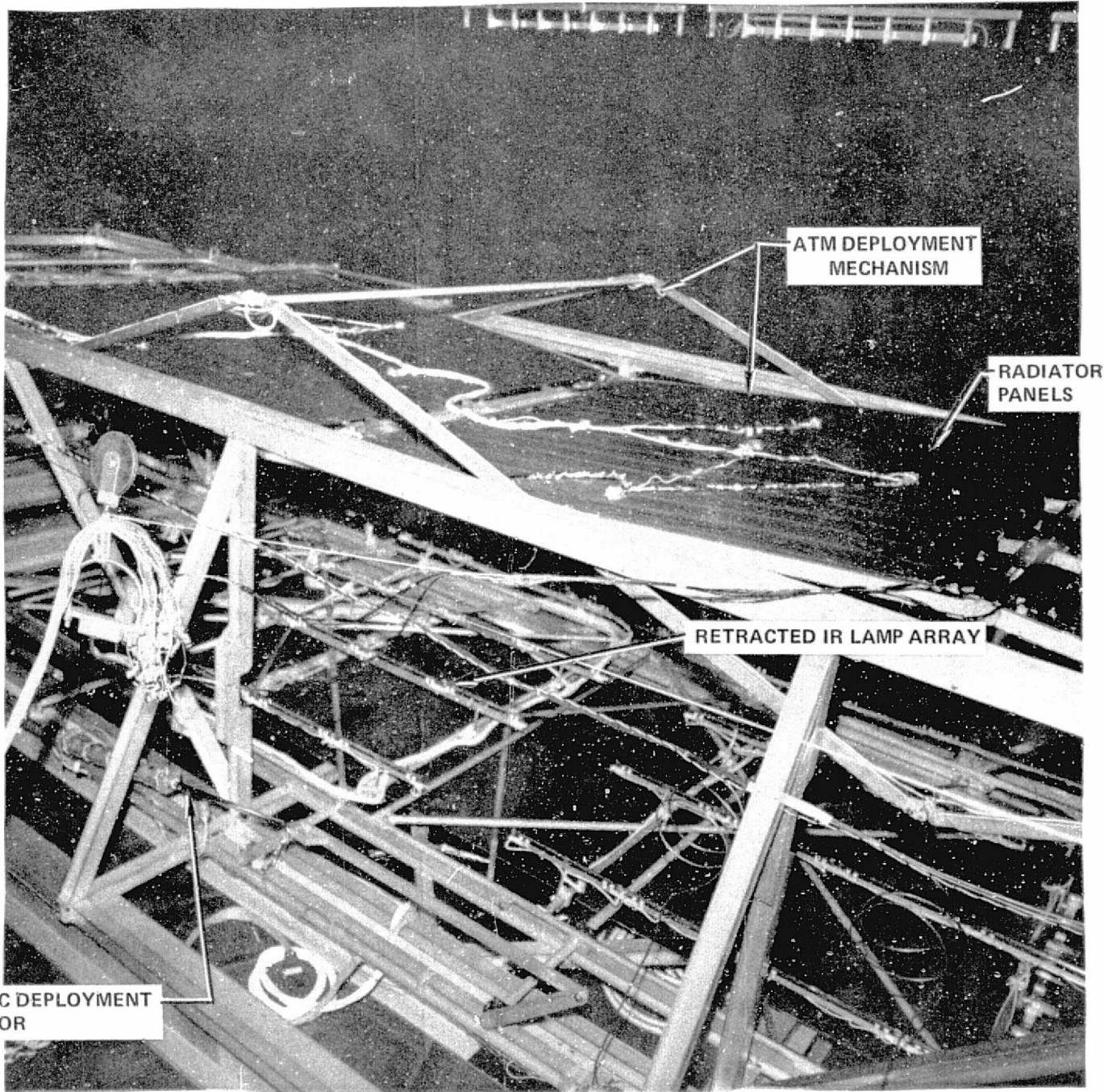
FIGURE 12- ENVIRONMENT SIMULATOR

3.0 TEST PLAN

The original test objectives and a detailed test plan were delineated in the detailed test procedures (Ref. 6). Deviations from the original plans were caused by the various hardware problems which are discussed in Section 4.0 of this report and test planning was performed on a continuing basis during week one. Between the two weeks of testing the results of week 1 and the status of the hardware were reviewed and a new test plan written for the second week of testing. This test plan was followed much more closely than the original one and was deviated from only slightly until the test was terminated due to a severe flex line leak. This section discusses the test objectives and original test plan and how the plan was deviated during the first week. The second week's test is then discussed.

3.1 Test Objectives and Original Test Plan

The specific test objectives for the Chamber A thermal vacuum test were:

1. Demonstrate deployment and retraction under realistic environment and heat load conditions. During these operations determine the loads and evaluate the fluid swivel design.

2. Determine heat rejection capability under pumped fluid radiator and refrigeration cycle modes and assess interaction of a system of condensing radiator panels.

3. Evaluate operation of radiator and refrigeration loop components used in a closed cycle system. The components to be evaluated were the contact heat exchanger, R-12 compressor, accumulator and liquid pump.

4. Obtain characteristics of "dual mode" control system in switching between pumped liquid radiator and refrigeration cycle operation.

5. Investigate system performance under off-nominal conditions including extreme heat loads, environments and partial deployment.

To accomplish these test objectives a test plan with 44 test points was prepared. A summary of these test points is given in Table 2. There were

18 planned tests of radiator mode operation, 17 refrigeration and 9 dual mode. These tests were organized into four phases as illustrated in the four charts of Table 2 which progressed from lowest to highest risk. First, pure pumped fluid radiator testing was to be conducted then pure refrigeration, next mixed mode tests demonstrating the controller were planned followed by a series of off-nominal conditions tests. The test points were designed to map both the radiator and refrigeration system capacities. The range of environments simulated cover earth orbital, translunar, full sun lunar orbit, and off-nominal conditions.

3.2   Revised Test Plan

During the first week of testing the test plan and sequence was revised as required by the hardware problems discussed in Section 4.0 and to add test points to insure sufficient data was obtained to define the system capabilities. The characteristics of the added test points will be discussed in the test results discussion in Section 4.0. Tests points 1 and 1A were conducted as scheduled then the sequence changed to run test point 8. Three other radiator system test points were conducted, 10A (a point added to document radiator performance in view of the level of contact heat exchanger performance), 4, and 5. The sequence was then altered to run a series of refrigeration points which were at the same environment since some difficulty had been incurred with the environment simulator. The mode switch was conducted and test points 13, 16, 16A, 21, 22, 14, 17, 18 and 19 were run in that sequence. A switch back to the radiator mode was made and test points 7, 6 and 11 were conducted which were skipped previously due to the environment simulator problem. A change in sequence was again made to switch back to refrigeration due to a liquid pump failure and test points 19A and 19B, which were added to further document refrigeration capabilities based on the test results thus far observed, were run. When the pump was again operational, test points 46, 47 and 48 were conducted plus 8A and 8B which were new points to further document radiator system performance. Then new refrigeration test points 14A and 17A were conducted and the week's testing terminated. No mode change experiments were conducted in week 1. The condition of the hardware would not support these operations in the latter part of week 1.

During the week between the tests a new test sequence for the second week was prepared based on the results of the first week's tests and the

28

TABLE 2   ORIGINAL TEST PLAN

SHEN TEST TIMELINE, PHASE I - RADIATOR SYSTEM TEST.

	TEST SEQUENCE	R-21 FLOW (lb/hr)	R-21 T IN (°F)	R-12 CONTROL TEMP	FLOW RATE	ENVIRONMENT (BTU/hr-ft²)	COMMENTS	ELAPSED TIME
Ambient deployment*	1	0	80°	ambient	2600	no lamps	deploy & retract	
Hot deployment	1A	2440	105	40	2600	41.6	deploy-bring to steady state	4 hrs.
Baseline rad performance	2		150	-	2600	41.6		2 hrs.
Baseline rad performance	3		outlet from 150° towards 80° to obtain 40° R-12 outlet	40	2600	41.6		2 hrs.
Check control at 40° Set point	4		ramp 80-45 in 2 hrs.	40	2600	41.6		4 hrs.
Check control at 40° Set point	5		ramp 45-80 in 2 hrs.	40	2600	41.6		3 hrs.
Determine radiation limit environment	6		105	40	2600	2 cycles 5-50 in 90 min.		4 hrs.
0° Control limits	7		at 49° inlet adjust in 5° increments to obtain 0° outlet	0	2600	20		3 hrs.
0° Control limits	8		at 63° inlet adjust in 5° increments to obtain 0° outlet	0	2600	5		3 hrs.
Check control valve at 0° set point	9		ramp 50-35 in 2 hrs	0	2600	5		2 hrs.
Check control valve at 0° set point	10		ramp 35-50 in 2 hrs	0	2600	5		2 hrs.
Determine radiometer limit environment	11		50	0	2600	2 cycles 5-20 in 90 min.		4 hrs.
Cold retract	12		40	0	2600	5	retract	4 hrs.

*To be conducted during chamber pumpdown prior to chamber cooldown.

TOAL 37 hrs.

29

TABLE 2   ORIGINAL TEST PLAN (CONT'D)

SHRM TEST TIMELINE, PHASE II - REFRIGERATION SYSTEM TESTING.

	TEST SEQUENCE	W21 (lbm/hr)	R-21 T IN (°F)	9-12 CONTROL TEMP (°F)	ENVIRONMENT BTU/Hr-FT²	COMMENTS	ELAPSED TIME
Baseline	13	2440	105	80	41.6	deploy	3 hrs.
Control check at steady state	14	2440	105	40	20.6		2 hrs.
Control check at steady state	15	2440	105	40	10		2 hrs.
Transient control temp check	16	2440	Ramp 105-60-105 in. 2 hrs.	40	41.6		3 hrs.
Max refrig limit point	17	2440	105	40	50		2 hrs.
Max refrig limit point	18	2440	105	40	60		2 hrs.
Max refrig limit point	19	2440	105	40	70		2 hrs.
Transient control check	20	2440	105	40	2 cycles 5-50 in 90 min.		4 hrs.
0° Baseline	21	2440	60	0	41.6		3 hrs.
Map to max performance	22	2440	at 50°, increase in 5° increments until capacity is reached	0	41.6		3 hrs.
Map to max environment	23	2440	60	0	50		2 hrs.
Map to max environment	24	2440	60	0	60		2 hrs.
Cycle for orbital environment	25	2440	60	0	2-90 min. cycles 5-50		4 hrs.

TOTAL 35 hrs.

*Capacity is defined as radiator inlet and radiator outlet temperatures, increases are the same.

TABLE 2 ORIGINAL TEST PLAN (CONT'D)

31

SHRM TEST TIMELINE, PHASE III - CONTROL SYSTEM TESTS.

	TEST SEQUENCE	R-21 FLOW (LBM/HR)	R-21 T IN (°F)	R-12 CONTROL TEST (°F)	ENVIRONMENT (BTU/hr-ft²)	COMMENTS	ELAPSED TIME
Meas stability during switch over	26	2440	60	0	41.6	optimize mode switch refrigeration to radiator	3 hrs.
Meas stability during switch over	27		60	0	41.6	optimize mode switch radiator to refrigeration	3 hrs.
Meas stability during switch over	28		105	35	41.6	optimize mode switch refrigerator to radiator	3 hrs.
Meas stability during switch over	29		105	35	41.6	optimize mode switch radiator to refrigerator	3 hrs.
Demonstrate switch for heat load change	30		ramp 105-60 in 2 hrs.	35	41.6	optimize mode switch refrigeration to rad during ramp	3 hrs.
Demonstrate switch for heat	31		ramp 60-105 in 2 hrs.	35	41.6	automatic switch to refrigeration	3 hrs.
Demonstrate switch for environment change	32		105	35	2-90 min. cycls 5-50	manual switch to rad, auto switch back	4 hrs.
	33		60	0	2-90 min cycls 5-50	manual switch to rad, auto switch back	4 hrs.

TOTAL 26 hrs.

TABLE 2 ORIGINAL TEST PLAN (CONT'D)

SHAM TEST TIMELINE, PHASE IV - OFF NOMINAL PERFORMANCE.

TEST SEQUENCE	R-21 T IN (°F)	R-21 FLOW LBM/HR	R-12 CONTROL TEMP (°F)	R-12 FLOW RATE	ENVIRONMENT (BTU/hr-ft²)	COMMENTS	ELAPSED TIME
34	150	2440	40	2600	75	Radiator mode	2 hrs.
35	150	2440	40	2600	20-100	Radiator mode	2 hrs.
35A	ramp 80-150	2440	40	2600	100		2 hrs.
36	150	2440	40		.75	Refrigerator mode	1 hrs.
37	150	2440	40		100	Refrigerator mode	2 hrs.
38	150	2440	40		5	Refrigerator mode	3 hrs.
39	105	2440	40		5	Refrigerator mode	2 hrs.
40	45 adjust for min. load		40	2000	5	Fully deployed radiator mode	6 hrs.
41	43 adjust for min. load		40	2600	5	Partially deployed radiator mode	6 hrs.
42	adjust for min. load		40	2600	5	Fully retracted radiator mode	6 hrs.
43	ramp 40-105 in 3 hrs.		40		ramp 5-41.6 in 3 hrs.	Deploy radiator as heat load increases automatic switch to refrigerator mode	8 hrs.
44		0	0	0	5	Retract panel at -250° F	6 hrs.
45	80	2440	40	2600	100	Deploy	3 hrs.

TOTAL 47 hrs.

TOTAL 4 PHASES 185 hrs.

32

changes in hardware. The test points were renumbered in sequence. A summary of the week 2 Test Plan is shown in Table 3. This new sequence was designed to:

1. Evaluate the changes/improvements to the test equipment between tests.

2. Obtain the originally planned test data not accomplished in week 1, especially the mode change tests and low load limits.

3. Map performance at a new (10°F) return temperature.

The week 2 test plan was followed quite closely with no major perturbations until the low load points were attempted. A flow stoppage to panel 4 caused some compromise in the quality of test points 114 and 115 which will be discussed later, then a severe leak which resulted when retraction was attempted caused the cancellation of test points 116-121.

TABLE 3 REVISED TEST PLAN FOR WEEK 2

OBJECTIVE			TEST POINT NUMBER	TOTAL SYSTEM FLOW (LB/HR)		DURATION (HR)		ENVIRON-MENT (BTU/HR °F)
				F12 *	F21	T.P.	CUM.	
Evaluate HX Grease			101 /?:·2 102 15.°C	2050 2050	2440 ~~1886~~ 1777	3 3	3 6	82
External Pump			103	2600	2440	3	9	82
Switchover	Rad to Refrig		104	2050 → 700	1886	6	15	100
	Refrig to Rad		105	700 → 2050				100
	Rad to Refrig		106	2050 → 700				100 → 150 in 1 hr
35° Set Point Repeat			107	700	2440	3	18	120
10° Set Point Capacity Demonstration	Rad.		108,109,110	2050	1886	8	26	40, 80, 120
	Ref.		111,112,113	400	1886	8	34	40, 80, 120
Low Load	100% Deploy	(-211°F) (-250°F)	114 115	2050	1886 1886	8 6	42 48	0 0
Cold Retract			116	0	1886	1	49	0
Low Load	0% Deploy	(-211°F) (-250°F)	117 118	2050	1886 1886	8 6	57 63	0 0
	50% Deploy	(-211°F) (-250°F)	119 120	2050	1886 1886	8 6	11 77	0 0
1/2 Retract, Cold Deploy/Recov.			121	2050	1886	1	78	0

* VALUES ARE APPROXIMATE, EXCEPT TEST POINT 103

34

4.0 TEST RESULTS

The results of the Thermal Vacuum Testing of the SHRM provided sufficient data to evaluate both system and component performance. A total of 42 test points were conducted during the two weeks of testing compared to the planned 44. Of these there were 22 radiator, 17 refrigeration and 3 dual mode points compared to 18, 17 and 9 planned. A summary of the test points conducted are given in Table 4. Retraction and deployment were demonstrated at ambient and at cold (average panel temperatures -4 to -40°F) conditions with no anomalies. Deployment and retraction were also demonstrated at very cold temperatures (-140 to -273°F) with damage incurred to one flex line. All the test objectives were achieved with the exception that only limited low load test data were obtained. Deployment and retraction of a deployable radiator system was successfully demonstrated. This section will discuss the hardware problems, their resolution and impact. The system thermodynamic test results and the evaluation of the components based on the test data will then be presented.

4.1 Hardware Problems and Corrective Actions

During the testing there were several hardware problems which had various effects on the system design, schedule, test planning and test sequence. Since much of the rationale for test activities involved the status of the hardware the major hardware problems incurred are delineated, the subsequent corrective actions taken are discussed and the impact on the conduct of the test explained. The problems are discussed in chronological order beginning with the pre-test activities of panel calibration and ambient checkout then the first week of testing followed by the week of refurbishment then the final week of testing.

4.1.1 Pre-Test Activity Hardware Problems

During the pre-test activities three problems were noted:

1. In pumped fluid mode an unequal flow split among panels was observed.
2. The fluid pump output was only 2070 lbm/hr with full radiator flow.
3. Damage of expansion valves during proof pressure test.

TABLE 4 TEST POINT SEQUENCE SUMMARY — 1ST WEEK

TEST POINT	MODE	R21 HEAT T_{IN} (°F)	T_{OUT} (°F)	R12 HX TEMPS T_{IN} (°F)	T_{OUT} (°F)	ENVIRONMENT (BTU/HR-FT^2)	NET HEAT REJECTION (BTU/HR)	COMMENTS
1A	Radiator	113.4	61.9	36.0	101.5	73.5	32,610	
8	Radiator	74.5	20.3	-7.0	61.9	Lamps Off	33,040	
10A	Radiator	61.9	27.1	13.6	55.5	68.7	21,360	
4	Radiator	87-55	47.1-38.3	33.8	49.2	83	Variable	2 hr inlet temp ramp
5	Radiator	55-87	38.3-47.1	33.8	76.6	83	Variable	2 hr inlet temp ramp
13	Refrigeration	105.4	49.2	33.8	31.5	83	37,600	
15	Refrigeration	105-60	47.1-38.3	33.8	31.5	83	Variable	2 hr inlet temp ramp
16A	Refrigeration	119.3	59.8	36.0	38.3	89 3	38,820	
21	Refrigeration	61.9	36.0	-16.4	59.8	82.0	13,040	
22	Refrigeration	27.1	0.1	-16.4	27.1	82.0	13,370	
14	Refrigeration	105.4	47.1	36.0	33.8	39.3	35,960	
17	Refrigeration	105.4	49.2	36.0	33.8	104.9	34,700	
18	Refrigeration	107.4	51.3	36.0	36.0	121.7	33,620	
19	Refrigeration	107.4	53.4	38.3	38.3	141.6	31,070	
7	Radiator	60.8	17.0	-2.1	51.3	40.0	26,460	
6	Radiator	107.4	51.3	34.9	91.4	10-90	Variable	Environment cycles
11	Radiator	57.0	11.4	-4.5	45.0	10-40	Variable	Environment cycles
19A	Refrigeration	105.4	55.5	38.3	38.3	155.4	32,500	
19B	Refrigeration	107.4	61.5	45.0	51.3	200	28,600	Run aborted due to temp
46	Radiator	161.6	76.6	33.8	138.2	16.4	51,805	
47	Radiator	146.9	72.4	36.0	125.3	43	45,663	
48	Radiator	80.8	49.2	36.0	72.4	121.4	18,050	
8A	Radiator	29.3	4.6	-4.5	24.8	79.1	14,560	
8B	Radiator	11.4	0.1	-4.5	6.9	106.1	5,260	
14A	Refrigeration	125.3	59.8	38.3	36.0	42.3	39,873	
17A	Refrigeration	111.4	53.4	36.0	38.3	101.3	36,190	

36

TABLE 4 (CONT'D)
TEST POINT SEQUENCE SUMMARY - 2ND WEEK

TEST POINT	MODE	R21 HEAT SOURCE T_{IN} (°F)	T_{OUT} (°F)	R12 HX TEMPS T_{IN} (°F)	T_{OUT} (°F)	ENVIRONMENT (BTU/HR-FT^2)	NET HEAT REJECTION (BTU/HR)	COMMENTS
101	Radiator	110.7	56.7	36.9	102.6	82.7	33,210	
102	Radiator	116.7	44.1	34.5	102.6	78.4	32,250	
103	Radiator	96.1	44.1	36.1	85.9	80.3	31,430	
104	Rad - Ref	85-110	405-87-43	36-40	Variable	105.0	Variable	Mode switch, T_{in} ramp
105	Ref - Rad	110-103	44-102-42	36	Variable	100.6	Variable	Mode switch, T_{in} ramp
106	Rad - Ref	85.9	40-75	36	Variable	100-150	Variable	Mode switch, envn. ra:
107	Refrigeration	101.1	42.5	36.1	56.7	120.1	36,420	
110	Radiator	38.5	17.5	15.0	34.5	120.1	9,140	
109	Radiator	71.4	21.6	15.0	59.8	80.7	22,440	
108	Radiator	101.1	24.8	14.2	81.4	40.6	35,410	
111	Refrigeration	106.9	32.9	14.2	12.6	42.4	33,240	
112	Refrigeration	85.5	24.0	8.5	6.1	81.3	26,920	
113	Refrigeration	78.3	21.6	9.3	8.5	119.4	24,450	
111A	Refrigeration	103.3	32.1	12.6	11.8	48.2	32,590	
114	Radiator	70.9	36.1	35.3	40.1	Lamps off	2,730	Low load
115	Radiator	36.1	36.1	35.3	36.1	Lamps Off	380	Low Load

37

1. A test was devised to determine the flow split among the four panels in the pumped fluid mode. The panels were orificed to provide an equal flow split in the vapor compression mode and some flow skew was expected. The test was conducted to determine what the actual distribution was so the acceptability could be determined. To accomplish this a flowmeter was installed on the inlet side between panels 1 and 2, 2 and 3, 3 and 4 (see Figure 3). Total flow was read from FM2 in the flow module. It was impossible to install a flowmeter to measure each panel flow due to the manifold and panel design. The flow to panel 1 was calculated by subtracting the flow between panels 1 and 2 from the total flow, the flow to panel 2 by subtracting the flow between panels 3 and 4 from the flow between 1 and 2, etc. The result was:

<div align="center">

Panel 1 - 920

Panel 2 - 520

Panel 3 - 365

Panel 4 - <u>215</u>

2020 lbm/hr - Total Flow Reading 2060

</div>

These resulted in laminar flow through panel 4 which would not result in acceptance fluid to tube heat transfer. Analysis indicated the presence of the flowmeters in the line could have significantly affected the distribution. The test was subsequently run with all the flow meters removed except the two which measured total flow and flow through panel 4. The result was:

<div align="center">

Panel 4 -   310 lbm/hr

Total   - 2120 lbm/hr

</div>

This would give a turbulent Reynold's No. in panel 4 and with the final flowmeter removed for the test configuration, it would further equalize the flow. For these reasons the flow split was accepted for test. The exact flow split was not known since this was impossible to measure and thus can only be estimated from the test data. No further action was taken on this problem.

2. In the Dallas checkout of the fluid pump a flowrate of 2689 lbm/hr was obtained at a pressure drop of about 35 psi. During this checkout the pump was installed in the flow module, however, there was a small heat exchanger in place of the radiator panels since the radiator panels were in Houston. This flow was somewhat below the 3000 lbm/hr which had been planned. With the radia-

tor panels installed in the thermal vacuum test configuration in Chamber A
the flow delivered was only 2080 lbm/hr. The indicated pressure rise was
36 psi. Since this flow was lower than expected, an investigation was under-
taken to determine if the pump was operating properly. All the power inputs
to the pump were confirmed to be proper. The pressure taps on the pump inlet
and outlet were connected to a pressure differential transducer and as much
of a flow vs ΔP curve was defined as was possible without removing the pump
from the system. More flow could be obtained by bypassing about half the flow
around the panels through manual operation of the radiator control valve.
This was done and the subsequent data compared to a pump performance curve
furnished by Sunstrand. The pump performance was close to predicted, indi-
cating that the cause of the low flow was higher flow resistance in the fluid
loop. It is a characteristic of centrifugal pumps for the ΔP - flowrate curve
to be non-linear and even to have a positive relationship between ΔP and flow-
rate over a part of the curve thus explaining the lower flow at a low pressure
drop. As flow resistance is decreased flowrate increases with little change
or even an increase in pressure drop. Ways to decrease the flow resistance
were investigated. Flow meter 4 was removed with no significant effect and
was subsequently re-installed. The decision was made to accept the lower flow-
rate. No further action was taken.

    3. During the pre-test activities a proof pressure test was con-
ducted at 375 psig, 1-1/2 times the max operating pressure of 250 psig. The
pressure was held for five minutes. The system remained intact, however, leak-
age was observed from the expansion valves. The valve bodies were tightened
and the leakage stopped at 250 psig. A review of the design indicated that the
full proof pressure was placed against the regulator diaphram during the test
and could have possibly damaged it. A check with Refrigerating Specialities,
the valve manufacturers, indicated the diaphram would probably be good to
250 psig. The valve bodies are tested to 1500 psig. An operational check of
the valve indicated the diaphrams had been damaged. Replacement diaphrams
were ordered and received the next day. The valves were repaired and proofed
to 250 psig. They were adjusted to the proper pressure settings again (32
psig for 35°F evaporator and 4.5 psig for -10°F evaporator). A pressure limit
of 250 psig was placed on test conditions to prevent further damage. No
further action was required during the remaining testing.

4.1.2   Week 1 Test Hardware Problems

During the first week of testing the following problems were noted:

1. Loosening of shear panels on empty 1st frame.
2. Apparent low performance of contact heat exchangers.
3. Failure of drive sprocket on variable frequency 1 variable voltage power source.
4. Failure of SV4 position switch, apparent failure of SV4 to respond and indication of internal leakage.
5. Failure of liquid pump to start.
6. Leakage on panel 1 manifold.

1. A visual inspection of the test hardware early in the thermal vacuum test revealed an object apparently hanging from the first frame of the ATM mechanism. A subsequent investigation revealed the object to be a coating from a dummy solar panel which had been left on this frame to provide shear strength during shipment and manipulation. It was at first feared, however, that it was the panel itself and might fall on the IR simulator lamps which are directly below when the lamps are in the deployed position. If the panel had fallen on the lamps it could have broken one and possibly caused an electrical short. During the period which it was thought the hanging object was a panel the IR lamps were kept in their retracted position, out of possible harm. This resulted in changes in the test sequences to run the test points first which did not require lamp deployment. The coating fell to the chamber floor during this period and the nature of the hanging object was discovered. The test was continued with the only impact being the change in test sequence.

2. During the first radiator test points it was noted the R-21 return temperature was higher than expected. $43 \pm 5°F$ was expected and $61.4°F$ was experienced. This temperature represented the coolant return to the payload thermal control system and temperatures around $43°F$ could be required for condensing dehumidifiers in life support systems. It had been planned to operate the R-12 system at a baseline of $100°F$ inlet to the radiators controlling the R-12 return to the contact heat exchanger to $38 \pm 5°F$ which was thought to be the correct temperature to return the R-21 at $43 \pm 5°F$. Other

parameters affect this, however, other than the contact heat exchanger performance, such as the R-12, flowrate which was low. In order to achieve the necessary heat rejection to return 43°F at 105°F in on the R-21 side of the heat exchanger with R-21 flow of 2440 lbm/hr requires a heat rejection of (2440 lbm/hr)(.25 BTU/lbm-°F)(105 - 43°F) = 37,820 BTU/hr. At an R-12 inlet to the radiators of 101.5°F and a return of 36°F, the heat rejection was only (2050 lbm/hr)(.23 BTU/lbm-°F)(101.5 - 36.0)°F = 30,883 BTU/hr. The return could only be 54°F if the heat exchanger were 100% effective. The lower heat rejection resulted in part from the lower R-12 flow discussed previously. Analysis of the heat exchanger performance, however, did indicate a low effectiveness (.845 compared to design of .87) and a low contact conduction heat transfer coefficient. The following actions were taken to alleviate the problems during the first week's testing:

1. The R-12 control temperature was lowered to 25°F to attempt to lower the R-21 return to 40°F at the baseline 105°F R-21 inlet. This did not work, however, since it served only to lower the heat rejection from the radiators which was already too low to return 40°F at the R-21 flow of 2440 lbm/hr.

2. The R-21 flow was lowered to 2000 lbm/hr to equalize the heat capacities on both sides (ṁCp). This effectively lowered the R-21 outlet but not to the 40°F.

3. For the remainder of the week 1 testing the R-21 flow was left at 2440 lbm/hr and testing was concentrated on establishing the desired R-12 temperature. The R-21 temperatures were adjusted to give the desired R-12 inlet temperature to the radiators.

After the first week of testing the following actions were taken with regard to the contact heat exchanger:

1. For the second week's testing the R-21 flowrate was set to equalize the heat capacities (ṁCP). This set R-21 flow to approximately 0.92 of the R-12 flowrate. Equal ṁCp was assumed in the heat exchanger design.

2. An investigation was conducted into the heat exchanger design which revealed the design R-12 to R-21 temperature difference to be 10°F rather than the 5°F which was assumed

during the week 1 testing. The investigation also
revealed the Uc (contact heat conduction) was an order
of magnitude lower during week 1 testing than the design
value (69.7 BTU/hr-ft-°F compared to design 800 BTU/hr-
ft-°F). As a result of these analyses the contact heat
exchanger was disassembled, the Dow corning 380 thermally
conductive grease removed, and General Electric 641 in-
sulgrease applied. The GE 641 grease indicated better
performance in Vought element tests. The DC 380 had been
installed at the manufacturer.

During subsequent testing the heat exchanger performed at the design temperature
differences (10°F) and at overall efficiencies of 0.89 compared to design value
of 0.87. Preliminary analysis indicates the contact conductance was improved
to 114.4 BTU/hr-ft-°F which is still considerably below the design value of 800.
This, however, did not affect the overall performance of the heat exchangers.

3. The variable frequency/variable voltage compressor power source
is controlled by the speed of a vari-drive electric motor. A small electric
motor was connected to a chain drive which was in turn connected to the vari-
drive speed control. The small motor was remotely operated from the SHRM con-
troller console thus providing regulation of power frequency and subsequently
compressor speed during the refrigeration testing. During TP-16 (a variation
in heat load test requiring compressor speed control) a failure of the drive
sprocket on the vari-drive speed control occurred. The unit was repaired;
however, there was approximately a 2 hour delay before TP-16 could be restarted.
No futher problems with speed control were observed during the remainder of
the testing.

4. As was shown in Figure 4, SV4 is used to isolate the system from
the metal bellows accumulator. As discussed earlier, this accumulator is
sized to provide system pressure when operating in the pumped liquid mode and
is isolated during the refrigeration mode. SV4, as discussed previously, is
a solenoid, latching valve which was given to Vought on consignment from
Carleton Controls for use in this test. In the third day of testing the valve
indicator failed to indicate the true valve position. This indication is
used as an input to the controller and produces an error signal if indicating
closed while the system is in the pumped fluid mode. This error signal prevents

42

the liquid pump from starting. In a subsequent mode switch the valve failed to respond to a command to open, but finally opened upon repeated cycling. When in the pumped liquid mode the valve position is easily determined by monitoring the system pressure. If the system pressure rises with GN_2 pressure on the accumulator the valve is open. The cycling of the valve caused a reduction of power to the controller and set erronous valve positions in some of the other valves. When the valve was closed for refrigeration operation, leakage through the valve was evidenced by changes in the amount of liquid present in the accumulator. The following actions were taken regarding SV4:

1. The controller logic which prevented pump operation with SV4 indicating closed was bypassed electrically to enable pumped liquid operation with a failed indicator.

2. The timeline was modified such that the pumped liquid test points were to be run first so the system would not be operated in the refrigeration mode with a leaking valve which could vary the Freon charge.

3. Later, when other considerations forced a return to the refrigeration mode, SV4 was left open and the charge kept constant by maintaining the liquid level in the accumulator through variation of the GN_2 pressure on the accumulator. SV4 control was not operated for the remainder of the first week's test to prevent further controller difficulties.

4. Between week 1 and week 2 tests SV4 was replaced with a pneumatically operated Nupro valve similar to the rest of the remotely operated valves described previously, and this new valve operated normally for the whole second week's testing. No further difficulties with the controller were experienced.

5. During a switch in R-12 control points to set up TP46 the pump's 5 amp breaker switch tripped. The switch could be reset and the pump started but either the breaker tripped immediately or the pump ran nominally for about

15 seconds then the breaker tripped. An ampmeter indicated a sudden rise to 7 amps at the time of the breaker trip. The pump vendor, Sunstrand, was contacted and could provide no solution. The test sequence was changed to return to the refrigeration mode and run those test points while the pump problem was being studied. Upon completion of the refrigeration test points the pump was tried again and found to be operating properly as before the failure. No further problem was experienced with the pump for the remainder of the 1st week's testing. The following action was taken between week 1 and week 2 tests:

1. An auxiliary gear pump was installed outside the chamber and plumbed in parallel to the in-chamber pump to insure operation in the pumped fluid mode in case the pump failed again.

2. In the period between the two weeks testing the pump was examined and back flushed to remove any possible contamination, none was found and the pump appeared to be good.

3. An examination indicated the wiring terminals on the flow module were blackened indicating possible arcing at these points. The terminals were removed and the pump wired directly to the power source.

4. Toward the end of the week between the two weeks testing the breaker trip phenomona appeared again and the cause was isolated to be a short in the wiring on the flow module where a wire leading to pump had been damaged. The wire was repaired and no further trouble was experienced during the second week's testing.

6. Upon return to pumped fluid operation after the pump had been restarted following the failure a decrease in liquid quantity in the accumulator was noted indicating leakage from the system. The test was continued with no impact and the leakage made up by periodically refilling the metal bellows accumulator from the auxiliary accumulator external to the chamber. Between the two weeks testing the following action was taken with respect to the leak:

1. The leak was found to be from panel 1 inlet
   manifold at the point where the frame attach-
   ment bracket was welded on. It was concluded
   from a subsequent investigation and examina-
   tion that the damage was caused by differen-
   tial thermal expansion between the panel and
   the frame.

2. The leak was repaired by rewelding the bracket
   on the manifold. The attachment brackets bolt
   holes were enlarged and the attachment bolts
   loosened on all the attachment points to pre-
   vent any damage during the second week testing.
   No further differential thermal expansion damage
   was experienced.

4.1.3   Period Between Week 1 and Week 2 Test Hardware Problems

The weeks period between the two weeks testing was used to take action
on the problems discovered during the 1st weeks testing as was discussed in
the previous paragraphs. In addition, the following new hardware problems
were incurred during this period:

1. The flex lines connecting the flow module and
   the radiator panels were observed to be damaged
   although not leaking.

2. The refrigeration system Heli-rotor compressor
   failed.

3. The belt on the vari-drive motor which powered
   the compressor power generator broke.

4. A welded T-joint used to splice in the auxiliary
   pump indicated pin hole leakage.

1. During the refurbishment operations it was noted that the Teflon
lining of the 1-1/8 in. flex hose which connected the flow module and the radia-
tor panels was badly deformed on the inside. The damage appeared to have been
caused by evacuation of these lines in servicing the system with R-12. Although
no leakage was observed it was feared that further vacuum inside these lines
would result in leakage. New hoses of 1-in. diameter were obtained and exposed

45

to vacuum on the inside. Since they suffered no apparent damage they were installed in place of the 1-1/8 in. diameter hoses previously used. No leakage was experienced from these hoses in subsequent operations or in the second week of testing.

2. After refurbishment of the system was completed, ambient operation was being conducted as a checkout and to readjust one of the expansion valves to a new, +10°F, evaporator temperature setting. While this adjustment was being made the refrigeration system, including the compressor, was operating normally. The compressor was shut-down for switch to the 35°F evaporator expansion valve operation. At this time the compressor would not restart. The amperage and voltage readings indicated a locked rotor condition. The compressor was removed and partially disassembled and the failure was found to be due to a broken bearing race, the pieces from which had been ingested into the rotors and resulted in a locked condition. The compressor manufacturer was contacted and reported that the unit could not be repaired in time to support the second weeks testing. An identical unit was available and was obtained. The replacement compressor was received 3 November 1975 instead of the expected 1 November and a subsequent slip in pumpdown preops from 12 AM – 3 November to 12 noon was necessary to accommodate the installation of the compressor. The new compressor was installed and operated normally for the remainder of the testing.

3. During the checkout of the new compressor the belt on the vari-drive which drives the compressor power generator broke. This piece of hardware is external to the chamber and it was decided to support pumpdown with the then current level of checkout. A new belt was located at Vought – Dallas and shipped by plane to Houston where it was received by 10 PM and subsequently installed prior to pumpdown. Pumpdown had been delayed due to a R-12 leak discussed later. The vari-drive operated nominally for the remainder of the test.

4. During final inspection prior to pumpdown a pin hole leak was observed in a weld joint on the flow module. The leak was in a T-fitting used to connect the auxiliary gear pump discussed previously. Vought recommended acceptance of the slight leak since it was apparently due to a porous weld and not likely to worsen. The decision was made by NASA/JSC to fix the leak since it would still be possible to accomplish the entire planned testing

in the remaining time available. Pumpdown was slipped to 12 AM 4 November and the leak repaired. The system was evacuated and recharged and pumpdown began at 12 AM.

4.1.4   Week 2 Thermal Vacuum Test Hardware Problems

The only two hardware problems which occurred during the second week of testing were:

1. Flow stoppage to panel 4 during low load testing.

2. Leakage from flex line which connected panel 3 outlet manifold line to the fluid swivel between panel 2 and 3.

1. During the first low load test point (pumped liquid mode) flow was decreased by the radiator control valve to the radiator panels to lower the heat rejection as inlet temperature was decreased. The flow is bypassed around the radiator in order to return 35°F R-12 at the mixed outlet of the control valve. The test plan was to decrease inlet temperature until the coldest temperatures on the panels are close to -210°F, the freezing point of R-21. At a relatively high load the flow apparently stopped at panel 4 and it soaked to below -210°F very quickly. Inlet temperature was increased to 105°F and flow to panel 4 re-established. When the inlet was decreased to 75°, however, panels 1, 2 and 3 appeared to stabilize but panel 4 temperatures continued to decrease indicating flow had stopped to this panel. The decision was made to run the low load test based on panel 3 temperatures and let panel 4 soak out at no flow. This was done and test points 114 and 115 taken based on this criteria. It is felt that the panel 4 flow anomaly was not caused by a new system malfunction, but was the natural behavior of the system which had lower flow in panel 4 at higher load, as discussed previously in this section. No fix could be made to this problem during the test, however, the problem will be considered in future design of parallel panel systems.

2. After test point 115 was completed the plan called for retraction of the panels to a 50% deployed position for another set of low load points. Prior to the retraction, panel 4 was warmed to above the R-12 freezing point of -252°F by turning on the IR lamps. During the retraction a severe leak developed which was visible in the chamber between panels 2 and 3 in the area

47

of the outlet line swivel. When the panels were returned to the deployed position the leak stopped or at least decreased to where it was not detectable visually or by changes in the level of liquid in the accumulator (less than 1 lb/hr). Each time the deployment device was retracted the leak occurred and worsened upon full retraction. The panels were deployed and the leak stopped. Since all the remaining testing was to be conducted at partially deployed positions and leakage into the chamber at these rates was not acceptable to JSC, the test was terminated at that time.

Examination of the test article after repressurization revealed that the leak was from the 5/8" flex hose which connects the outlet manifold of panel 3 to the swivel between panels 2 and 3. The nature of the damage to this flex line was a crease indentation appearing to be caused by twisting of the flex line. There was no leakage from the swivel and it turned freely at ambient temperature after repressurization. The characteristics of the flex line failure indicated that when the mechanism was retracted the swivel did not rotate thus putting the rotational torque on the flex line causing it to twist and rupture. There were four possible causes considered in a failure investigation after the test:

1. Frozen R-12 prevented the swivel from turning.
2. A differential thermal expansion problem caused by temperatures below $-200°F$ at which the swivel was acceptance tested caused seizing.
3. A side load force caused binding.
4. Frozen refrigerant oil outside the seal between the shaft and body prevented the swivel from rotating.

A detailed examination of the swivel temperature test data indicated it was $-225°F$ at the time of retraction which is well above the $-252°F$ freezing point of R-12. An analysis of the swivel clearances and the metal coefficient of thermal expansion indicated a temperature difference of over $100°F$ between the shaft and body would be necessary to cause a locked condition. This was judged to be very unlikely. The swivel attachment was deliberately designed using flex hoses to prevent any side load from occurring since the swivel was not designed to maintain no leakage with a side load. Any side load force on the shaft would have to be transmitted through the flex line and it is unlikely

48

that enough force could be transmitted to cause a locked swivel. The R-12 used in the test contained about 4% Sunisco 3GS refrigerant oil to provide for compressor lubrication when the system operates in the refrigeration mode. This oil is infinitely soluable in liquid R-12 at any temperature and since a hard liquid system was maintained during the pumped liquid portion of the testing no residual pockets of oil would be expected in the pressurized portion of the swivel. If there had been leakage across the seal as there would have been had a side load been inadvertently placed on the swivel during test preparation then liquid R-12 containing the oil could pass into the close tolerance area between the shaft and body. The R-12 would evaporate leaving a residue of oil in this area. The freezing point of the oil was found to be -45°F indicating any residue present would have been frozen at the time of retraction. An examination of one of the returned swivels (not the one which failed) revealed the presence of some oil on the shaft outside the seal. The swivel in question, S/N 2, was installed in the acceptance test fixture in the as removed condition and the rotational torque measured as temperature was reduced to attempt to simulate the failure conditions. The swivel turned freely at 5 in/lb of torque until a temperature of -50°F was reached. At this temperature the swivel would not rotate with up to 150 in/lb torque. When the temperature was gradually increased again the swivel again began to rotate at -40°F. The swivel was then disassembled and found to indeed have a thick film of oil on the shaft outside the seal. To confirm these results the swivel was cleaned, new seals installed and retested. The results showed a freely turning swivel at 8 in/lb torque at temperatures as low as -200°F. It was concluded from these tests that the frozen oil outside the seal caused the swivel seizure and subsequent line rupture.

4.2   SYSTEM TEST RESULTS

4.2.1   Steady State Performance

4.2.1.1   Maximum Performance Maps

        System performance of the SHRM included mapping of the steady state maximum performance of the system in both the radiator and refrigeration modes over a range of environmental flux for different coolant return temperatures. In addition, system tests were conducted to determine the characteristics of the heat rejection system during a mode change precipitated by either changes in heat load or environmental flux.

        The maximum system heat rejection at R-12 return temperatures of approximately 35° and 15°F is shown in Figure 13 as a function of environmental flux. The radiator operation line defines the maximum heat rejection which can be achieved over the environment range by the system operating in the radiator mode and continuously returning 35°F R-12 to the contact heat exchanger. At a given point on the line, should the heat load (R-12 delivery temperature) or the environmental flux be increased this would cause the R-12 return temperature to exceed the desired 35°F return. Obviously, should a higher return temperature be allowed, higher heat rejections could be obtained. Thus, the system capacity described in this Figure represents the maximum heat rejection only for the given return temperature (35°F). The refrigeration operational line of similar nature is also shown in Figure 13. As can be seen in the figure the refrigeration heat rejection changes less with increases in heat flux than does the radiator. This is due to the characteristics of the closed cycle vapor compression system. As the environmental flux increases there is a subsequent increase in the condensing temperature in the radiator panels. The higher radiator panel temperature results in higher emissive power (σT^4) which offsets, in part, the increase in absorbed heat flux as environmental flux is increased. The constant return temperature is achieved by evaporating the liquid at a 35°F saturation pressure for R-12 by means of the constant pressure expansion valve. The increase in panel temperature with environmental flux does not occur in radiator operation and heat rejection falls off more rapidly. The intersection of the two operation lines form ranges of operation for the system. Below and to the left of the radiator operation line radiator operation can meet the heat rejection
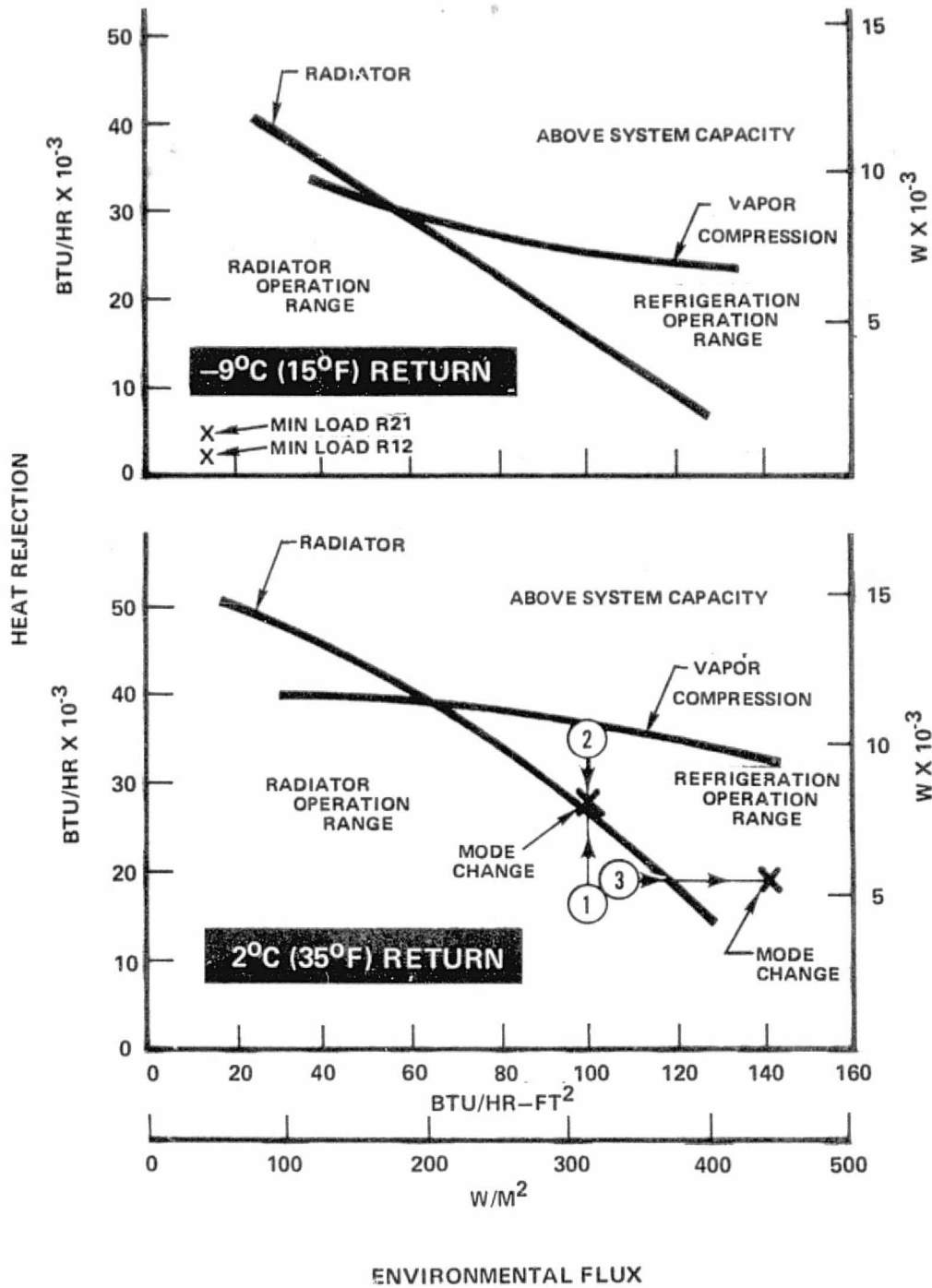
FIGURE 13   MAXIMUM SYSTEM HEAT REJECTION MAPS

and return temperature requirements. Although the refrigeration system could be used in this range for heat loads below the refrigeration operation line it would logically not be used because of the much higher power consumption. The region on the plot above and to the right of the radiator operation line but below the refrigeration line defines the region of operation in which the refrigeration system would logically be used. In this region the desired return temperature of 35°F can only be achieved by use of vapor compression. Heat rejections above both of the lines cannot be achieved with this system size and a 35°F return. The 15°F return temperature was evaluated during the second week. The results of this testing are also shown in Figure 13. Ranges of operation in both modes were well defined and the system operated satisfactorily in both modes. Also shown in Figure 13 is the low load data taken in the fully deployed position. It should be noted that these points are based on the first three panels only since the flow stopped in panel 4 at the outset of the low load test points. These were the only two low load points taken due to the ruptured flex hose terminating the test. The R-21 simulation test was based on no temperature falling below -210°F, the freezing point of R-21. The R-12 test was based on -252°F, the freezing point of R-12. As can be seen there is considerable heat load range even with the panels deployed. More heat load range could be obtained by retracting the panels until only one surface of panel 4 is exposed.

Figure 14 shows data from -10°F R-12 return temperature tests of the first week similar to that given in Figure 13 for 35° and 15°F. While the radiator operation curve was defined sufficiently, only one point on the refrigeration curve was obtained. At environments above 80 BTU/hr-ft^2 the compressor discharge overheated (> 300°F) and testing at these conditions was terminated. Since refrigeration system operation in the radiator operation range is not logical, no further refrigeration testing was conducted at the -5°F return temperature. With this system and compressor there is no refrigeration operation range for the -10°F return temperature. As a result of these tests the 15°F return was selected for evaluating in the second week.
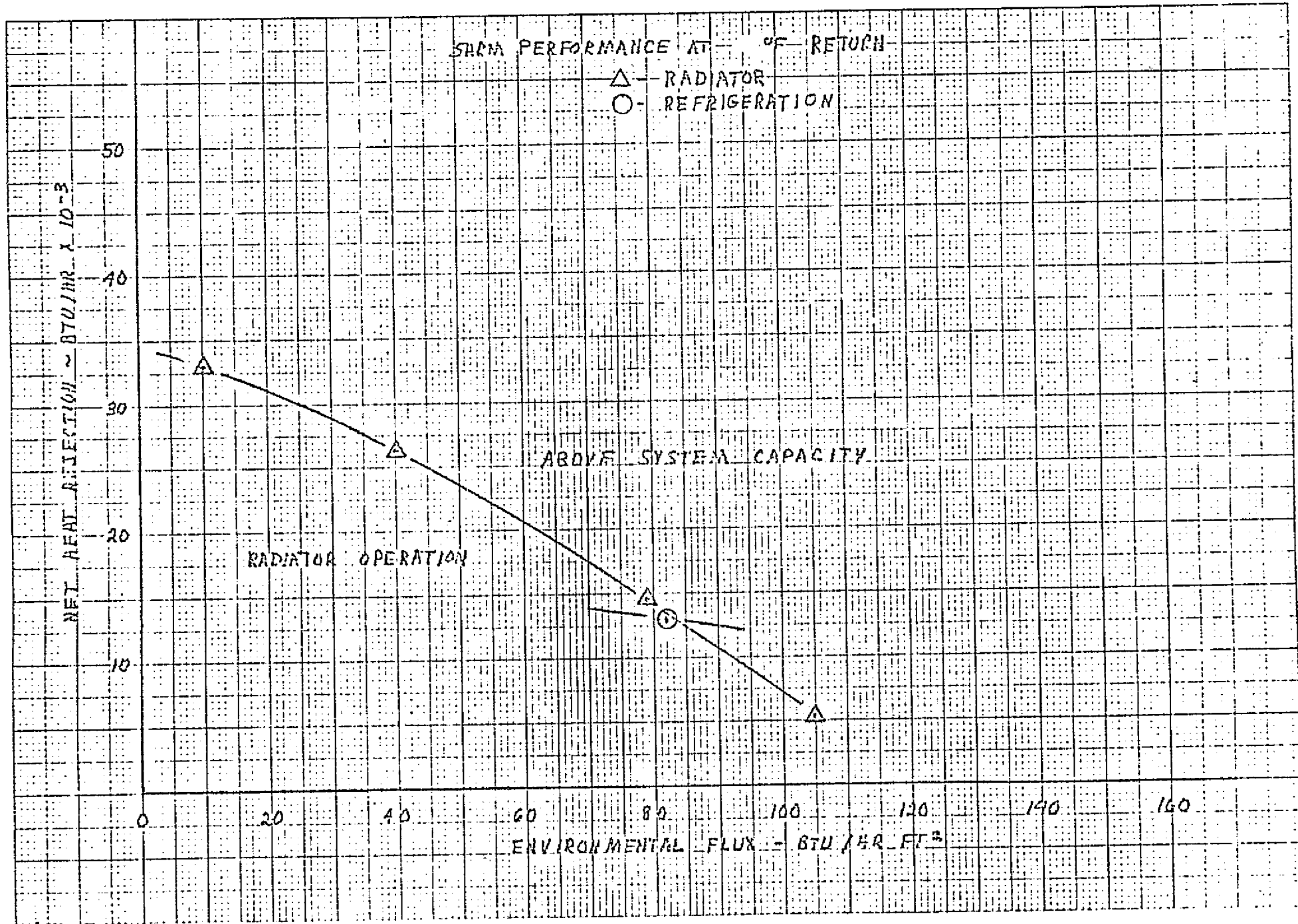
FIGURE 14 HEAT REJECTION MAP AT -10°F R-12 RETURN TEMPERATURE

4.2.2   Mode Switching

As discussed in Section 2.0 of this report, it is necessary to remove liquid R-12 in an amount equal to about 2/3 the system volume from the flow system in order to switch from pumped liquid to vapor compression mode operation and return it to switch back. During the time this transfer is being accomplished neither the pump or compressor is operating and therefore the only source of cooling is the thermal capacitance of the payload thermal control system. It is obviously desirable to minimize the switching time to the greatest extent possible. The mode switching tests were designed to evaluate the feasibility of mode switching and to evaluate the techniques developed for accomplishing the switching. No attempt was made to simulate the thermal capacitance of a payload thermal control loop in these tests.

Three mode change test points were taken. All of these were at a 2°C (35°F) return temperature. The first mode change test point was a mode change initiated by an increase in heat load. Referring again to Figure 13 at the circled 1, the heat load was increased at a constant 312 W/m^2 (100 ETU/hr-ft^2) environment to move into the refrigeration operation mode. The electronic controller is designed to initiate a mode switch from radiator to refrigeration operation when the return temperature of the R-21 side of the contact heat exchanger reaches 6°C (43°F), indicating loss of return temperature control due to the increased heat load (inlet temperature). The automatic mode change was initiated by the controller as planned and was successfully accomplished. The results are shown in Figure 15 . During the period where no heat rejection was being effected the R-21 to the payload thermal control system increased to 87°F. The loss of control, however, encompassed a period of only 6 minutes and this was judged to be satisfactory for payload thermal control. The period and extent of control loss could have been improved with a more efficient accumulator such as a larger metal bellows device and with simulation of the thermal capacitance of a payload thermal control system.

The second mode switch was the opposite of the first, a switch from refrigeration to radiator. The heat load starting at the circled 2 on Figure 13 was reduced and a switchover was initiated at the previous
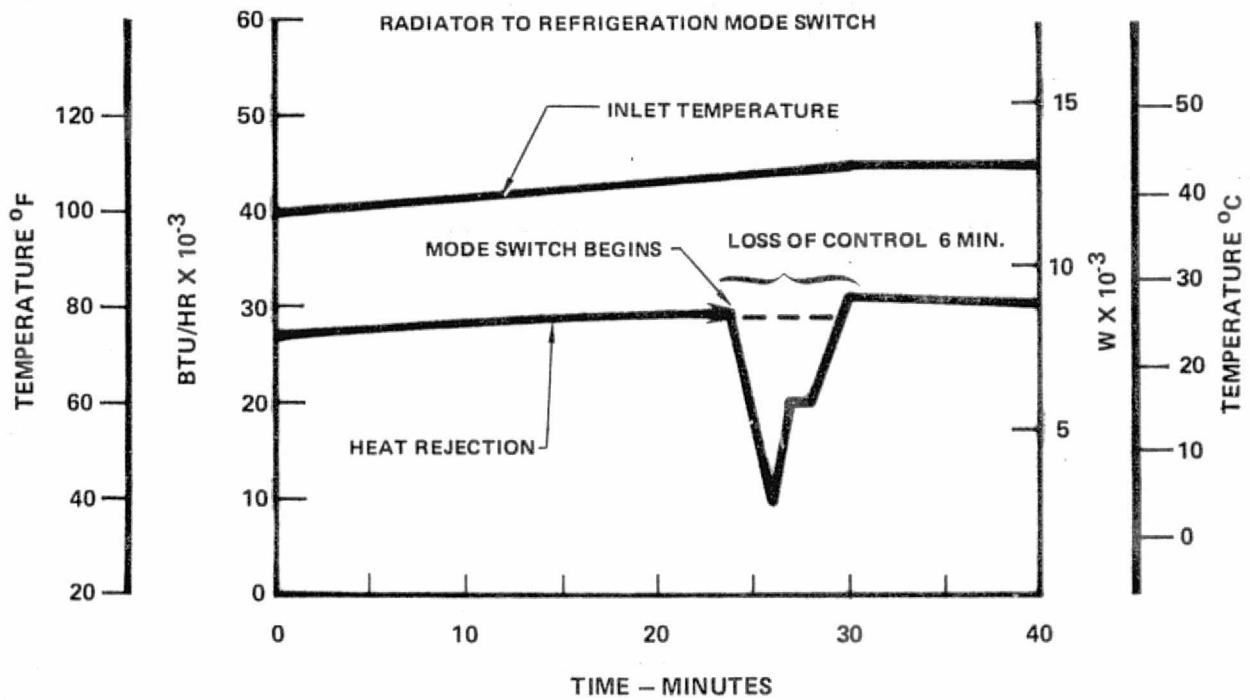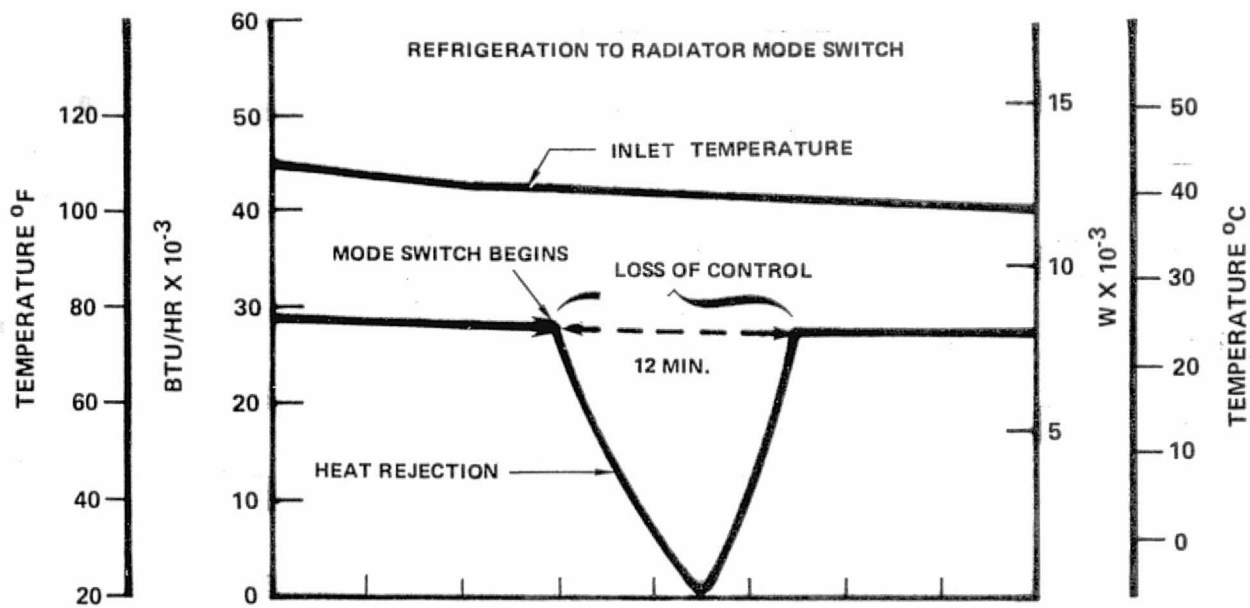
MODE SWITCH CHARACTERISTICS

FIGURE 15

switchover point heat load. The results of this test are also shown in Figure 15. As can be seen, the switchover was successfully achieved with a maximum R-21 return of 101°F. Return temperature control was lost for a period of 12-1/2 minutes. Again this was judged to be adequate but improvable.

The third switchover was a radiator-to-refrigerator initiated by an increase in environment. This is shown on Figure 13 starting at the circled 3. As can be seen, operation was well within the refrigeration operation range before the switchover occurred. The reason for this was a lag in the time for the increase in the environment to cause an increase in return temperature due to the thermal capacity of the radiator panels. The automatic controller initiated switchover at the proper temperature and the results were almost identical to the previous radiator-to-refrigeration switch shown in Figure 15 with loss of control to 75°F maximum for a 6 minute period.

4.2.1.2   Steady State Radiator System Performance

The pumped liquid radiator system effected heat rejection from the array of radiator panels as expected during the testing. There was some problem with flow distribution, as discussed previously, due to the complex manifolding system necessary to obtain parallel flow to the panels and to operate in the vapor compression mode. Steady state temperature maps of the panels for the steady state radiator test points are included in Figures A1 - A15 of Appendix A. An examination of these maps serve to illustrate the flow distribution. Lower panel temperatures are observed in the outer panels (panels 2, 3, and 4) indicating lower flow rates. Equal flow rates would have resulted in near equal temperature losses through each panel except for some slight differences due to lower inlet temperatures resulting from heat losses from the manifolds. The panel maps indicate increases in temperature loss moving outward from panel 1 to panel 4. However, since the total emmissive power of the radiators is approximately proportional to the fourth power of the average absolute temperature of the panel array which varies much less than the outlet temperature of each panel with differences in flow distribution, the system heat rejection is affected little by the flow distribution. Previous radiator testing of parallel and series banks of eight radiator

panels (Reference 7) have shown little dependence in total heat rejection with panel flow distribution. An examination of the tube outlet temperature distribution indicates normal flow distribution between the panel tubes. The distortion on the tube outlet temperatures at the edge of the panels is due to manifolds which are attached to the panels at these locations.

Figures A14 and A15 illustrate the panel temperatures at the two low load points discussed previously. These temperatures illustrate the flow stoppage in panel 4 since the temperatures are below the -252°F freezing point of R-12. The other three panels, however, indicate flow by temperatures above the freeze point and high temperature losses across the panel. The low load data taken, therefore, is indicated to be valid for a three panel fully deployed system. Note that for test point 114 illustrated in Figure A14 the lowest temperature on panels 1-3 are approximately -210°F, the freezing point of R-21 and similarly for test point 113 the lowest panel temperatures are as near to the -252°F freezing point of R-12 as possible. Thus the low load with both fluids was simulated using R-12.

4.2.1.3   Steady State Refrigeration System Performance

The array of radiator panels acted as condensers when the system was operating in the radiator mode. The panels effectively rejected heat during this phase of operation and no severe anomolies were noted. Panel temperature maps for the condensing radiators during steady state refrigeration operation are excluded in Appendix A, Figures A16 - A32. Characteristic operation of a condensing radiator panel is indicated by a high temperature at the inlet as the superheated vapor from the compressor enters which quickly cools to the saturation temperature at the condenser pressure as evidenced by a rigid temperature decrease at the panel inlet. A large portion of the radiator just downstream of the inlet remains at approximately a constant temperature as the vapor condenses. The panel temperatures here are slightly below saturation temperature at the condenser pressure due to the fluid to tube temperature loss. Near the outlet side of the panel the temperatures begin to decrease again as the liquid begins to subcool after condensation. The trend of the actual data was an described except that little or no subcooling was observed

from Panels 1 and 2 and considerable from Panels 3 and 4 indicating the first two panels may have been receiving more flow than the outer two. The data, however, also indicates the R-12 had lost most of its superheat by heat rejection from the manifolds which were attached to the panel edges prior to reaching Panel 3 and 4 inlets. This contributed to the greater amount of subcooling in Panels 3 and 4. The return from the four panel system indicated little or no subcooling during the first week of testing. One reason for this was thought to be that the inlet and outlet flex hoses which connected the panels to the flow module were bundled together inside the same insulation package which could have resulted in some regeneration between the hot condenser inlet and the outlet thus resulting in less subcooling. During the second week the lines were separated and approximately 5°F of subcooling was obtained at the 35°F evaporator and 10-15° at the 15°F evaporator temperature. Test point 107 was conducted at conditions identical to test point 18 to evaluate this change and indicated a 5°F subcooling from the panels compared to no subcooling for test point 18.

The refrigeration system steady state cycle performance was plotted on R-12 pressure enthalpy diagrams for illustration and evaluation. These plots are included in Appendix A, Figures A33 through A48. Approximate evaporator temperature and measured flowrate, environment and power are also given on each figure. The net cooling (heat rejection) of the system was calculated by two methods and both are included for comparison. The cooling was obtained from the change in temperature of the R-21 flow through the contact heat exchanger which simulated the payload thermal control system. A second value for cooling was obtained from the change in enthalpy of the R-12 flow through the contact heat exchanger (evaporator). The measurements indicated fair agreement with the cooling indicated by the R-21 generally lower than that indicated by the R-12 for the first week of testing and generally higher for the second week. Since the cooling calculations from the R-21 used fewer measurements (3) than the R-12 calculation (5) and were more consistant these were accepted as the system heat rejection. In addition it was felt the R-21 flow measurements were more accurate and the fluid was all R-21 where the R-12 contained at least 4% refrigerant oil which could affect the calculations somewhat.

The efficiency of refrigeration cycles is usually measured by the coefficient of performance (COP) which is defined as the cooling effect divided by the input power. The COP for the refrigeration steady state points was also calculated by two methods and both and included on the figures. The first method divided the cooling calculated from the R-21 temperature loss through the heat exchanger by the measured power input to the compressor. The second method ratioed the enthalpy changes of the R-12 across the evaporator and compressor illustrated in the P-h diagrams as obtained by pressure and temperature measurements. The COP for the nominal 35°F return temperature varied from 1.6 at the highest environment (155 BTU/hr-ft^2) to 2.8 at the lowest environment tested (42 BTU/hr-ft^2). As discussed previously the condensing pressure increases with the environment and as a result the theoretical vapor cycle COP also decreases with environment. The test results followed this expected trend. The cooling effect reported did not consider the waste heat from the electrical power source. If, for instance, Shuttle fuel cells were used to provide power to the compressor additional heat rejection is necessary for fuel cell cooling. This should not be directly subtracted from the cooling, however, since fuel cell waste heat is at a much higher temperature (approximately 175°F) than either the 35 or 15°F return temperatures and could use a pumped liquid system under nearly all conditions. Disregarding this difference in cooling temperature, however, and applying the Shuttle fuel cell thermal efficiency of 0.568 a COP greater than 0.76 can be shown to be necessary to obtain a net cooling effect considering fuel cell waste heat. Since all the COP values measured are at least double this value a significant net cooling effect was demonstrated even under the worst case condition of cooling the fuel cells at the low return temperatures.

4.2.3   Transient Performance

In actual operation a heat rejection device such as the SHRM is subjected to transient conditions during most of its operation life. Payload cooling requirements vary with the activity of the various equipment and experiments in the payload and the heat sink to

which the heat is rejection is a function of the orbital position for most orbits. For these reasons it is necessary to provide control techniques to insure the desired return temperature is maintained under heat load and environment transients.

In order to provide a test of the heat load control techniques employed in the SHRM operation in both modes five transient test points were conducted. Four of these were in the radiator mode and one in the refrigeration mode. As discussed earlier, control of the return temperature to the simulated payload thermal control R-21 loop was provided by control of the R-12 return to the contact heat exchanger. A flow control valve developed for use in the Shuttle radiator flow control assembly was employed for this purpose. In the refrigeration mode compressor speed was varied manually to adjust system capacity to the heat load.

Transient results of the four pumped liquid radiator transient points are given in Appendix A, Figures A49 through A59. The results at test point 4 are given in Figures A49 through A50. Test point 4 was a heat load ramp (R-21 inlet temperature) at a constant 83 BTU/hr-ft^2 environment with a 35°F return temperature. Figure A49 presents computer plots of the test data illustrating the total heat rejection, panel heat rejection, temperature changes across the contact heat exchanger, and environment. A flux adjustment was made near the end of the test point to increase the environment to the desired value. Continuous reviews of the flux were made and the levels adjusted as necessary. Figure A50 illustrates the inlet and outlet temperatures of the contact heat exchanger for both the R-21 and R-12 systems and the radiator panel inlet and outlet temperatures. The top curve illustrates the decrease in heat load and the control of the R-12 return temperature. The R-12 return was held constant throughout the transient by the flow control valve. The R-21 return varied somewhat, however, this was due to the contact heat exchanger performance which will be discussed later. Successful control was demonstrated during the transient. Figures A51 - A52 show the return increasing heat load transient of test

point 5 conducted at the same flux. Again temperature control was demonstrated throughout the transient. Figures A53 and A54 present the same data for test point 6 which was a cyclic variable environment at a constant heat load and a 35°F return temperature. The environment was cycled between 10 and 100 BTU/hr-ft^2 as shown in the lower plots on Figure A53. Figure A54 illustrates that the R-12 return temperature was maintained at a constant 33°F throughout the cycles again demonstrating successful control. Figures A55 and A56 present the results of test point 11, a cyclic environment at a constant heat load with a -5°F return temperature. This test point was included to demonstrate control at a second set point in addition to the 35°F. The environment was cycled between 10 and 40 BTU/hr-ft^2 as shown on Figure A55. Figure A56 shows that control was successfully demonstrated at the lower control temperature. The R-12 return to the contact heat exchanger was maintained at -5°F throughout the cycles. Figures A57 - A59 show the results of test point 16, the final transient test. This test was conducted in the refrigeration mode at a constant environment of 85 BTU/hr-ft^2 under a variable heat load which began at about 40,000 BTU/hr, decreased to 20,000 and returned to 40,000 in a two hour period. This was accomplished by ramping the R-21 inlet temperature to the contact heat exchanger from 105°F to 60°F in one hour and returning to 105°F in one hour. Figure A57 illustrates the resulting cycle in heat rejection as the heat load was reduced and the compressor speed reduced to adjust the system capacity. The results demonstrated a 2:1 heat load control range using this technique. Figure A58 illustrates the temperature ramp and the R-12 return to the heat exchanger which was held at a constant 33°F by the constant pressure expansion valve. The range of control of the R-21 return to the simulated payload thermal control system is also shown on this figure. The lower figure shows the wide range of compressor outlet (panel inlet) temperatures over the range of compressor speed operation. Figure A59 illustrates the compressor power, discharge and suction pressure variations during the transient. The power was reduced from 4910 watts to 660 watts over the range of control, thus maintaining high cycle

efficiency over the entire range. The 2 to 1 range demonstrated should be quite adequate for vapor compression system operation for payload thermal control.

4.3   Component Evaluation

An evaluation of several of the components can be made based on the test results. Specific components which were individually evaluated are the accumulator, contact heat exchanger, liquid pump, compressor and fluid swivels.

The metal bellows accumulator performed as expected during the entire test. The design was evaluated to be adequate for future use, however, the size was too small to service the system completely and an auxiliary tank external to the chamber was used. An accumulator design which does not have strict limits on ΔP across the bellows (100 psi expanded and 15 psi collapsed) would allow the use as a receiver also and remove the requirement for this component. Using the present accumulator design of adequate size should improve the mode change transition times significantly, especially the refrigeration to radiator change which took 12 minutes.

The contact heat exchanger performance is illustrated in Figure 16. The contact heat exchanger was designed for an efficiency of 0.865 and 800 BTU/hr-ft-°F as was discussed in Section 2.0. The results shown here illustrate the improvement between weeks 1 and 2 after the repacking of the device with new thermal grease as previously discussed. As is shown in Figure 11, with the proper flowrates to balance the $\dot{m}Cp$'s on both sides of the heat exchanger not only are good efficiencies obtained but also return temperatures of the R-21 are within the desired $40 \pm 5°F$. There is one possible area of improvement, contact conductance, which was calculated as 69.7 BTU/hr-ft-°F the first week and 114.4 BTU/hr-ft-°F the second week. Bringing this conductance up should provide even better performance. The results of the second week's testing indicated the concept of the heat exchanger is valid and suitable for use in the SHRM or other devices where a similar requirement exists.

Some redesign of the heat exchanger was indicated, however, to improve the ease with which the mechanical coupling of the two halves

63

R-12
2050 LBM/HR

$T_{out} = 101.5°F$ $T_{in} = 36.0°F$

R-12
749 LBM/HR

$T_{out} = 36°F$ $T_{in} = 36°F$

Week 1
Radiator   32,810 BTU/hr

Week 1
Refrigeration   33,620 BTU/hr

$T_{in} = 113.4°F$ $T_{out} = 61.9°F$

$T_{in} = 107.4°F$ $T_{out} = 51.3°F$

R-21
2440 LBM/HR

R-21
2435 LBM/HR
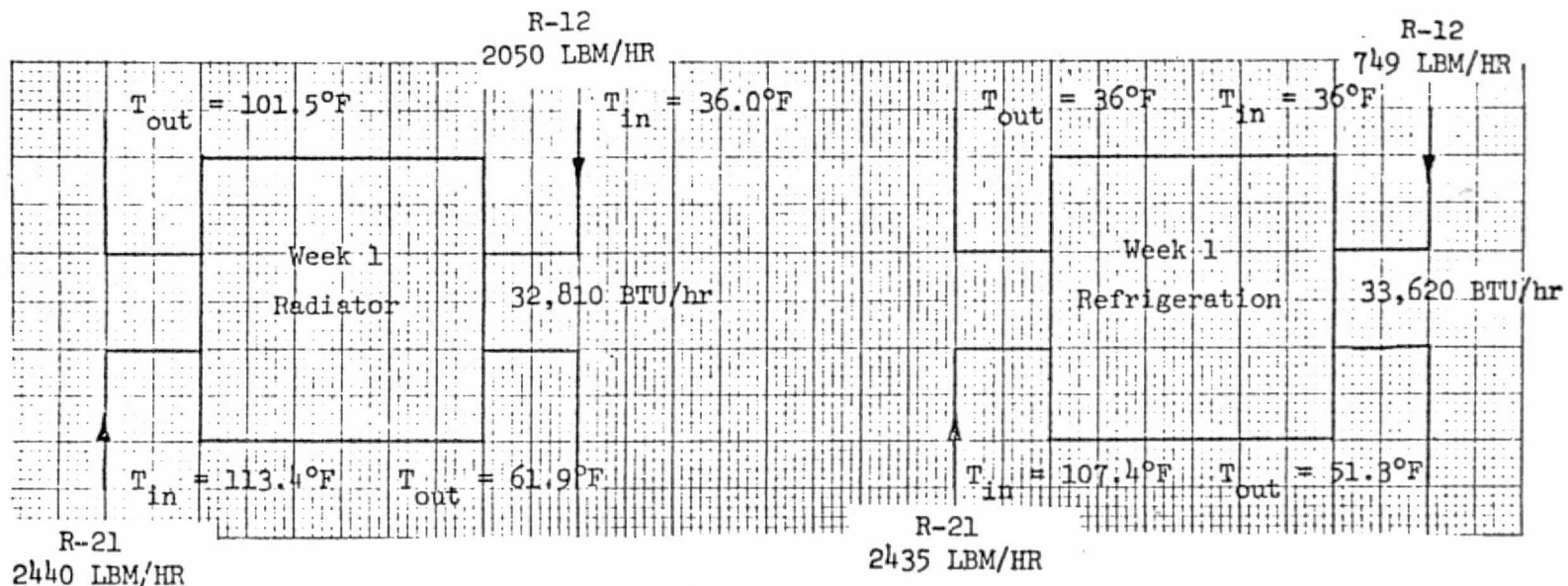
$$\eta = \frac{101.5 - 36}{113.4 - 36} = \underline{0.846}$$

Design η = 0.865

R-12
1900 LBM/HR

$T_{out} = 102.6°F$ $T_{in} = 36.9°F$

R-12
682 LBM/HR

$T_{out} = 56.7°F$ $T_{in} = 36.1°F$

Week 2
Radiator   33,210 BTU/hr

Week 2
Refrigeration   36,420 BTU/hr

$T_{in} = 110.7°F$ $T_{out} = 56.7°F$

$T_{in} = 101.1°F$ $T_{in} = 42.5°F$

R-21
2460 LBM/HR
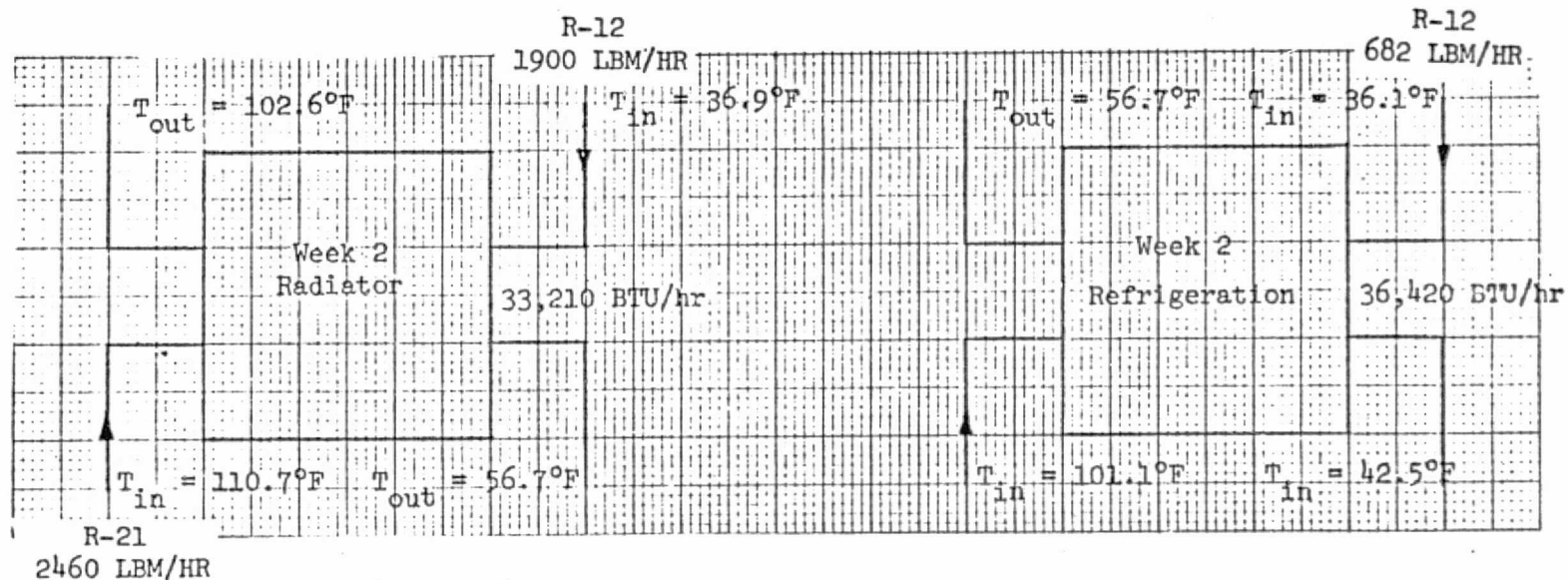
$$\eta = \frac{102.6 - 36.9}{110.7 - 36.9} = \underline{0.890}$$

FIGURE 16   CONTACT HEAT EXCHANGER PERFORMANCE

R-12
1916 LBM/HR

T_{out} = 102.6°F

T_{in} = 34.5°F

32,250 BTU/HR

T_{in} = 116.7°F T_{out} = 44.1°F

R-21
1777 LBM/HR

R-12
2567 LBM/HR

T_{out} = 85.9°F

T_{in} = 36°F

31,430 BTU/HR

T_{in} = 96.1°F T_{out} = 44.1°F

R-21
2448 LBM/HR
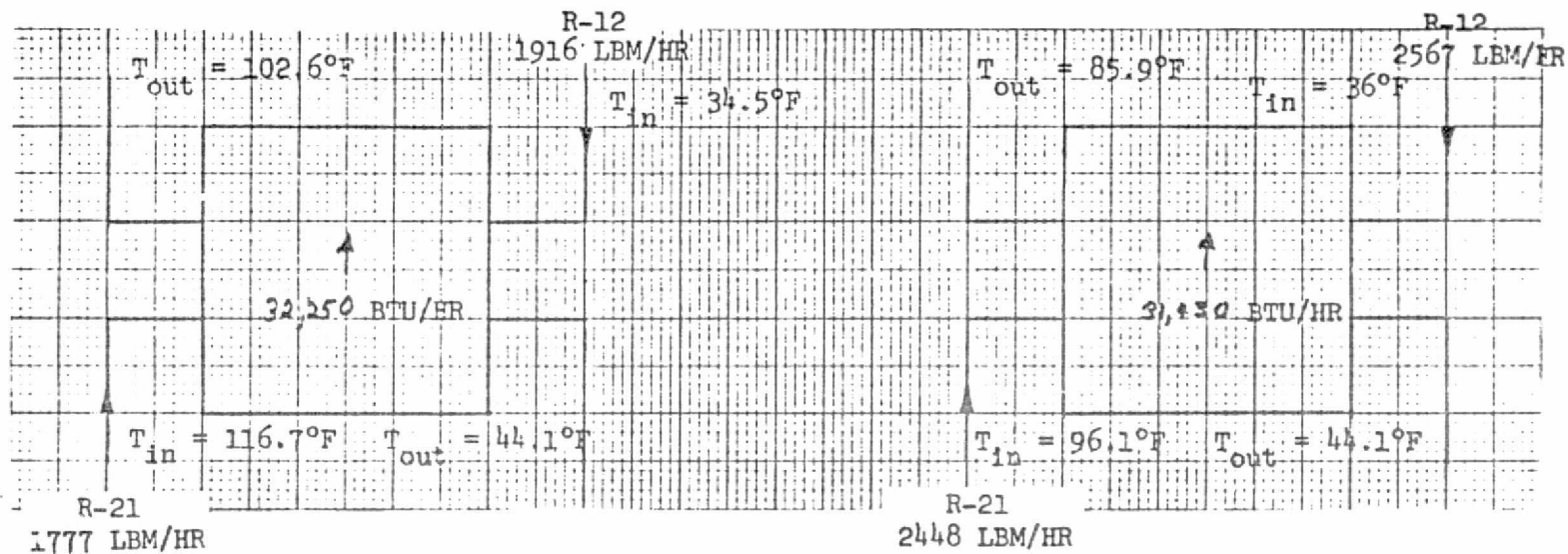
$$\eta = \frac{116.7 - 44.1}{116.7 - 34.5} = .883 \qquad\qquad \eta = \frac{96.1 - 44.1}{96.1 - 36.1} = .867$$

EQUAL ṁCp's

Design Uc   - 800 BTU/hr-ft-°F
Level 1 Test Uc - 69.7
Level 2 Test Uc - 111.4

FIGURE 16   CONTACT HEAT EXCHANGER PERFORMANCE (CONT'D)

can be performed. The experience between the two weeks of testing and a post test disassembly for inspection revealed that this particular design is difficult to mechanically disconnect and connect. Some suggestions for improvement are to increase the distance from the manifold which connects the plates to the mating surfaces and increase the gap sizes. This should allow the halves to mate more freely. In addition, improving the thermal grease to serve as a lubricant as well as a heat conduction path would greatly assist the assembly process. Both the Dow Corning 350 and the GE 641 were quite sticky and tacky when first applied to the surfaces and contributed to the friction in sliding the halves together and taking them apart.

Post-test examination of the GE 641 after the one week vacuum exposure and six months of ambient storage indicated no change in the spreading properties. The appearance and feel of the grease was similar to when it was first installed. No drying or flaking was present. This substance appeared to be acceptable for use in vacuum exposed devices if the assembly problem can be solved through changes in mechanical design.

The low flowrate from the liquid pump was discussed previously as well as the anomoly. Figure 17 illustrates the three data points which were obtained during the testing compared to the vendor supplied pump characteristic. This data indicates close to nominal performance for the pump. In order to achieve the higher flowrates which were desired it would be necessary to reduce the system flow resistance or secure a more powerful pump. The pump, however, was judged to have operated satisfactorily during the test and the design is suitable for future applications.

An indication of compressor performance is illustrated in Figure 18. Capacity and input power taken during both weeks of the test is compared to curves supplied by the compressor vendor. Also shown is the capacity of the compressor measured during the Phase I laboratory prototype test. The week 1 and week 2 data points represent two different units of the same design since, as discussed previously, the compressor

SPECIFICATION:
6 gpm (3898 LBM/HR R12 at 80°F)
30 psi
3000 hr. life

ΔP - PSI

FLOW - GPM

△ LTV HOUSTON TEST DATA
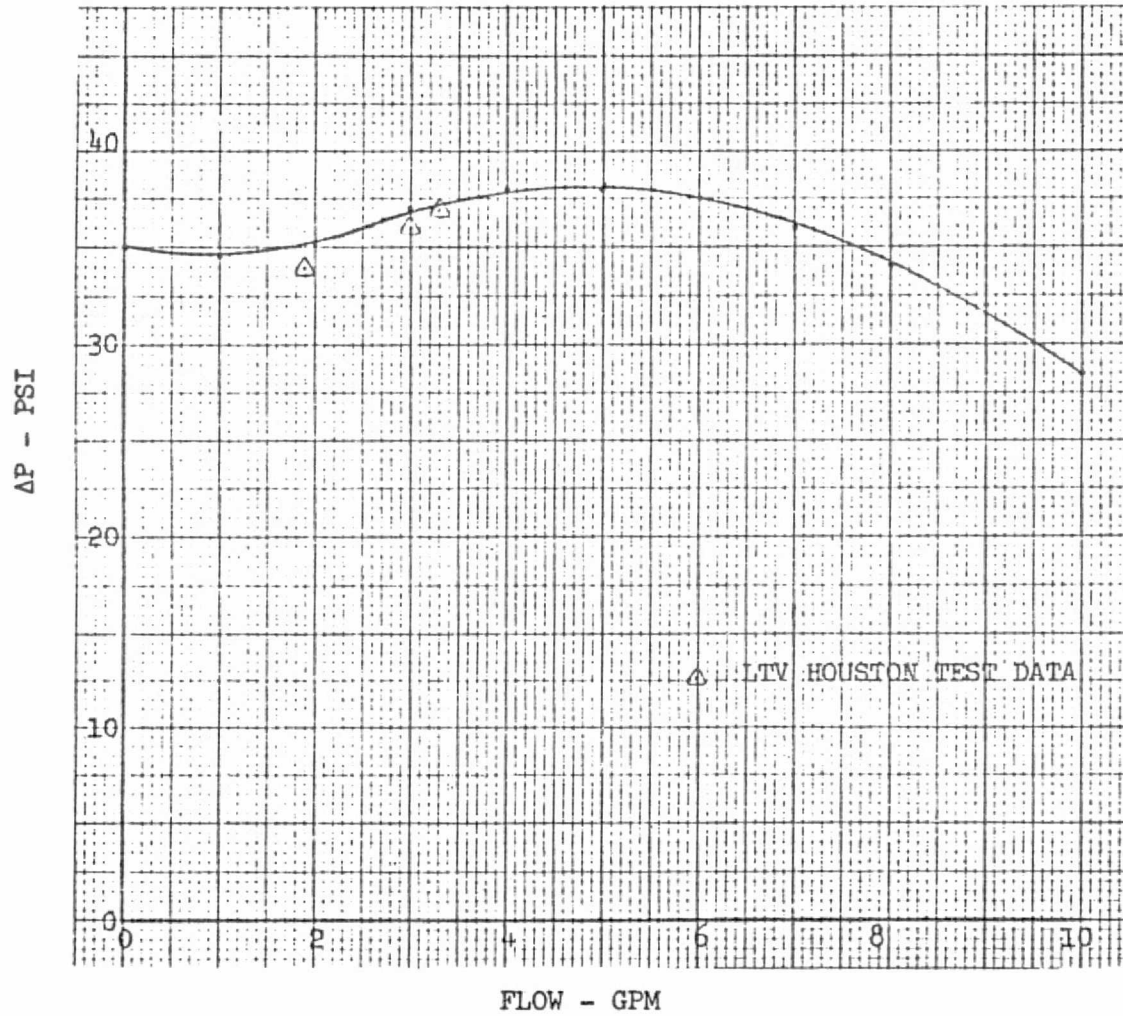
FIGURE 17   LIQUID PUMP EVALUATION
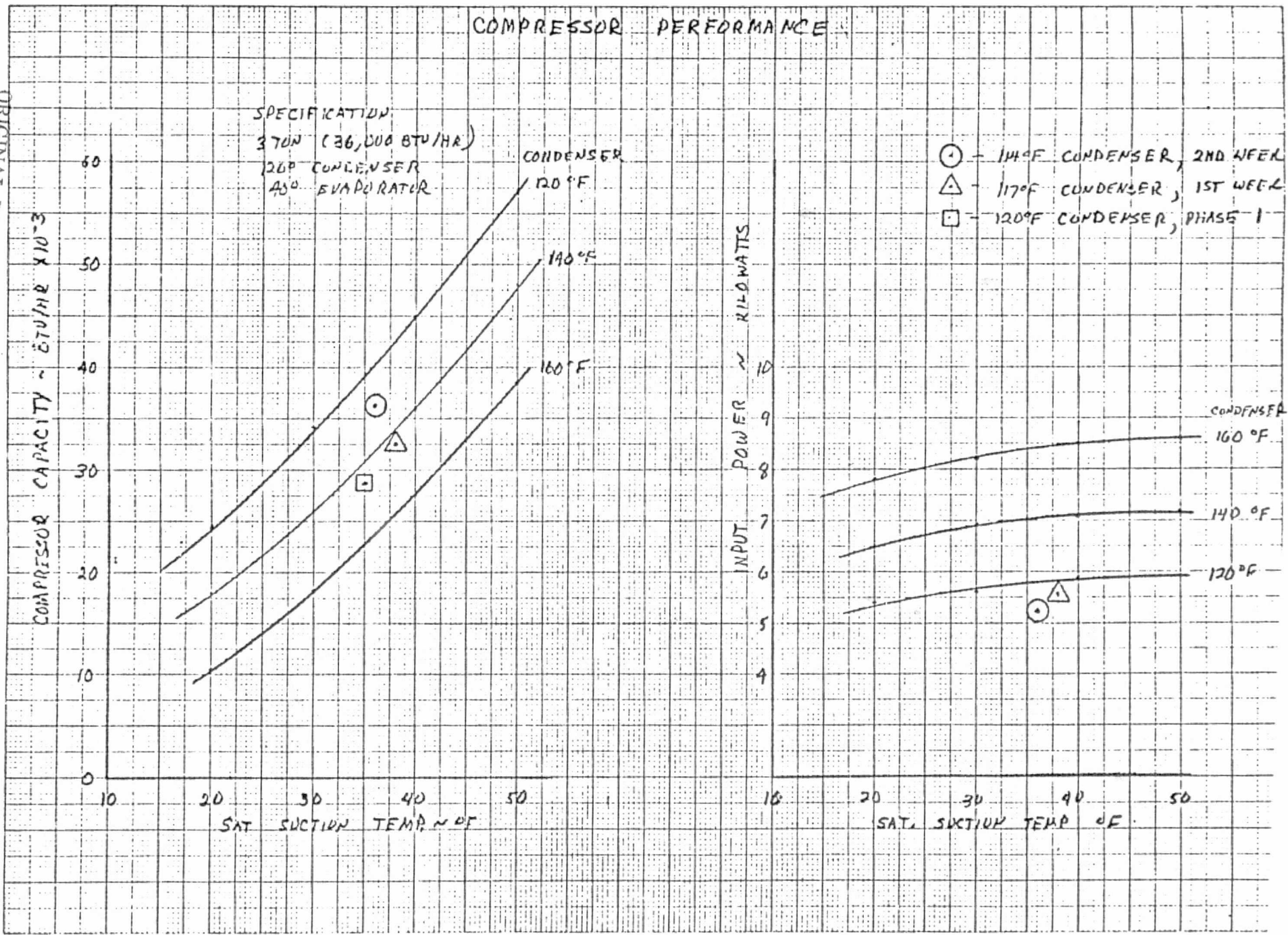
FIGURE 18 COMPRESSOR PERFORMANCE EVALUATION

was replaced between the two weeks of testing. As can be seen, the capacity was somewhat below the expected values, however, so was the input power at these conditions. The compressor did deliver about 35,000 BTU/hr net heat rejection and defined a refrigeration operation range in which the radiator system could not provide the desired conditions.

The fluid swivels performed nominally, with the exception of the cold retraction at the end of the test, throughout the test with no leakage detected. The failure of the swivel to turn was due to the frozen oil as discussed previously and is not judged to be a reflection on the swivel design. A possible fix to prevent a recurrence would be to move the seal as close to the Freon plenum as possible and to redesign the seal so that no leakage occurs due to side force or at low pressures. The swivel is judged to be completely acceptable for use with a pumped liquid system where no compressor oil is required. A compressor lubricant which freezes at a lower temperature is another possibility, however, none has been identified at this writing. Swivels for future deployable radiator systems should be designed to withstand both side and axial loads with no leakage and reasonable turning torque. Such a design would alleviate the necessity of flex lines or close tolerance alignment of the deployment fixtures.

5.0   CONCLUSIONS AND RECOMMENDATIONS

The test results demonstrated the feasibility of a full scale deployable radiator system and secured important technology for future deployable radiator systems. In addition a dual mode radiator/vapor compression feature was demonstrated for the first time. It was concluded that the scissor type ATM deployment mechanism is applicable to deployable radiators and that the vapor compression with a conventional aircraft compressor has sufficient efficiency to effect a net heat rejection effect at high environments while returning low temperature ($10°F$ and $35°F$) conditioned fluid to the payload thermal control system. The net heat rejection was significant even when considering waste heat of fuel cell power generation.

It is recommended that future dual mode designs contain an accumulator which will hold the necessary quantity of liquid for mode switching and can be used as a fluid receiver in vapor compression operation. It is further recommended that series flow connections of the panels be considered for the system to alleviate problems associated with obtaining the desired flow split between panels. Fluid swivels for future deployable radiators should be designed to withstand, with no leakage, both side and axial loads. If the swivels are to be used in a system containing refrigerant oil, the swivels must be designed to insure no oil deposits can occur in close tolerance areas where freezing of the oil will inhibit the proper operation of the swivel. Additionally care should be taken in future design to insure thermal expansion of radiator panels with respect to the deployment frame can be accommodated. The rapid transients in temperature during radiator panel operation, especially in the refrigeration mode in a dual mode system, can result in severe thermal expansion differences between the panel and the frame before sufficient heat is transferred to the frame to equalize the temperature.

The contact heat exchanger indicated good thermal performance, however, in future designs consideration should be given to ease of assembly recognizing that the characteristics of thermal conductive grease

provide no lubrication but rather contribute to the friction of large flat mating surfaces.

The results of the fabrication and testing of the prototype Self Contained Heat Rejection Module concluded that the state-of-the-art of a pumped liquid deployable radiator system is sufficiently advanced to proceed to design and fabrication of flight qualified systems with no further significant development effort. Some development will be required, however, for flight dual mode systems, in the problem areas discussed in this report and also in a high capacity, zero gravity compatible compressor and refrigeration system.

6.0 REFERENCES

1. "Development of a Self Contained Heat Rejection Module" (SHRM) – Phase I Final Report, Vought Report T211-RP-028, February 1976.

2. Williams, J. L.,et.al., "Development of A Direct Condensing Radiator for Use in A Spacecraft Vapor Compression Refrigeration System", ASME Technical Paper 73-ENAs-5, July 1973.

3. Tufte, R. J., "Wide Heat Load Range Space Radiator Development", ASME Paper 71-AV-5, July 1971.

4. Dietz, J. B., et.al., "Modular Radiator System Development For Shuttle and Advanced Spacecraft", ASME Paper 72-ENAv-34, August, 1972.

5. "SHRM Radiator Panel Installation", Vought Drawing 221-60056, January 1975.

6. "Self Contained Heat Rejection Module (SHRM) Test and OHRS Wide Cavity Test – Detailed Test Procedure and Test Rules", Test No. 55-A-75, October 1975.

7. Fleming, M. L., et.al., "Shuttle Active Thermal Control System Development Testing", ASME Paper 74-ENAs-43, July 1974.

APPENDIX A

TEST POINT 1A
DAY 294
TIME 11:00:27

Fe$_{12}$ Return
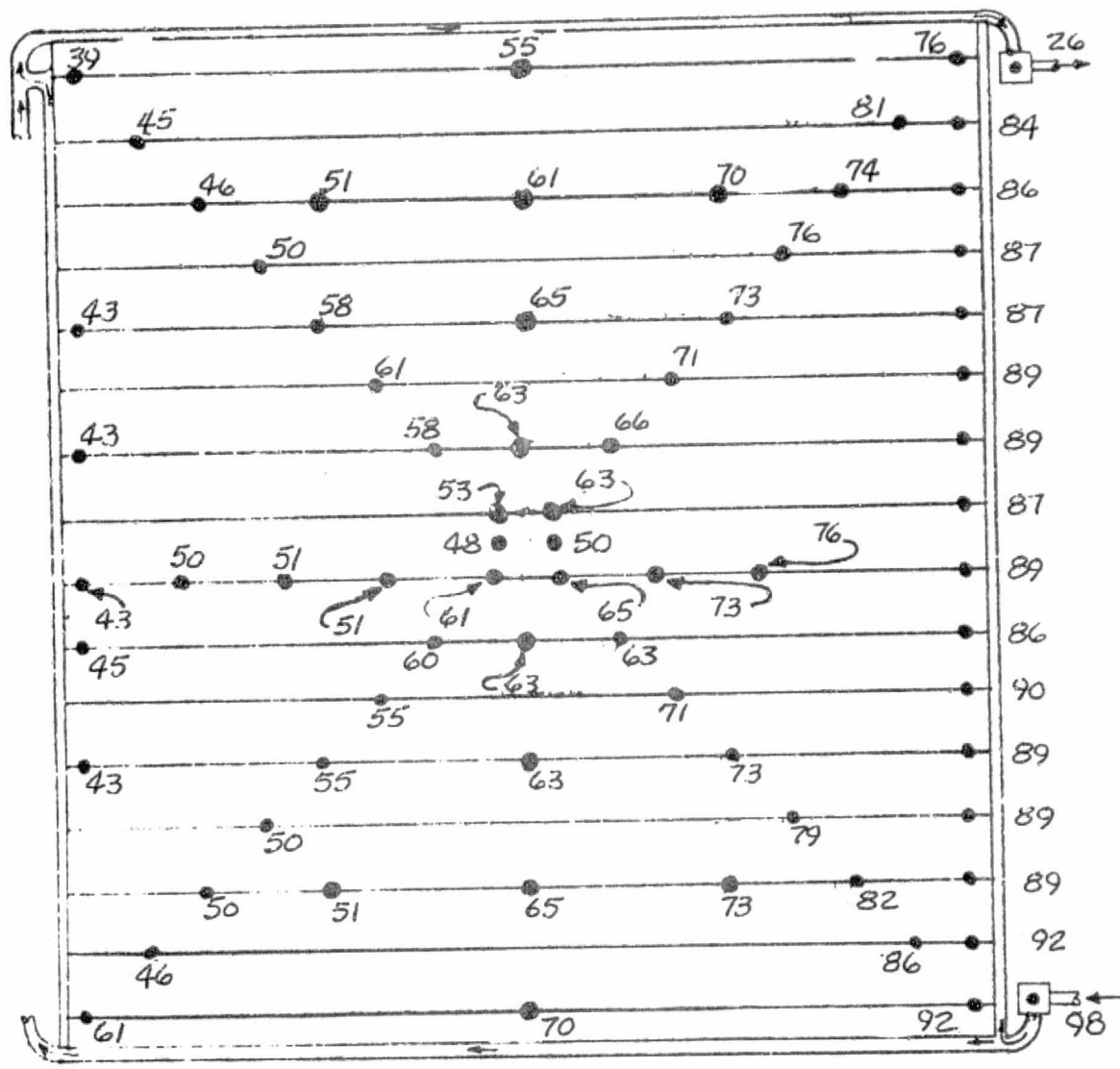
PANEL NO. 1

FIGURE A1

STEADY STATE LIQUID RADIATOR OPERATION PANEL TEMPERATURE MAPS

Fe$_{12}$ Supply

A-2

TEST POINT __IA__
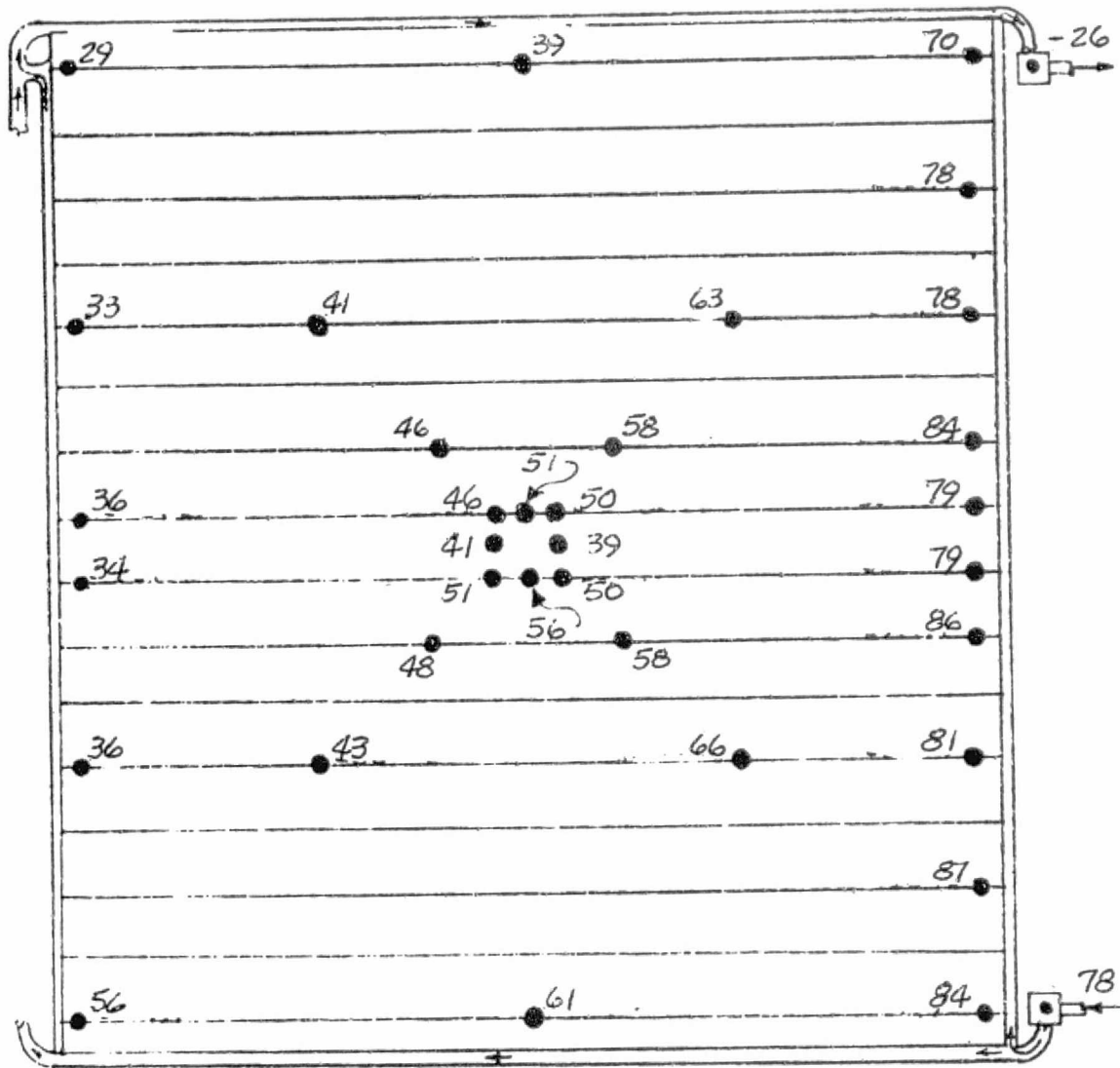
DAY __294__

TIME __11:00:17__

Fe$_{12}$ Return

PANEL NO. 2

FIGURE A1 (CONT'D)

A-3

TEST POINT _IA_

DAY _294_

TIME _11:00:17_
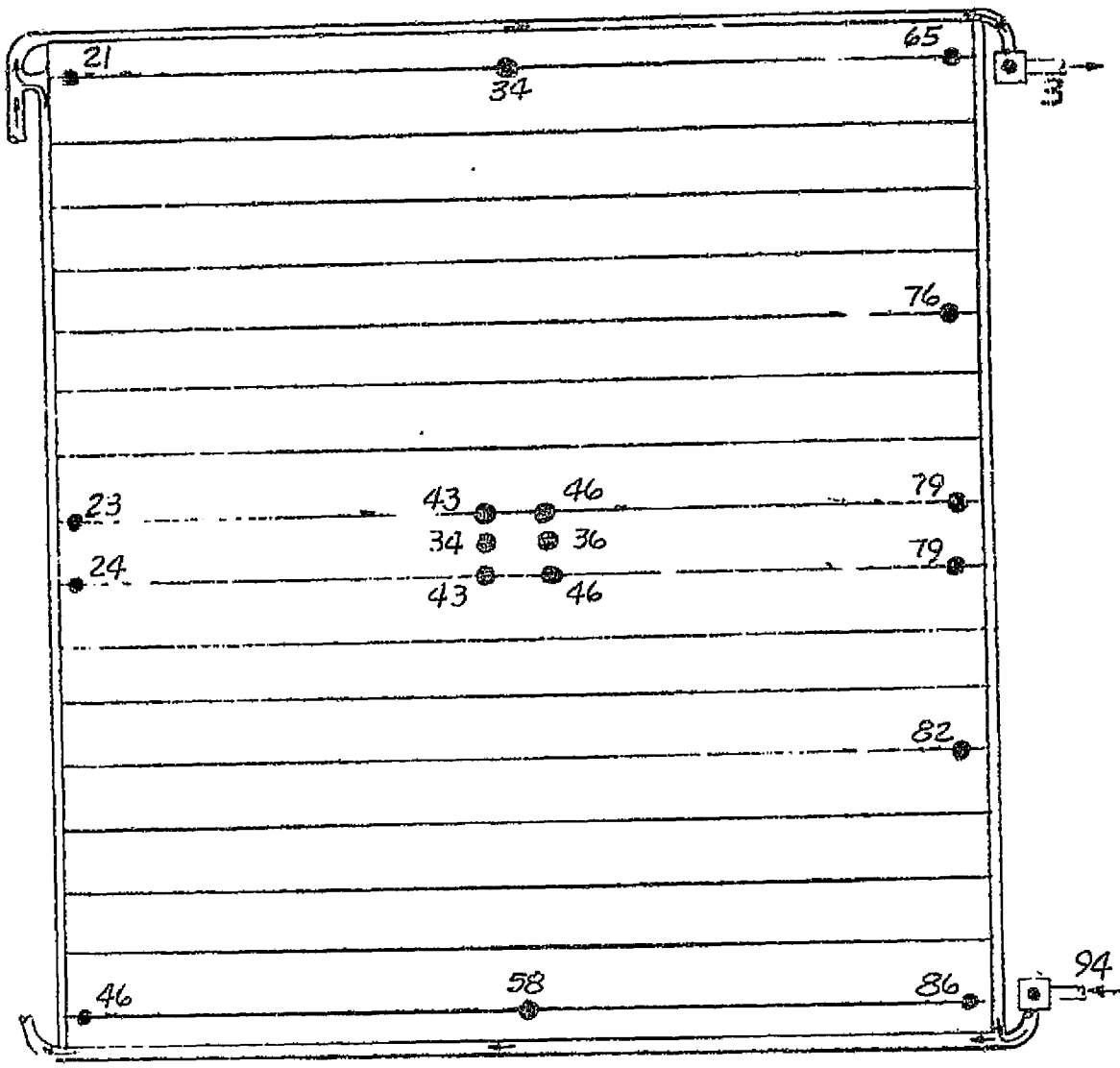
Fe$_{12}$ Return

Fe$_{12}$ Supply

PANEL NO. 3

FIGURE A1 (CONT'D)
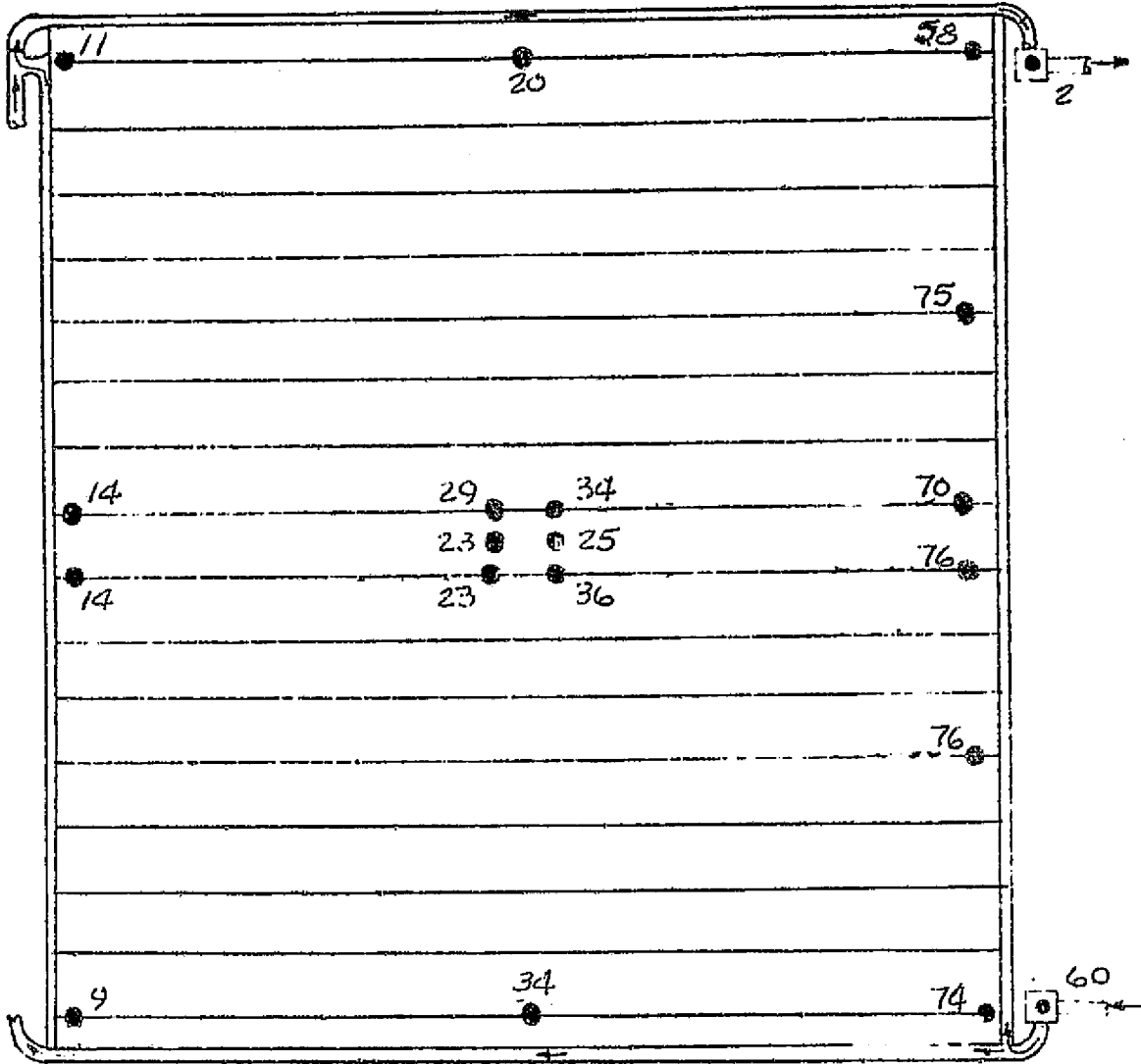
A-4

TEST POINT __1A__

DAY __294__

TIME __11:00:17__

Fe$_{12}$ Return

Fe$_{12}$ Supply

PANEL NO. 4

FIGURE A1 (CONT'D)

Fe$_{12}$ Return

−4   12   36   −36

1   41   45

3   10   23   29   36   46

5   36   48

1   15   24   33   48

19   34   50

23

17   26

1   50

15   23   50

7   8   38

1 8 8 12 21 26 34 51

3   19   26   48

23   53

15   33

1   12   24   33   51

8   41   51

7 12 24 33 43 51

46   53

23   31   53   58
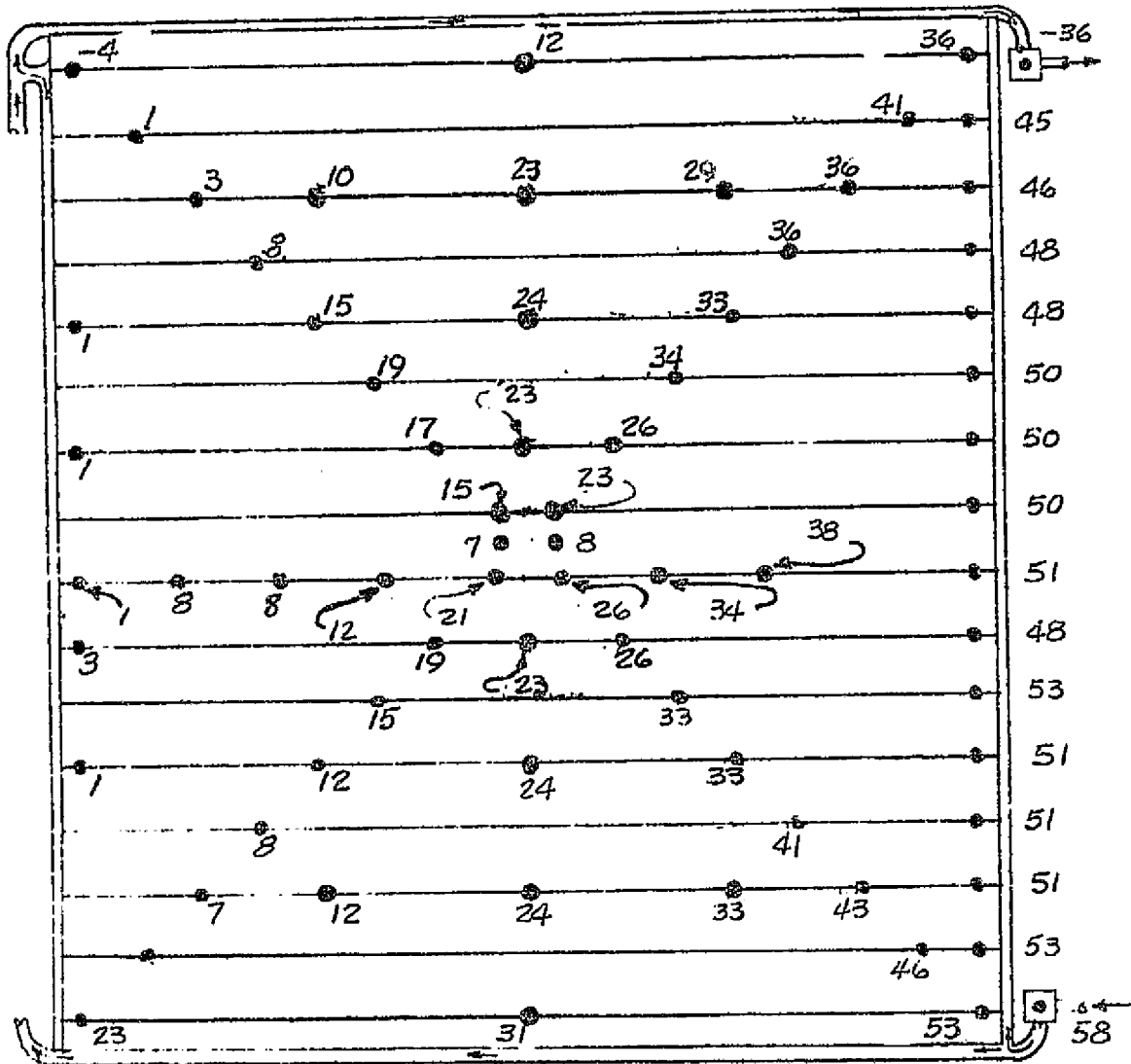
Fe$_{12}$ Supply

PANEL NO. 1

FIGURE A2

STEADY STATE LIQUID RADIATOR OPERATION PANEL TEMPERATURE MAPS

TEST POINT __8__

DAY __293__
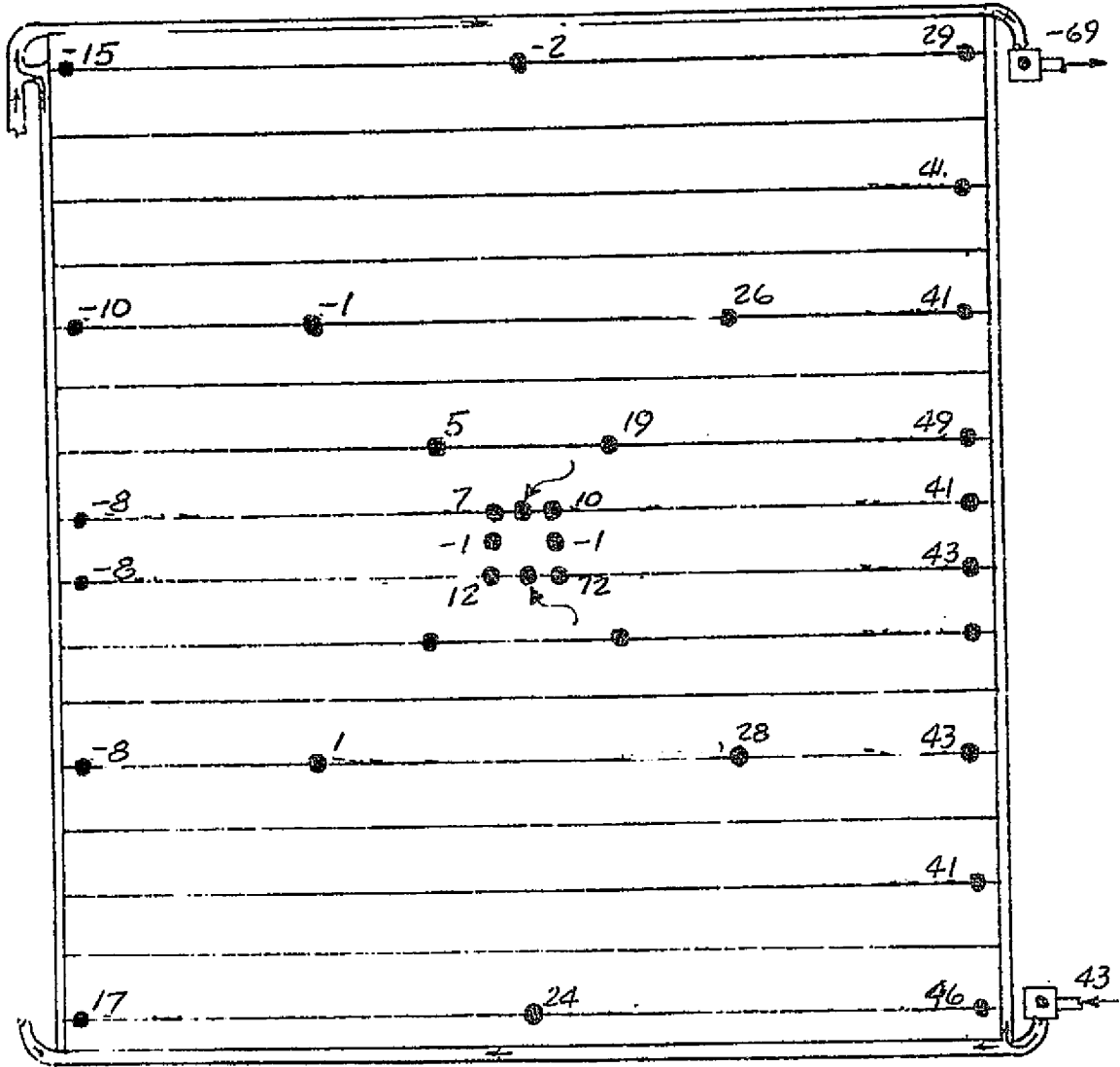
TIME __23:50:18__

Fe$_{12}$ Return

PANEL NO. 2

FIGURE A2 (CONT'D)

TEST POINT __8__

DAY __293__

TIME __23:50:18__

Fe$_{12}$ Return

-28   -10   26   -53

38

-24   -1 3   41
    -11 -7
-24   -1 3   41

45

5   -19   48   55
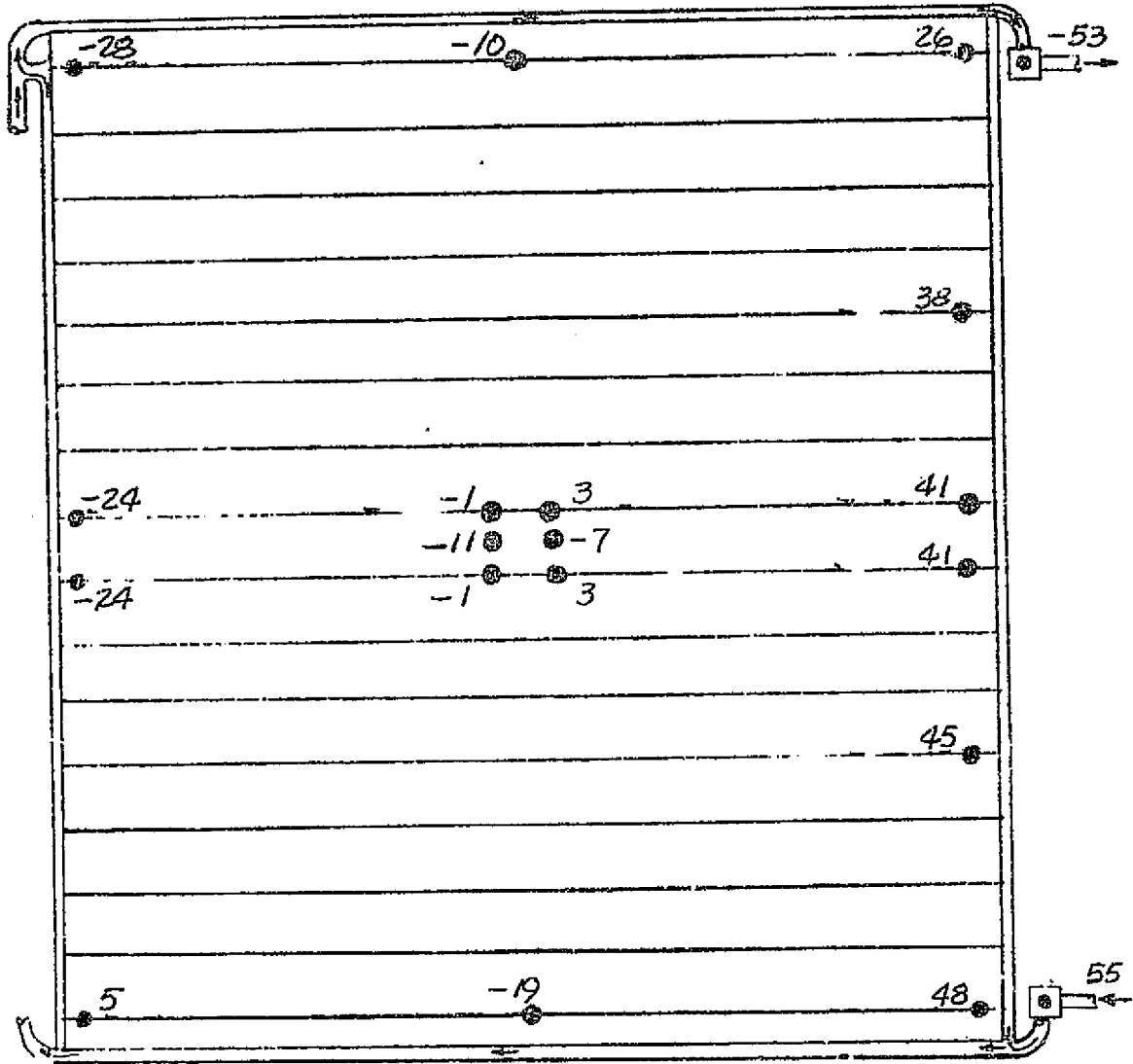
Fe$_{12}$ Supply

PANEL NO. 3

FIGURE A2 (CONT'D)

TEST POINT __8__

DAY __293__

TIME __23:50:18__
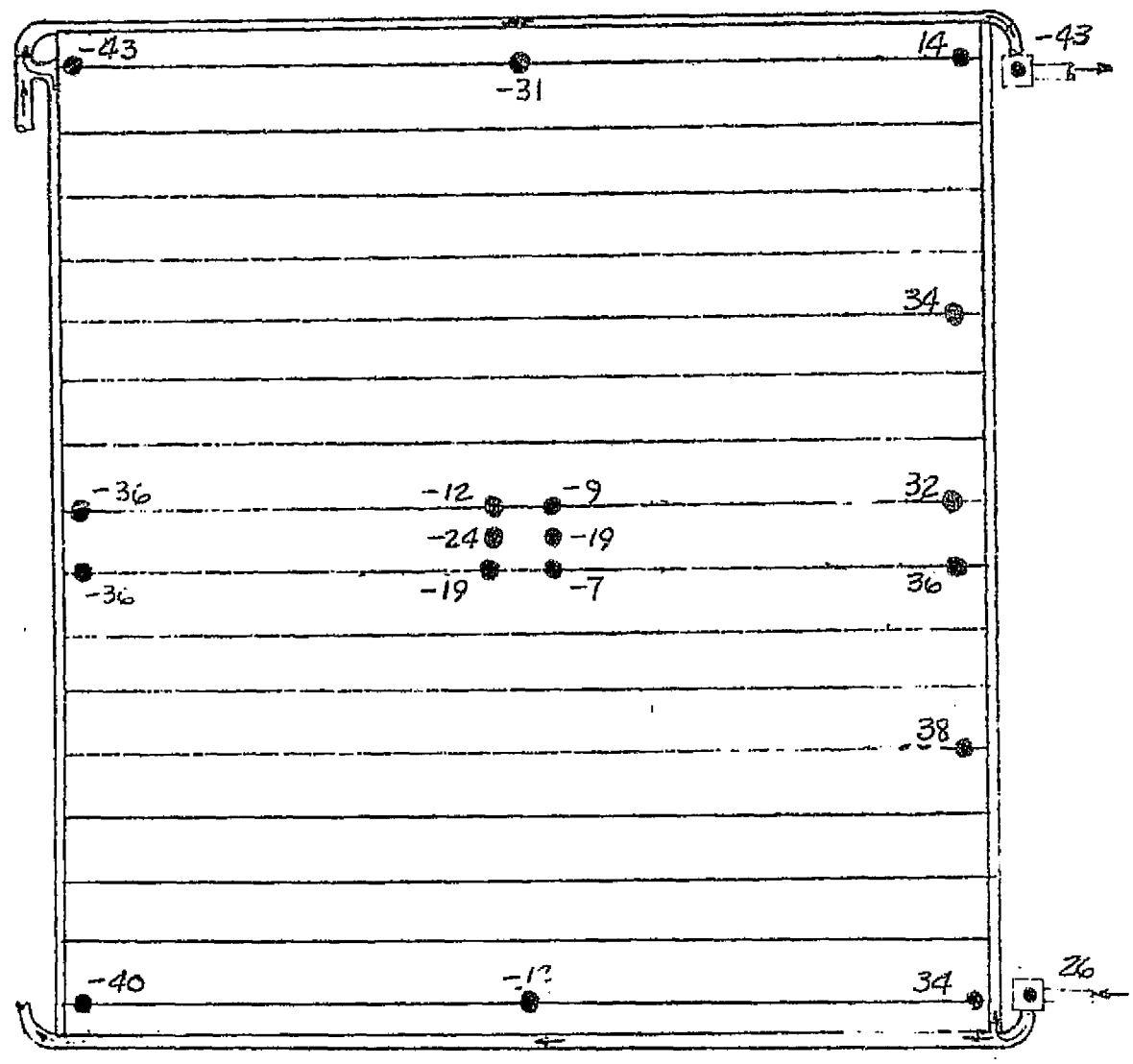
Fe_{12} Return

PANEL NO. 4

FIGURE A2 (CONT'D)

Fe_{12} Supply

TEST POINT _46_

DAY ___296___

TIME ___15:45:04___
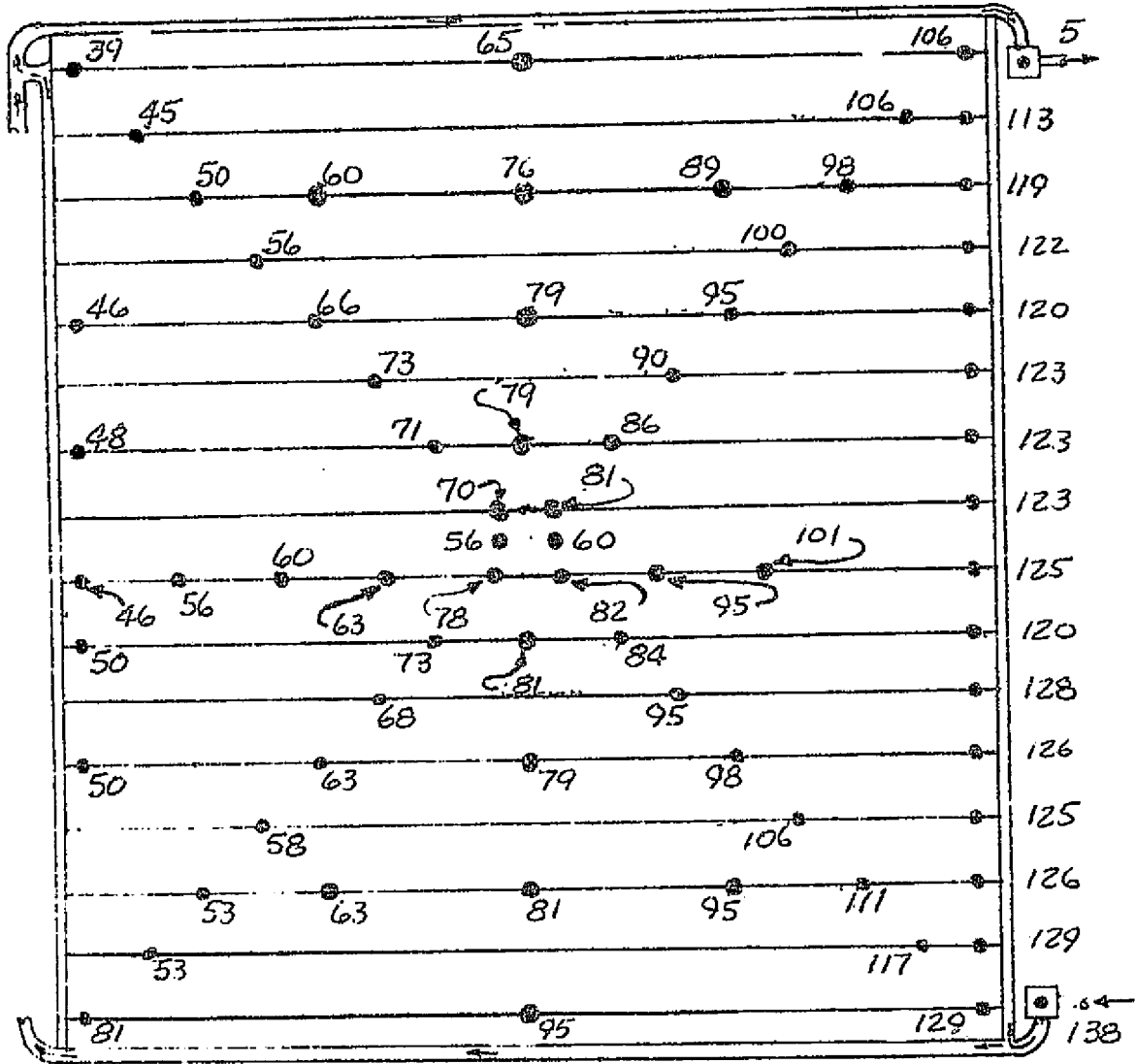
Fe$_{12}$ Return

Fe$_{12}$ Supply

PANEL NO. 1

FIGURE A3

STEADY STATE LIQUID RADIATOR OPERATION PANEL TEMPERATURE MAPS

TEST POINT _46_

DAY _296_
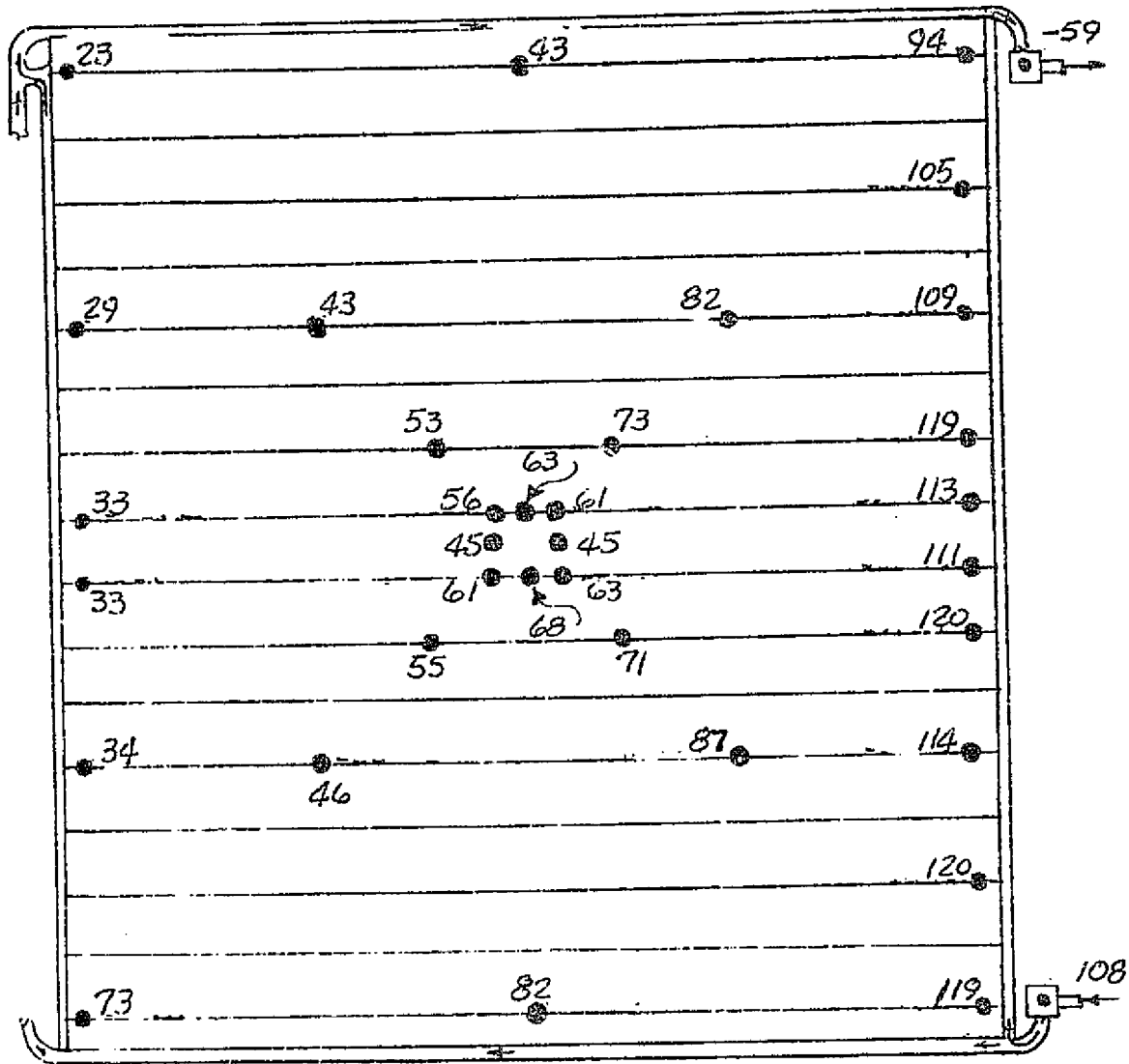
TIME _15:45:04_

Fe$_{12}$ Return

PANEL NO. 2

FIGURE A3 (CONT'D)

TEST POINT _46_

DAY _296_
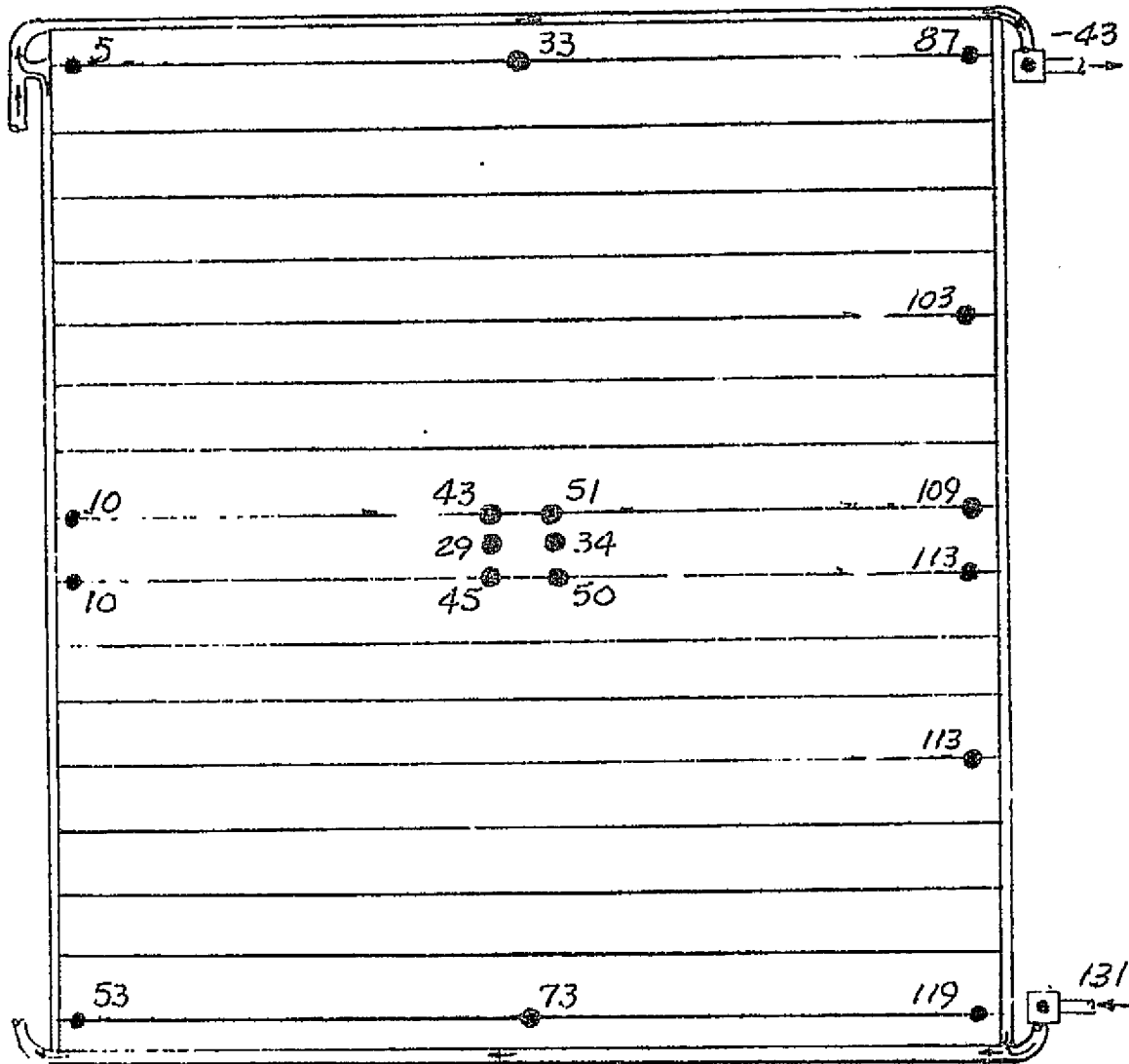
TIME _15:45:04_

Fe$_{12}$ Return

PANEL NO. 3

FIGURE A3 (CONT'D)

Fe$_{12}$ Supply

TEST POINT __46__

DAY __296__

TIME __15:45:04__

Fe$_{12}$ Return

−9   11   75   −16

98

−5   27   34   96

14   20

−7   18   36   101

103

−9   32   98   79
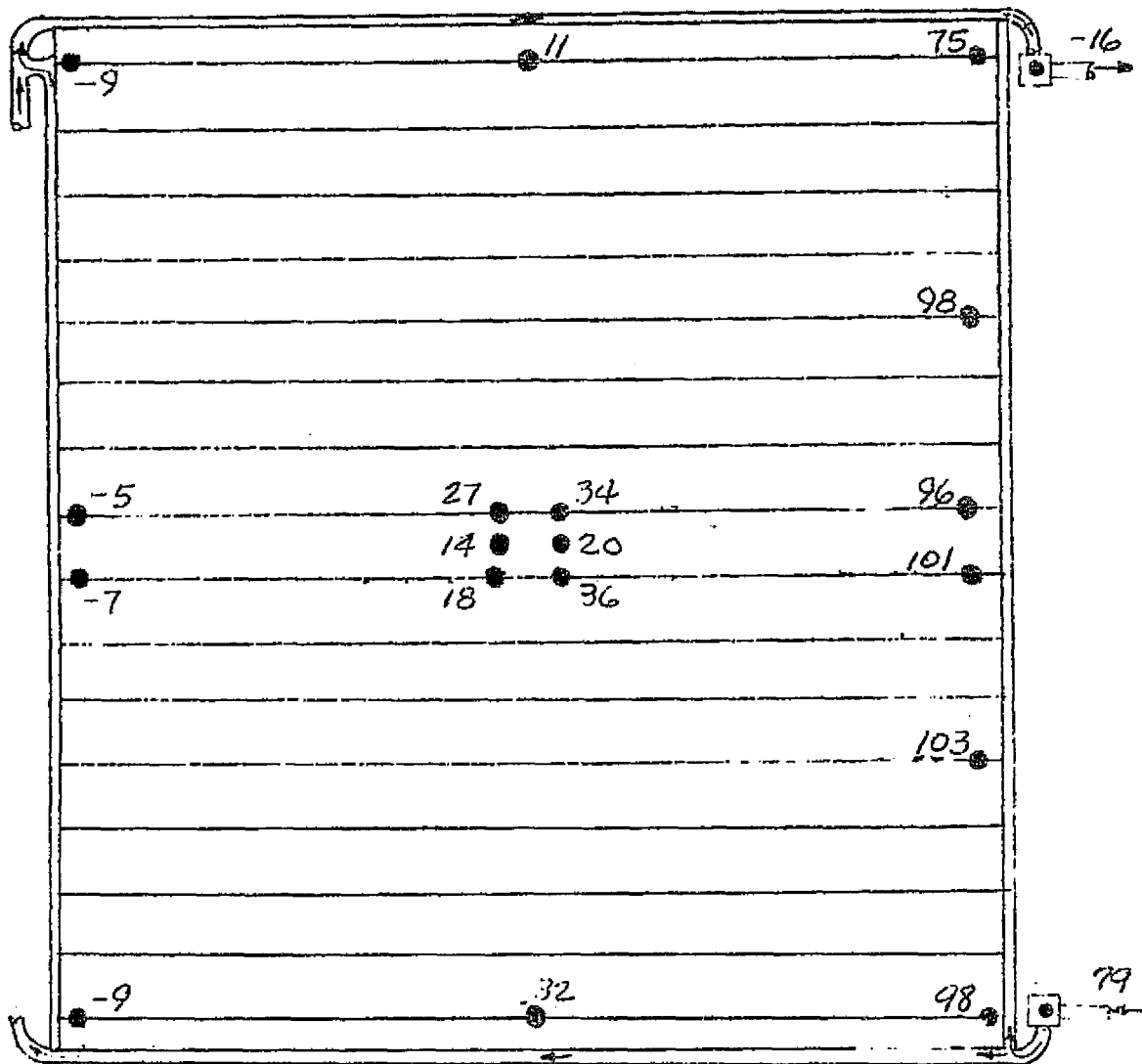
Fe$_{12}$ Supply

PANEL NO. 4

FIGURE A3 (CONT'D)

A-13

TEST POINT _47_
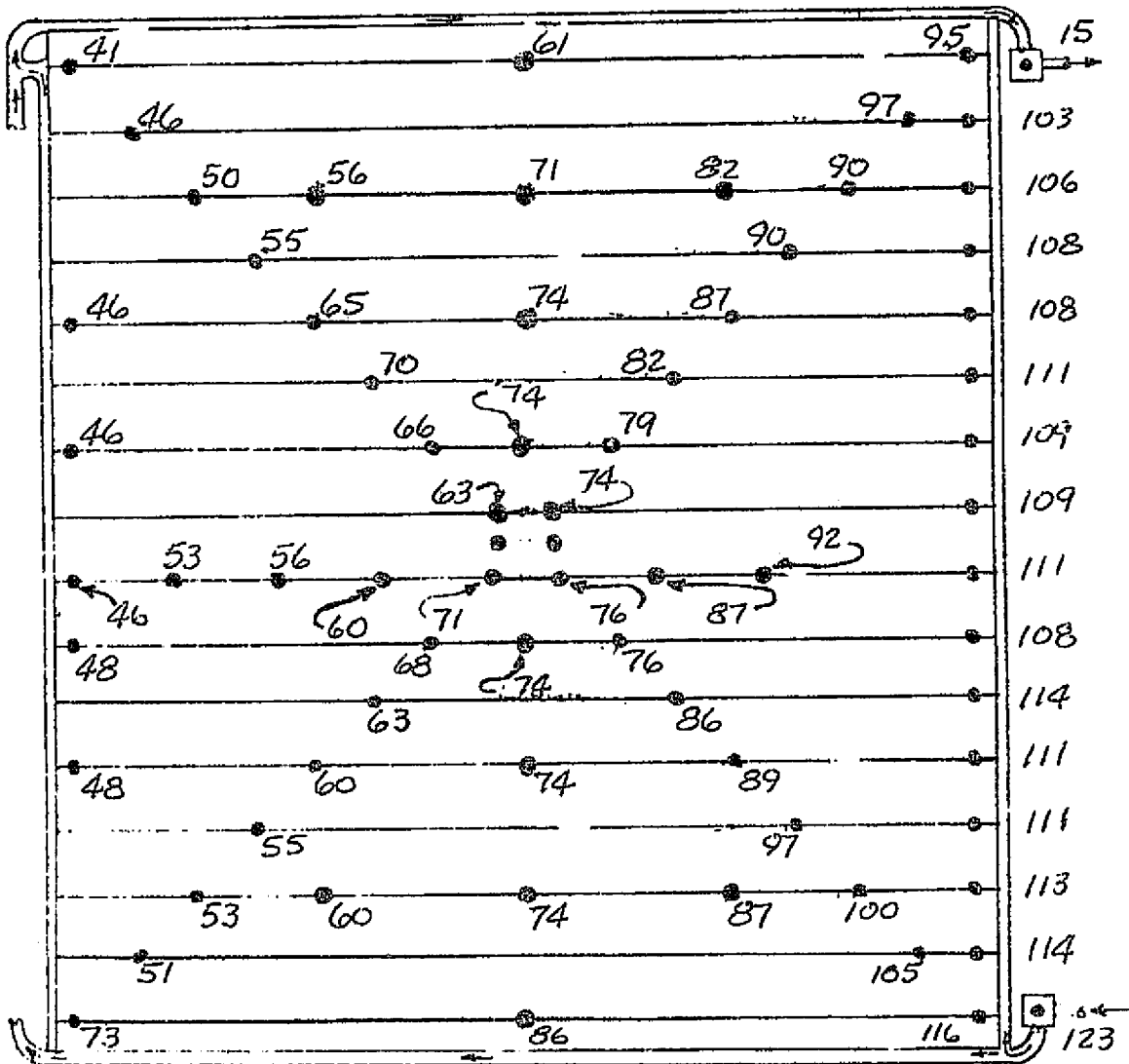
DAY _296_

TIME _19:30:03_

Fe$_{12}$ Return

PANEL NO. 1

FIGURE A4

STEADY STATE LIQUID RADIATOR OPERATION PANEL TEMPERATURE MAPS

Fe$_{12}$ Supply

A-14

TEST POINT __47__

DAY __296__

TIME __19:30:03__

Fe₁₂ Return

Fe_{12} Return

26   41   84   — 53

95

31   43   74   97

50   68   106

58

34   53   56   98

43   43

33   58   58   98

65   108

53   66

34   45   79   101

108

66   74   105

94
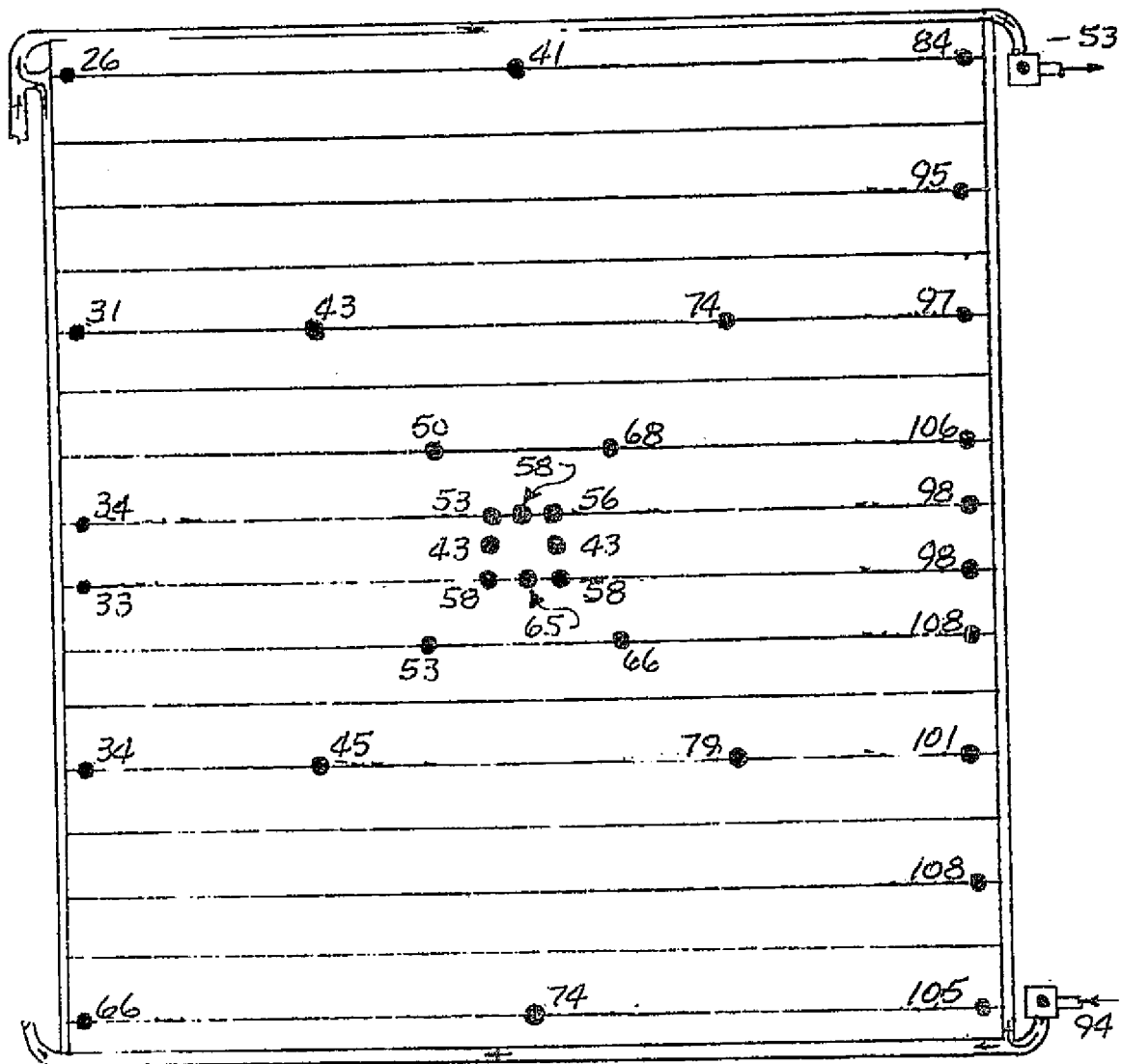
Fe_{12} Supply

PANEL NO. 2

FIGURE A4 (CONT'D)

A-15

TEST POINT   _47_____
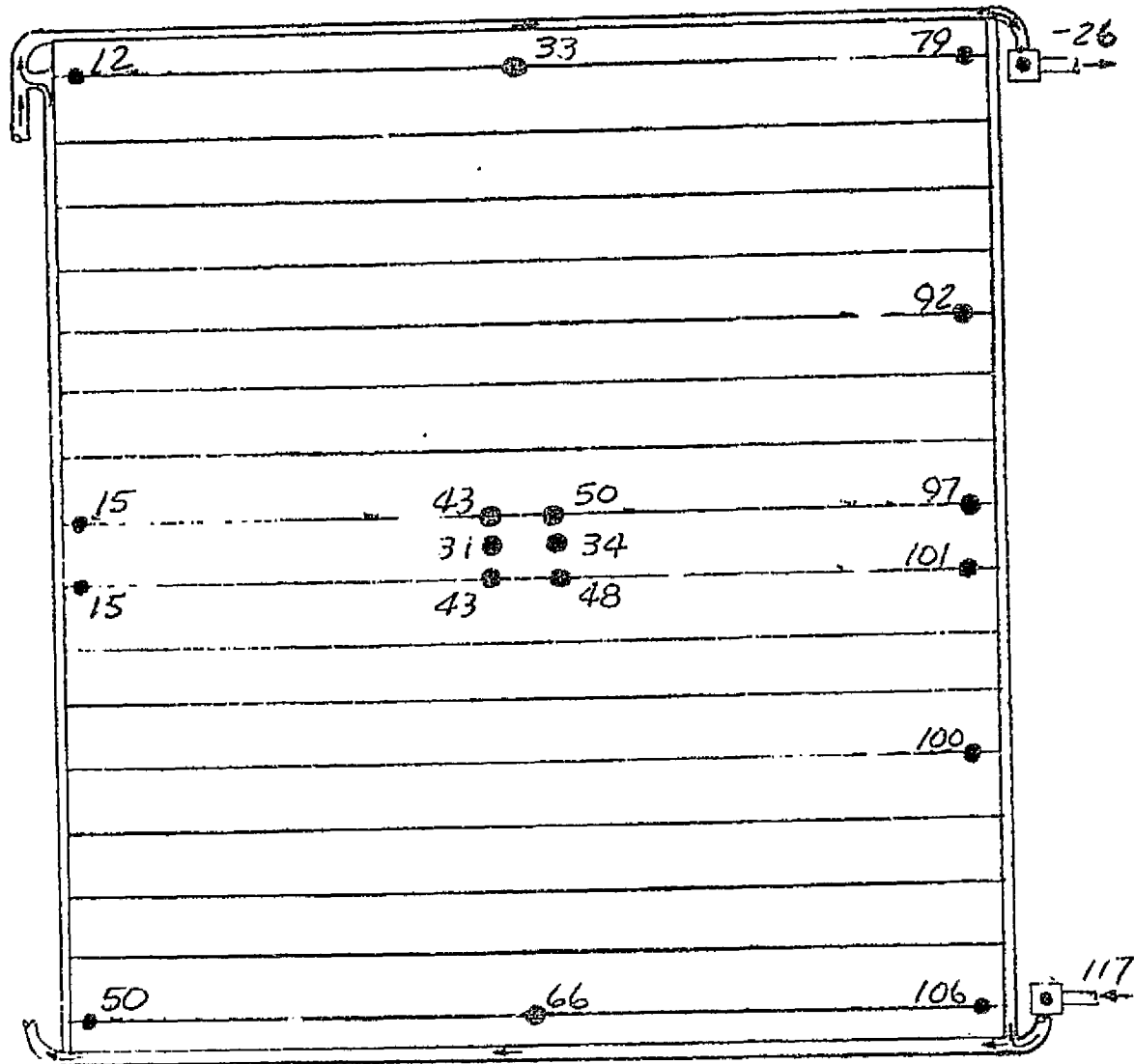
DAY _____ _296____

TIME _____ _19:30:03____

Fe_{12} Return

PANEL NO. 3

FIGURE A4 (CONT'D)

TEST POINT 47

DAY 296

TIME 19:30:03
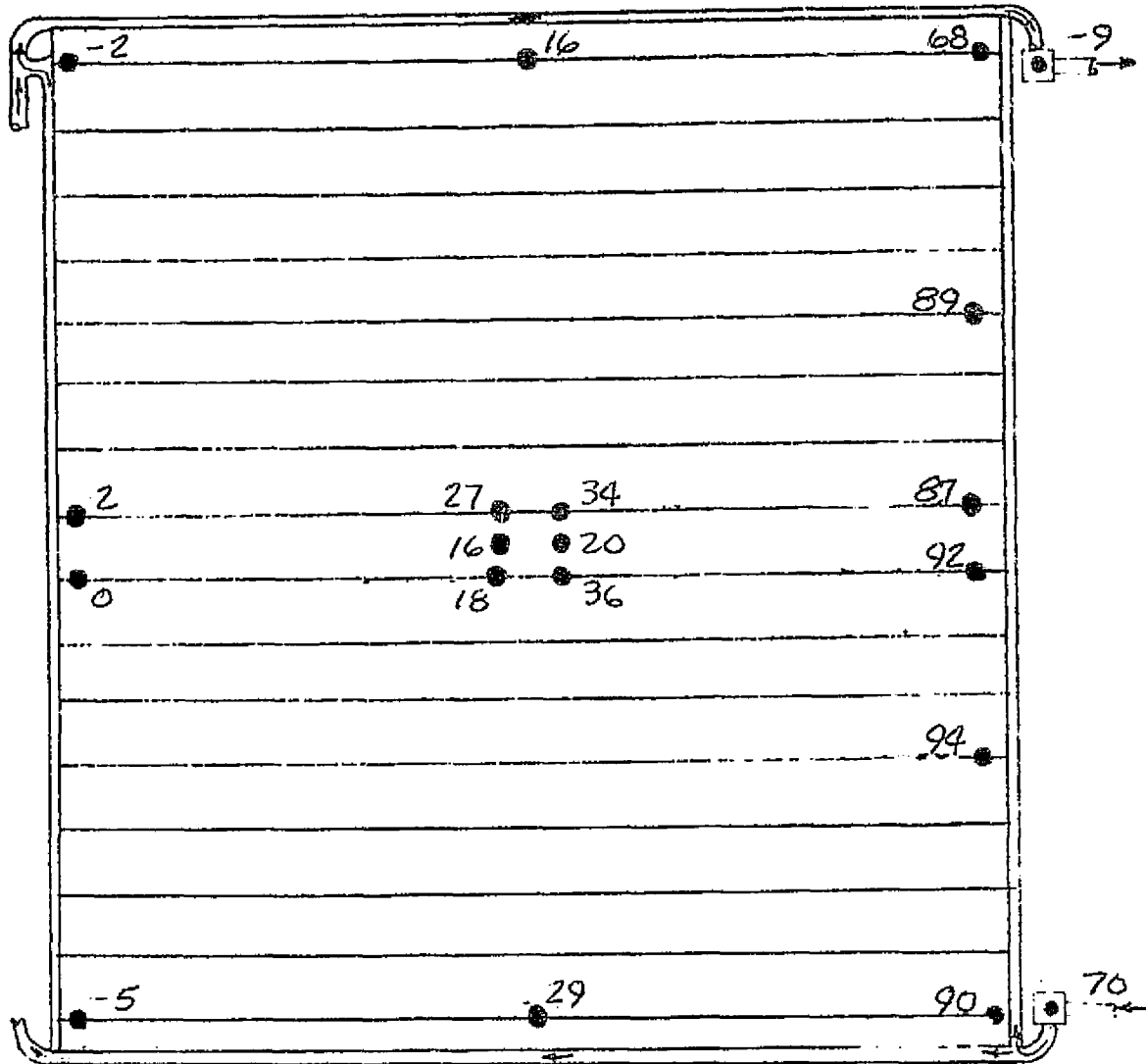
PANEL NO. 4

FIGURE A4 (CONT'D)

TEST POINT _48_

DAY _296_

TIME _22:00:03_
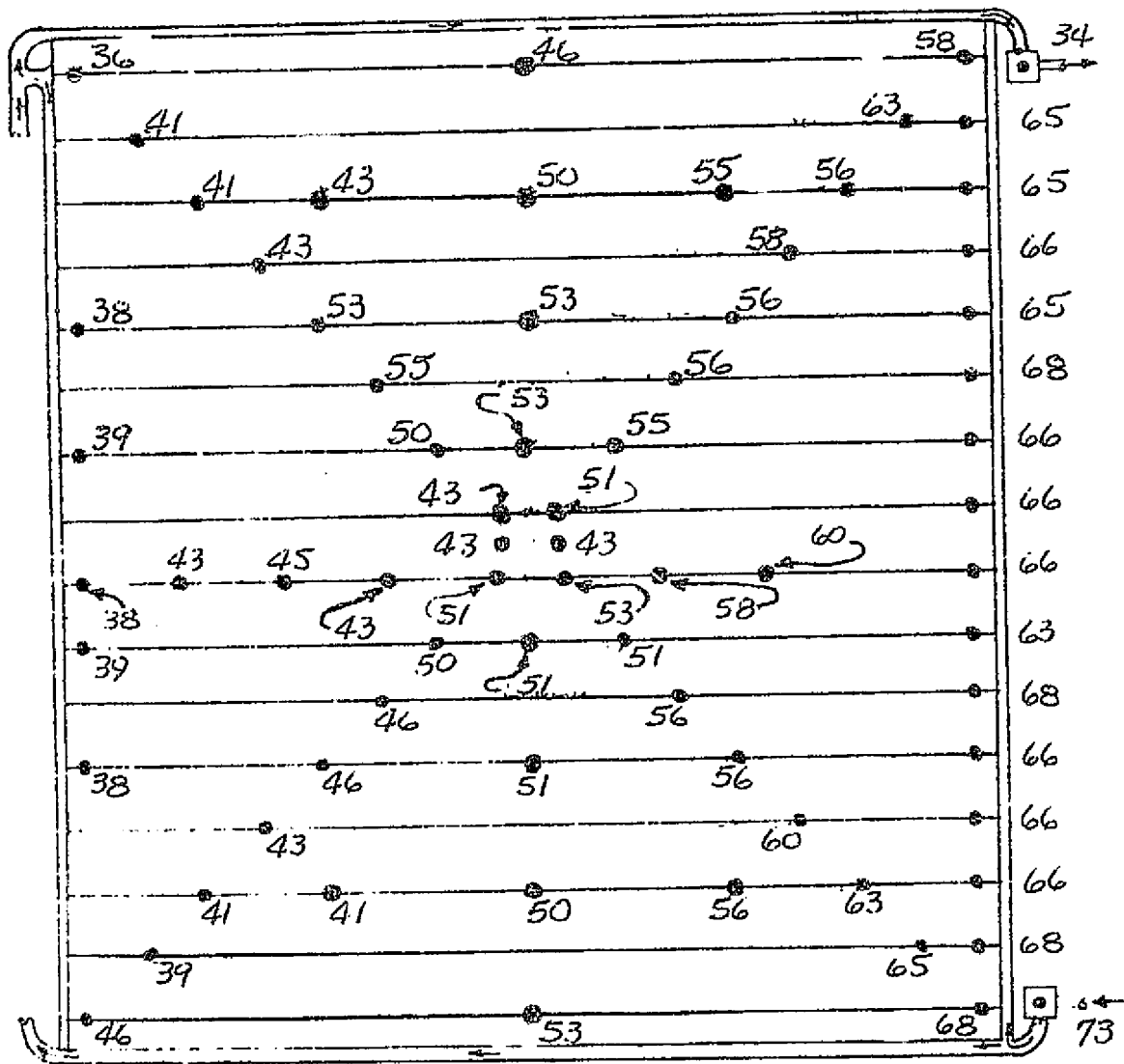
Fe$_{12}$ Return

Fe$_{12}$ Supply

PANEL NO. 1

FIGURE A5

STEADY STATE LIQUID RADIATOR OPERATION PANEL TEMPERATURE MAPS

A-18

TEST POINT __48__
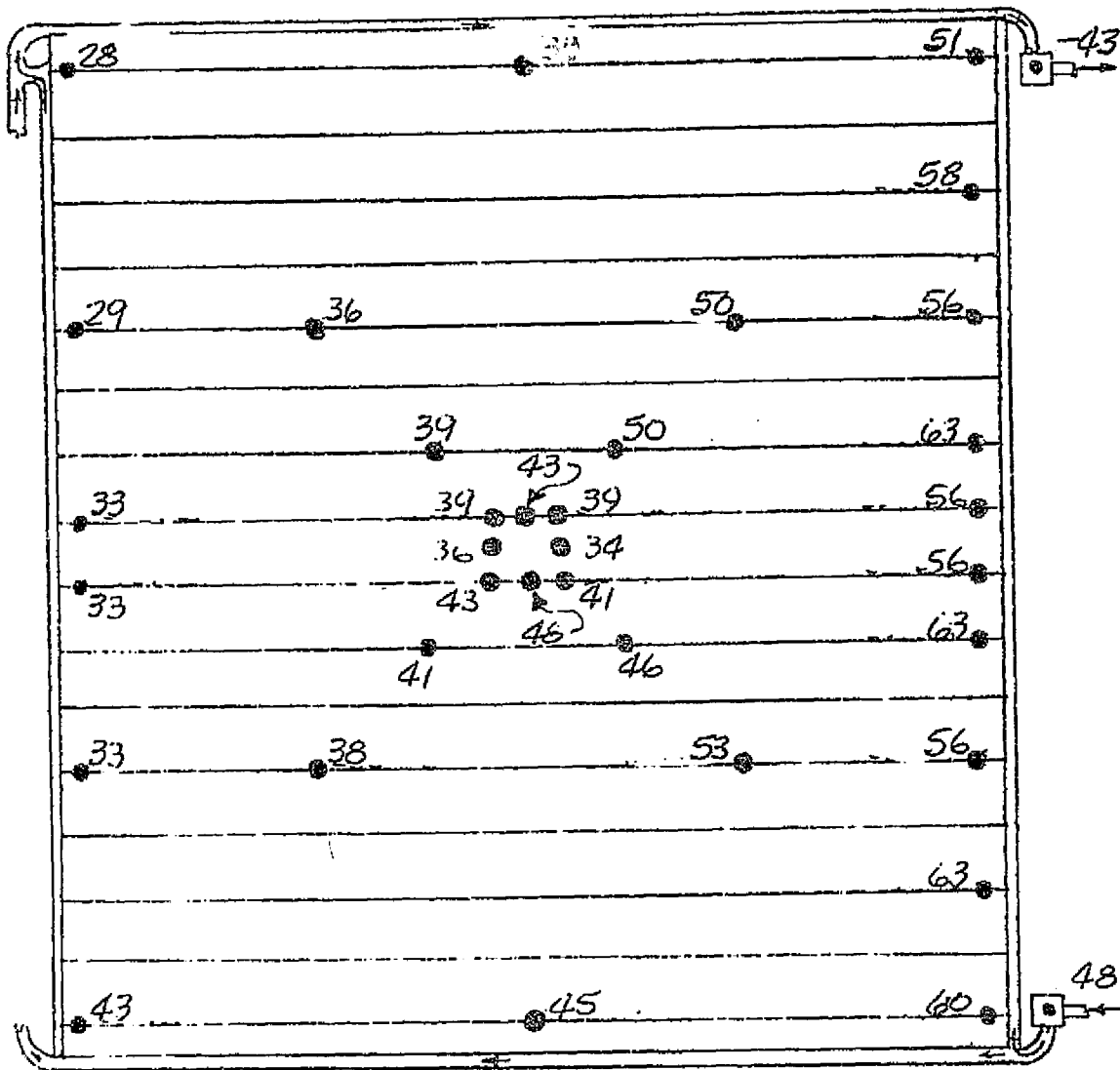
DAY __296__

TIME __22:00:03__

Fe_{12} Return

PANEL NO. 2

FIGURE A5 (CONT'D)

Fe_{12} Supply

TEST POINT __48__
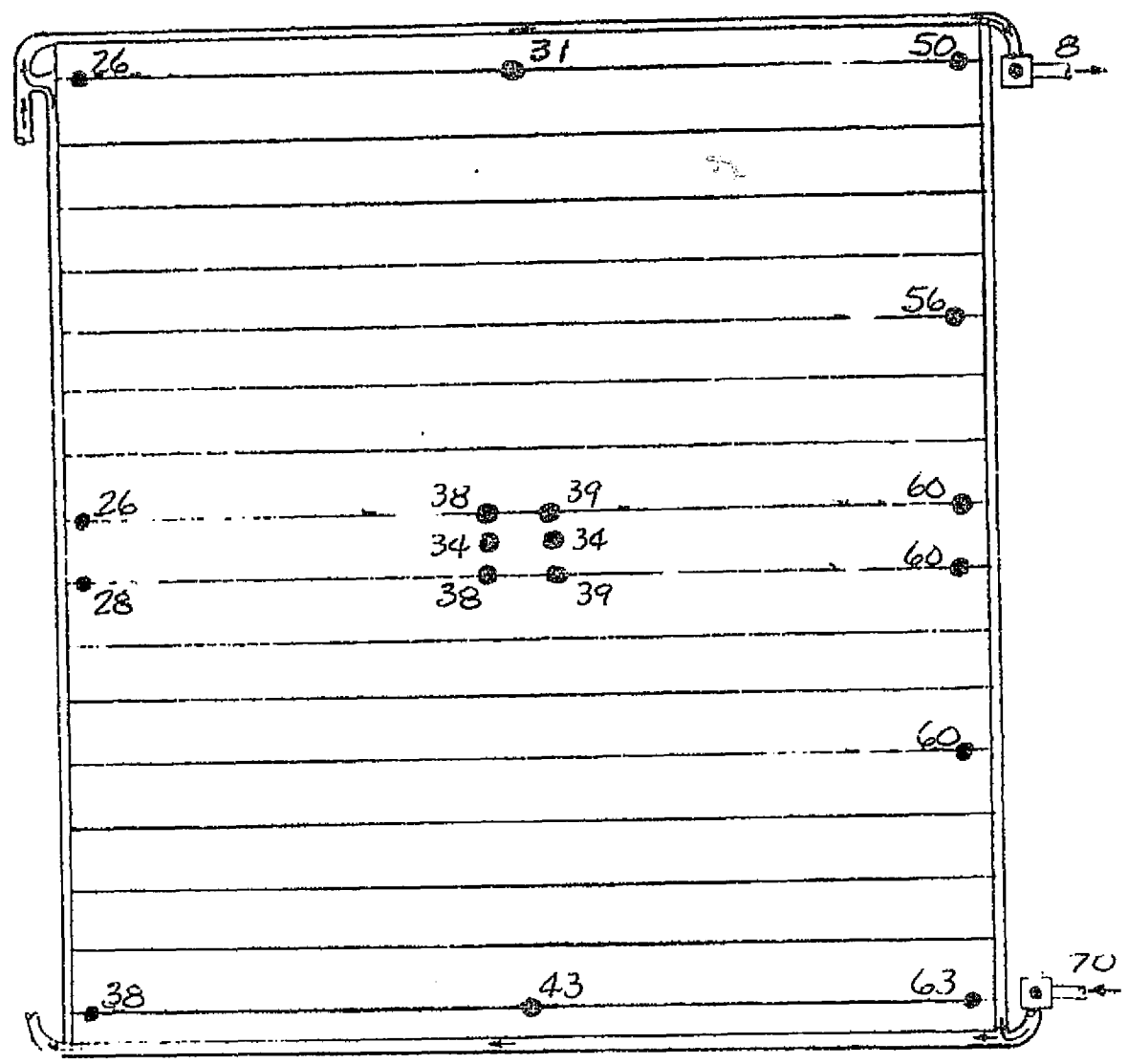
DAY _____296_____

TIME ____22:00:03____

Fe$_{12}$ Return

PANEL NO. 3

FIGURE A5 (CONT'D)

Fe$_{12}$ Supply

A-20

TEST POINT _48_

DAY _296_

TIME _22:00:03_

Fe$_{12}$ Return

PANEL NO. 4

FIGURE A5 (CONT'D)

TEST POINT __8A__

DAY __297__

TIME __00:30:03__

Fe_{12} Return

Fe_{12} Supply

PANEL NO. 1

FIGURE A6

STEADY STATE LIQUID RADIATOR OPERATION PANEL TEMPERATURE MAPS

TEST POINT **8A**
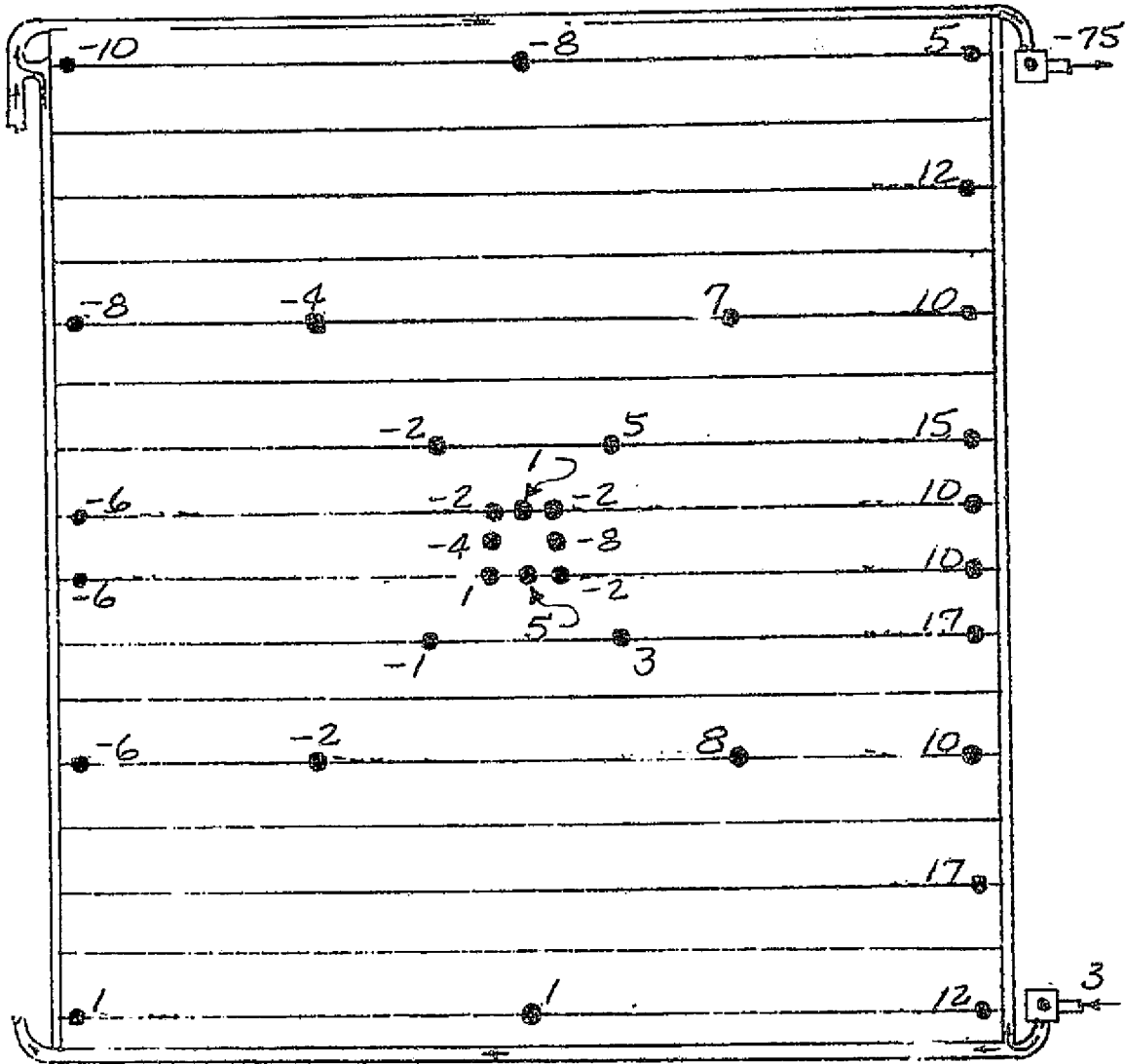
DAY **297**

TIME **00:30:03**

Fe_{12} Return

PANEL NO. 2

FIGURE A6 (CONT'D)

Fe_{12} Supply

A-23

TEST POINT __8A__

DAY ____297____

TIME ____00:30:03____

Fe$_{12}$ Return

PANEL NO. 3

FIGURE A6 (CONT'D)

A-24

TEST POINT: _8A_

DAY _297_

TIME _00:30:03_

Fe$_{12}$ Return

PANEL NO. 4

FIGURE A6 (CONT'D)

TEST POINT __8B__

DAY __297__

TIME __02:15:03__

Fe$_{12}$ Return
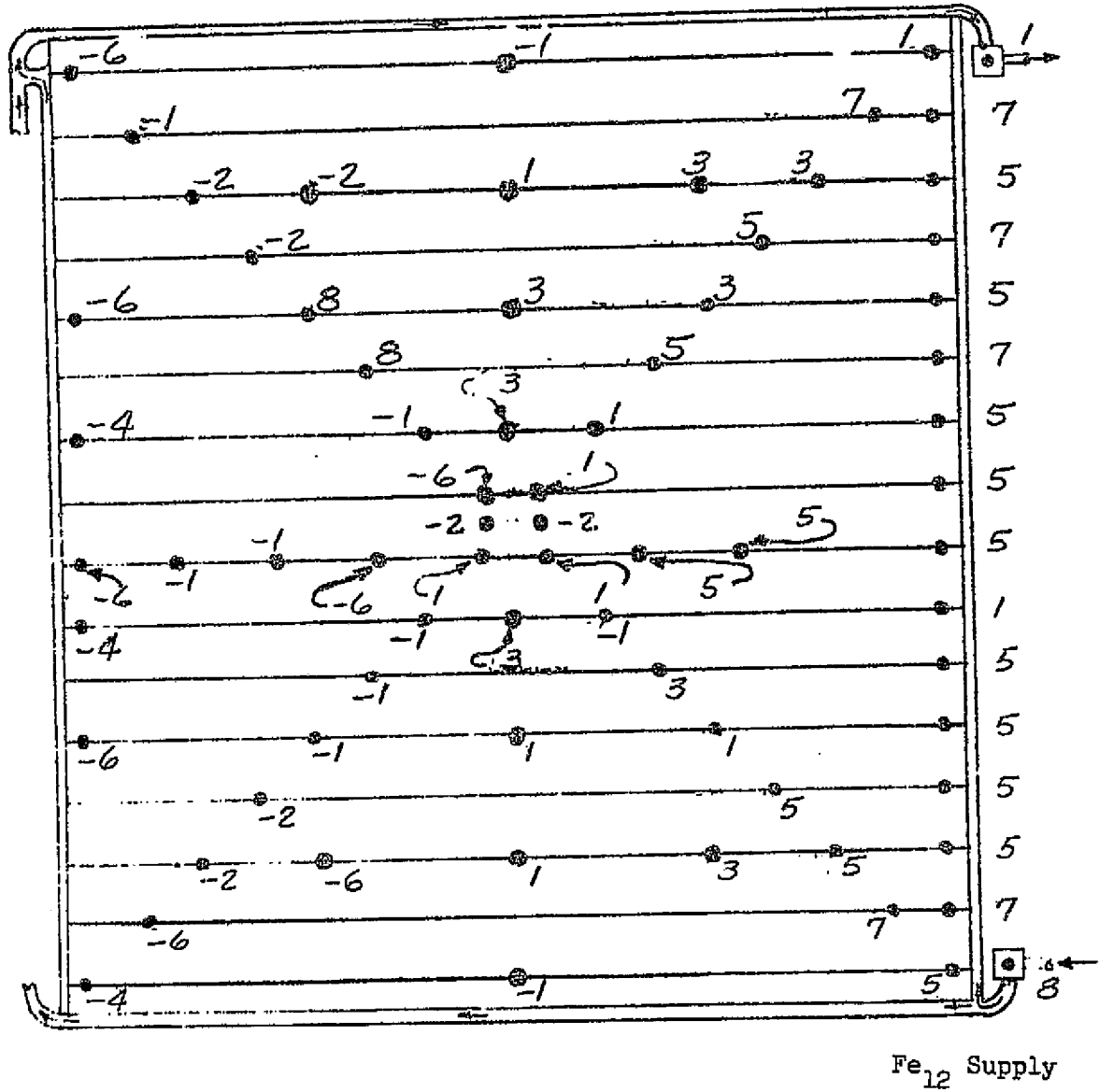
Fe$_{12}$ Supply

PANEL NO. 1

FIGURE A7

STEADY STATE LIQUID RADIATOR OPERATION PANEL TEMPERATURE MAPS
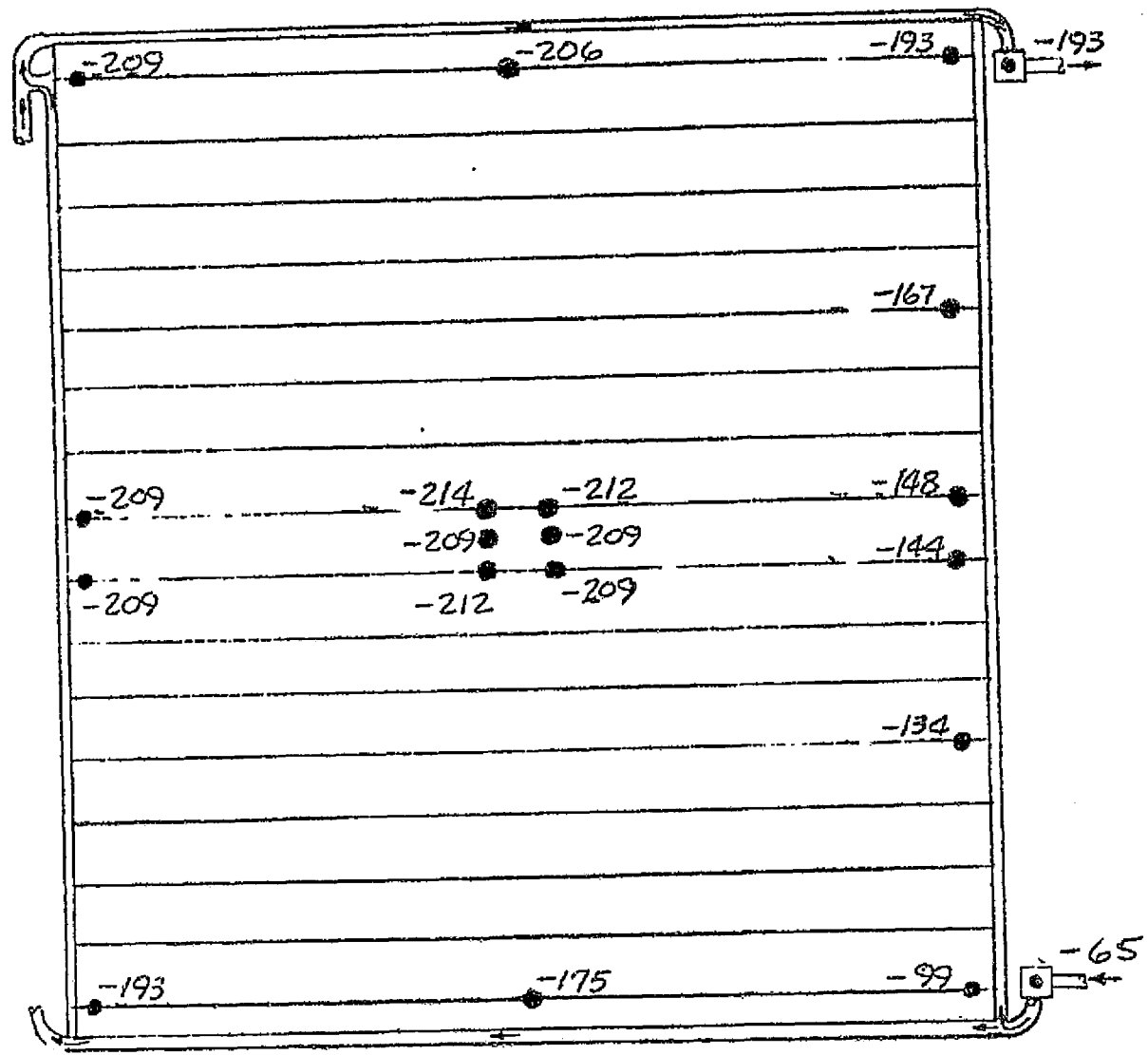
TEST POINT 8B

DAY 297

TIME 02:15:03
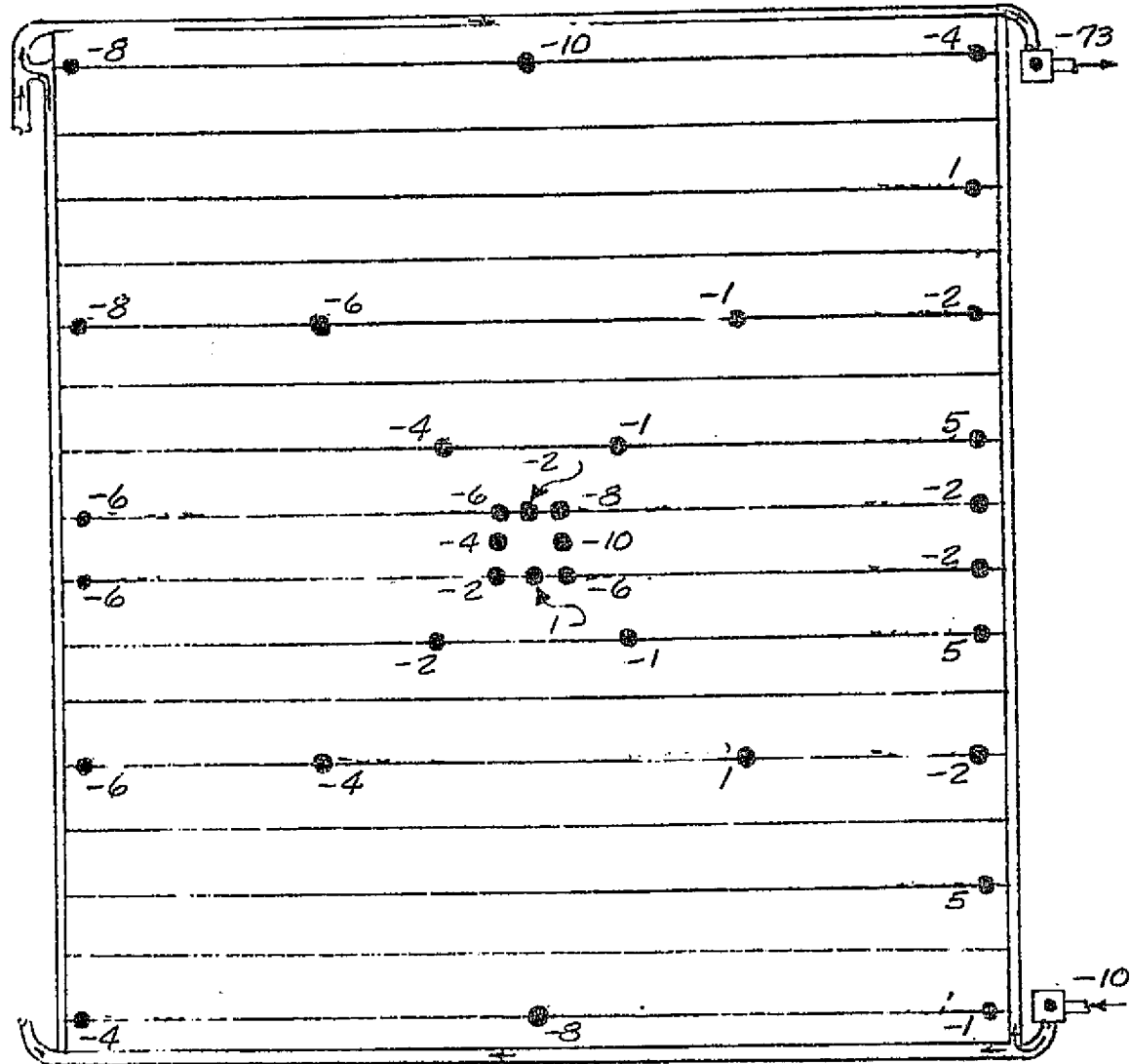
Fe_{12} Return

Fe_{12} Supply

PANEL NO. 2

FIGURE A7 (CONT'D)

A-27

TEST POINT __8B__
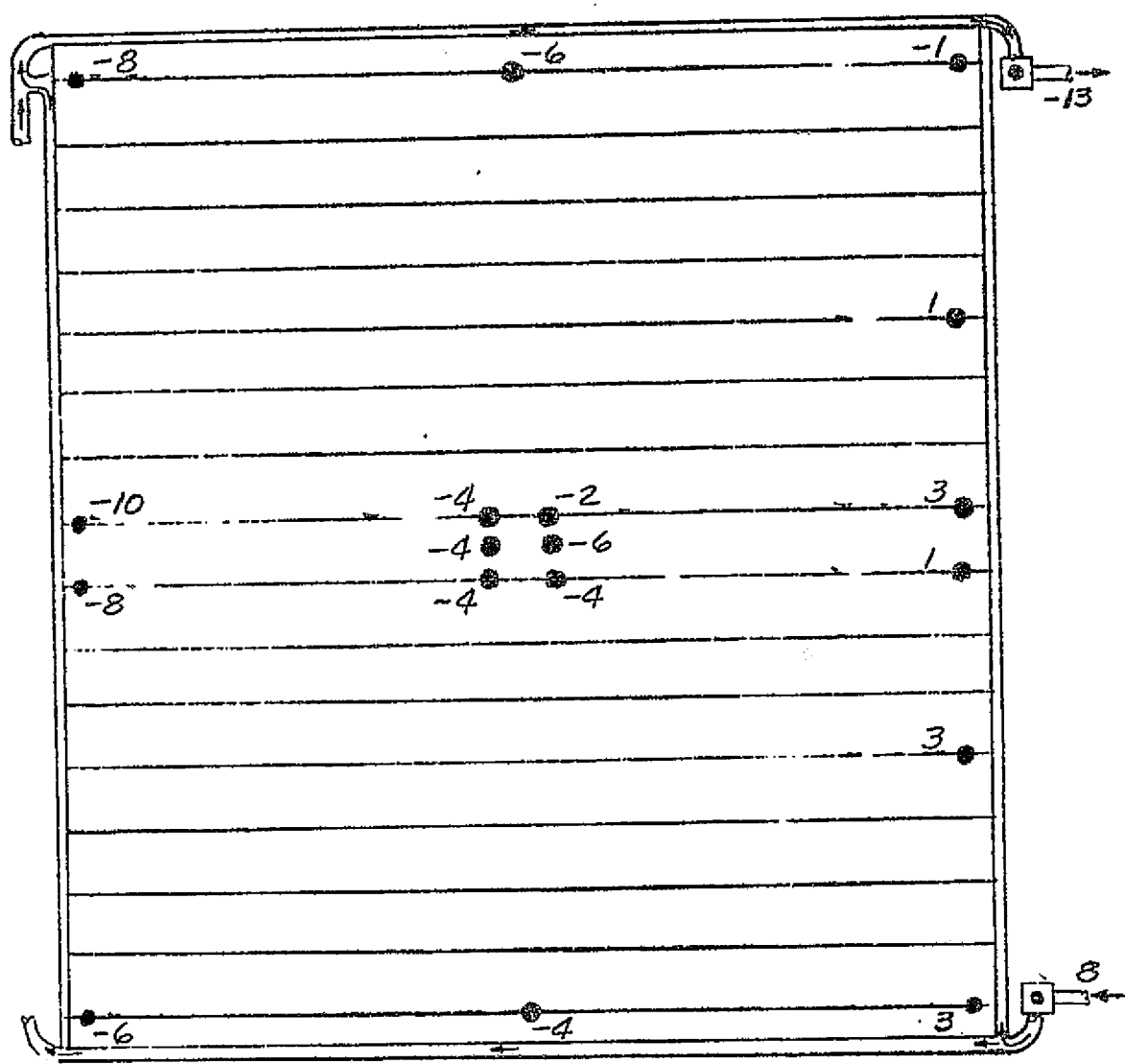
DAY __297__

TIME __02:15:03__

Fe_{12} Return

PANEL NO. 3

FIGURE A7 (CONT'D)

Fe_{12} Supply

TEST POINT _8B_

DAY _297_

TIME _02:15:03_
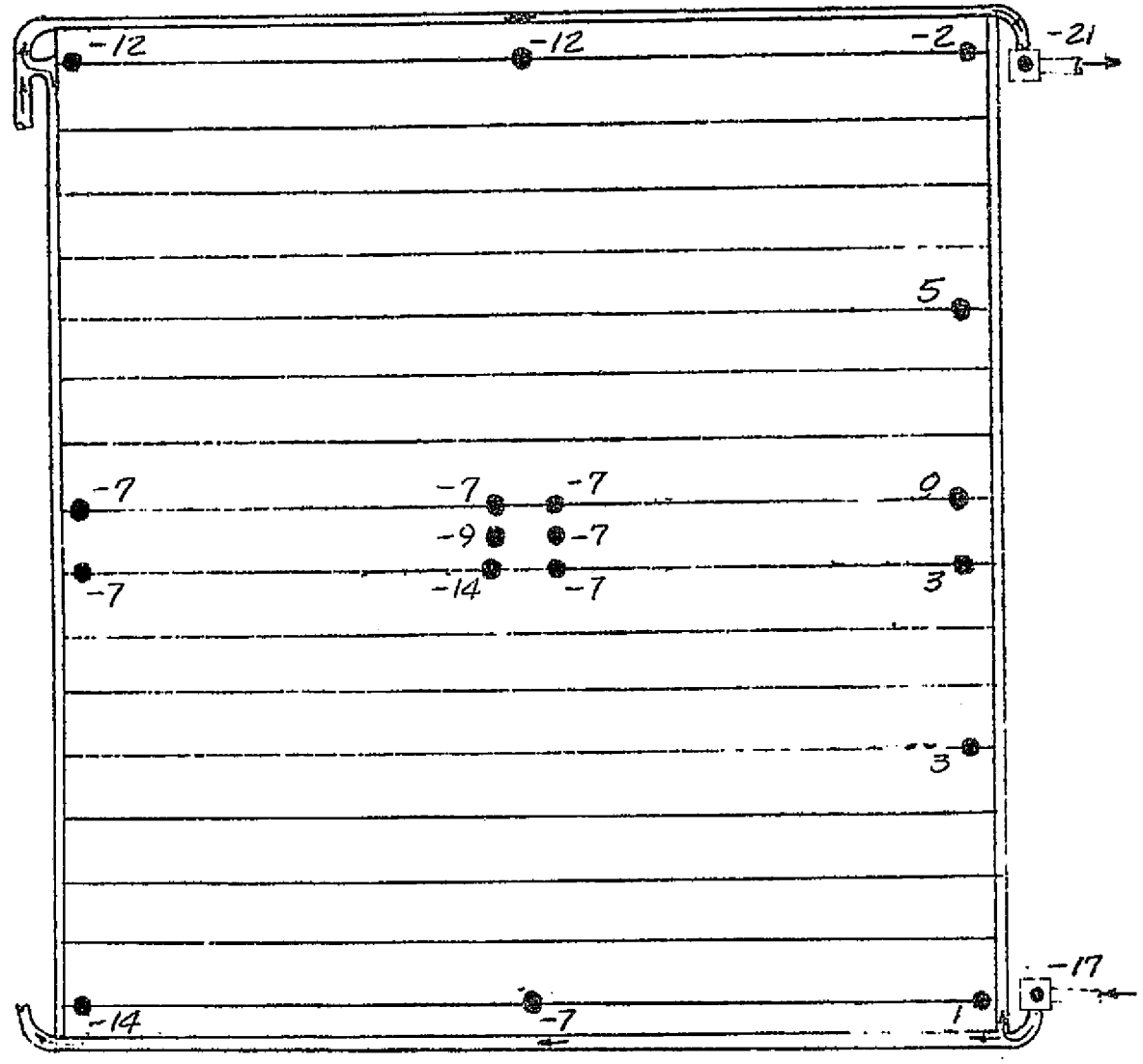
Fe$_{12}$ Return

PANEL NO. 4

FIGURE A7 (CONT'D)·

Fe$_{12}$ Supply

A-29

TEST POINT _101_
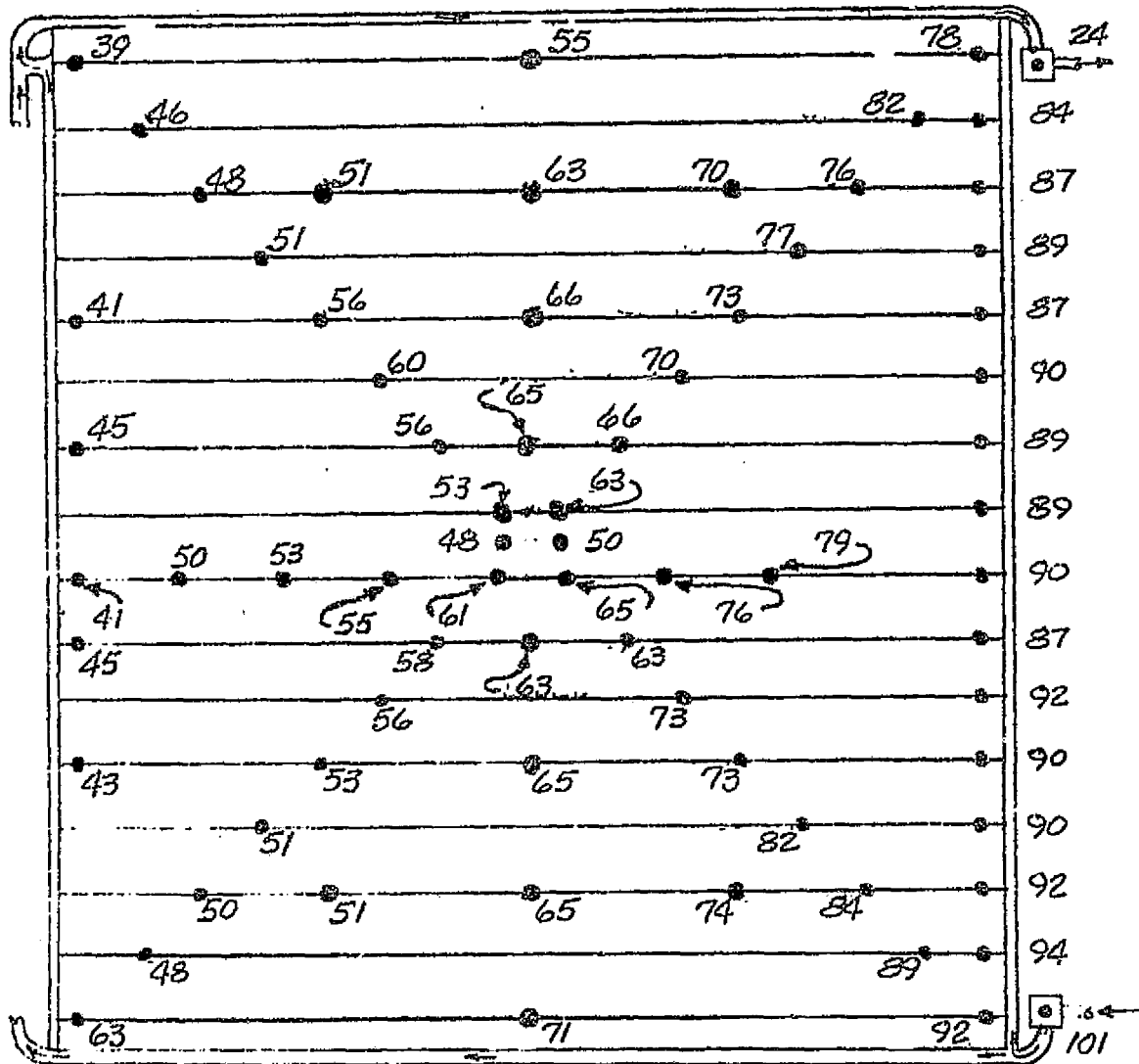
DAY _308_

TIME _13:00:05_

Fe$_{12}$ Return

PANEL NO. 1

FIGURE A8

STEADY STATE LIQUID RADIATOR OPERATION PANEL TEMPERATURE MAPS

Fe$_{12}$ Supply

TEST POINT ___101___

DAY ___308___

TIME ___13:00:05___

Fe$_{12}$ Return

28   43   73   28

79

29   41   63   82

45   56   86

50

33   45   53   84

41   43   84

33   53   53   87

56

46   56

34   41   66   86

87

58   66   89   82
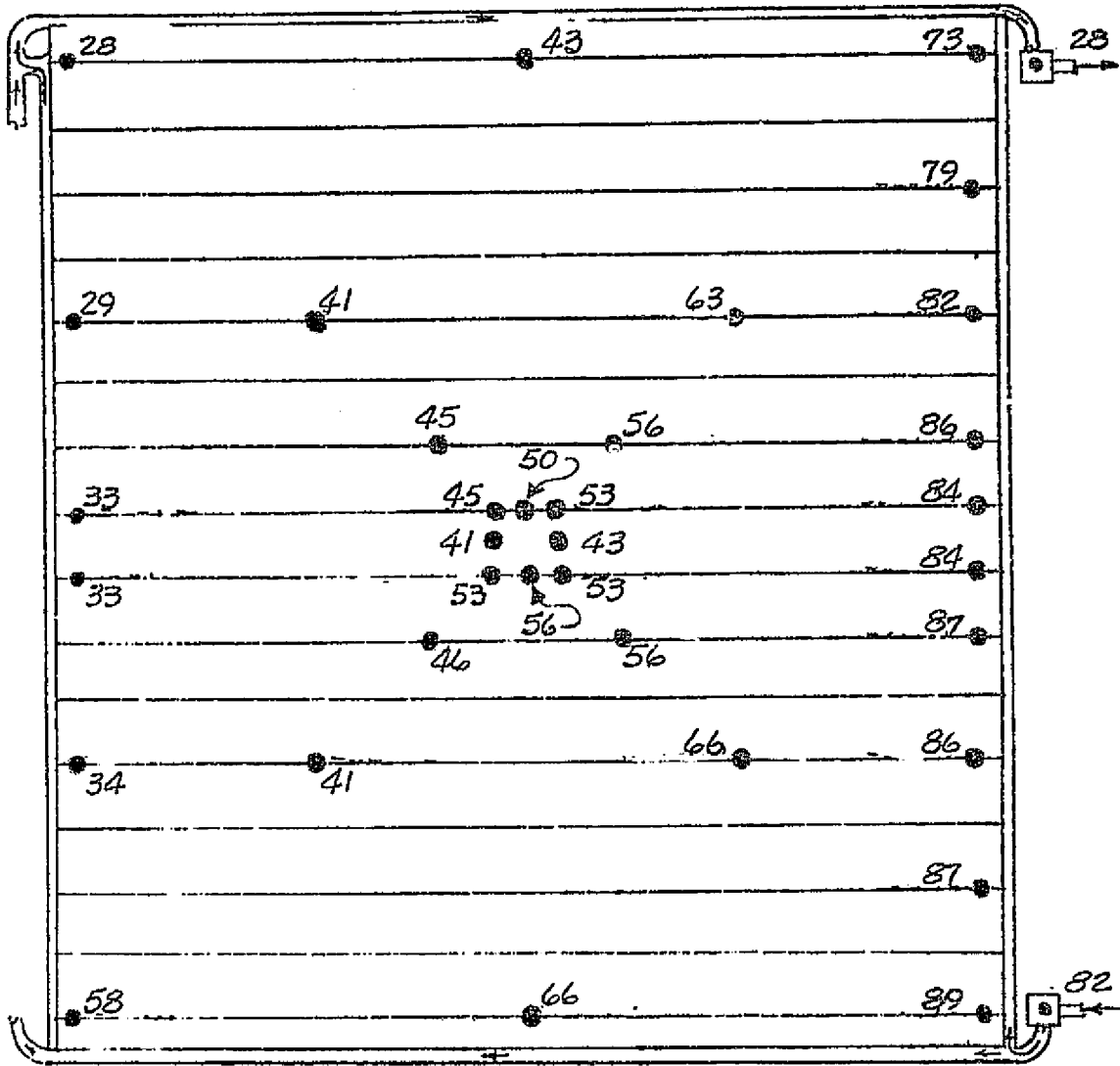
Fe$_{12}$ Supply

PANEL NO. 2

FIGURE A8 (CONT'D)

TEST POINT __101__

DAY __308__

TIME __13:00:05__

Fe$_{12}$ Return

19   33   65   23

76

19   39   43   79
          31   34   81
21   39   43

82

95
46   56   86
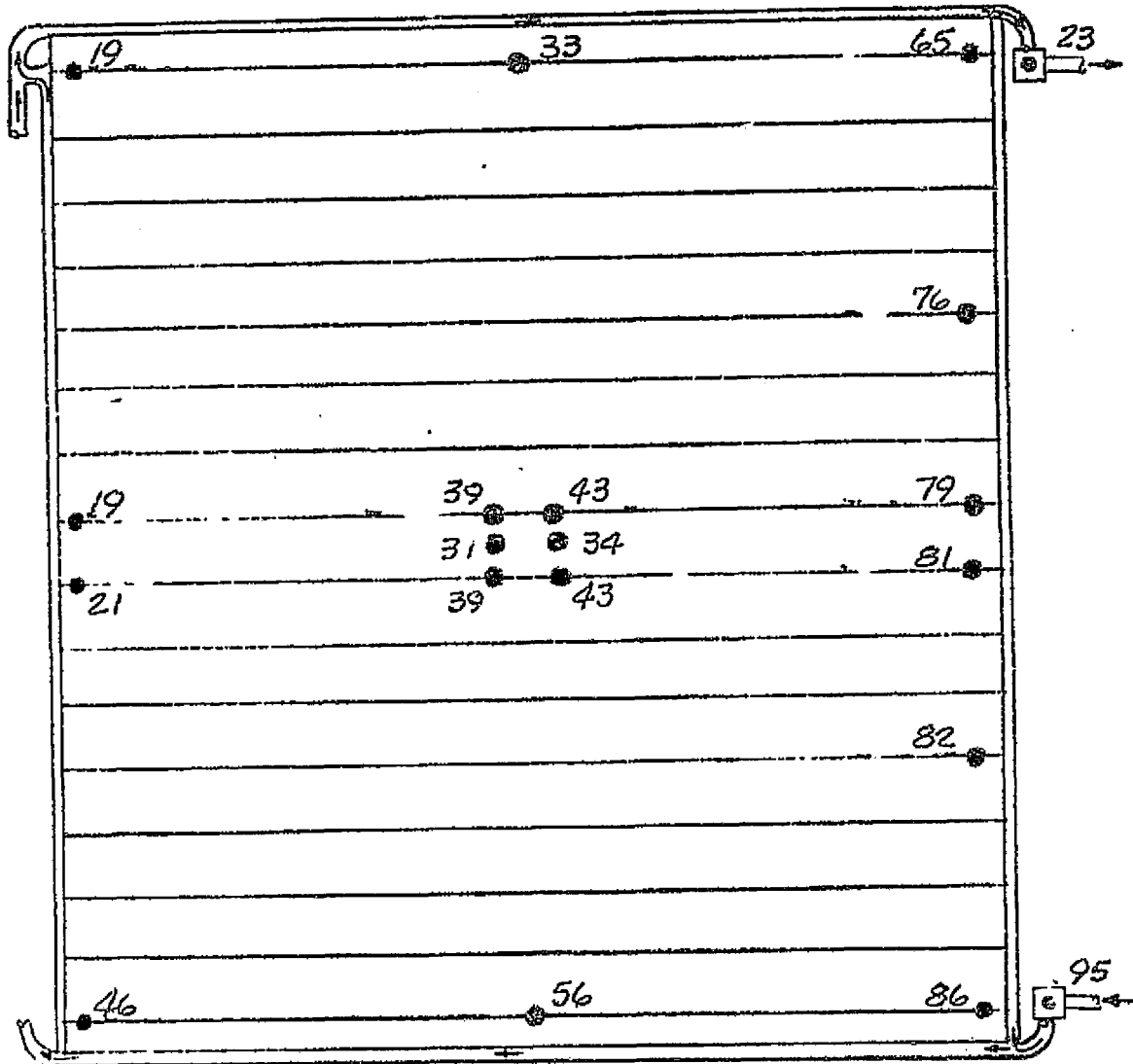
Fe$_{12}$ Supply

PANEL NO. 3

FIGURE A8 (CONT'D)

TEST POINT ___101___

DAY ___308___

TIME ___13:00:05___
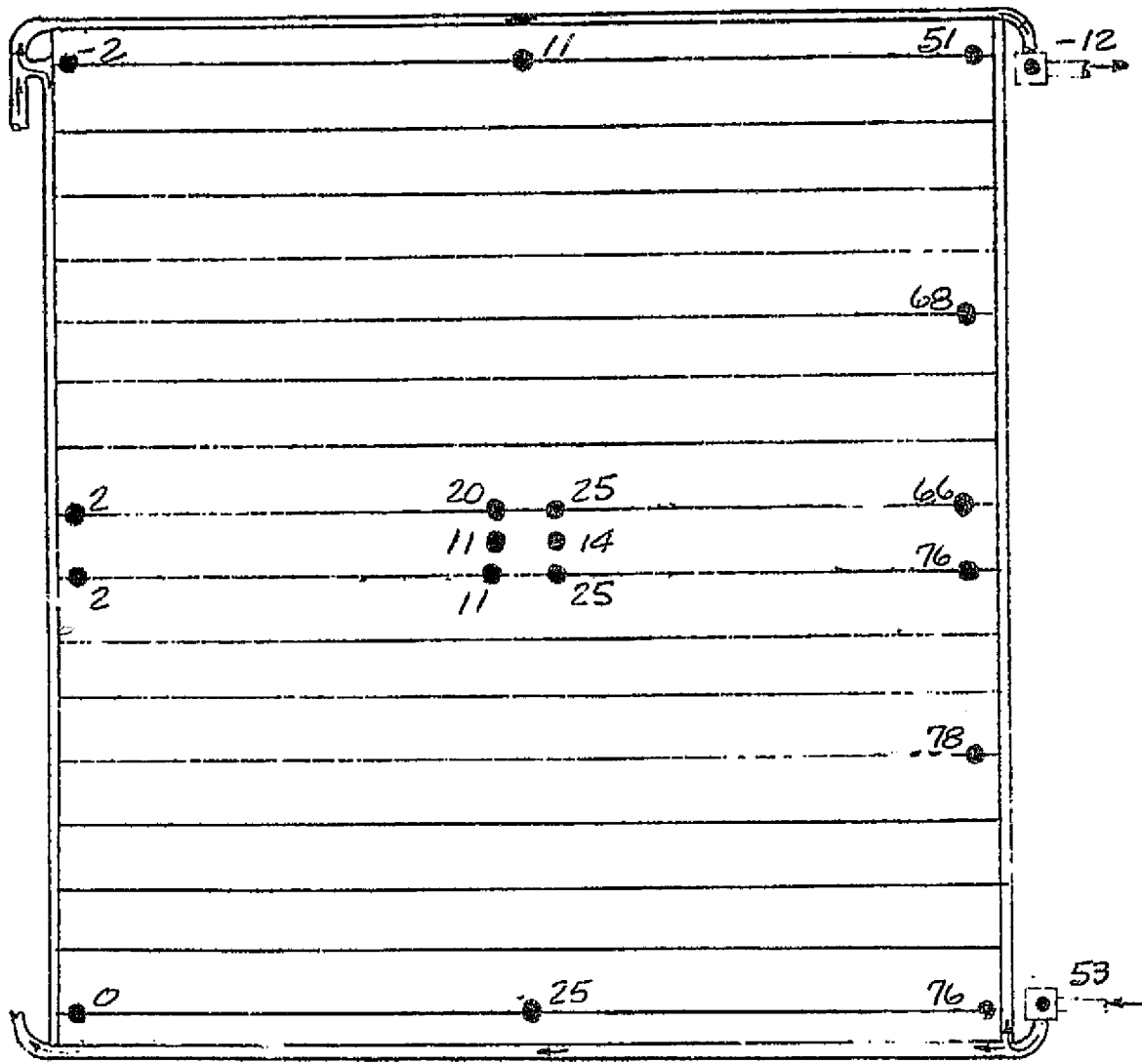
Fe$_{12}$ Return

Fe$_{12}$ Supply

PANEL NO. 4

FIGURE A8 (CONT'D)·

TEST POINT _102_
DAY _308_
TIME _15:00:05_
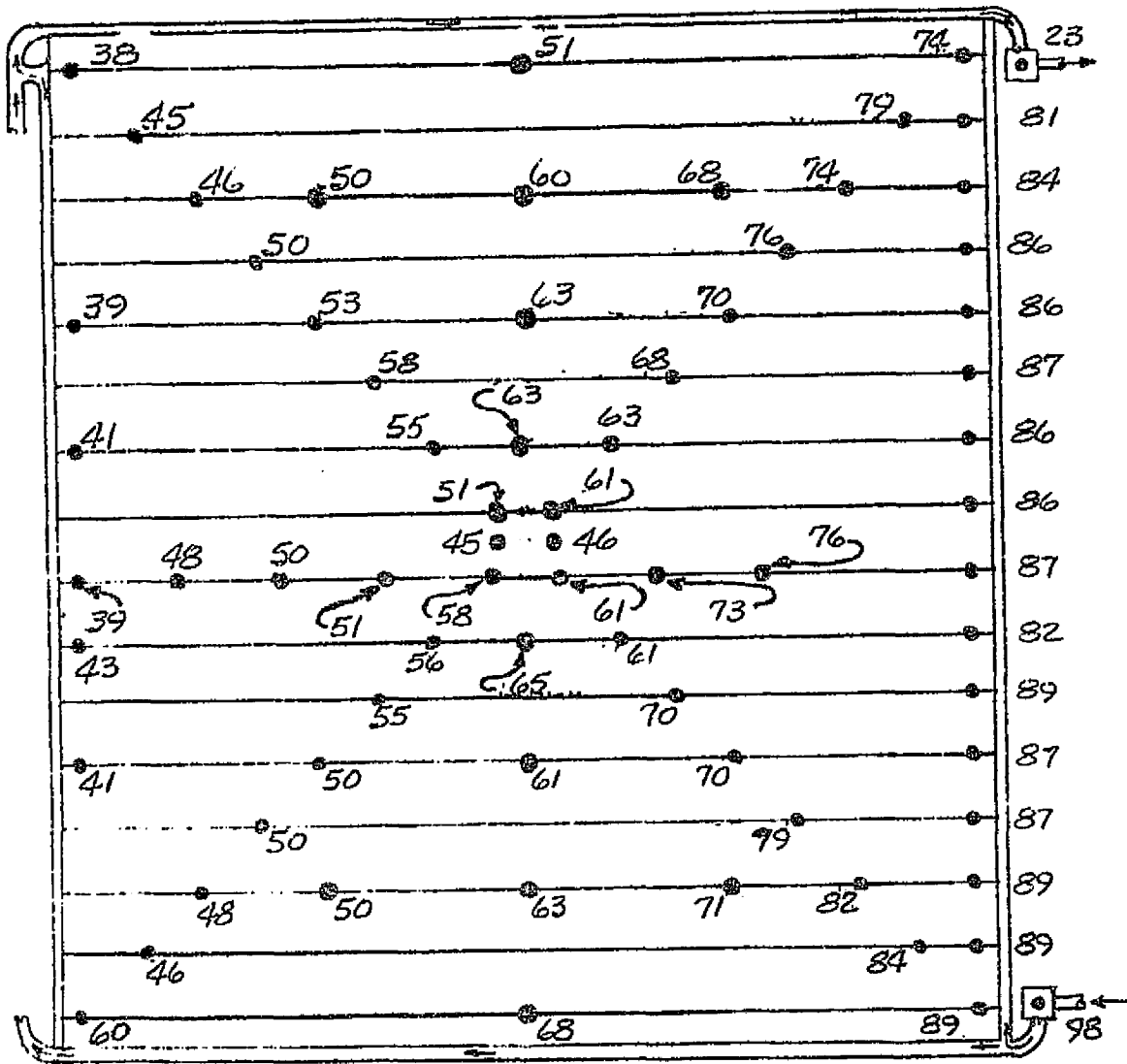
Fe$_{12}$ Return

PANEL NO. 1

FIGURE A9

STEADY STATE LIQUID RADIATOR OPERATION PANEL TEMPERATURE MAPS

TEST POINT _102_

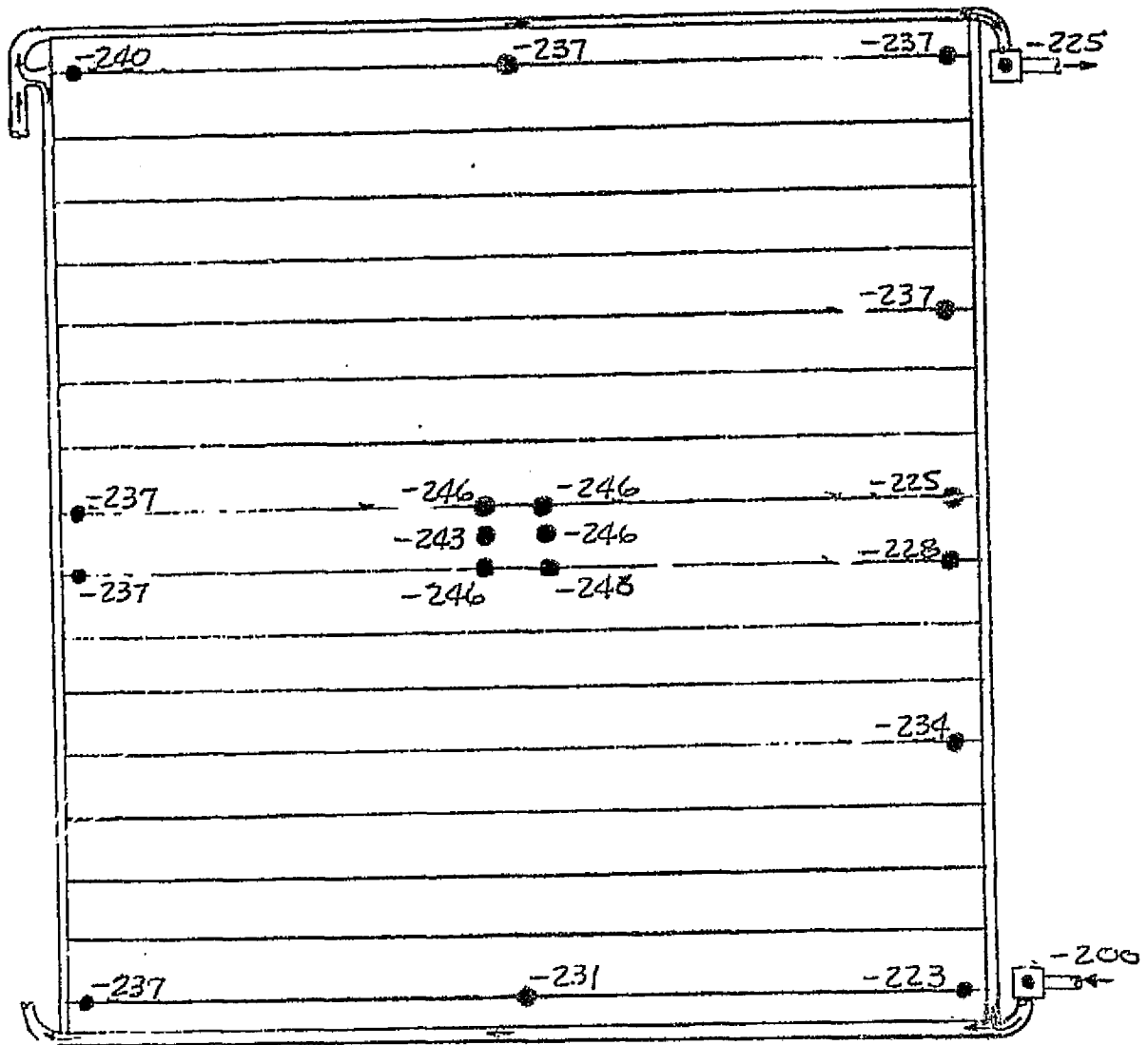DAY _308_
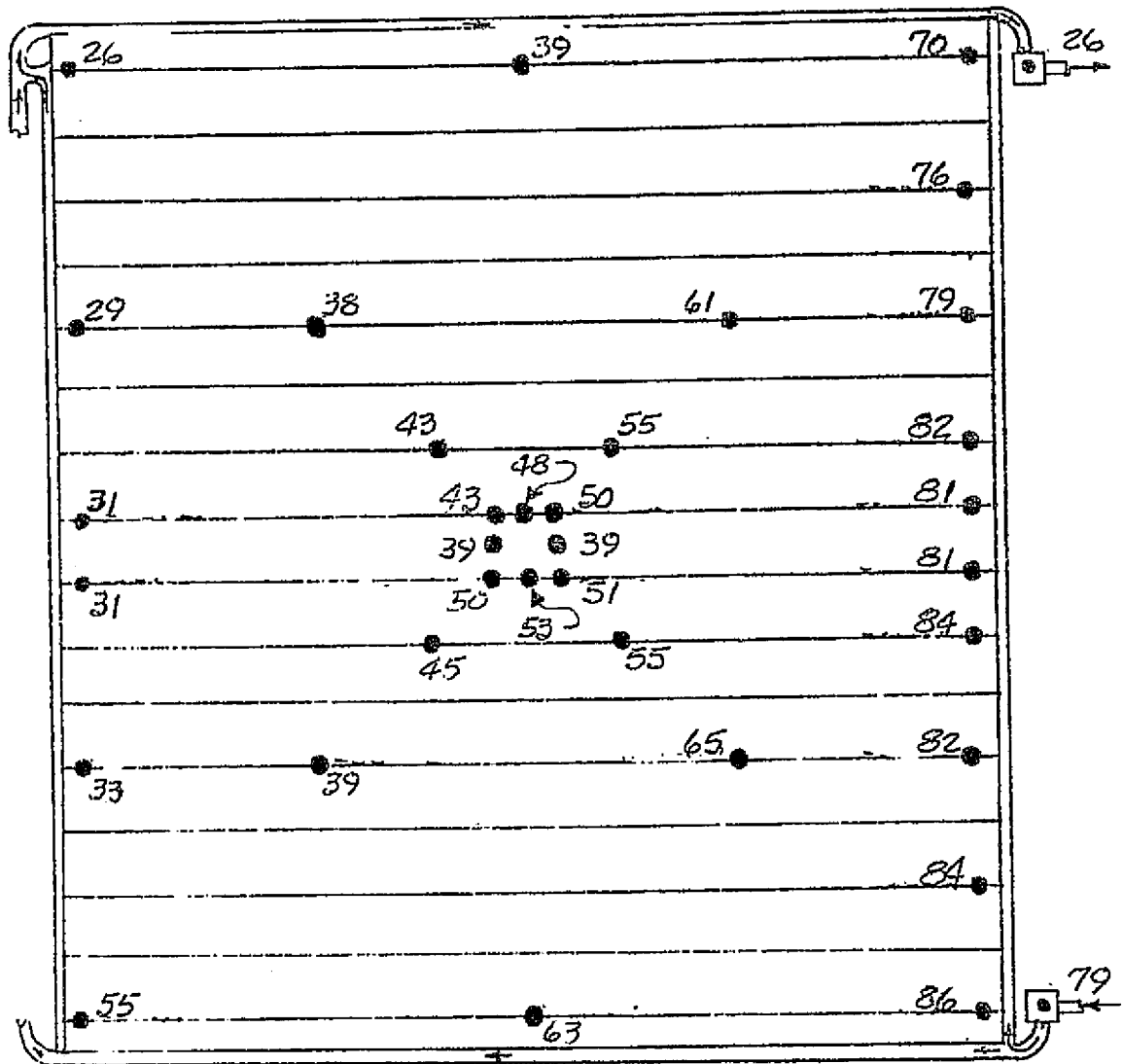
TIME _15:00:05_

Fe$_{12}$ Return

PANEL NO. 2

FIGURE A9 (CONT'D)

TEST POINT _102_

DAY _308_

TIME _15:00:05_

Fe$_{12}$ Return

17   31   61   19

73

17   36 41   78
     29 31
19   38 41   81

79

43   55   82   92
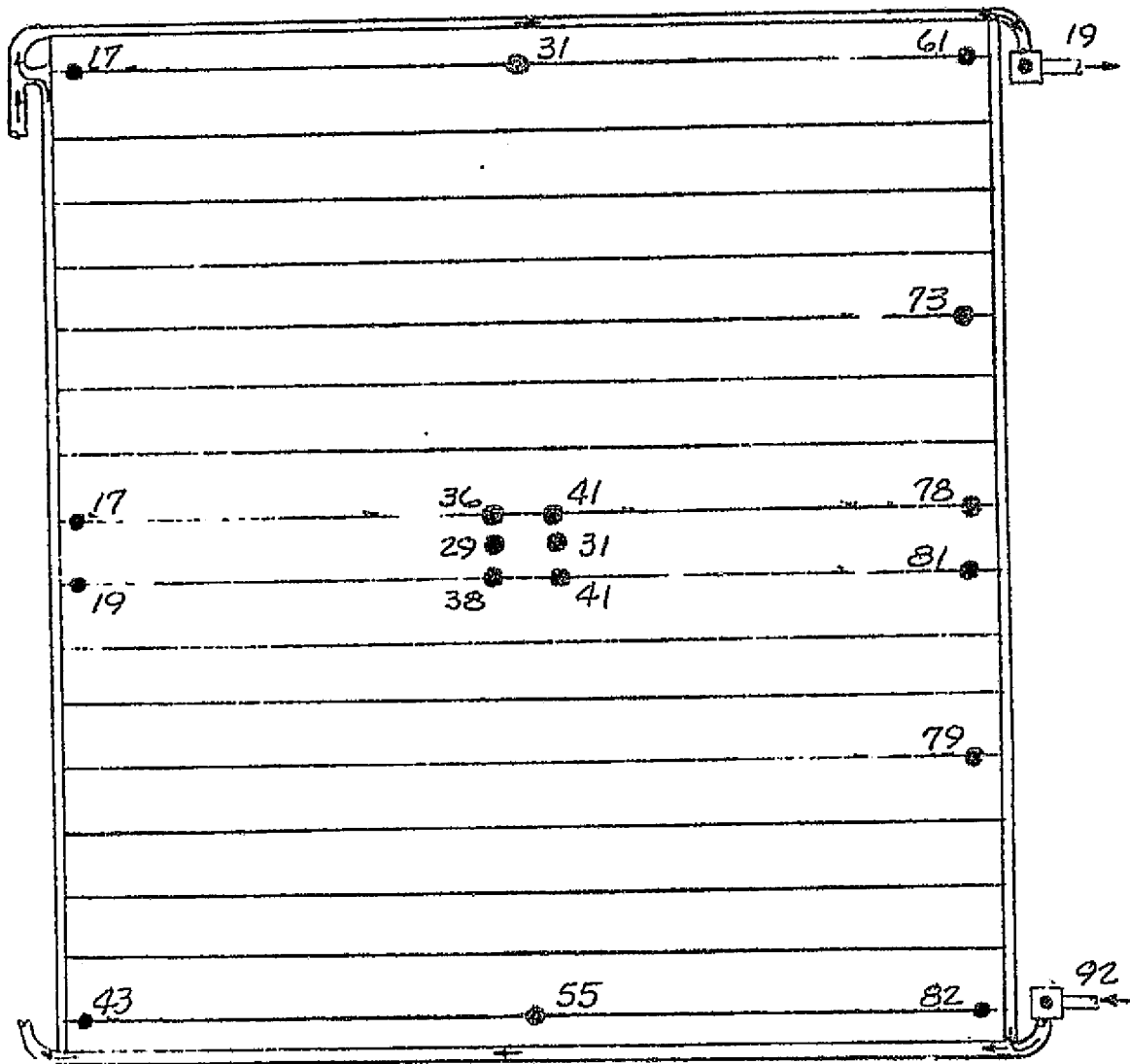
Fe$_{12}$ Supply

PANEL NO. 3

FIGURE A9 (CONT'D)

A-36

TEST POINT _102_

DAY _308_

TIME _15:00:05_

Fe$_{12}$ Return

−7   9   49   −16

64

0   16 20   62

9 11   73

0   9 25

74

−2   25   73   50
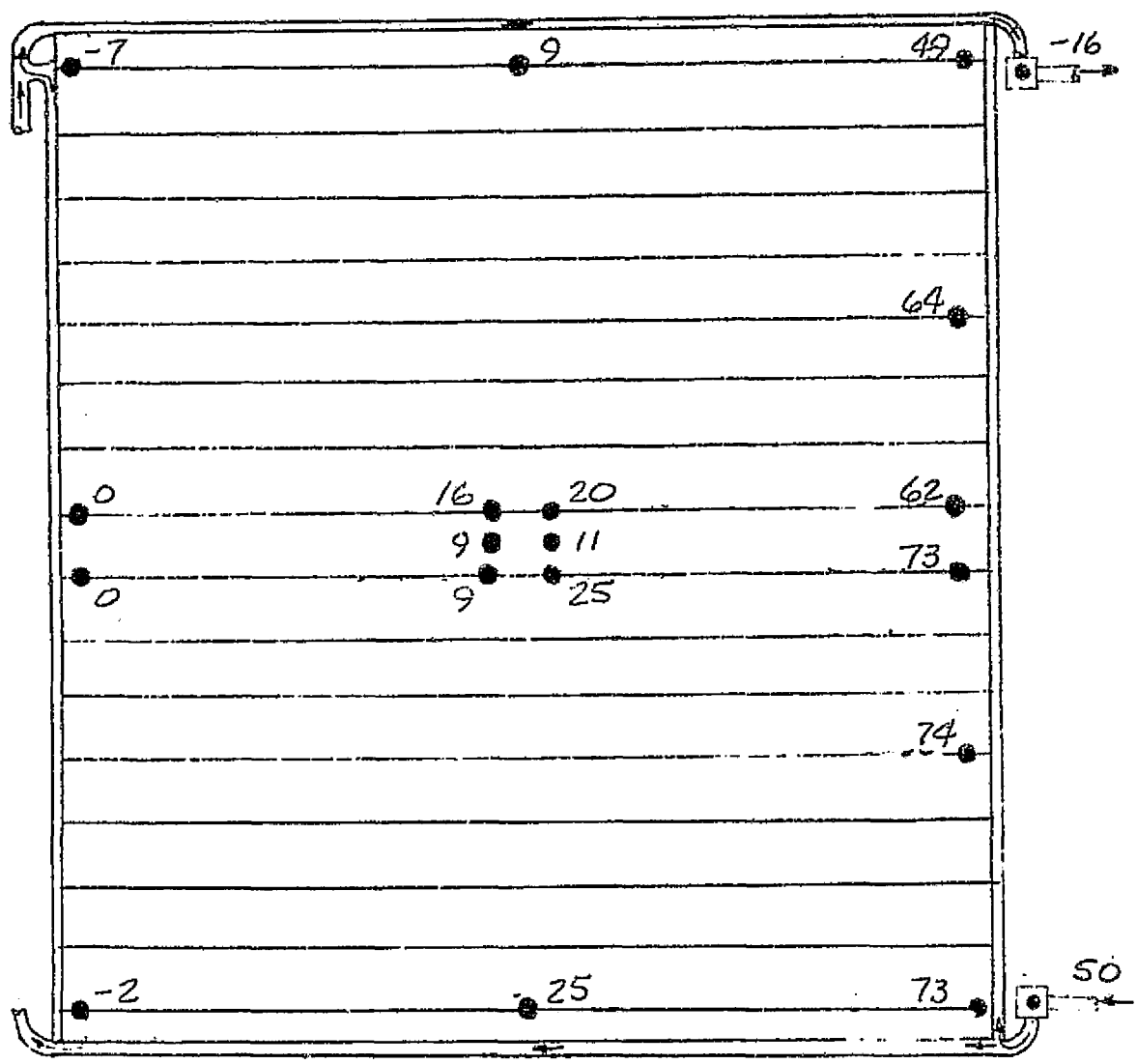
Fe$_{12}$ Supply

PANEL NO. 4

FIGURE A9 (CONT'D)

A-37

TEST POINT _103_

DAY _308_

TIME _18:00:05_

Fe$_{12}$ Return
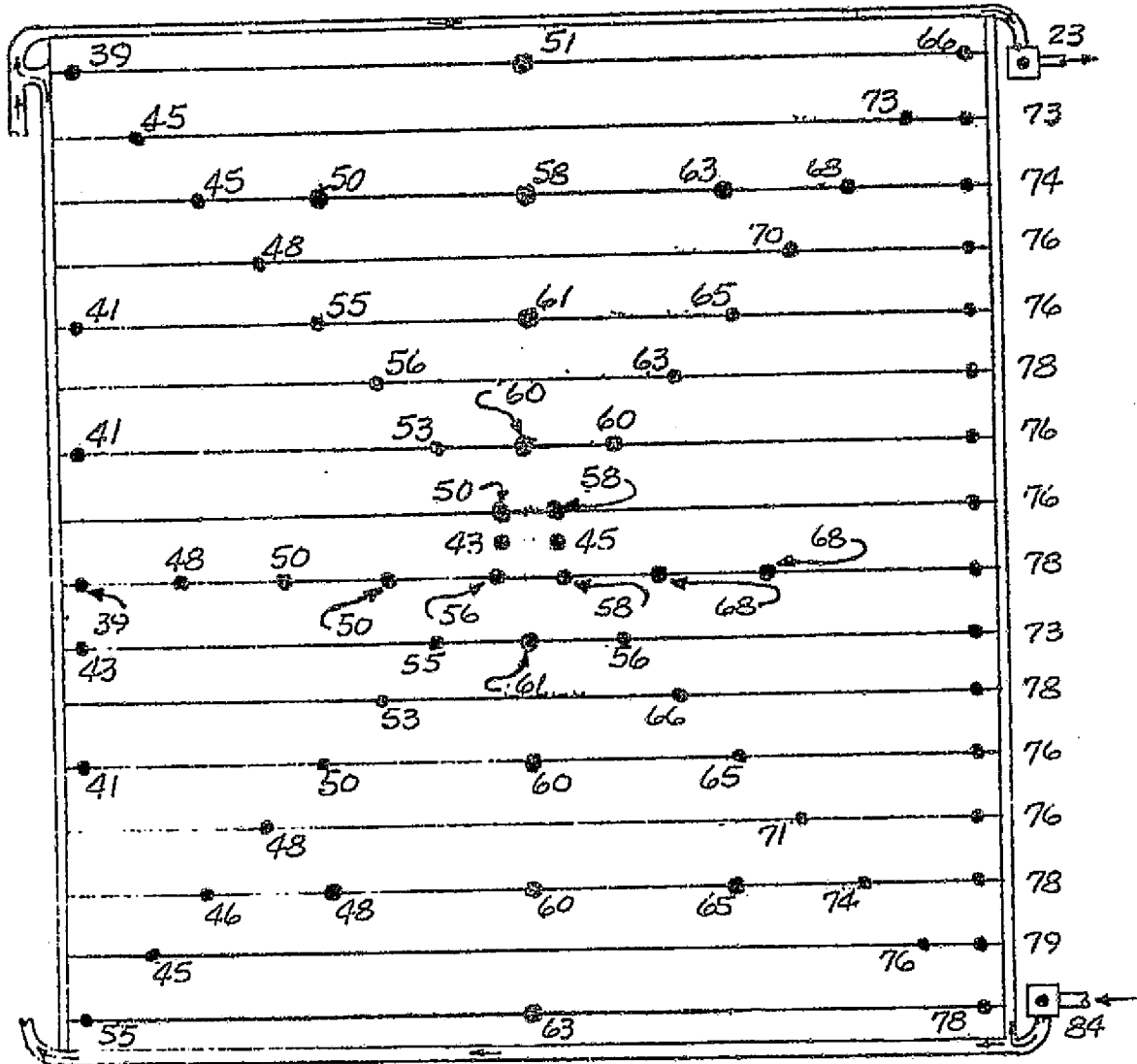
Fe$_{12}$ Supply

PANEL NO. 1

FIGURE A10

STEADY STATE LIQUID RADIATOR OPERATION PANEL TEMPERATURE MAPS

TEST POINT ___103___

DAY ___308___
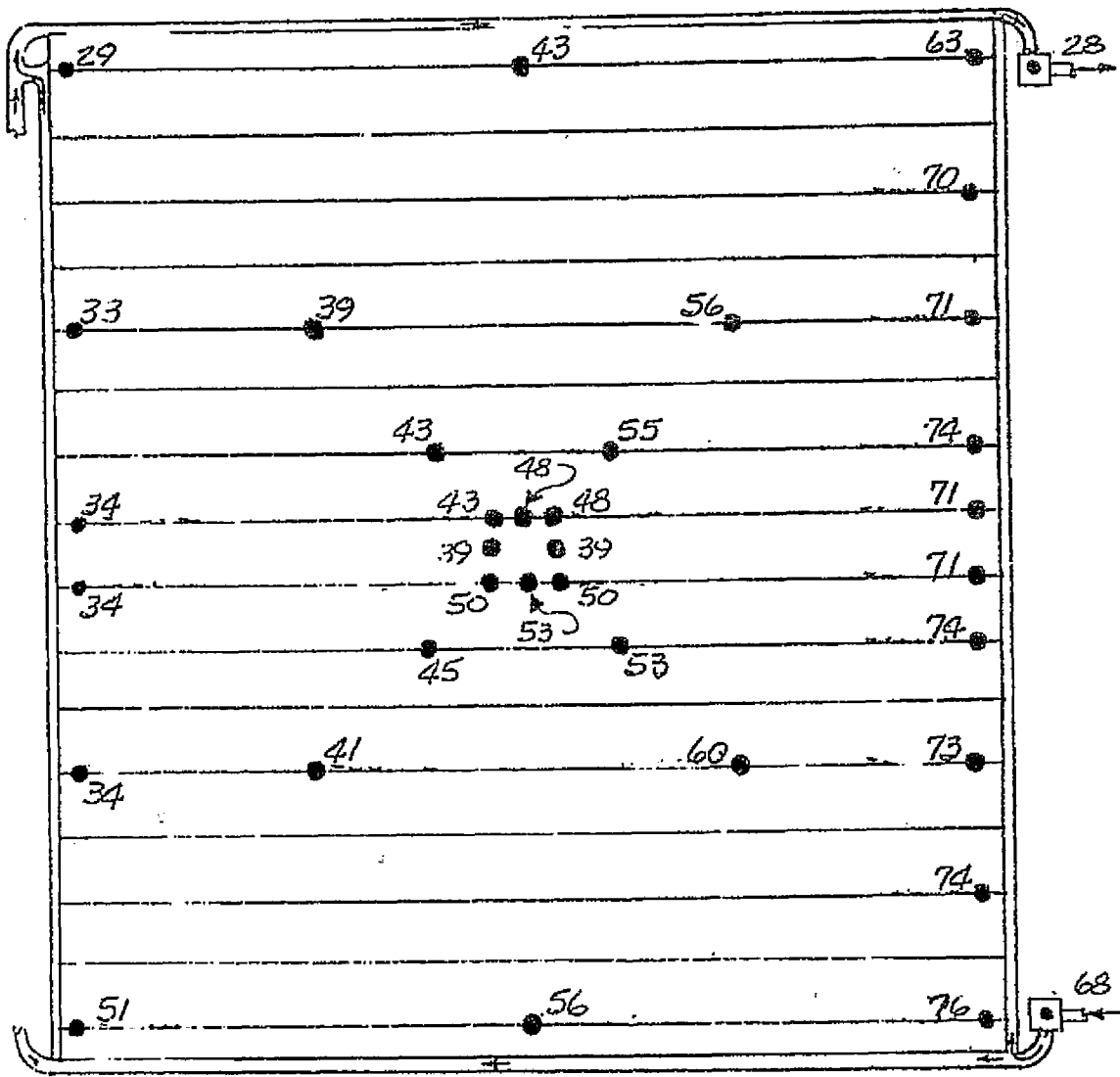
TIME ___15:00:05___   Fe$_{12}$ Return

PANEL NO. 2

FIGURE A10 (CONT'D)

Fe$_{12}$ Supply

A-39

TEST POINT ___103___

DAY ___308___

TIME ___15:00:05___

Fe_{12} Return

PANEL NO. 3

FIGURE A10 (CONT'D)

Fe_{12} Supply

A-40

TEST POINT ___103___

DAY ___308___

TIME ___15:00:05___

Fe_{12} Return

PANEL NO. 4

FIGURE A10 (CONT'D)

TEST POINT ___108___

DAY ___309___
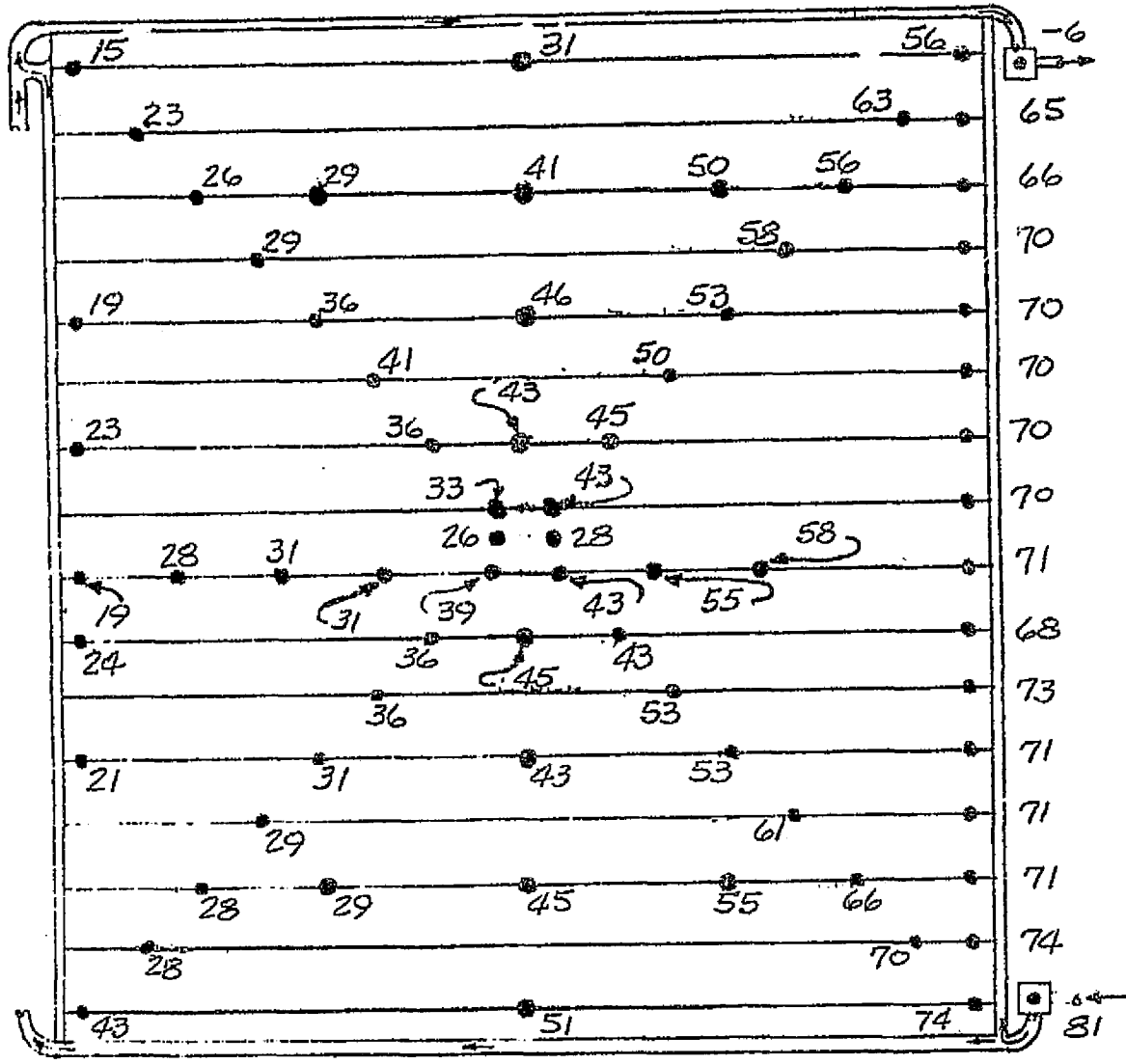
TIME ___12:45:06___

Fe$_{12}$ Return

PANEL NO. 1

FIGURE A11

STEADY STATE LIQUID RADIATOR OPERATION PANEL TEMPERATURE MAPS

TEST POINT _108_

DAY _309_
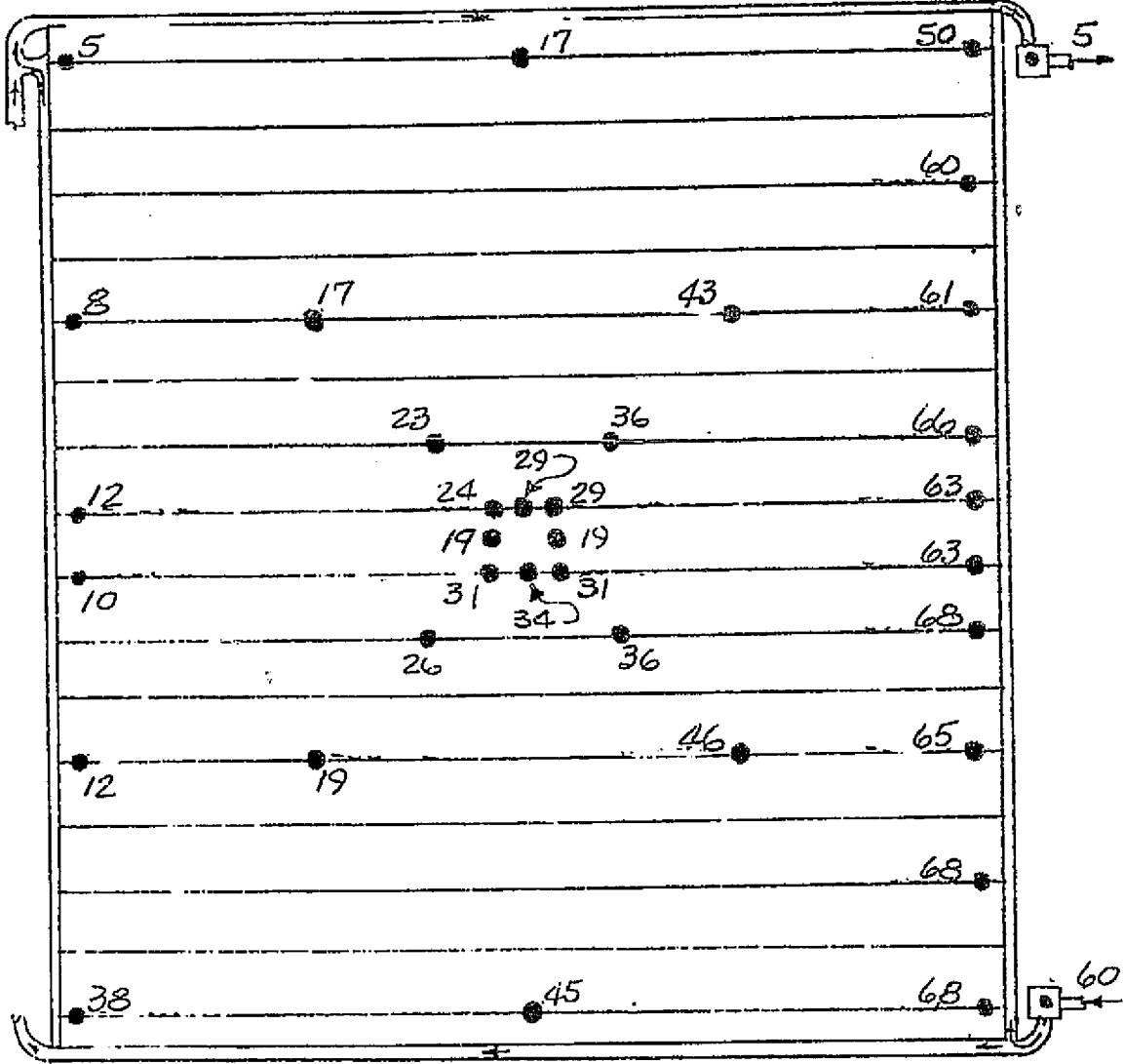
TIME _12:45:06_

Fe_{12} Return

PANEL NO. 2

FIGURE A11 (CONT'D)

Fe_{12} Supply

A-43

TEST POINT ___108___
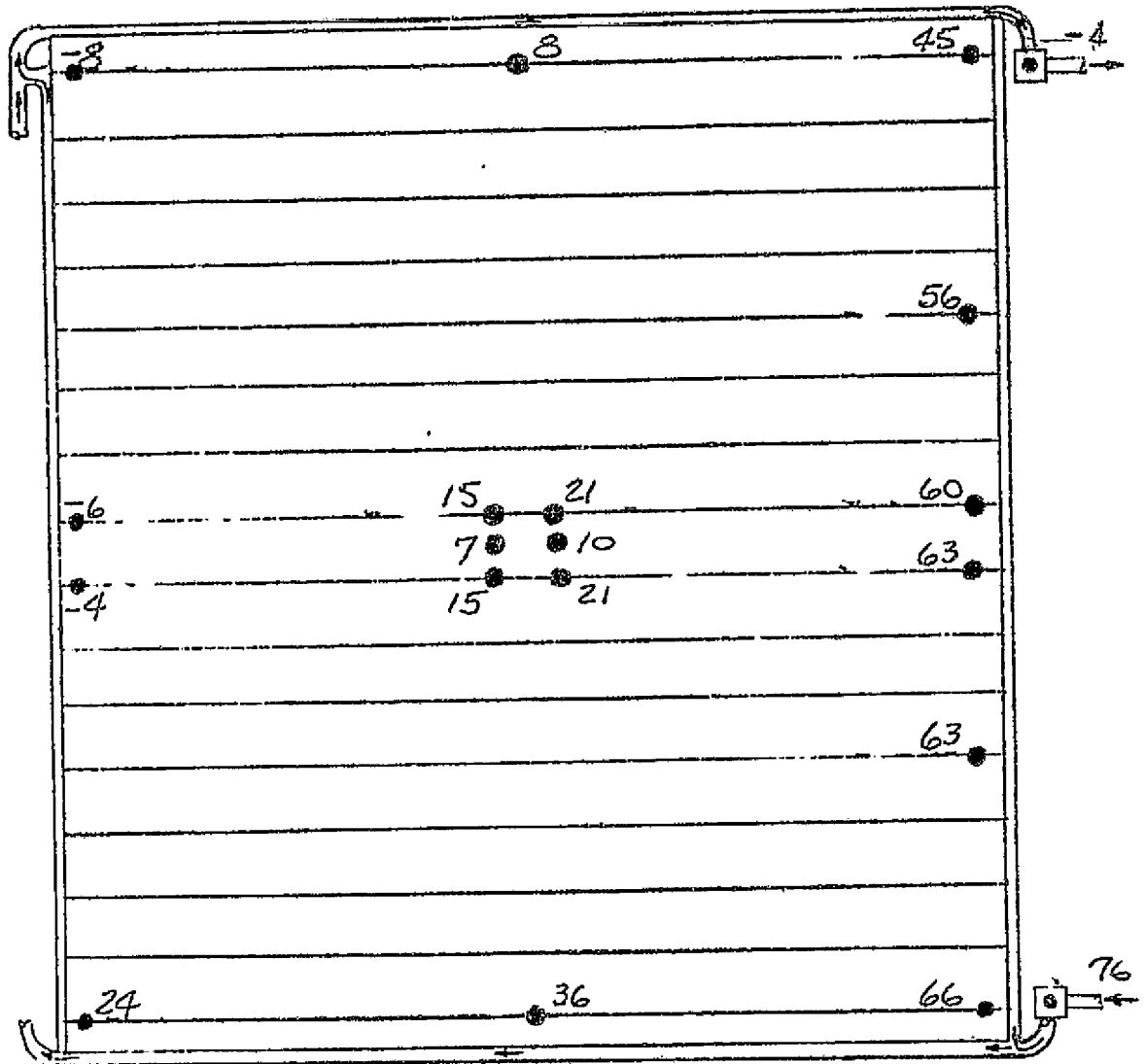
DAY ___309___

TIME ___12:45:06___

Fe_{12} Return

PANEL NO. 3

FIGURE A11 (CONT'D)

Fe_{12} Supply

A-44

TEST POINT ___108___

DAY ___309___

TIME ___12:45:06___

Fe_{12} Return

PANEL NO. 4

FIGURE A11 (CONT'D)

A-45
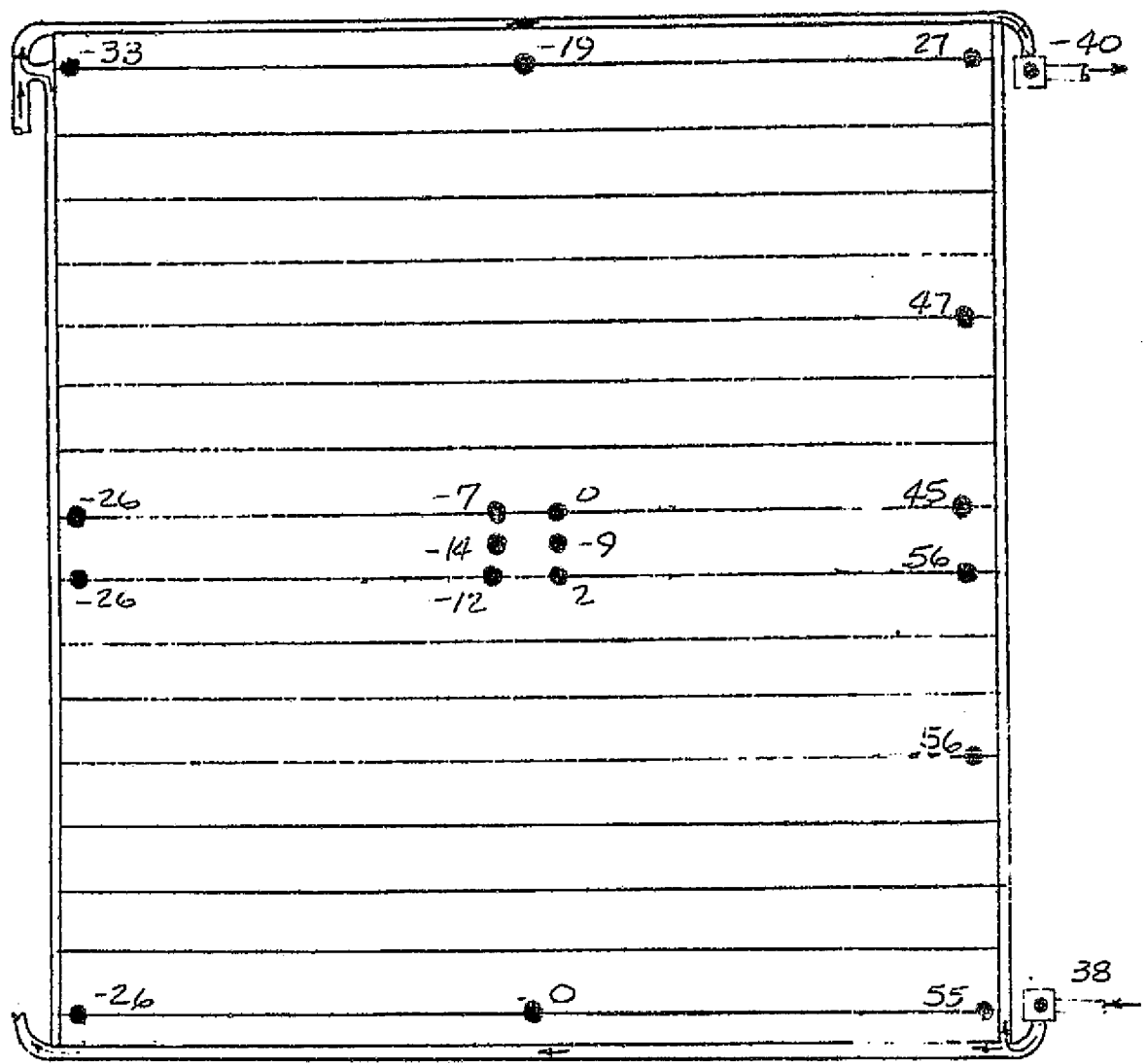
TEST POINT _109_

DAY _309_

TIME _11:15:06_
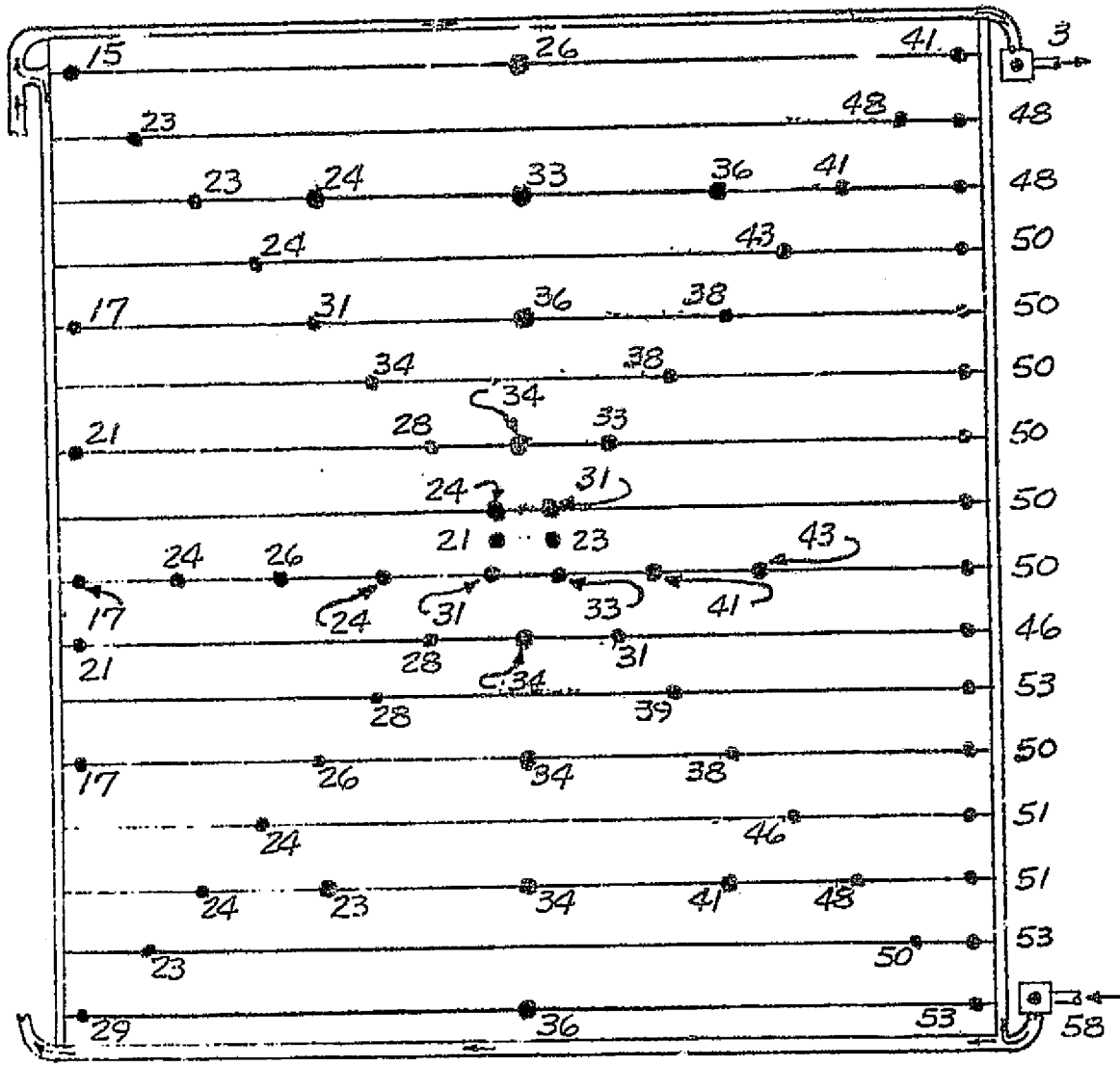
Fe$_{12}$ Return

Fe$_{12}$ Supply

PANEL NO. 1

FIGURE A12

STEADY STATE LIQUID RADIATOR OPERATION PANEL TEMPERATURE MAPS

A-46

TEST POINT ___109___
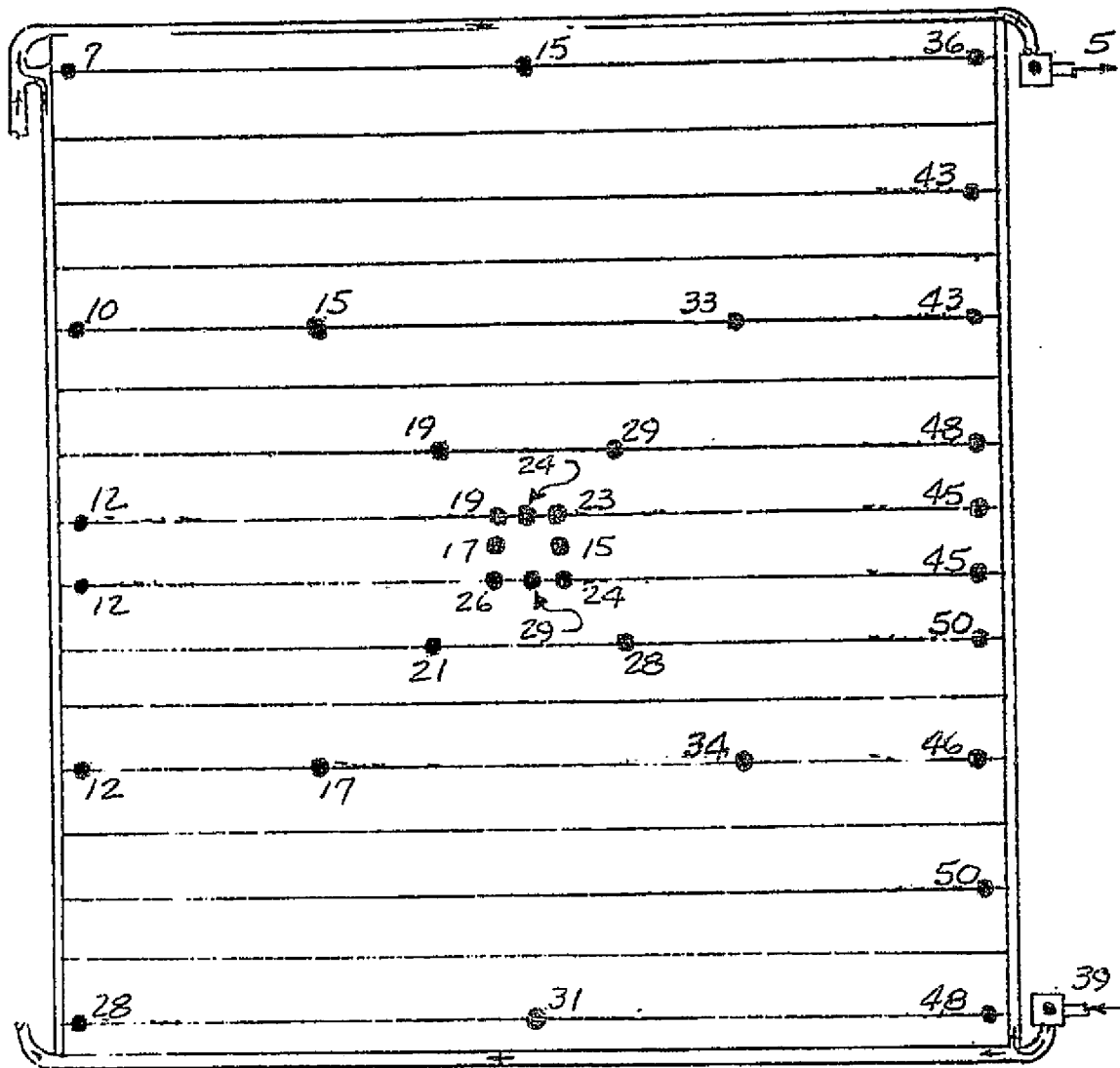
DAY ___309___

TIME ___11:15:06___

Fe$_{12}$ Return

PANEL NO. 2

FIGURE A12 (CONT'D)

Fe$_{12}$ Supply

A-47

TEST POINT ___IC___
DAY _____309_____
TIME ___11:15:06___
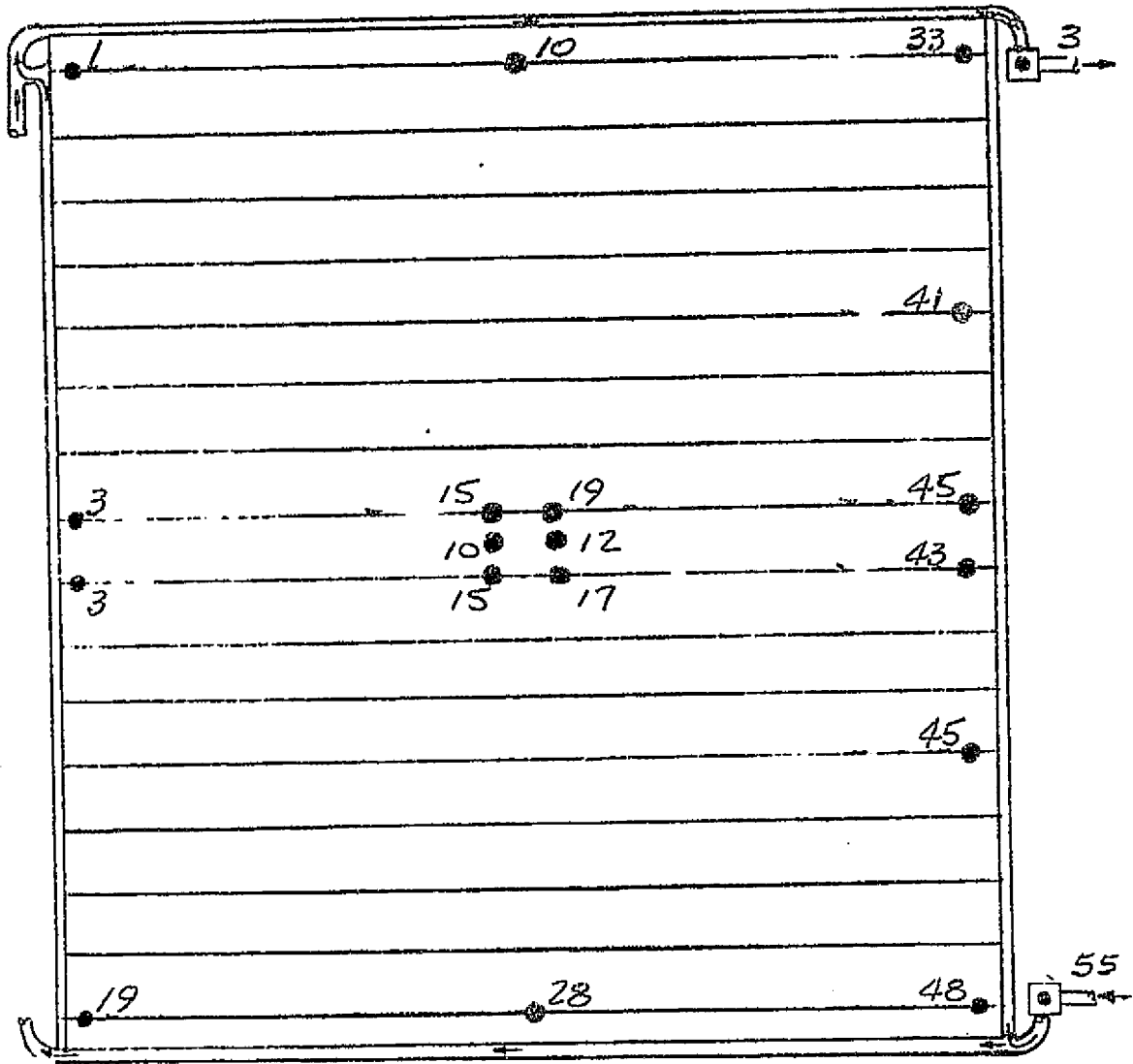
Fe_{12} Return

PANEL NO. 3

FIGURE A12 (CONT'D)

Fe_{12} Supply

TEST POINT ___109___

DAY ___309___

TIME ___11:15:06___

Fe$_{12}$ Return

-21   -9   18   -31

34

-16   -2   0   29

-9   -7

-16   -9   2   41

43

-19   2   41   23

Fe$_{12}$ Supply

PANEL NO. 4

FIGURE A12 (CONT'D)

TEST POINT _110_

DAY _309_

TIME _10:30:06_
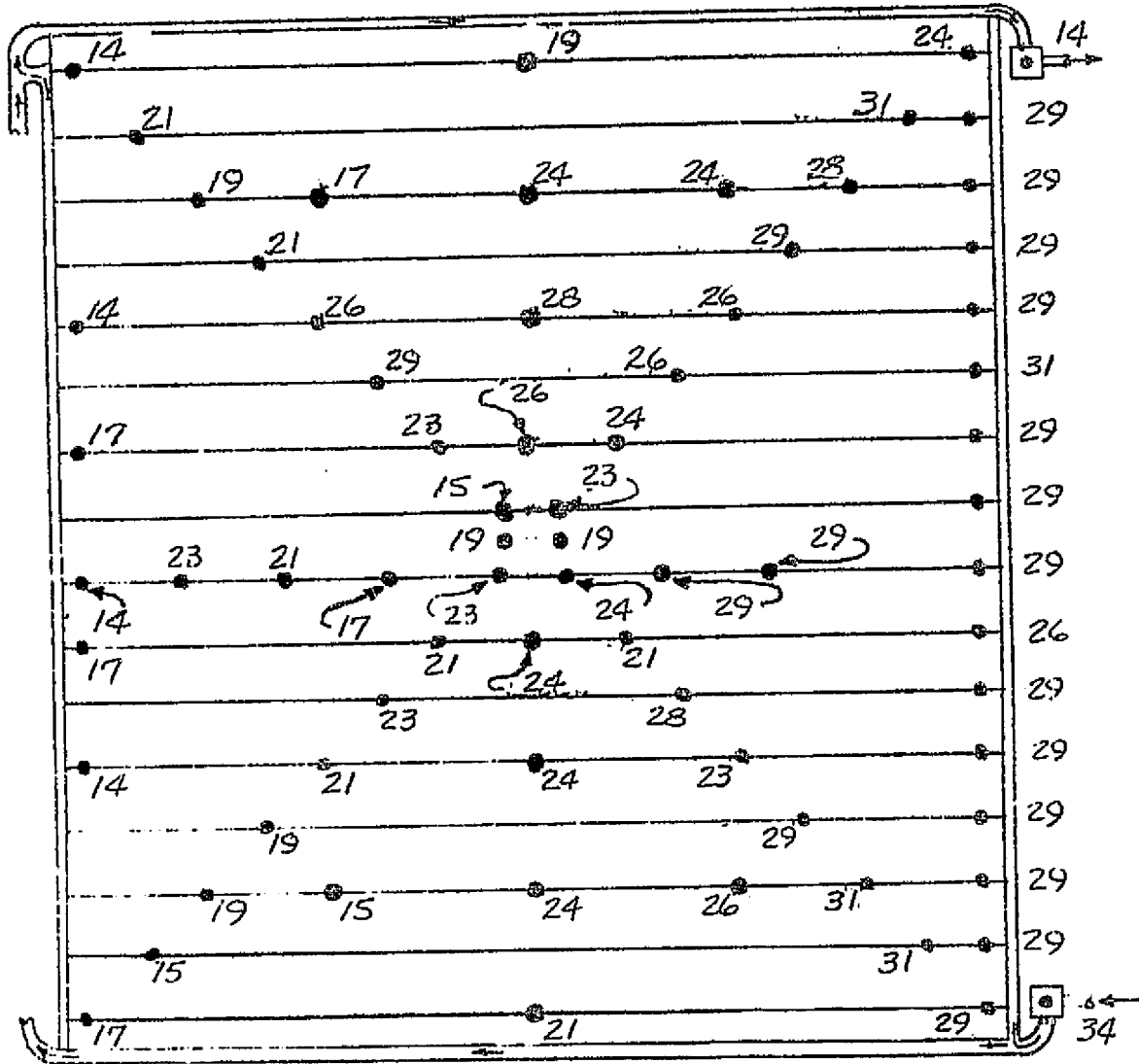
Fe$_{12}$ Return

Fe$_{12}$ Supply

PANEL NO. 1

FIGURE A13

STEADY STATE LIQUID RADIATOR OPERATION PANEL TEMPERATURE MAPS

TEST POINT __110__

DAY __309__
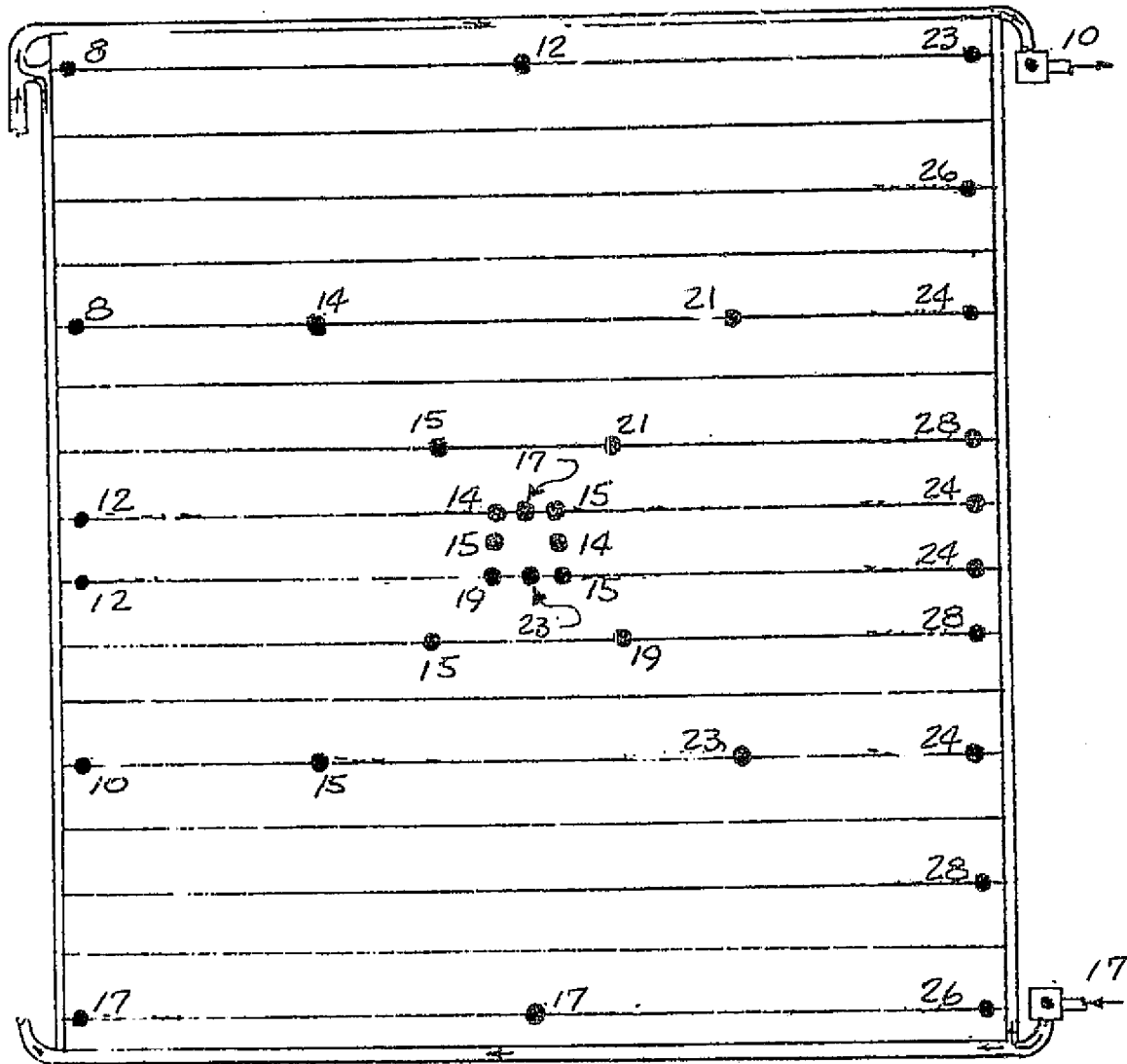
TIME __10:30:06__

Fe_{12} Return

PANEL NO. 2

FIGURE A13 (CONT'D)

Fe_{12} Supply

A-51

TEST POINT __110__

DAY __309__

TIME __10:30:06__

Fe$_{12}$ Return

8   10   19   10

23

8   14   15   26

14   14   26

8   15   15

26

15   15   28   33
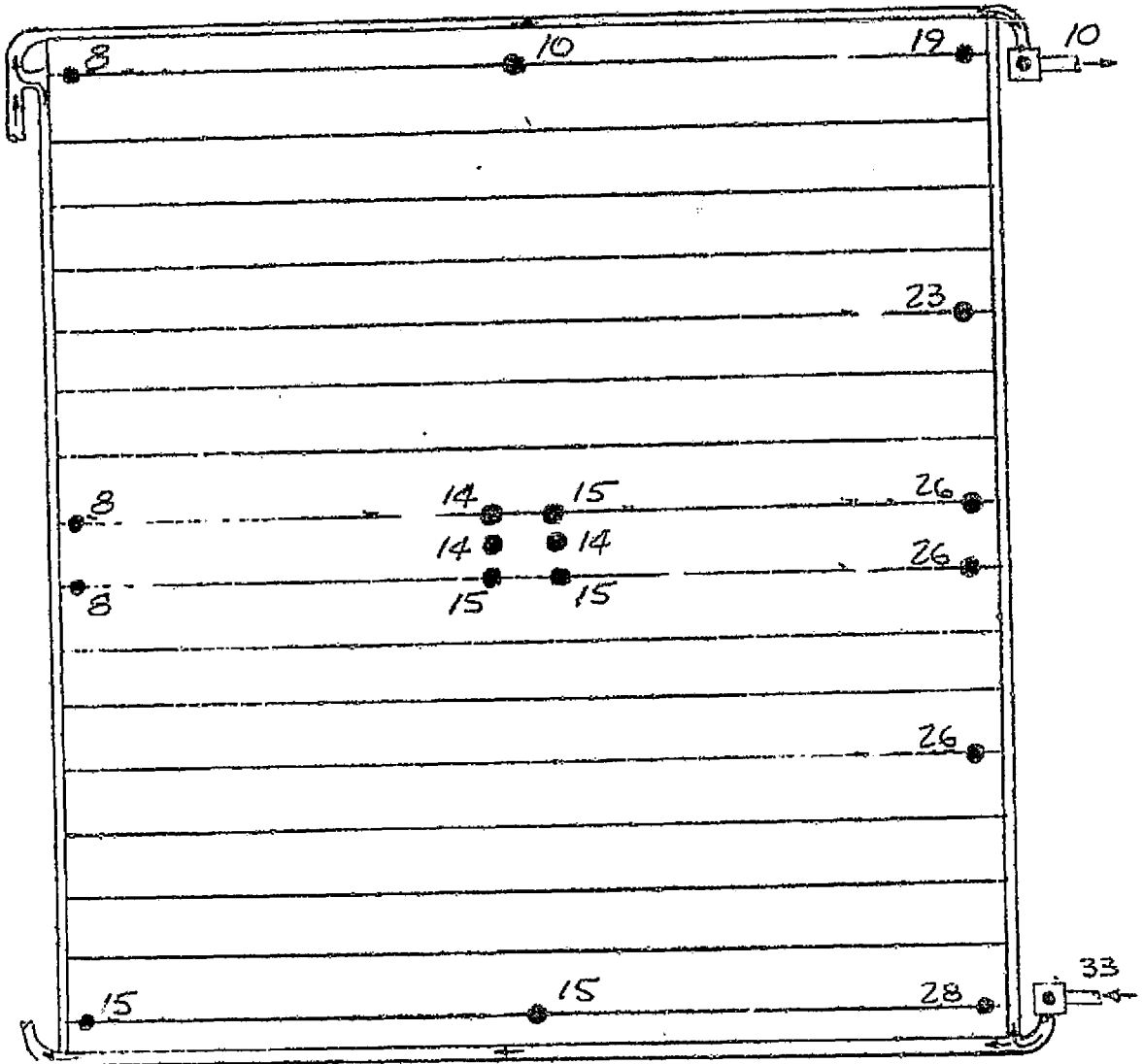
Fe$_{12}$ Supply

PANEL NO. 3

FIGURE A13 (CONT'D)

A-52

TEST POINT ___110___

DAY ___309___

TIME ___10:30:06___
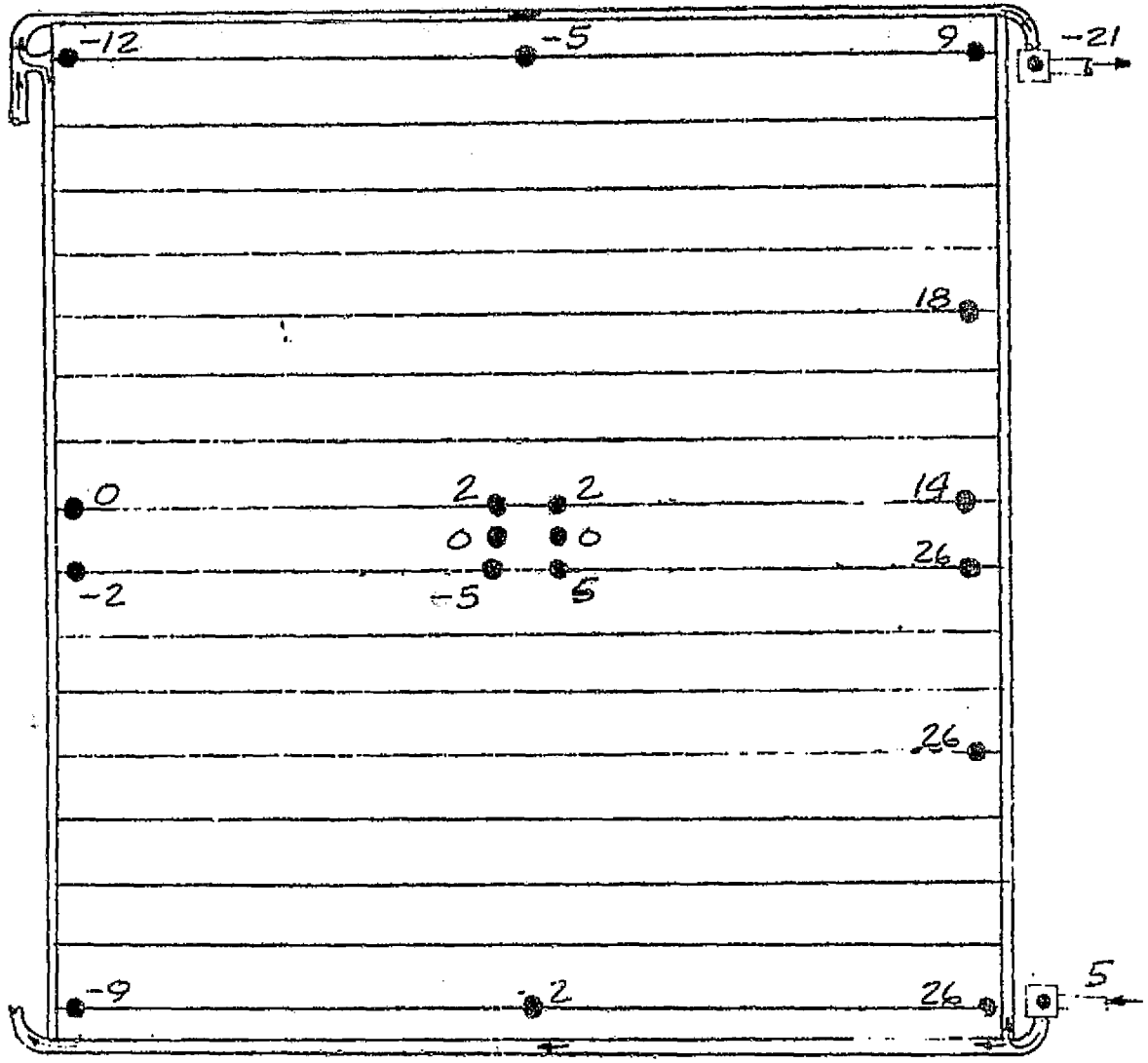
Fe$_{12}$ Return

PANEL NO. 4

FIGURE A13 (CONT'D)

Fe$_{12}$ Supply

A-53

TEST POINT ___114___
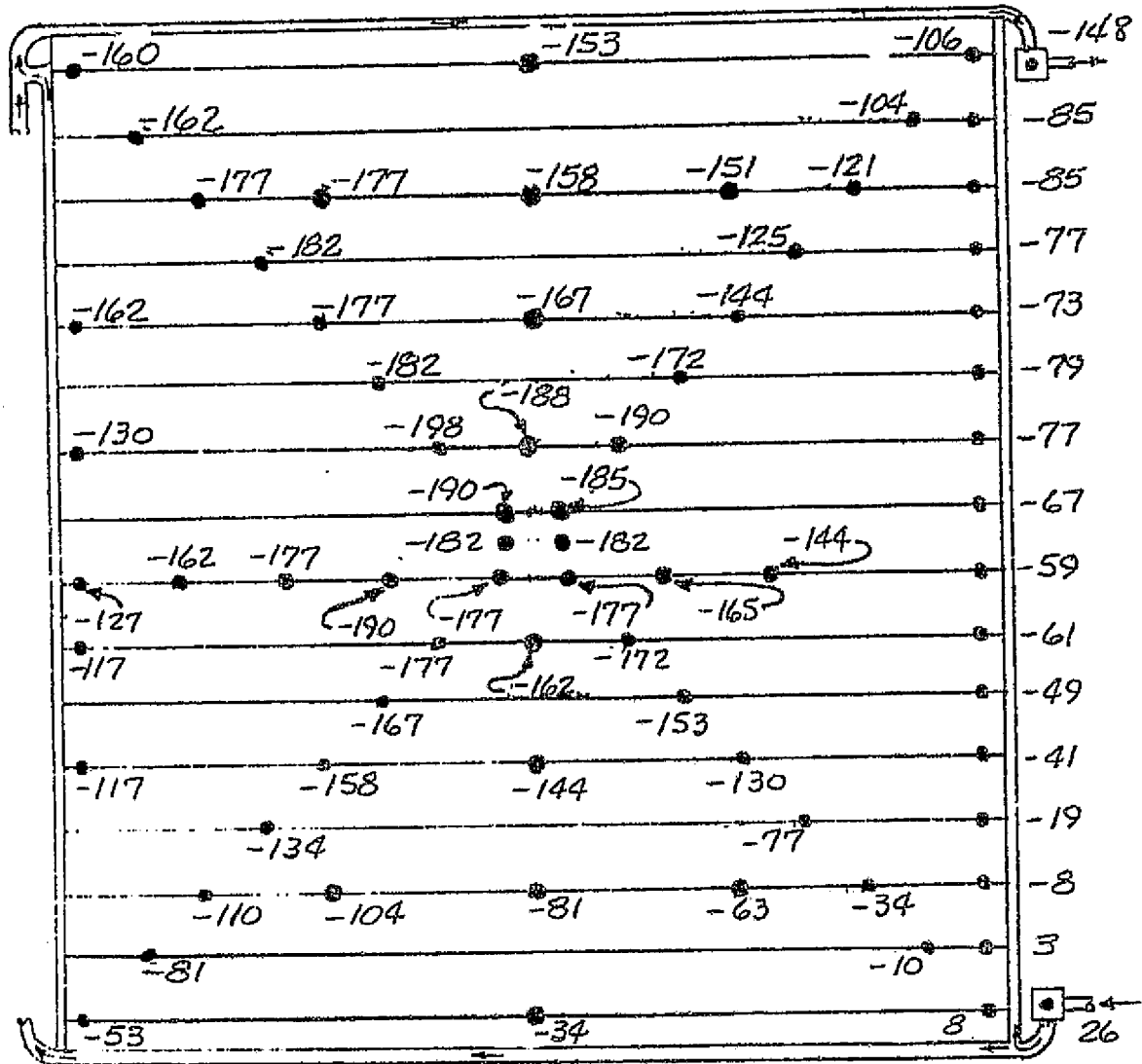
DAY ___310___

TIME ___7:15:06___

Fe$_{12}$ Return

PANEL NO. 1

FIGURE A14

STEADY STATE LIQUID RADIATOR OPERATION PANEL TEMPERATURE MAPS

A-54

Fe$_{12}$ Return

-167   -182   -175   -172

-165

-170   -203   -193   -158

-200   -193   -132

-188

-167   -190   -193   -130

-185   -190

-167   -180   -182   -125

-177   -117

-188   -180

-151   -182   -165   -112

-93

-95   -97   -75   -34
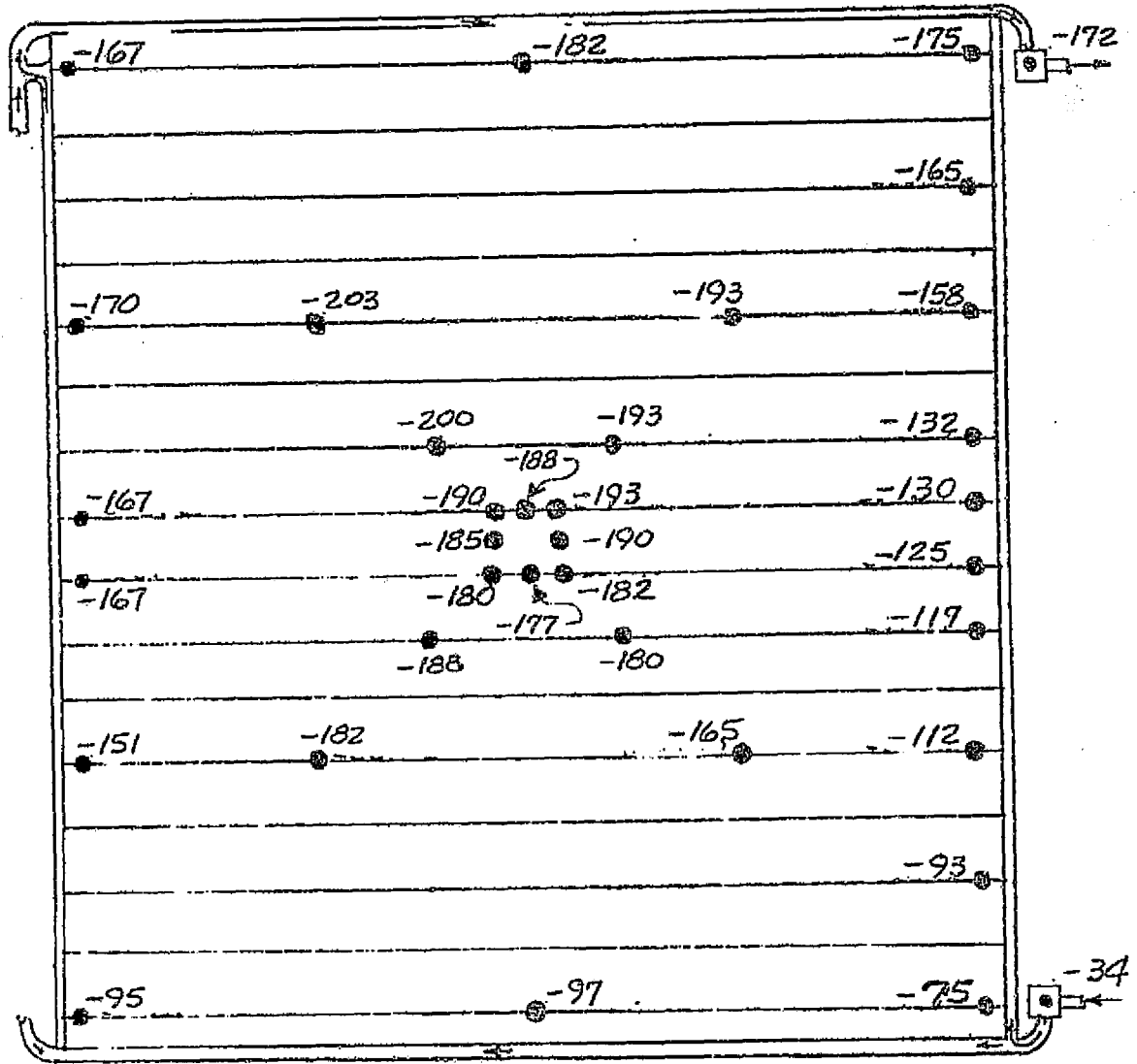
Fe$_{12}$ Supply

PANEL NO. 2

FIGURE A14 (CONT'D)

TEST POINT _114_

DAY _310_

TIME _7:15:06_

Fe$_{12}$ Return

PANEL NO. 3

FIGURE A14 (CONT'D)

Fe$_{12}$ Supply

TEST POINT ___114___

DAY ___310___

TIME ___7:15:06___

Fe$_{12}$ Return

-267   -258   -258   -217

-254

-262   -271   -271   -254

-271   -271   -214

-267   -271   -271

-214

-267   -258   -203   -177
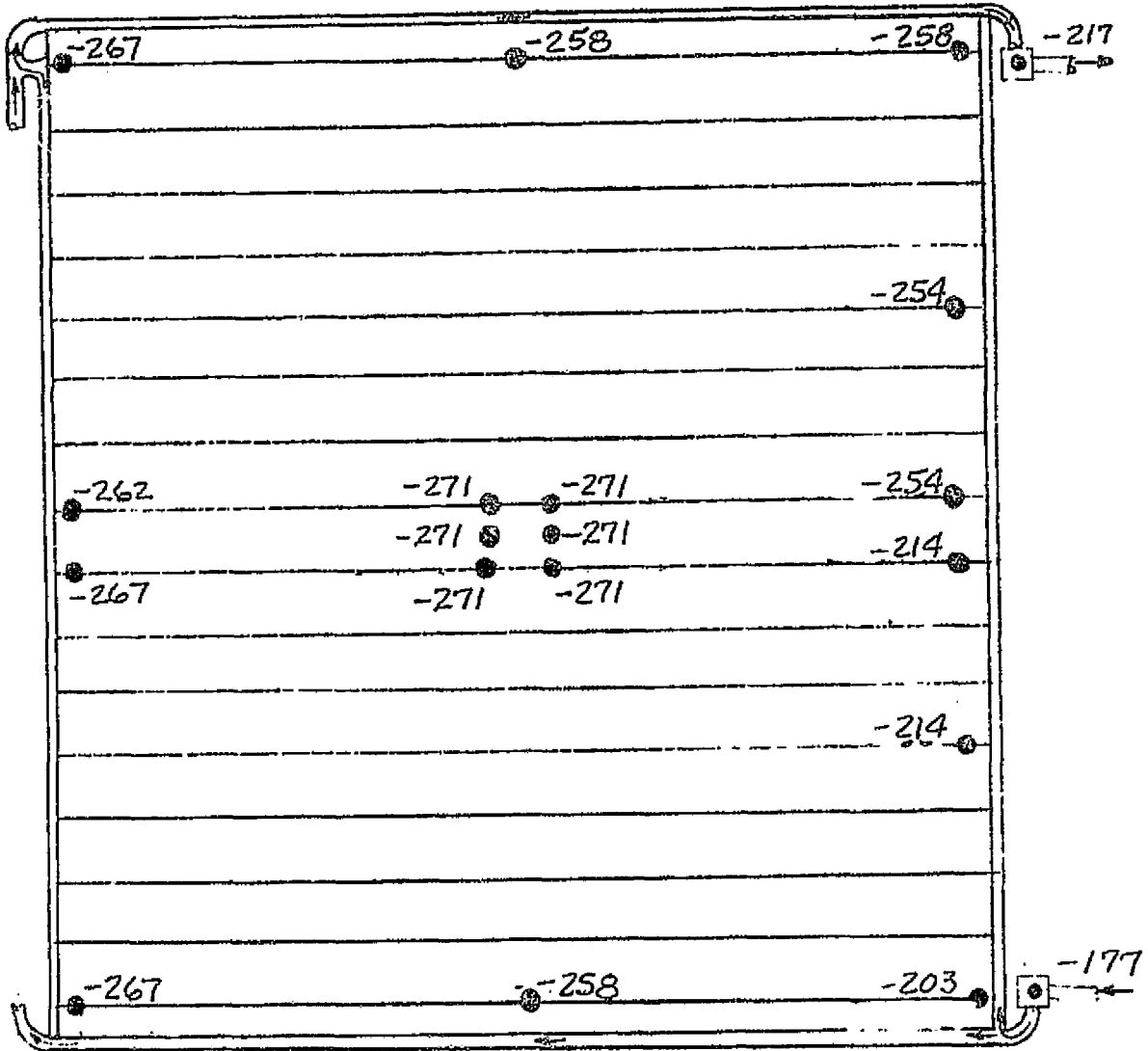
Fe$_{12}$ Supply

PANEL NO. 4

FIGURE A14 (CONT'D)

TEST POINT _115_

DAY _310_

TIME _11:30:06_

Fe$_{12}$ Return

-172   -177   -167   -170

-185   -167   -158

-200 -206   -190   -198 -175   -158

-206   -182   -151

-188   -200   -198   -193   -144

-195   -188   -134

-200

-172   -212   -203   -130

-206   -203   -123

-185 -198   -200   -167   -167   -117

-167   -209   -193   -195   -185   -110

-158   -200   -185   -195   -99

-193   -182   -91

-155   -188   -188   -170   -77

-172   -182   -55

-153 -148   -130   -119   -83   -38

-132   -182

-110   -79   -19   5
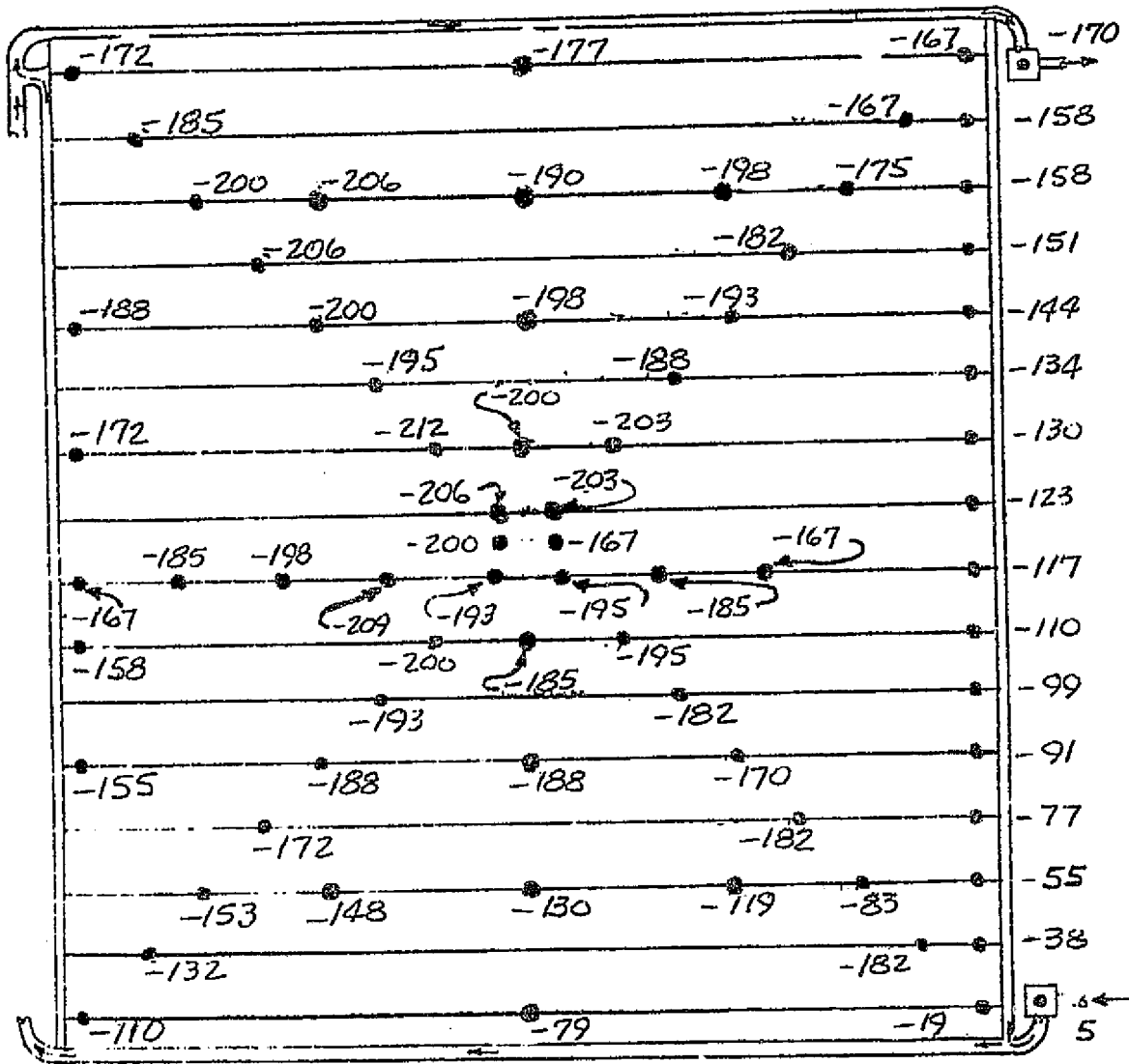
Fe$_{12}$ Supply

PANEL NO. 1

FIGURE A15

STEADY STATE LIQUID RADIATOR OPERATION PANEL TEMPERATURE MAPS

A-58

TEST POINT ___115___

DAY ___310___

TIME ___11:30:06___

Fe_{12} Return

-231   -225   -231   -206

-228

-228   -231   -228   -234

-228   -228   -214

-225

-220   -223   -231   -223

-220   -228   -220

-220   -217   -225   -214

-214   -223

-221

-225   -225   -225

-228

-214

-223   -217   -209   -141
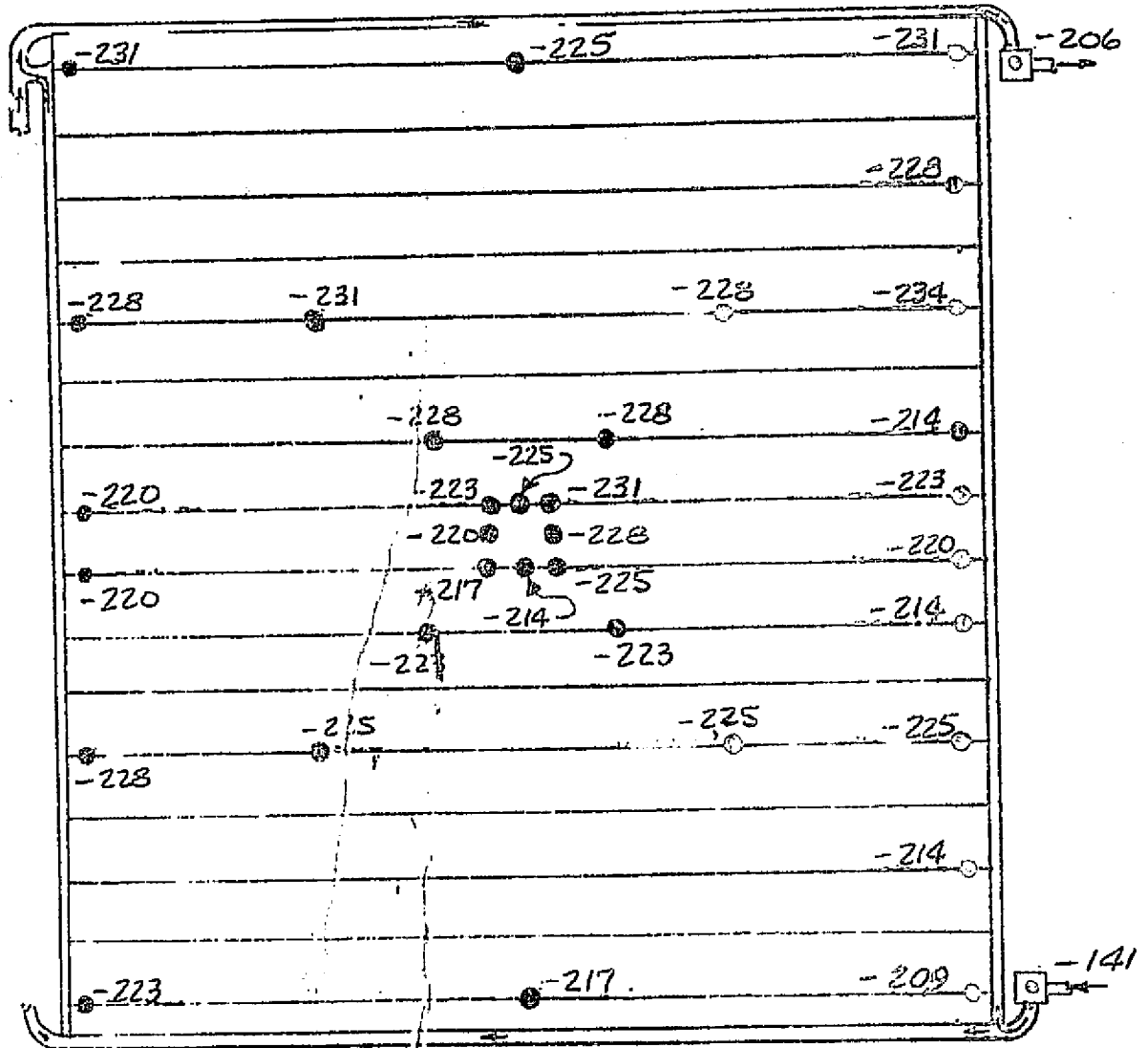
Fe_{12} Supply

PANEL NO. 2

FIGURE A15 (CONT'D)

A-59

TEST POINT _115_

DAY _310_

TIME _11:30:06_

Fe$_{12}$ Return

-240   -237   -237   -225→

-237

-237   -246   -246   -225

-243   -246   -228

-237   -246   -248   -234

-237   -231   -223   ←-200

Fe$_{12}$ Supply

PANEL NO. 3

FIGURE A15 (CONT'D)

TEST POINT ___115___

DAY ___310___

TIME ___11:30:06___
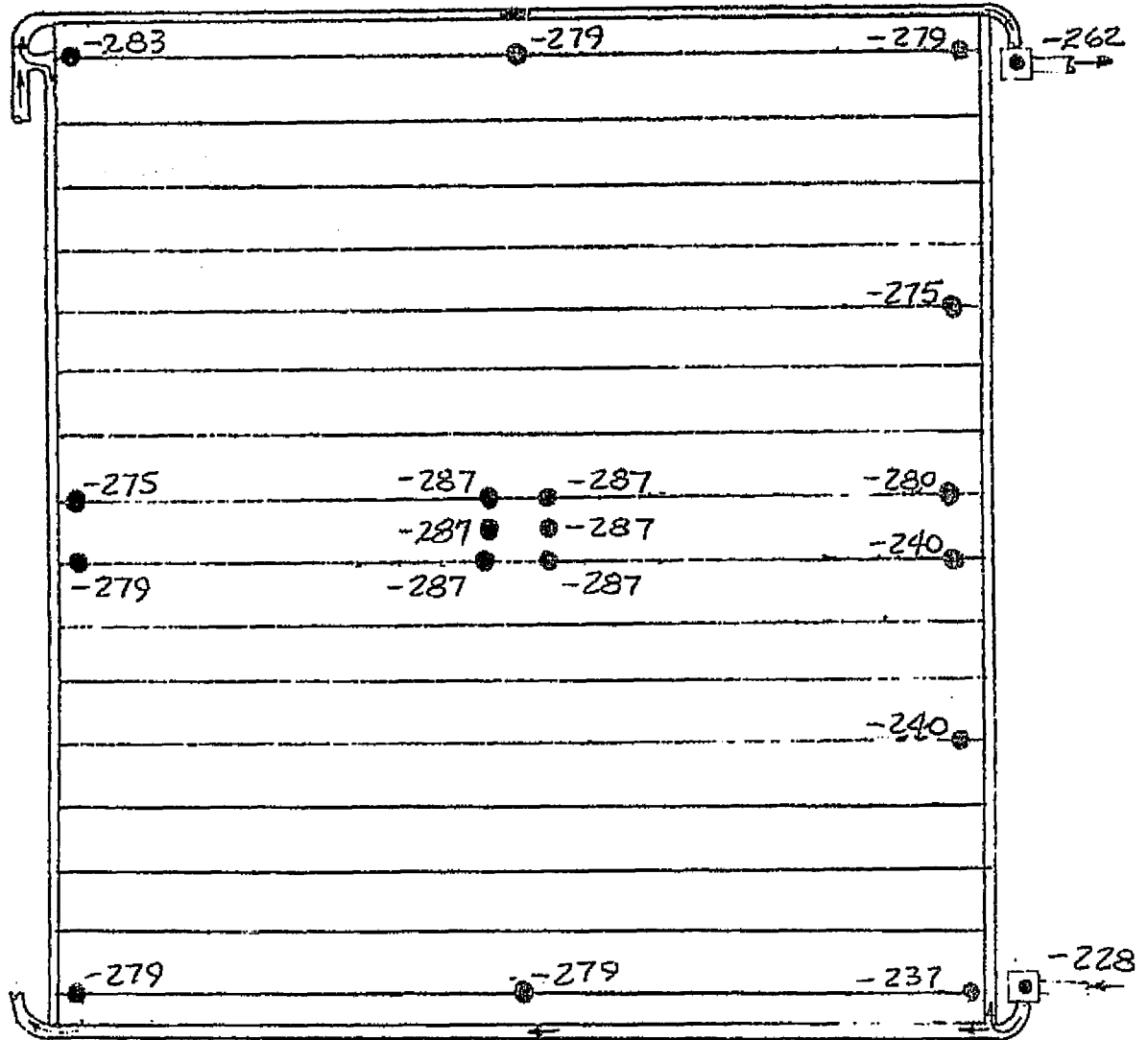
Fe_{12} Return

PANEL NO. 4

FIGURE A15 (CONT'D)

Fe_{12} Supply

TEST POINT __13__

DAY __194__

TIME __20:00:00__

Fe$_{12}$ Return
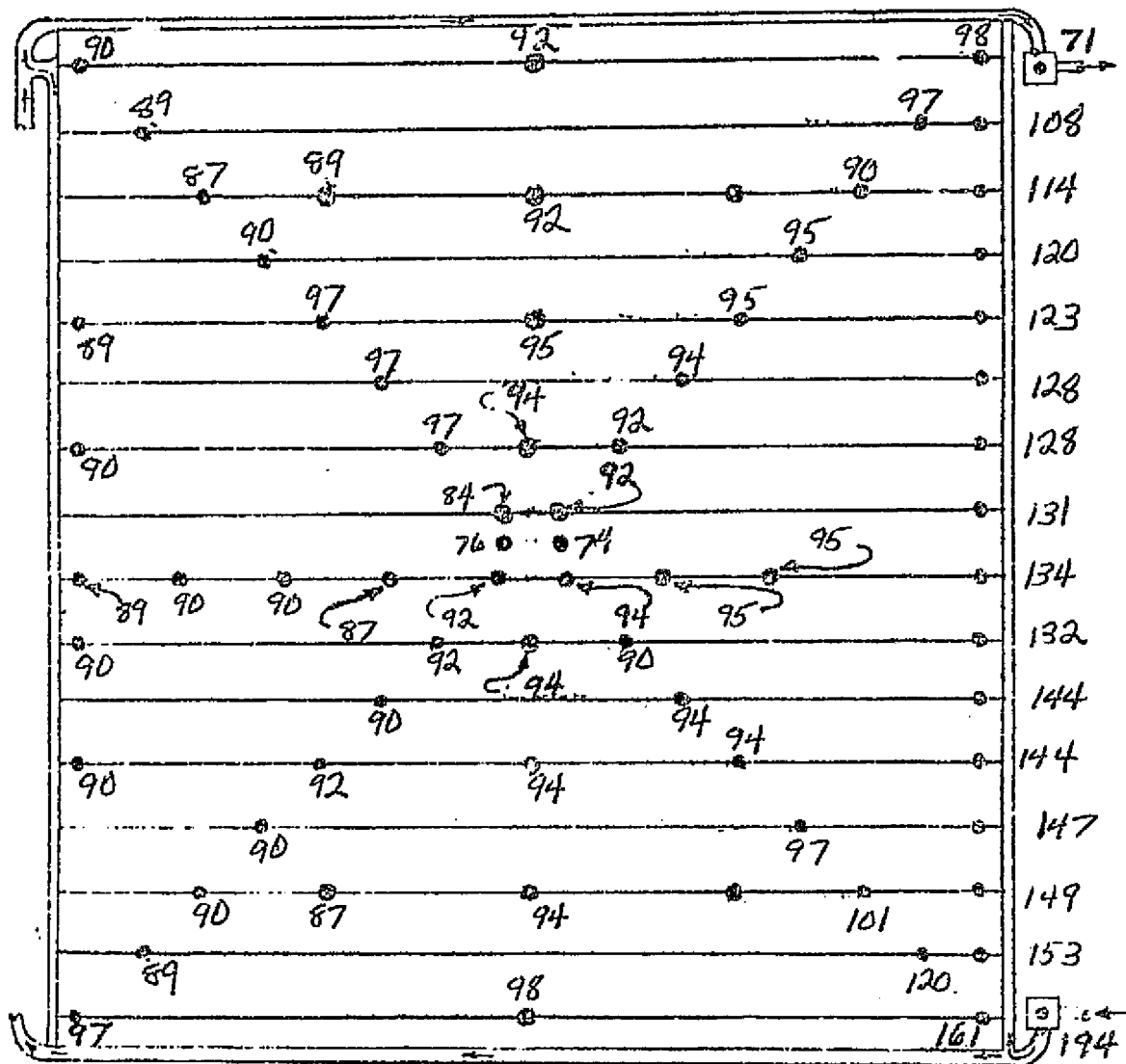
PANEL NO. 1

FIGURE A16

STEADY STATE VAPOR COMPRESSION OPERATION PANEL TEMPERATURE MAPS

Fe$_{12}$ Supply

TEST POINT ___13___

DAY ___294___

TIME ___20:00:00___

Fe_{12} Return

PAN⁺L NO. 2

FICURE A16 (CONT'D)

Fe_{12} Supply

A-63
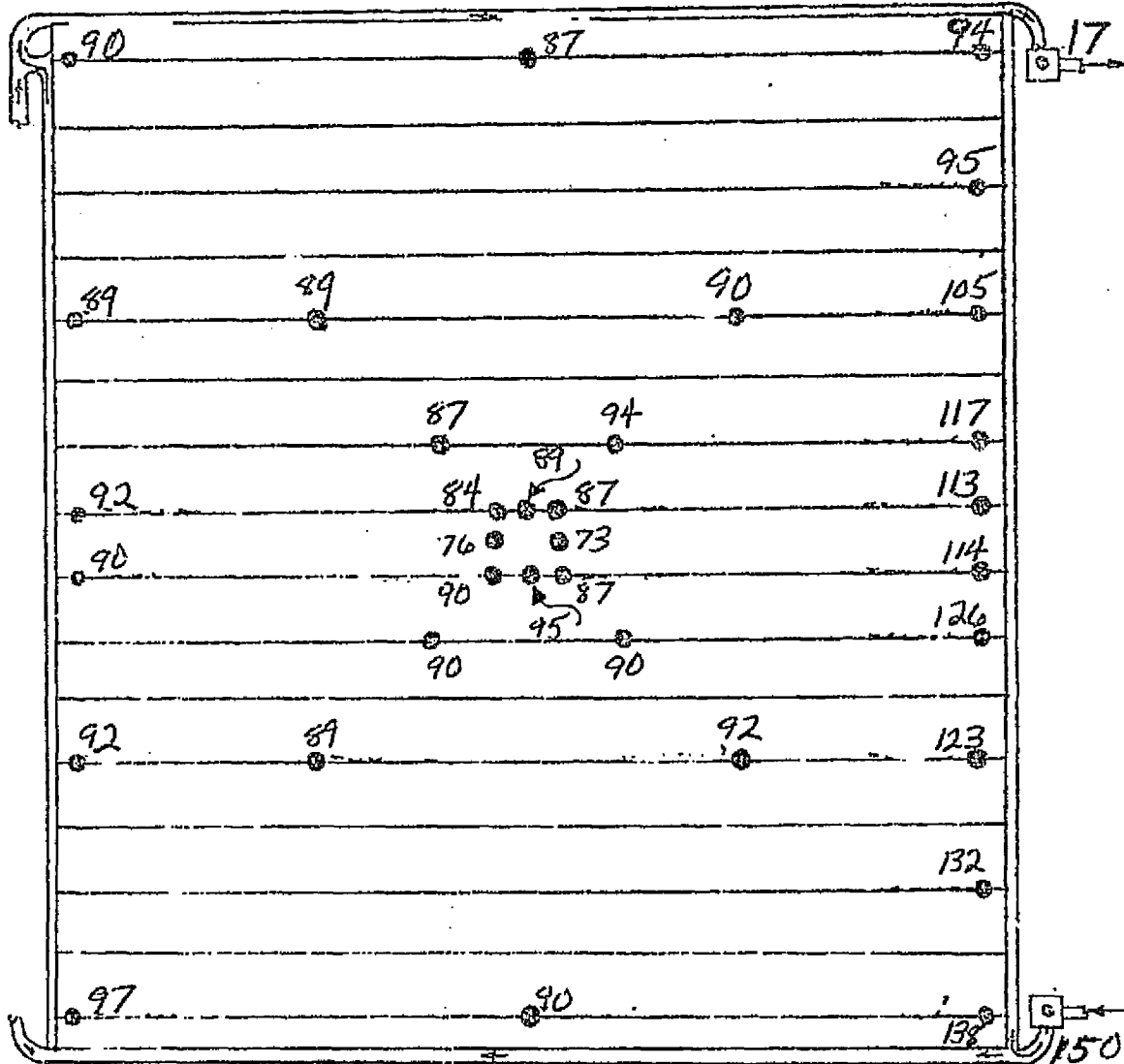
TEST POINT __13__
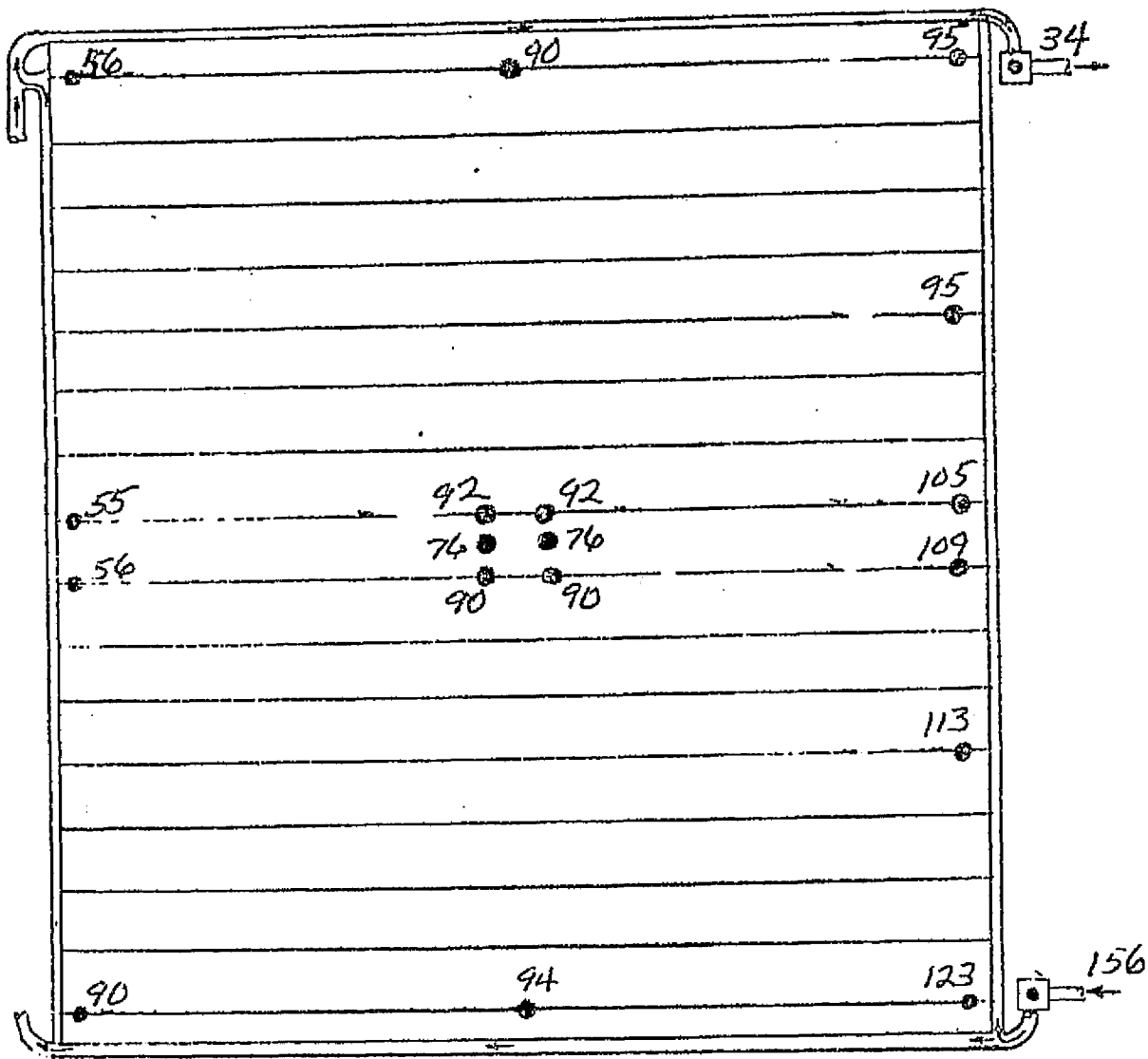
DAY __294__

TIME __20:00:00__

Fe$_{12}$ Return

PANEL NO. 3

FIGURE A16 (CONT'D)

A-64

TEST POINT ___13___
DAY ___294___
TIME ___20:00:00___
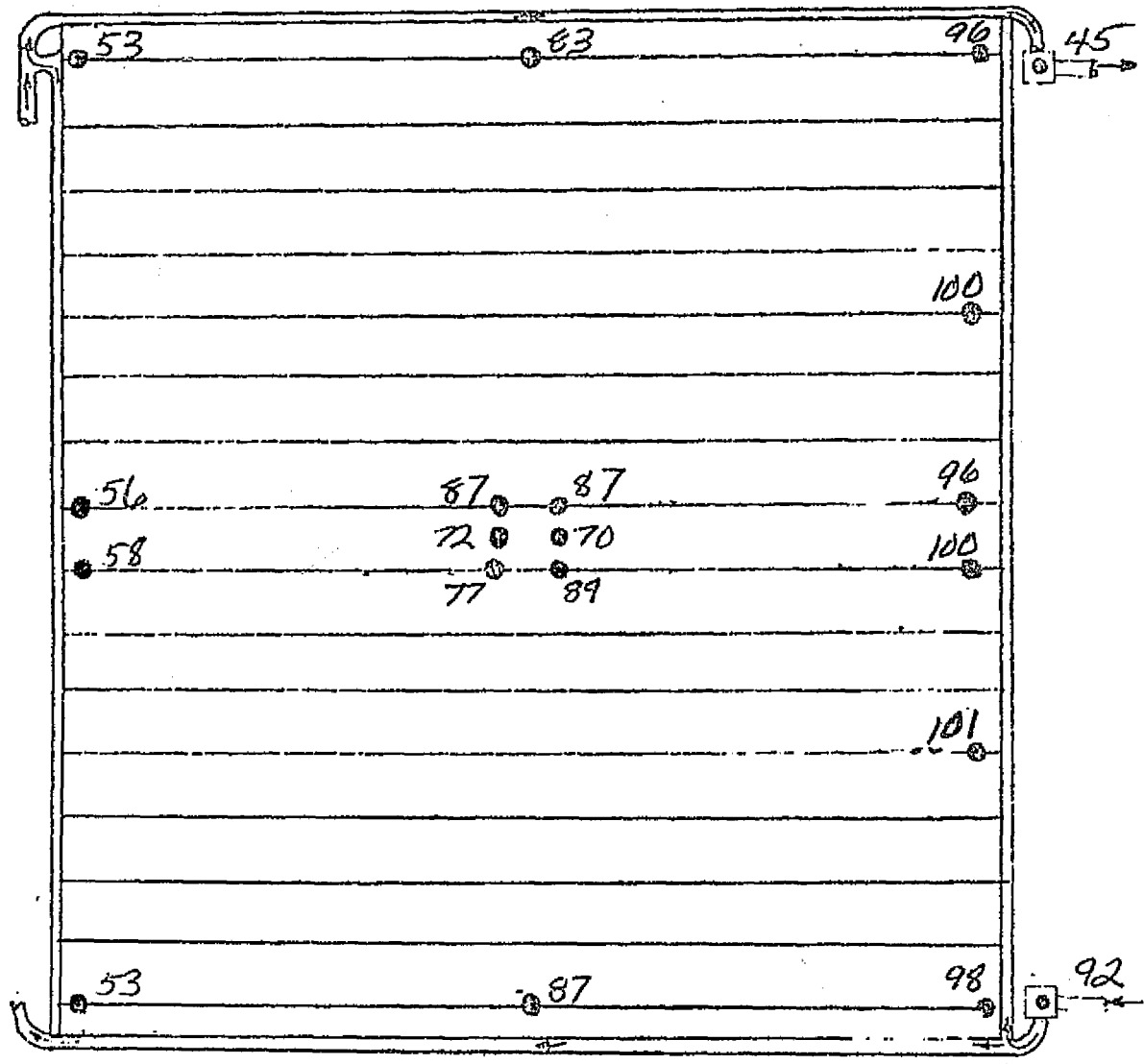
Fe$_{12}$ Return

PANEL NO. 4

FIGURE A16 (CONT'D)
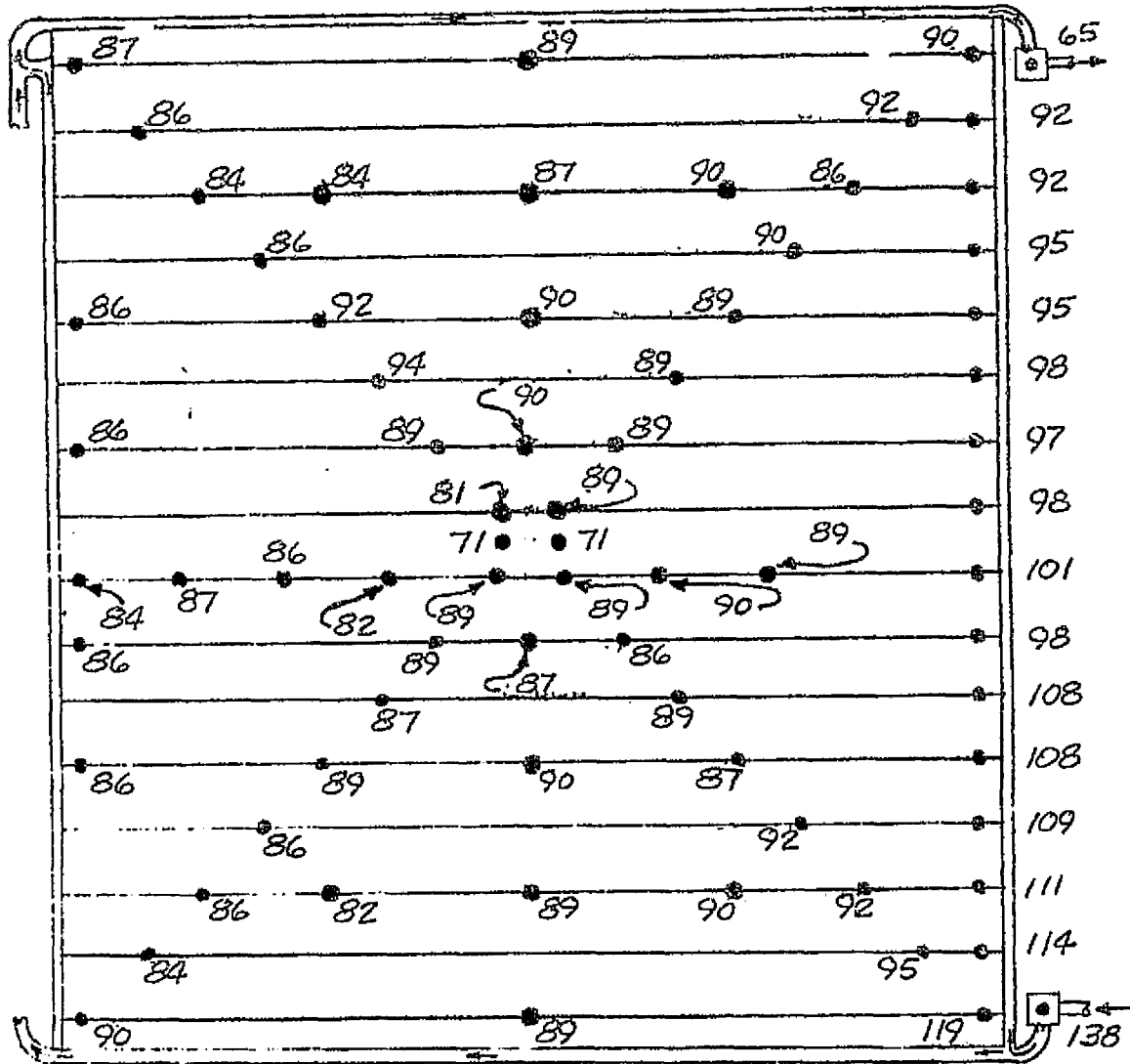
PANEL NO. 1

FIGURE A17

STEADY STATE VAPOR COMPRESSION OPERATION PANEL TEMPERATURE MAPS

TEST POINT __16__

DAY __295__
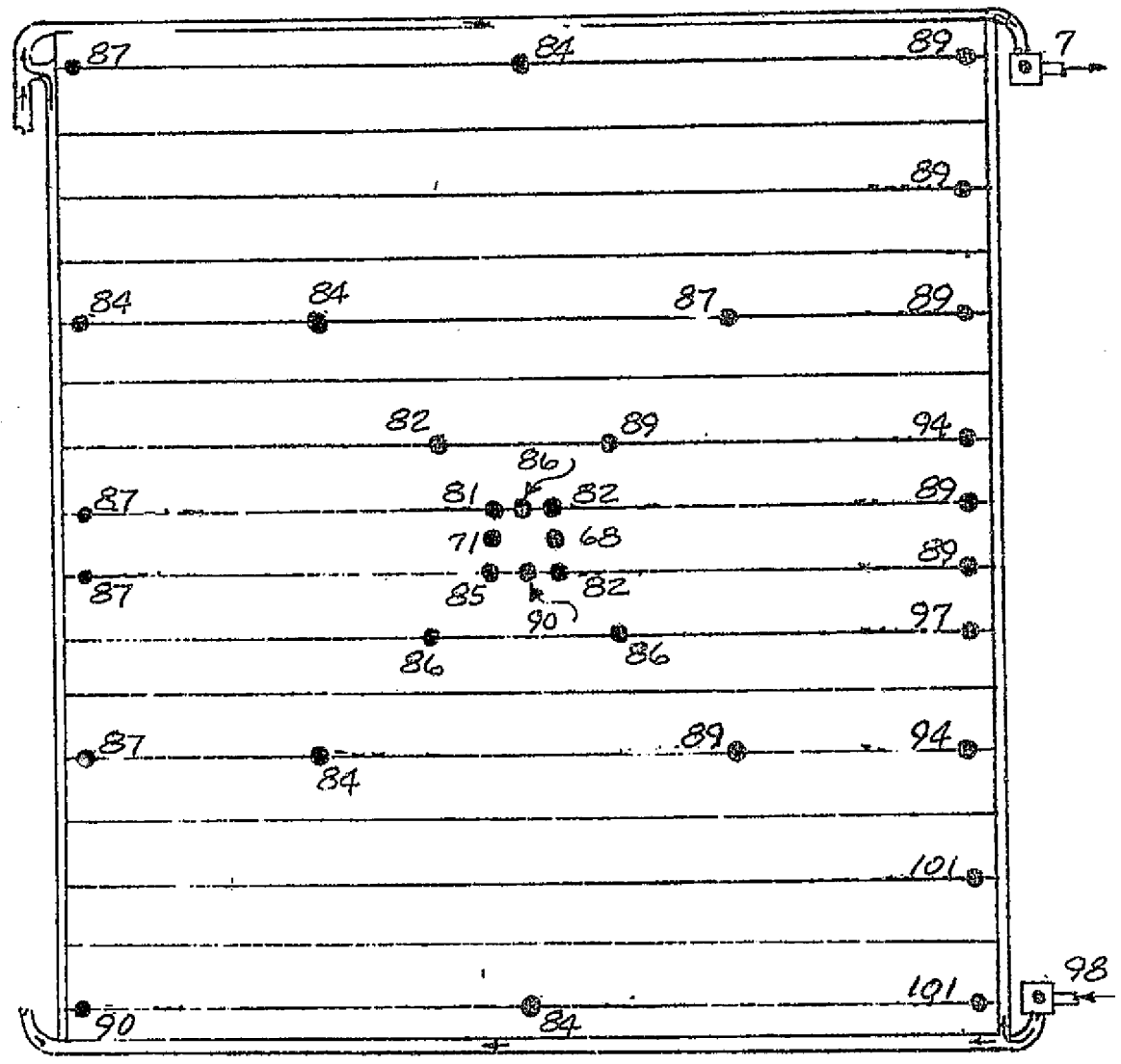
TIME __01:14:59__

Fe_{12} Return

PANEL NO. 2

FIGURE A17 (CONT'D)

TEST POINT ___16___

DAY ___295___
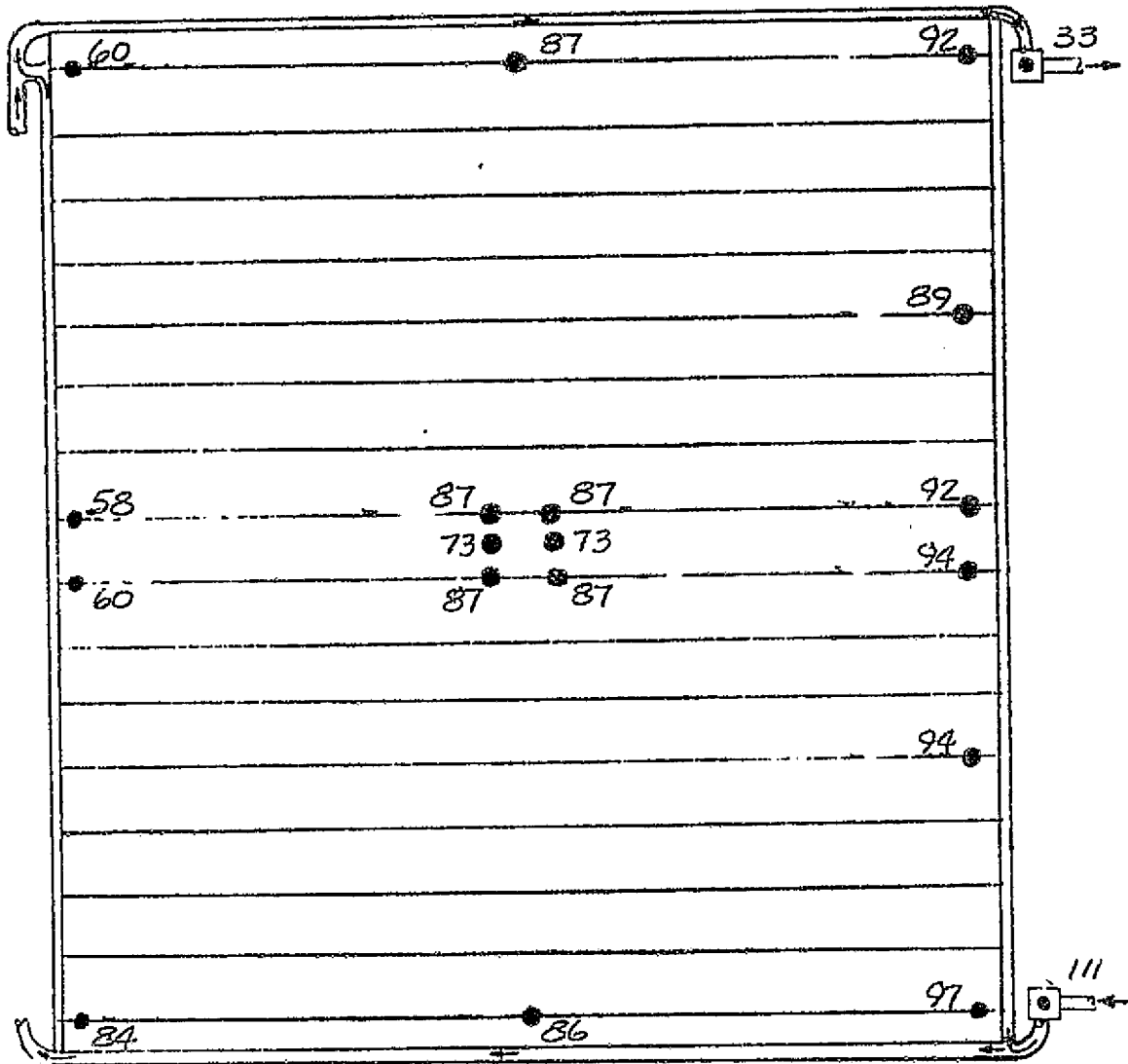
TIME ___01:14:59___

Fe_{12} Return

PANEL NO. 3

FIGURE A17 (CONT'D)

Fe_{12} Supply

TEST POINT ___16___

DAY ___295___

TIME ___01:14:59___
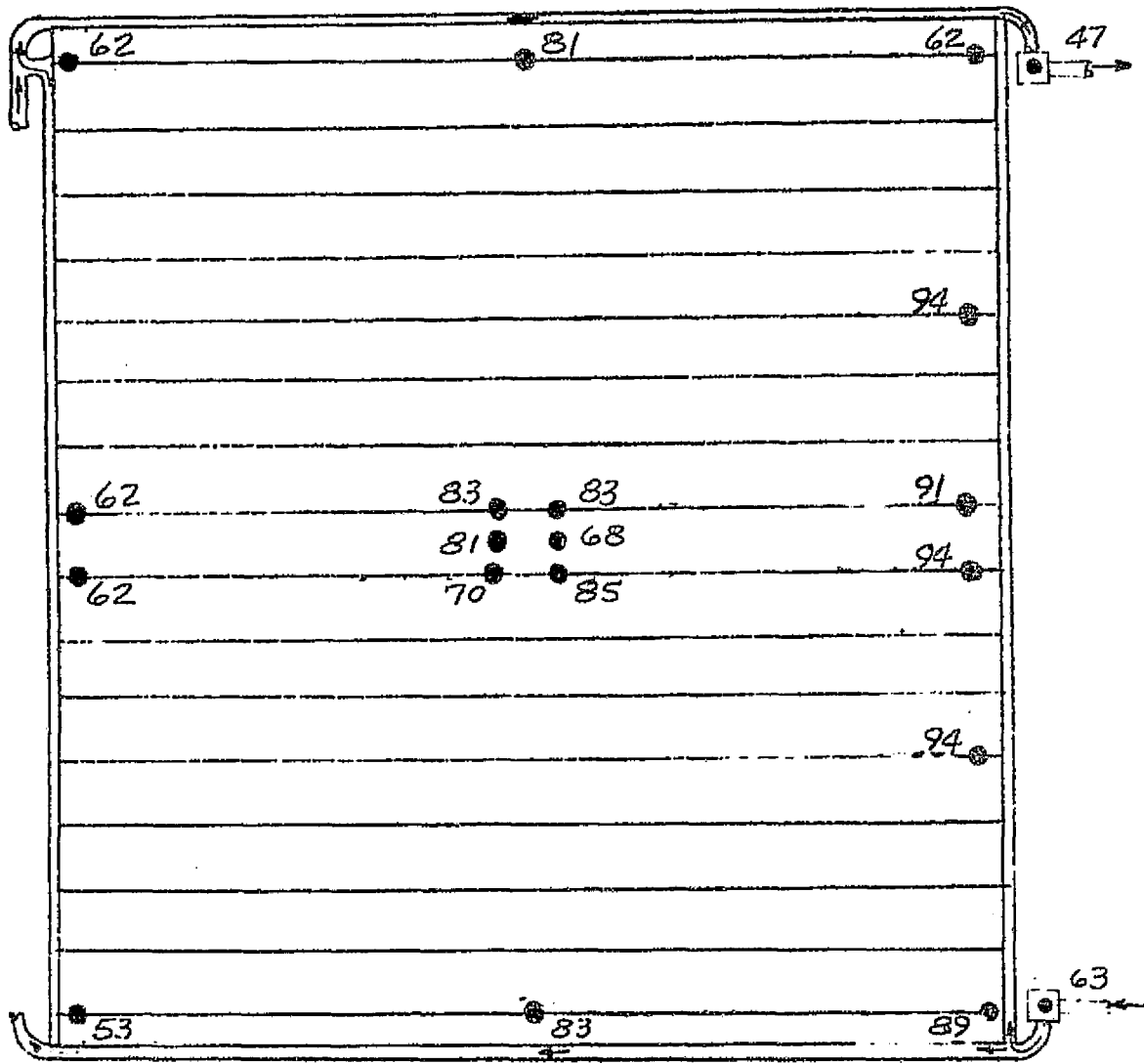
Fe$_{12}$ Return

PANEL NO. 4

FIGURE A17 (CONT'D)

Fe$_{12}$ Supply

TEST POINT __164__
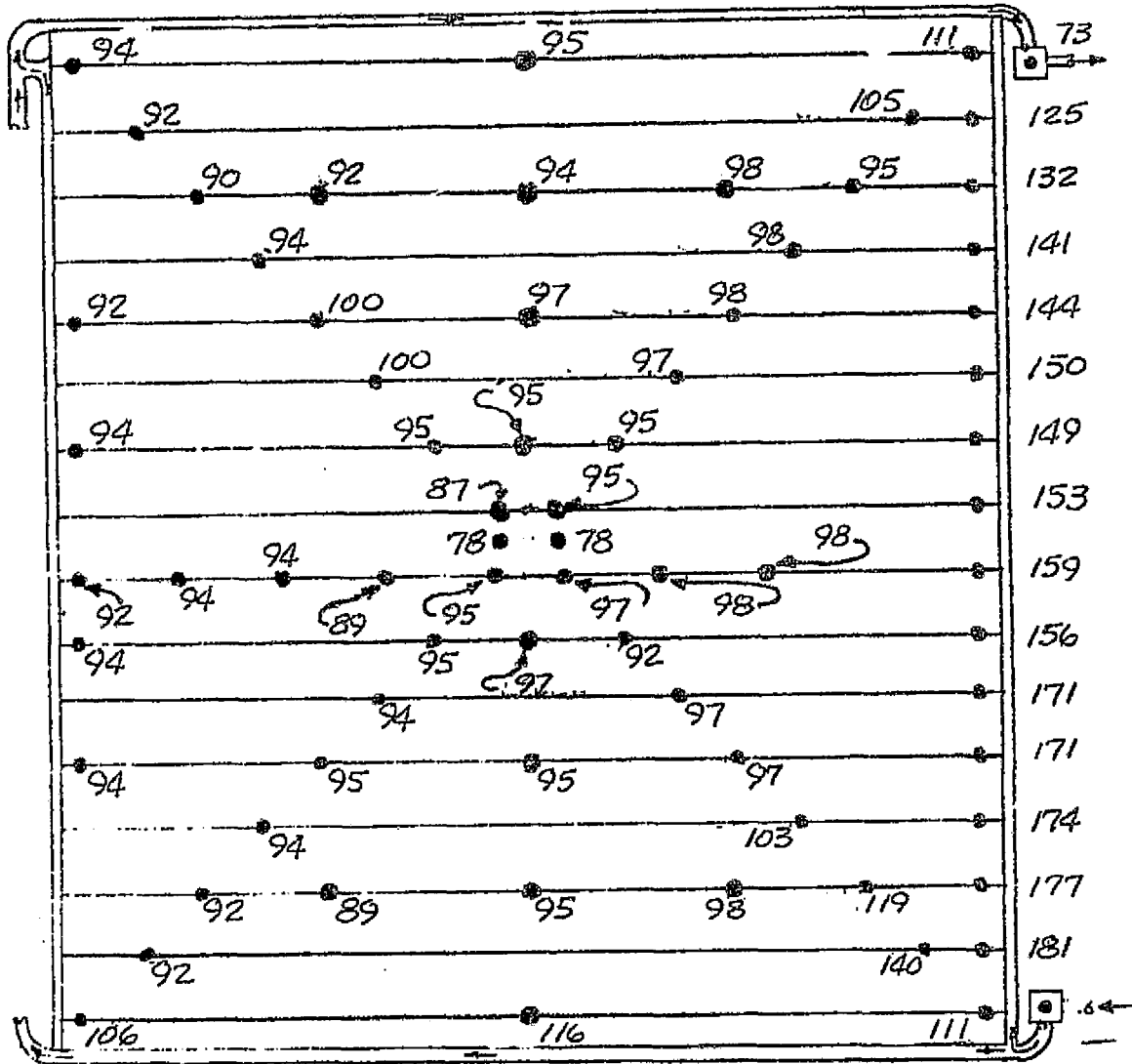
DAY __295__

TIME __02:14:59__
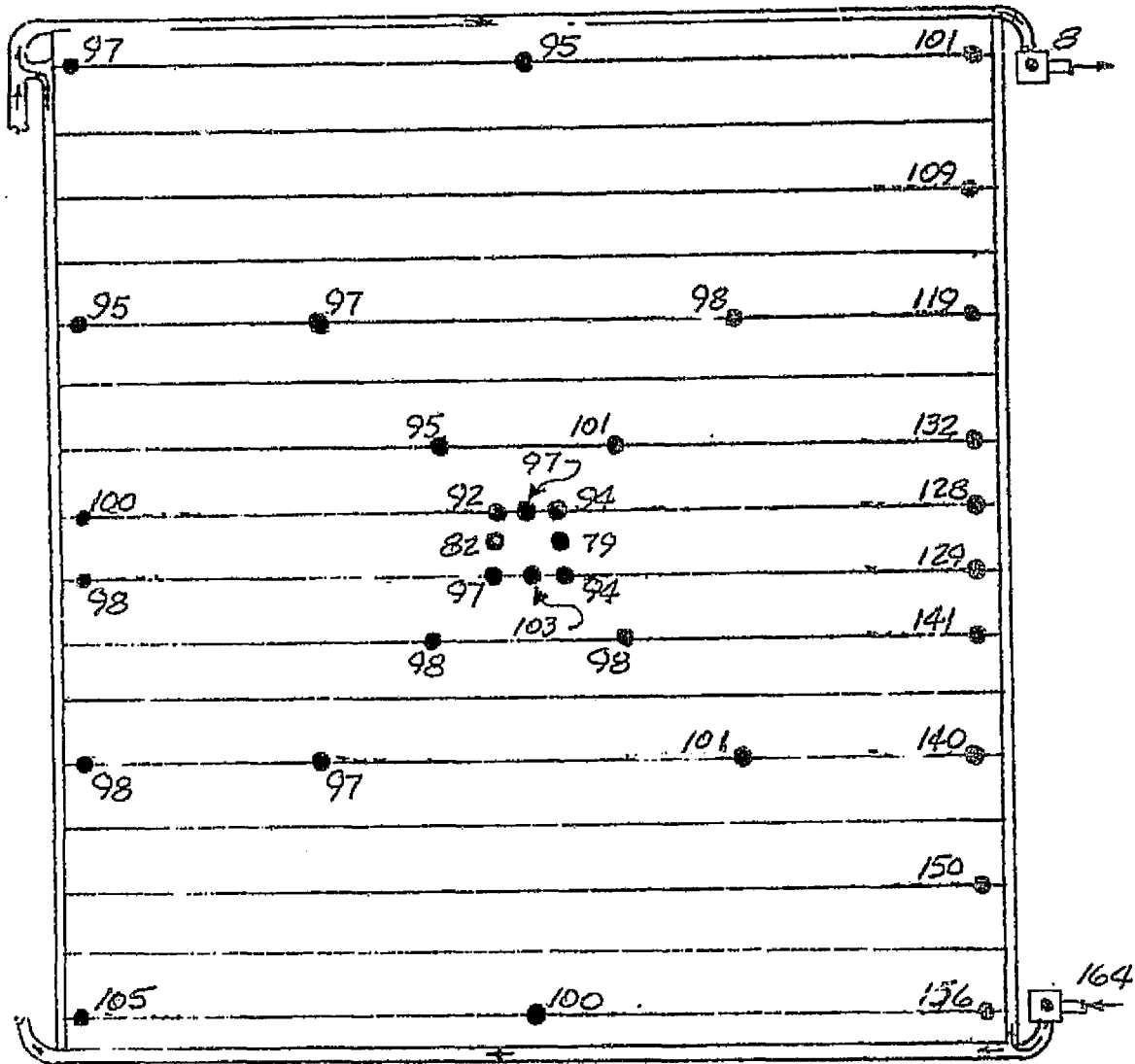
Fe$_{12}$ Return

PANEL NO. 1

FIGURE A18

STEADY STATE VAPOR COMPRESSION OPERATION PANEL TEMPERATURE MAPS

TEST POINT _16A_

DAY _295_
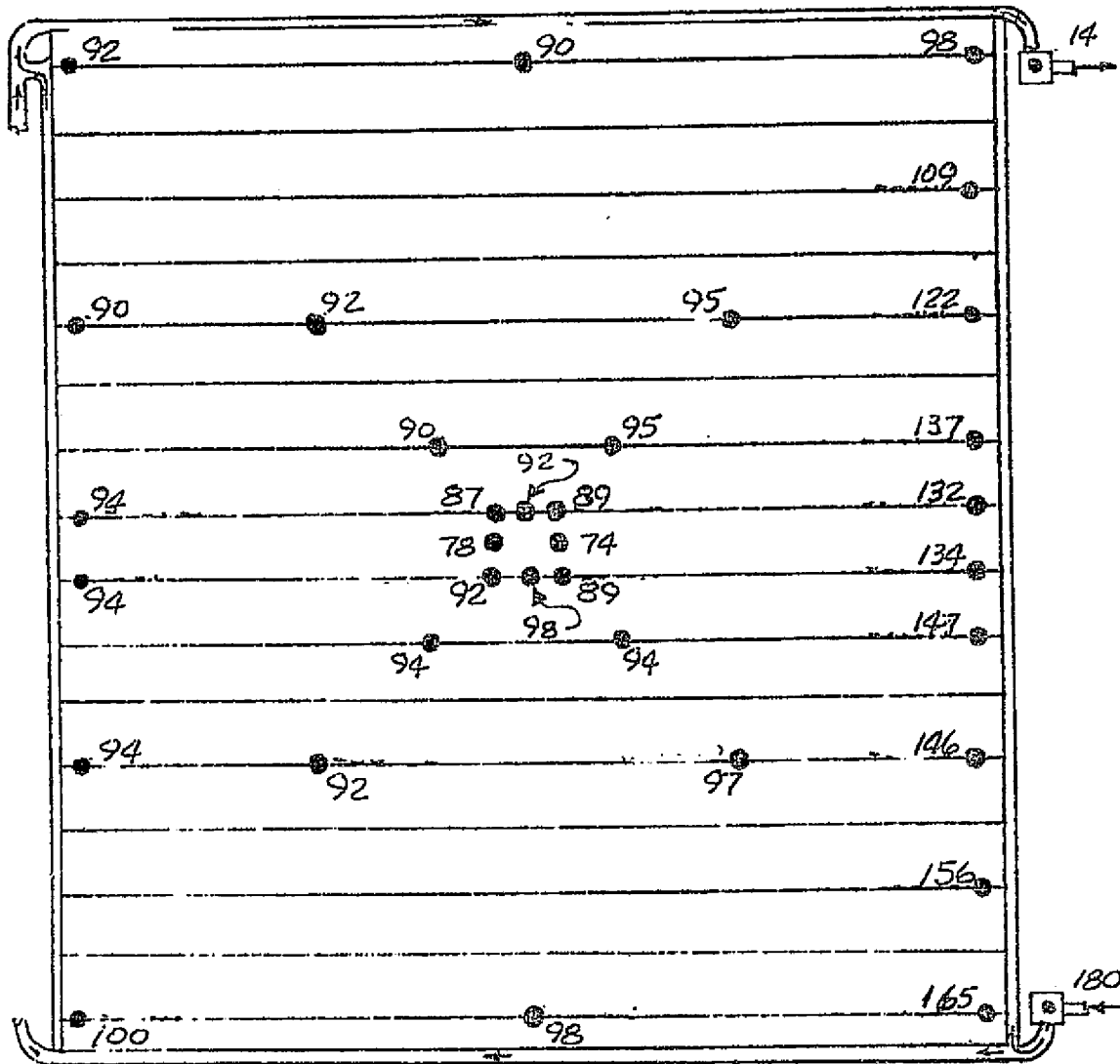
TIME _02:14:59_

Fe_{12} Return

PANEL NO. 2

FIGURE A18 (CONT'D)

Fe_{12} Supply

A-71

TEST POINT _16A___

DAY _____295_____

TIME ___02:14:59___

Fe$_{12}$ Return

55   94   98   33

101

56   94   95   117
      79   78
56   94   94   123

129

94   97   143   183

Fe$_{12}$ Supply

PANEL NO. 3

FIGURE A18 (CONT'D)

A-72

TEST POINT __16A__

DAY __295__

TIME __02:14:59__

Fe$_{12}$ Return

49   85   98   43→

102

56   89 89   102

75 72

53   77   91   102

111

51   89   111   106→

Fe$_{12}$ Supply

PANEL NO. 4

FIGURE A18 (CONT'D)

TEST POINT __21__
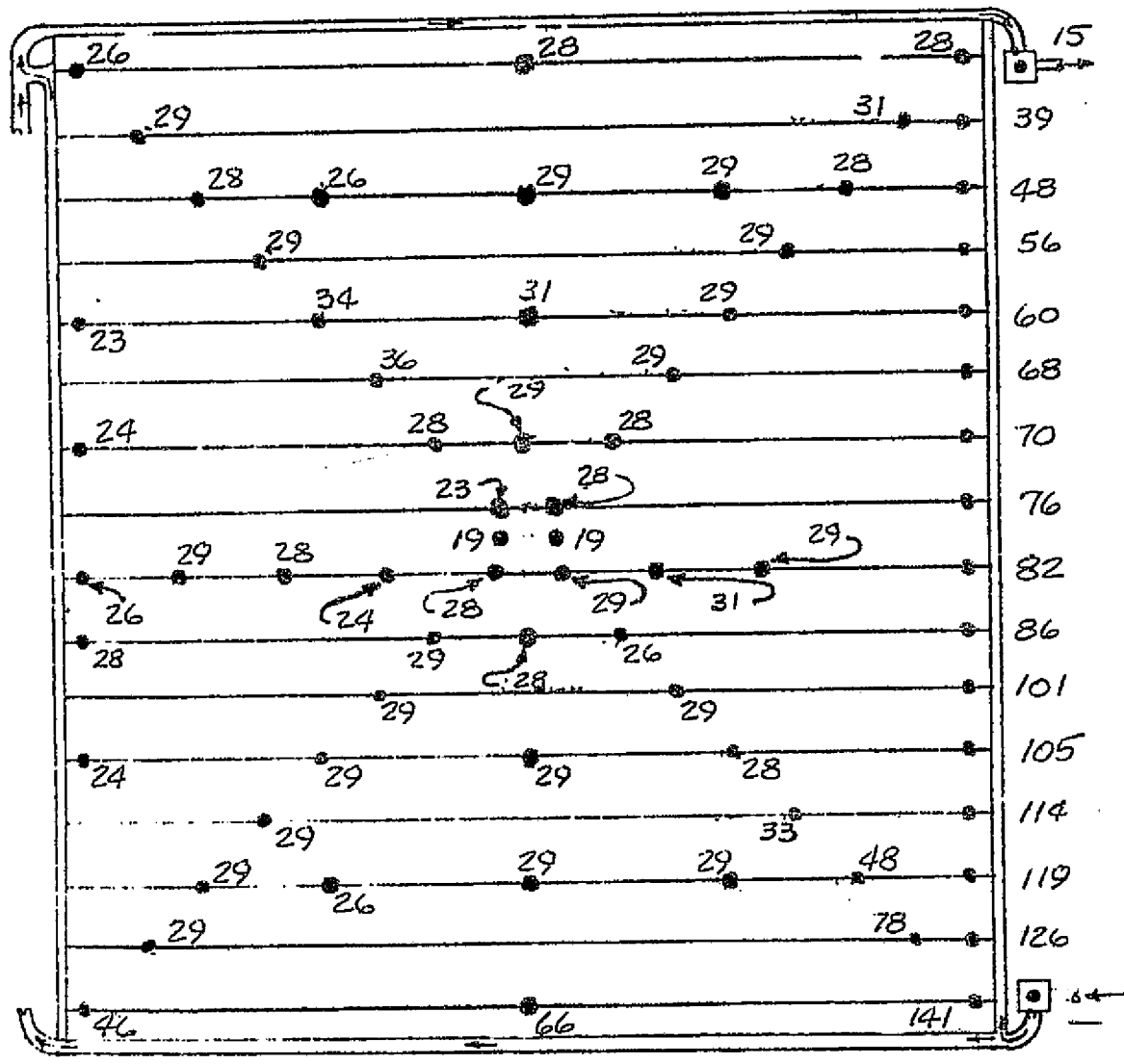
DAY __295__

TIME __04:29:59__

Fe$_{12}$ Return

PANEL NO. 1

FIGURE A19

STEADY STATE VAPOR COMPRESSION OPERATION PANEL TEMPERATURE MAPS

A-74

TEST POINT ___21___

DAY ___295___

TIME ___04:29:59___

Fe_{12} Return

15 23 26 -41

28

5 24 28 26

-15 -6 14

24

21 21 24

19 15

21 31

26 23

29

55

28 28

28 28 29 70

86

123

39 39 100
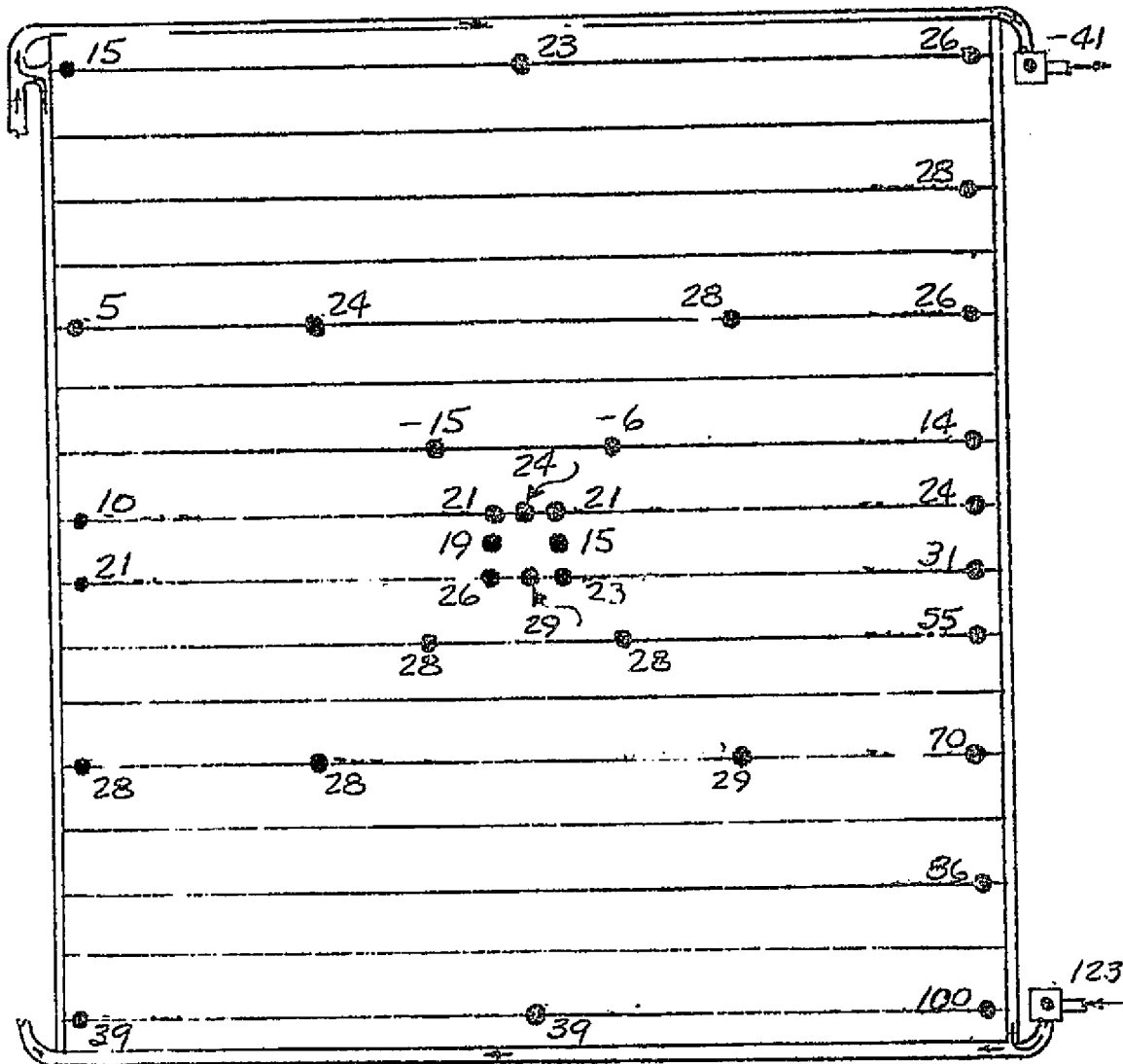
Fe_{12} Supply

PANEL NO. 2

FIGURE A19 (CONT'D)

A-75

TEST POINT __21__
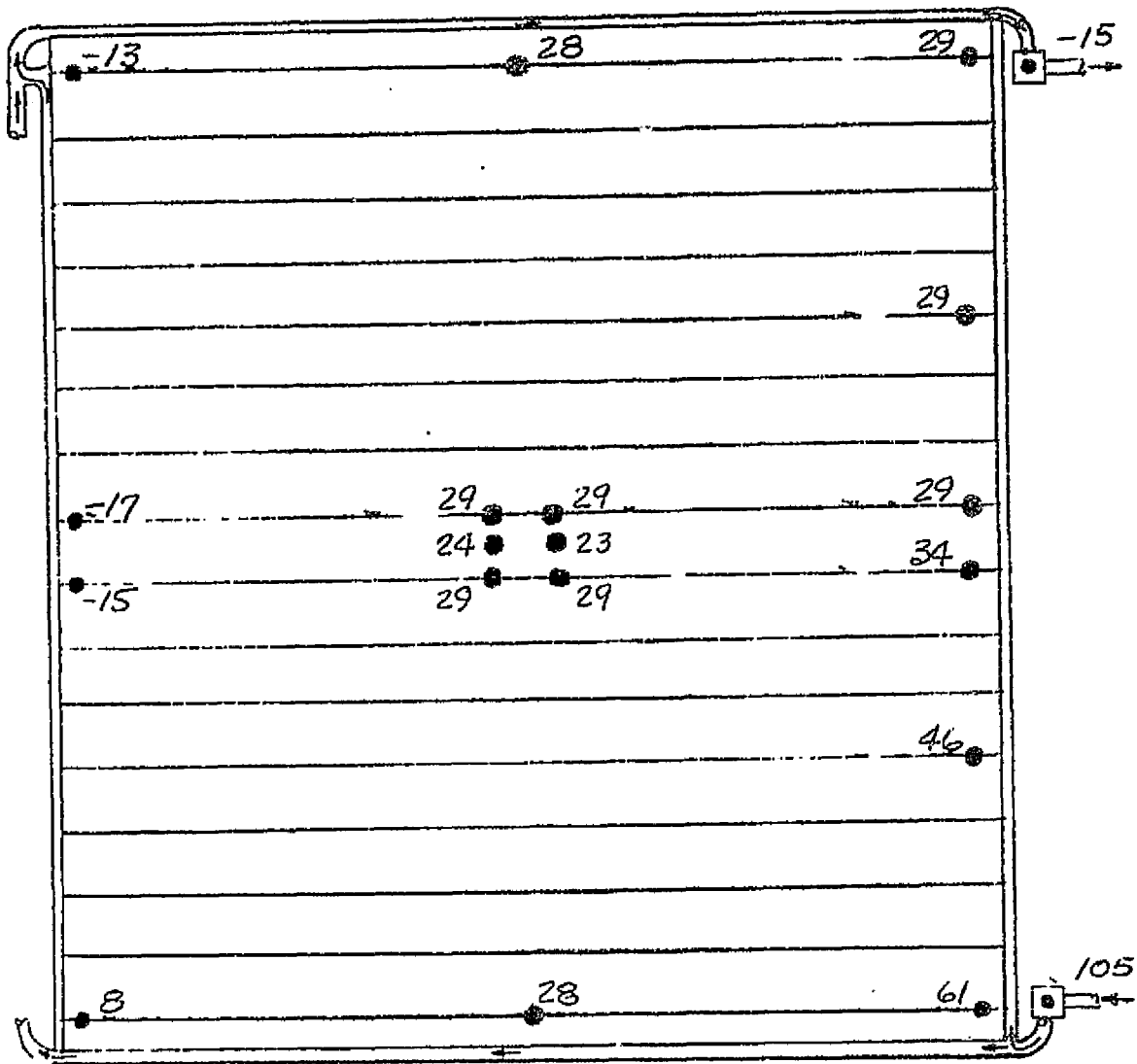
DAY __295__

TIME __04:29:59__

Fe_{12} Return

PANEL NO. 3

FIGURE A19 (CONT'D)

TEST POINT ___21___

DAY ___295___

TIME ___04:29:59___
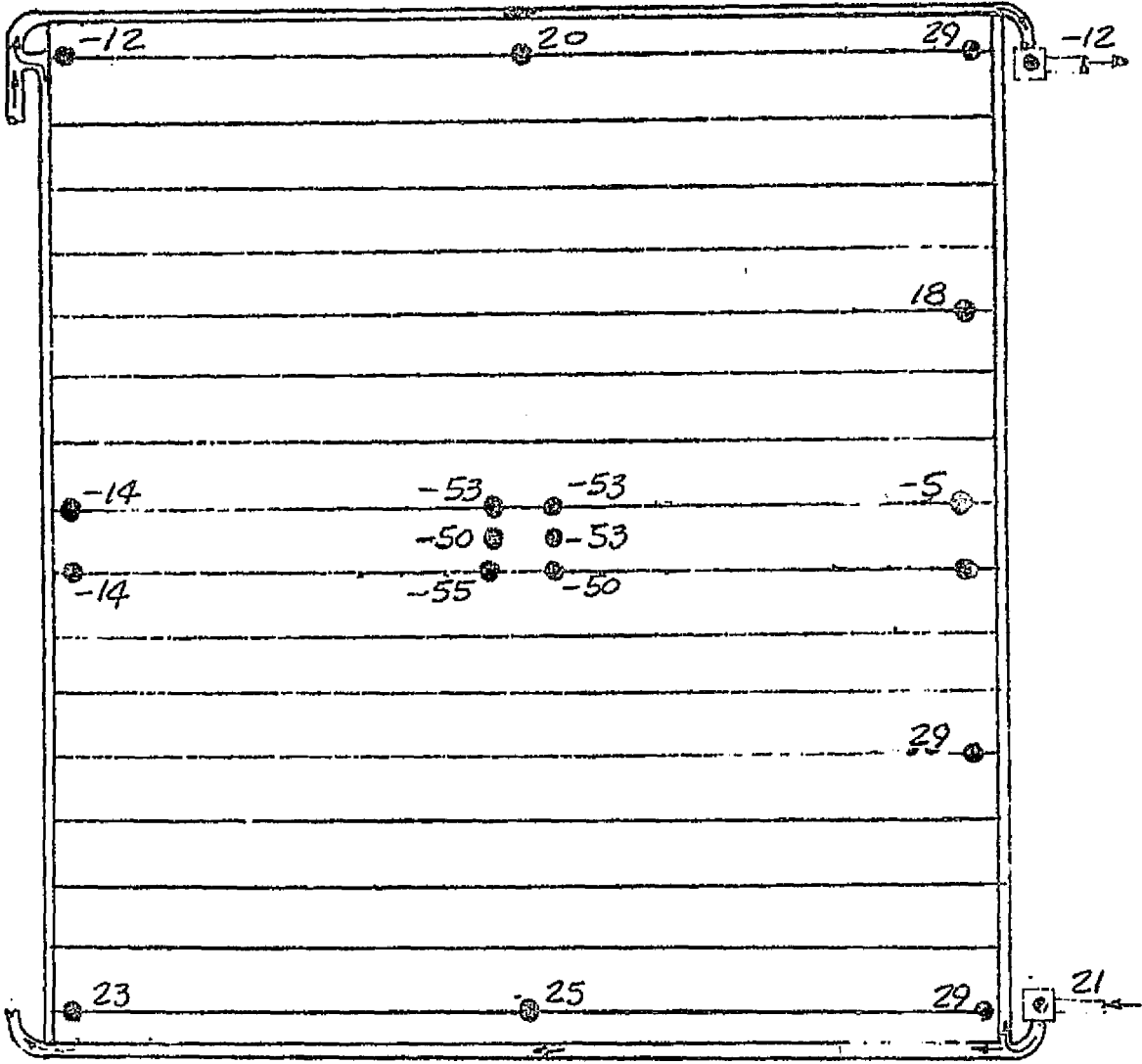
Fe_{12} Return

PANEL NO. 4

FIGURE A19 (CONT'D)

TEST POINT __22__
DAY __295__
TIME __06:59:59__
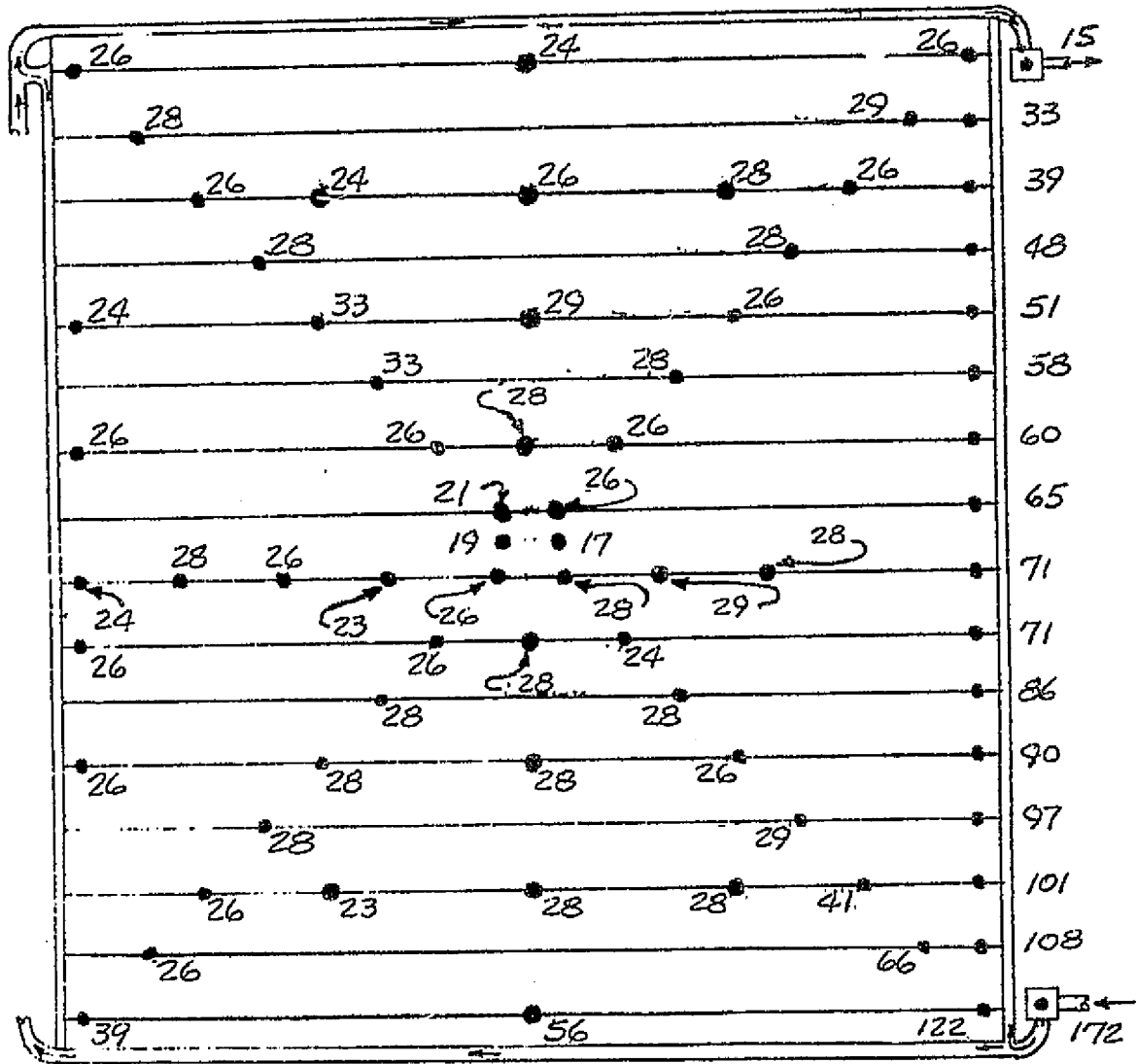
Fe_{12} Return

PANEL NO. 1

FIGURE A20

STEADY STATE VAPOR COMPRESSION OPERATION PANEL TEMPERATURE MAPS

TEST POINT   22

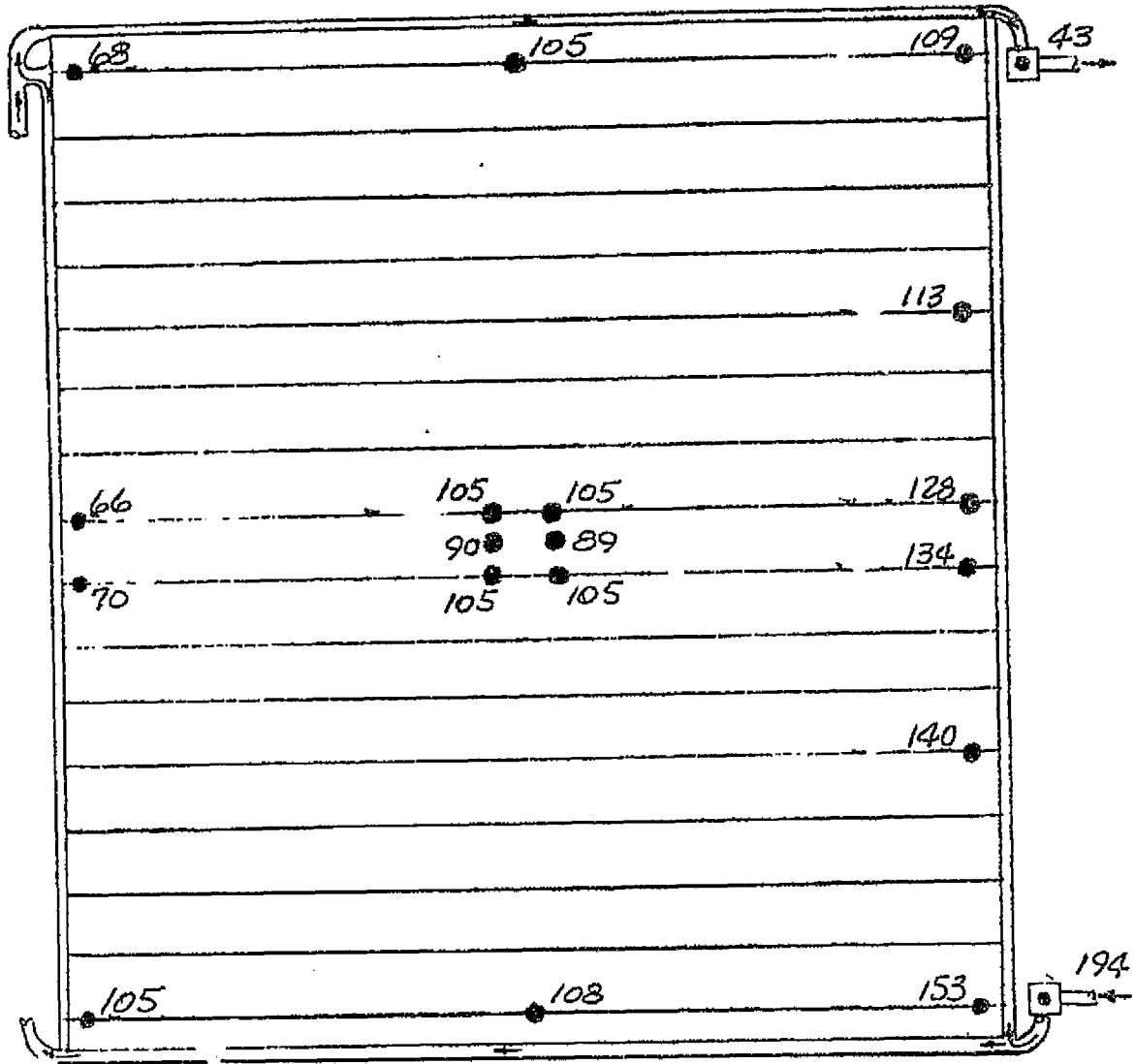DAY   295
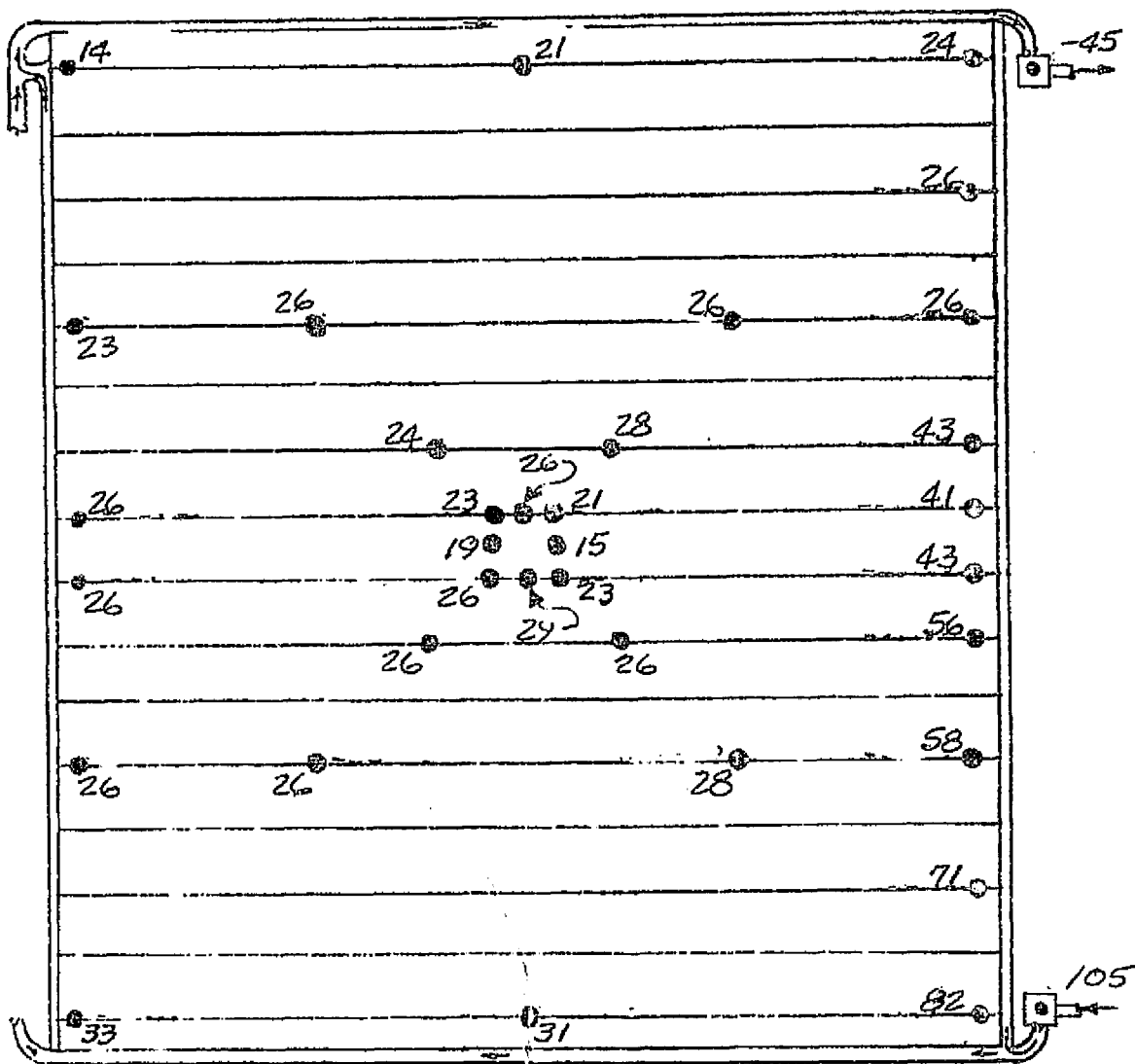
TIME   06:59:59

Fe$_{12}$ Return

PANEL NO. 2

FIGURE A20 (CONT'D)

Fe$_{12}$ Supply

TEST POINT 22

DAY 295

TIME 06:59:59

PANEL NO. 3

FIGURE A20 (CONT'D)

TEST POINT _22_

DAY _295_

TIME _06:59:59_
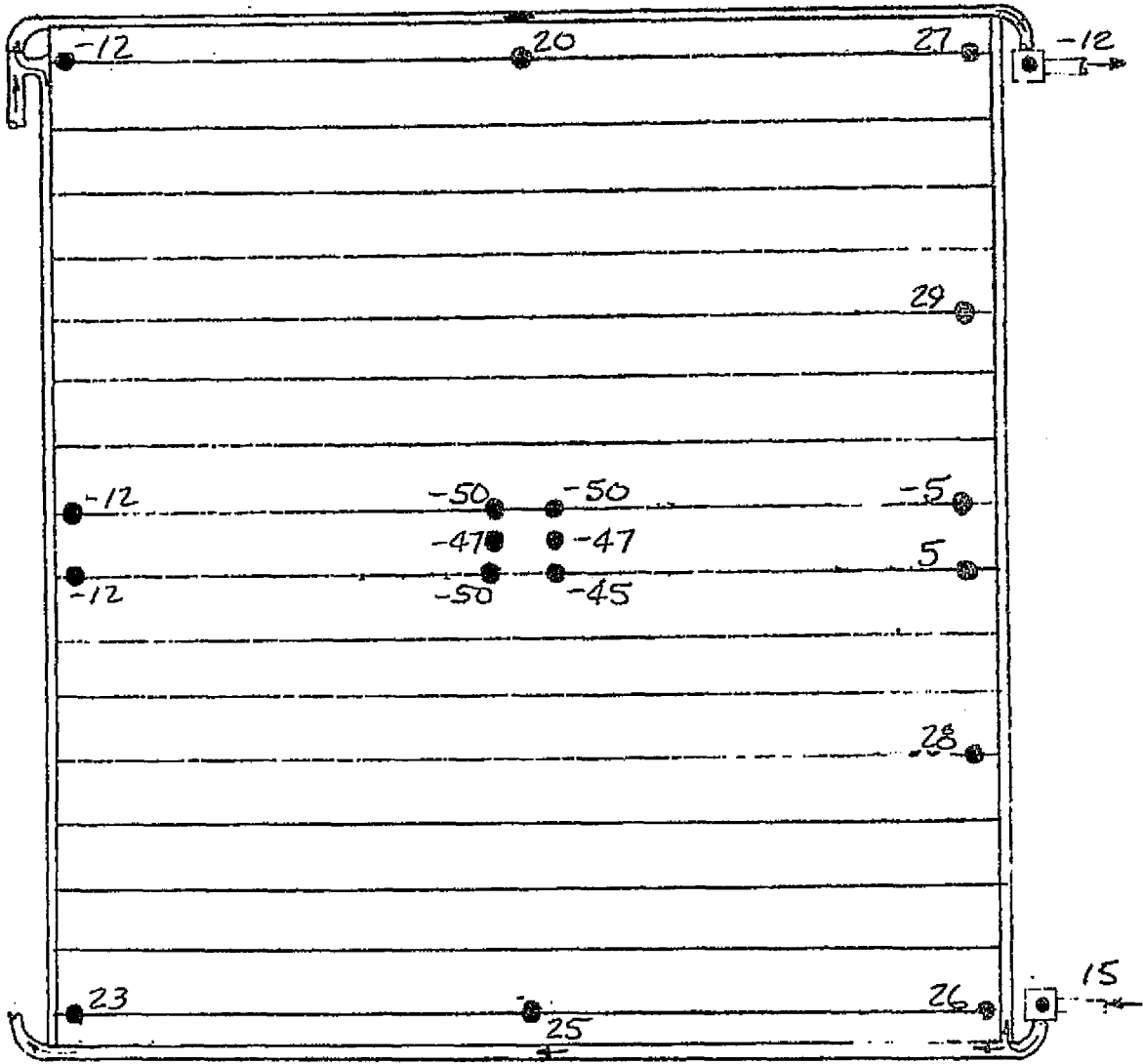
Fe$_{12}$ Return

Fe$_{12}$ Supply

PANEL NO. 4

FIGURE A20 (CONT'D)

Fe_{12} Return

PANEL NO. 1

FIGURE A21

STEADY STATE VAPOR COMPRESSION OPERATION PANEL TEMPERATURE MAPS

Fe_{12} Supply

TEST POINT _14_
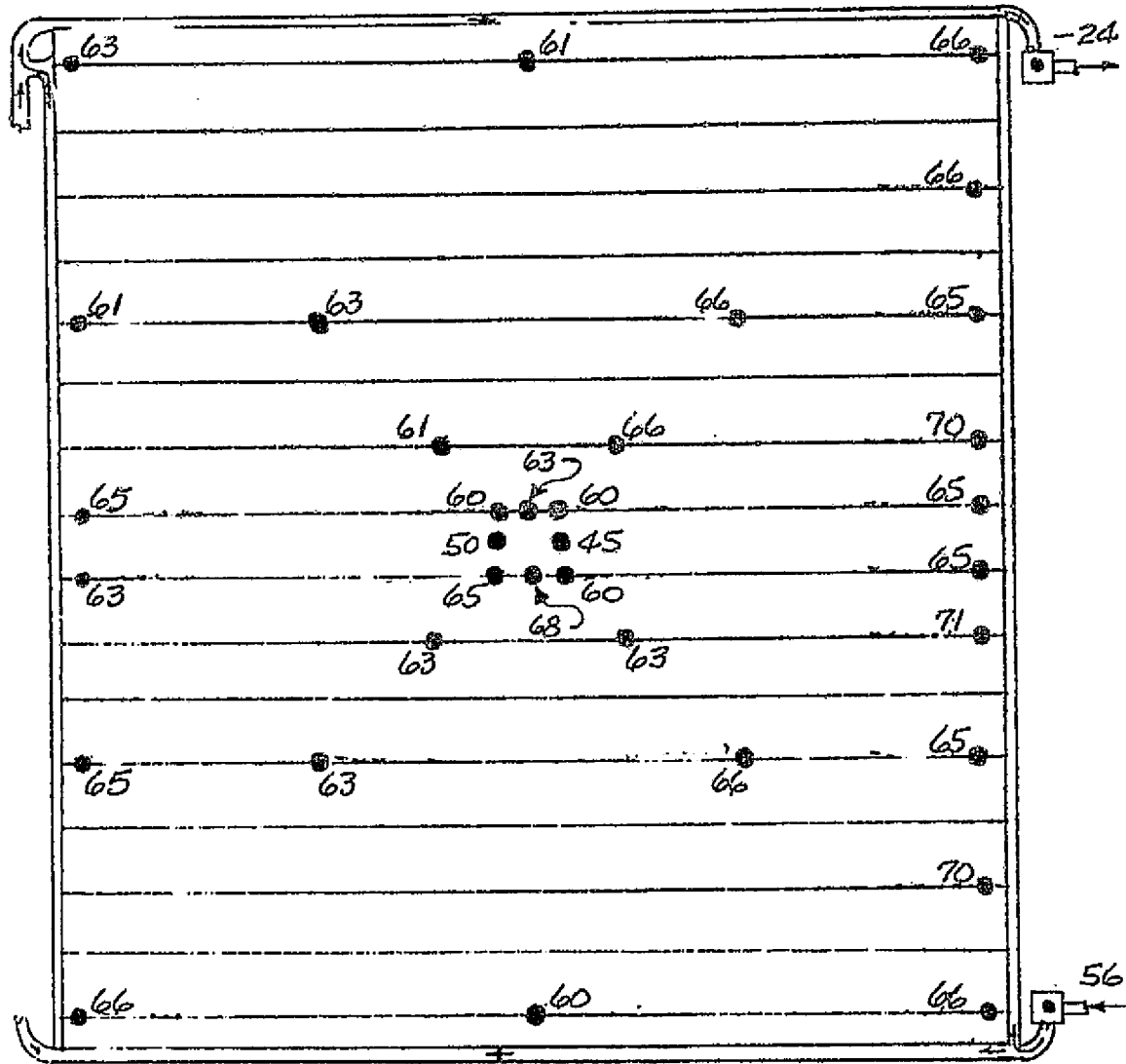
DAY _295_

TIME _11:30:05_

Fe$_{12}$ Return

PANEL NO. 2

FIGURE A21 (CONT'D)

TEST POINT _14_

DAY _____ 295_____

TIME _____ 11:30:05 _____
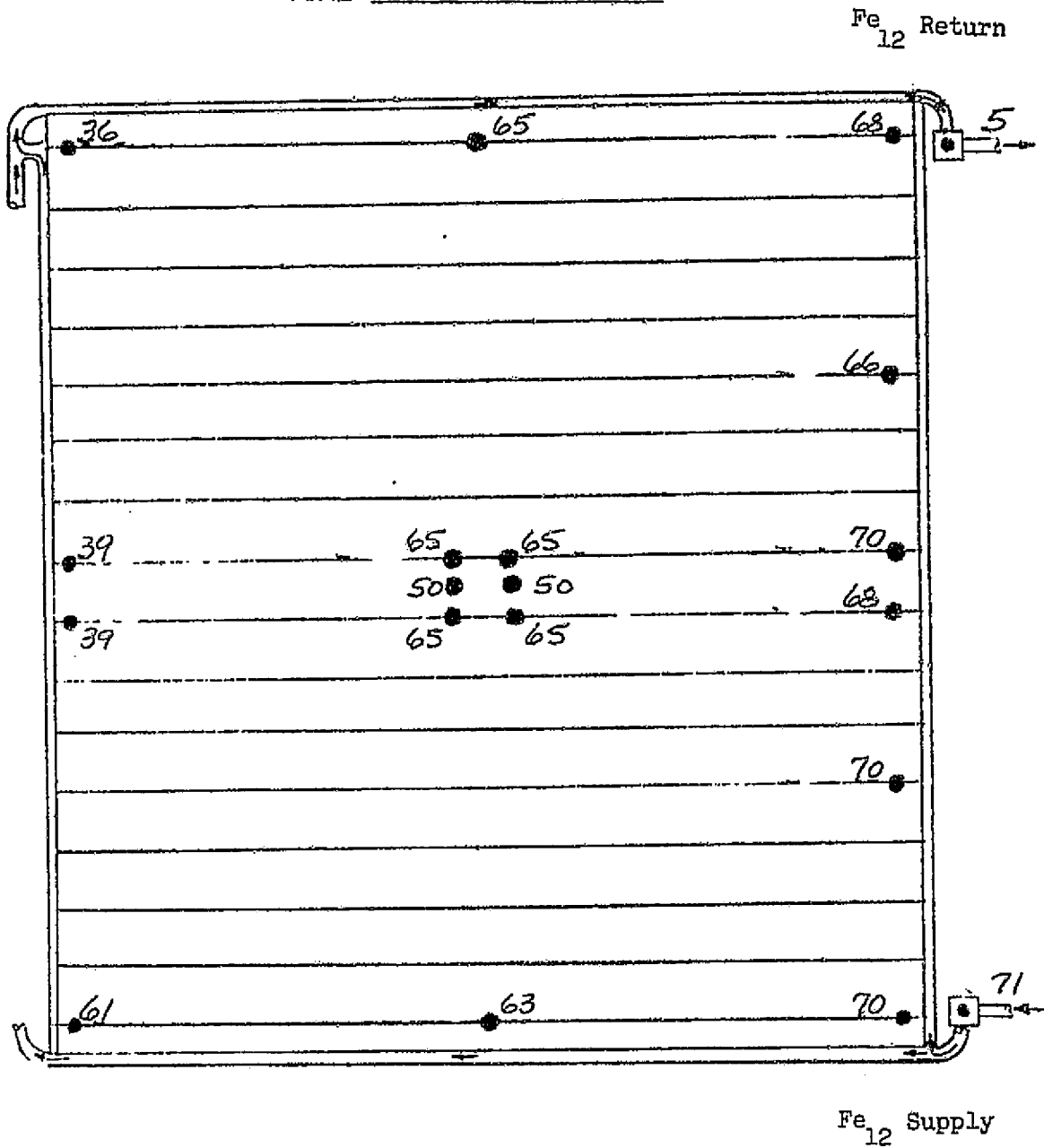
Fe$_{12}$ Return

PANEL NO. 3

FIGURE A21 (CONT'D)

Fe$_{12}$ Supply

TEST POINT ___14___
DAY ___295___
TIME ___11:30:05___
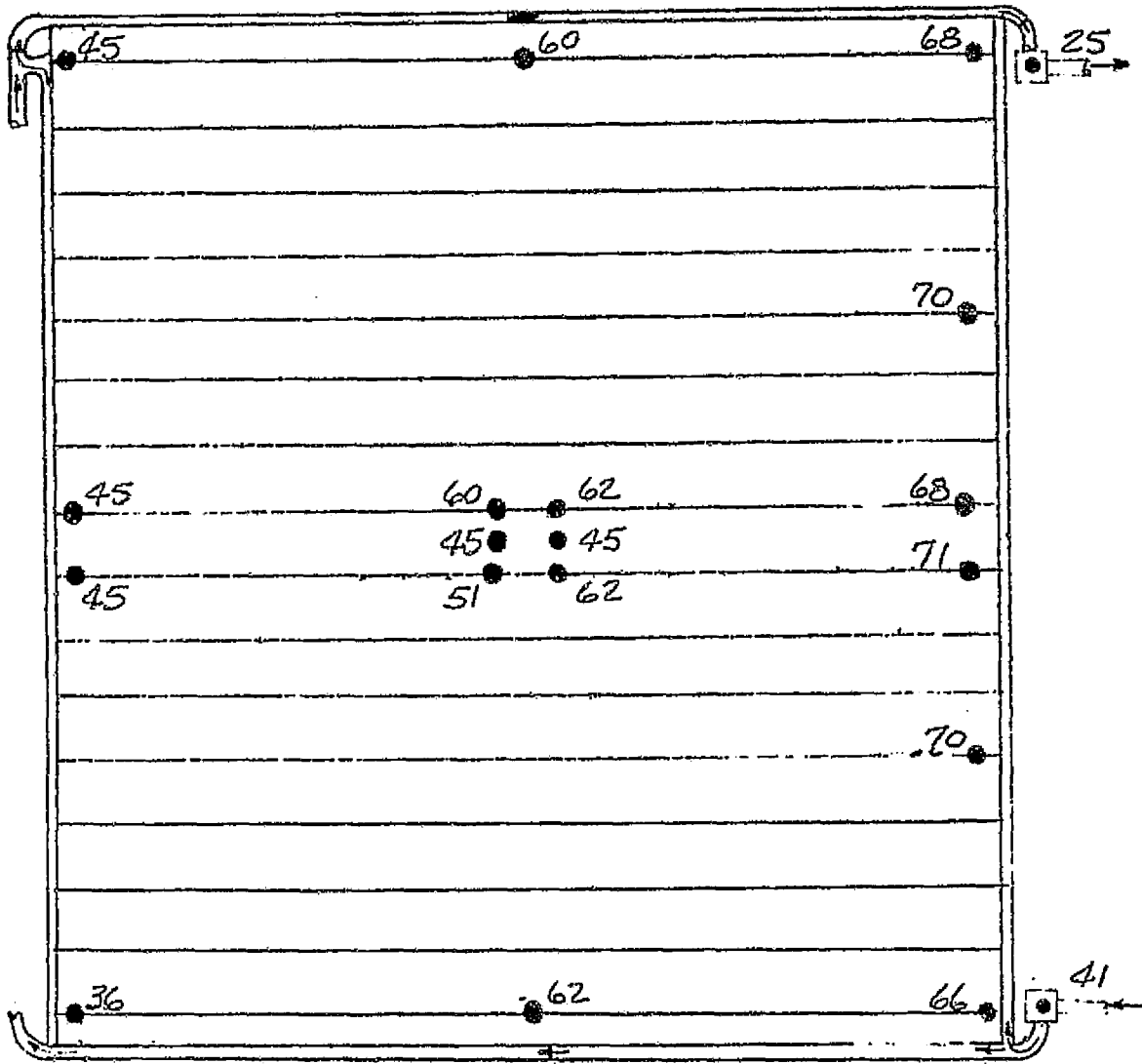
PANEL NO. 4

FIGURE A21 (CONT'D)

TEST POINT ___17___
DAY ___295___
TIME ___13:30:05___
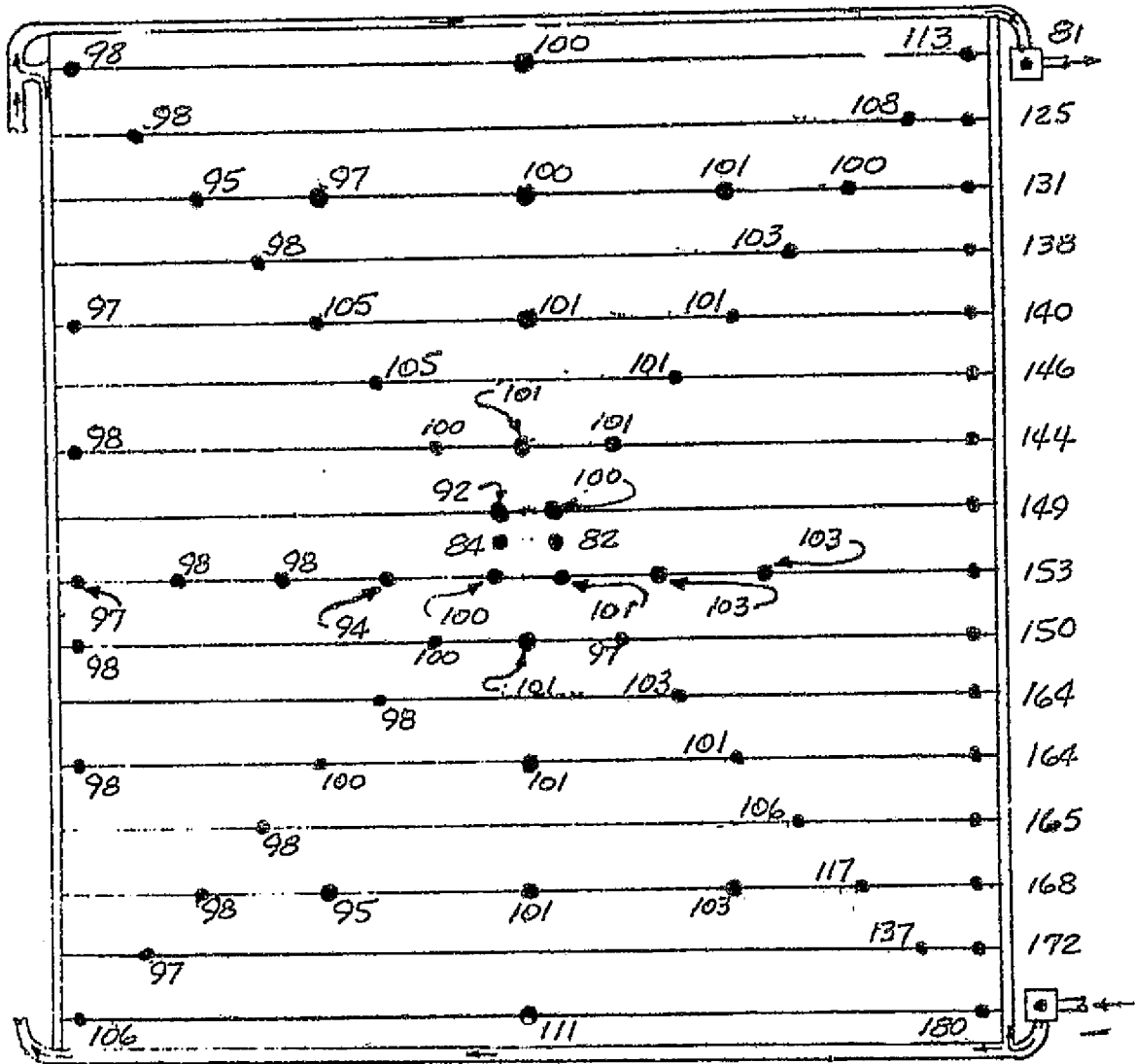
Fe$_{12}$ Return

PANEL NO. 1

FIGURE A22

STEADY STATE VAPOR COMPRESSION OPERATION PANEL TEMPERATURE MAPS

Fe$_{12}$ Supply

A-86

TEST POINT _17_

DAY _295_

TIME _13:30:05_

Fe$_{12}$ Return

PANEL NO. 2

FIGURE A22 (CONT'D)

Fe$_{12}$ Supply

A-87

TEST POINT ___17___

DAY ___295___

TIME ___13:30:05___
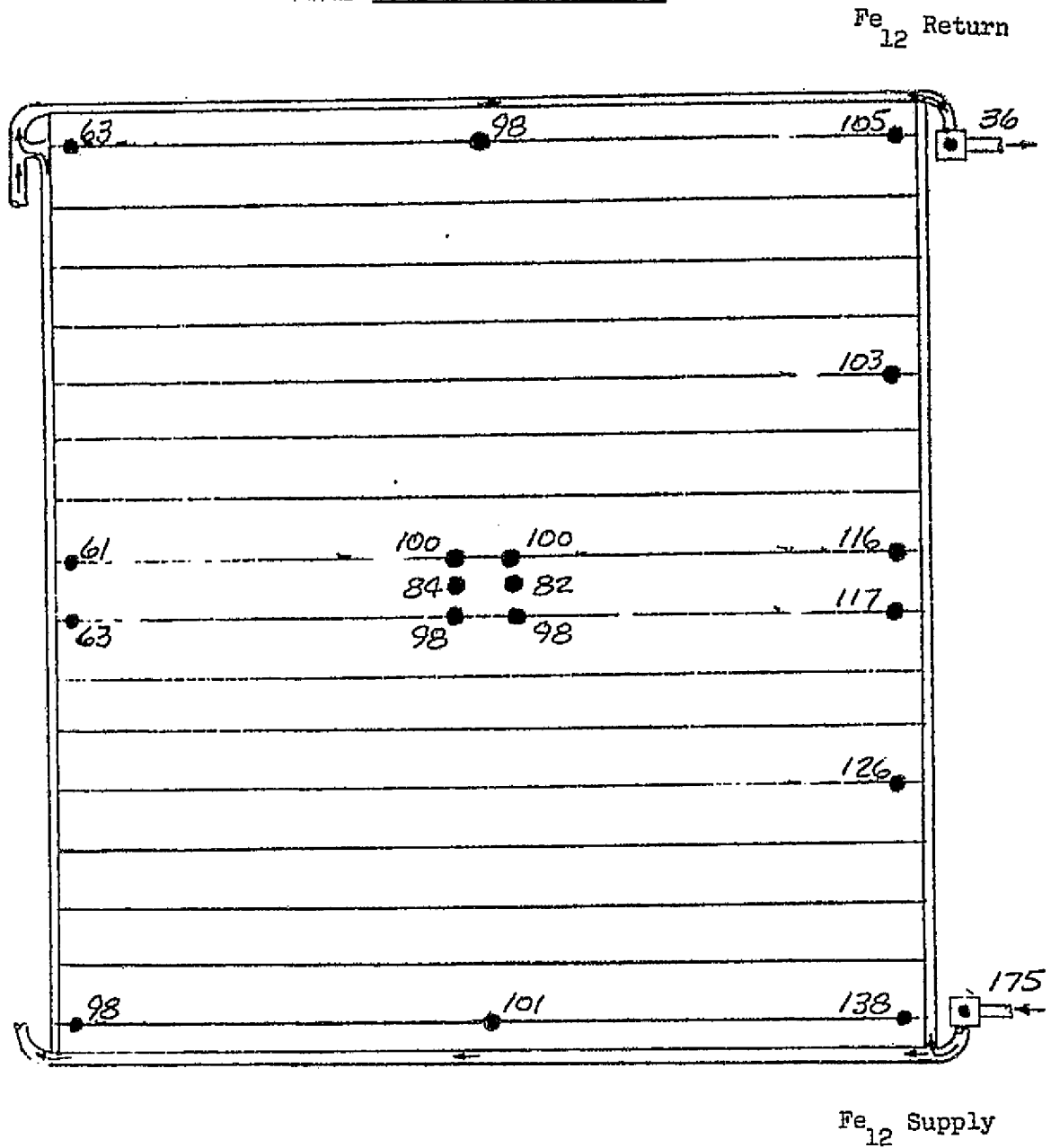
Fe_{12} Return

PANEL NO. 3

FIGURE A22 (CONT'D)

Fe_{12} Supply

TEST POINT ___17___

DAY ___295___

TIME ___13:30:05___

Fe$_{12}$ Return

60   89   102   49

107

64   96   96   103

79   79   109

64   83   98

113

60   96   111   103
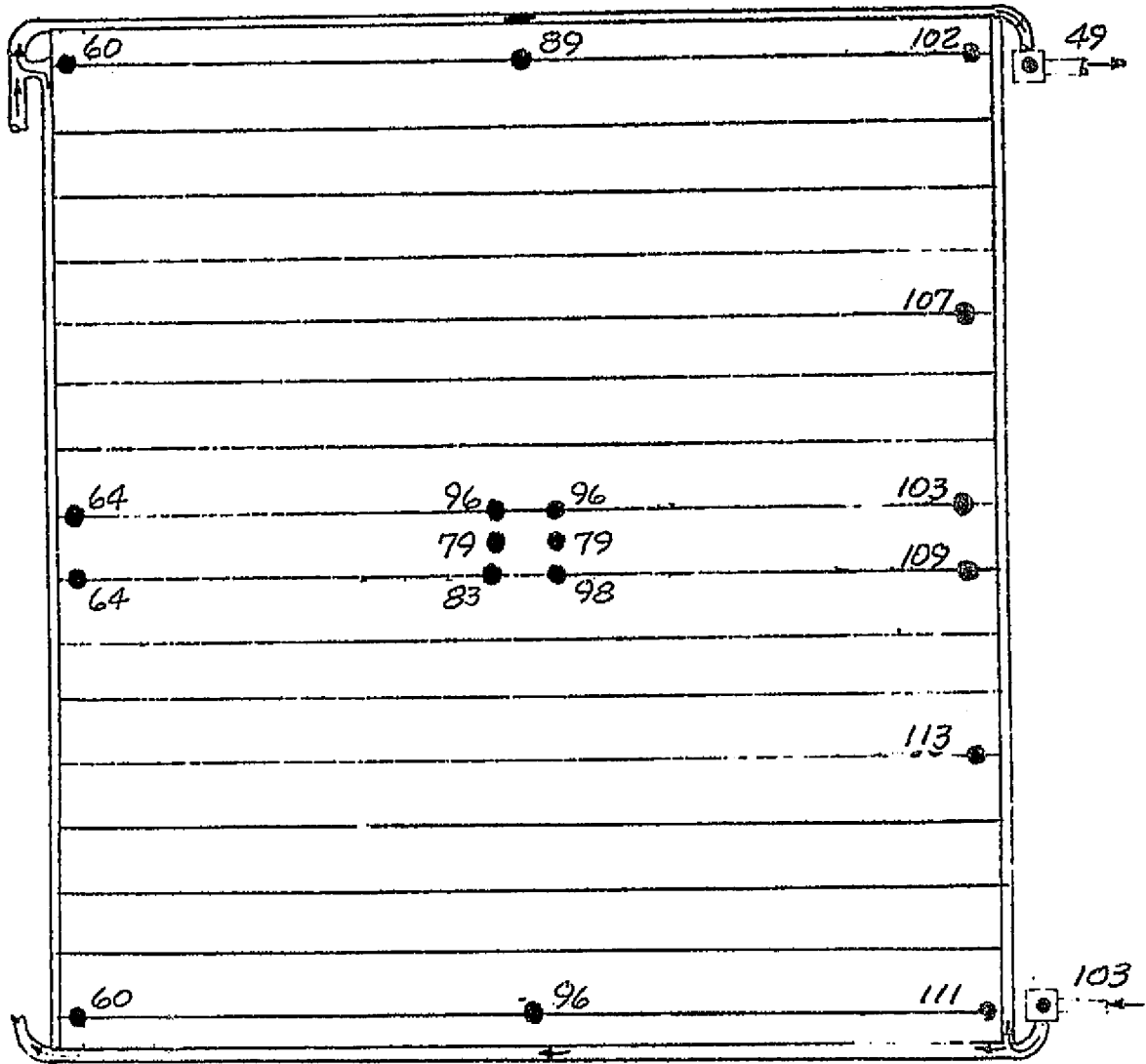
Fe$_{12}$ Supply

PANEL NO. 4

FIGURE A22 (CONT'D)

A-89

TEST POINT _18_
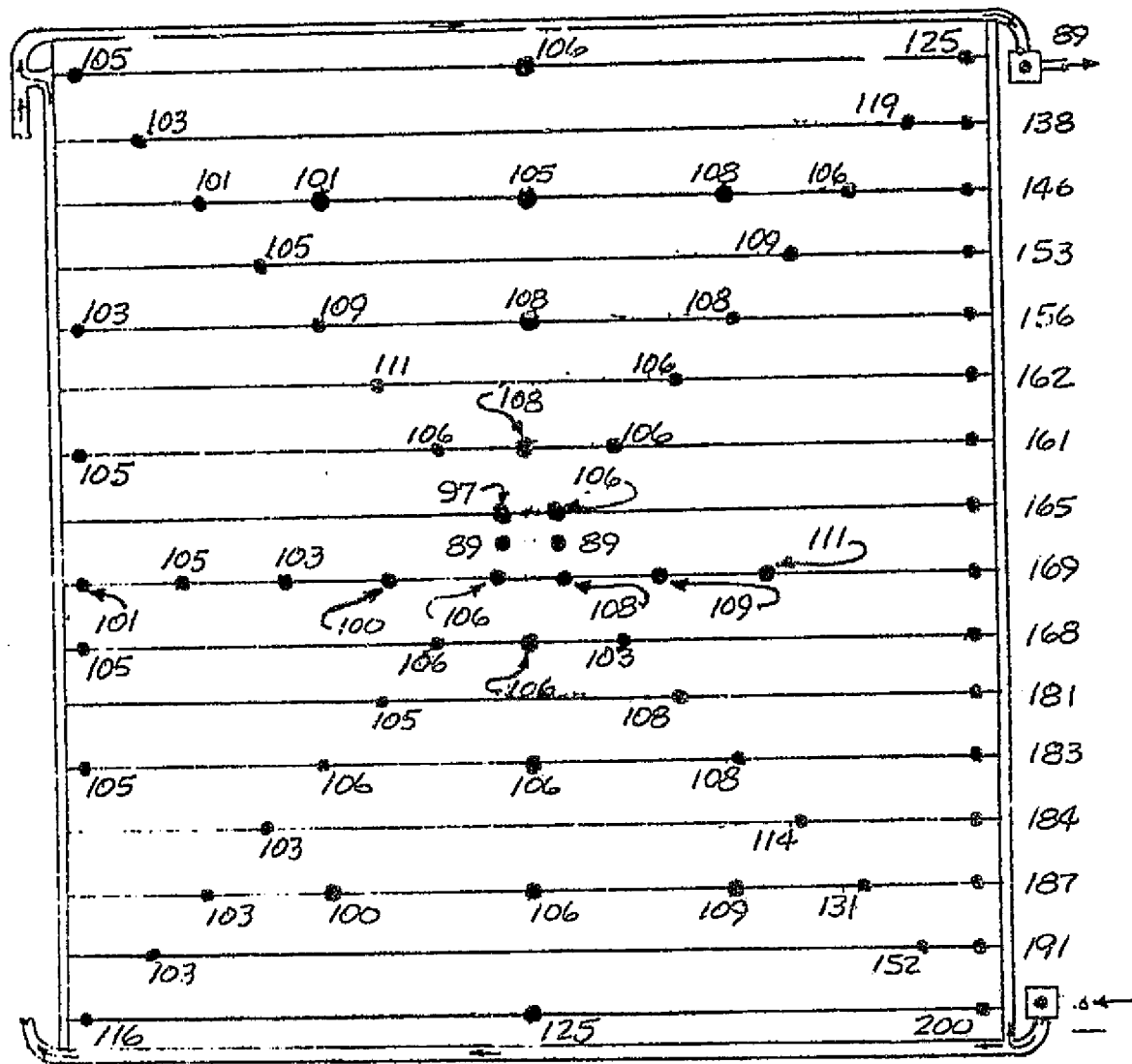
DAY _295_

TIME _14:45:05_

Fe_{12} Return

PANEL NO. 1

FIGURE A23

STEADY STATE VAPOR COMPRESSION OPERATION PANEL TEMPERATURE MAPS

Fe_{12} Supply

TEST POINT ___18___
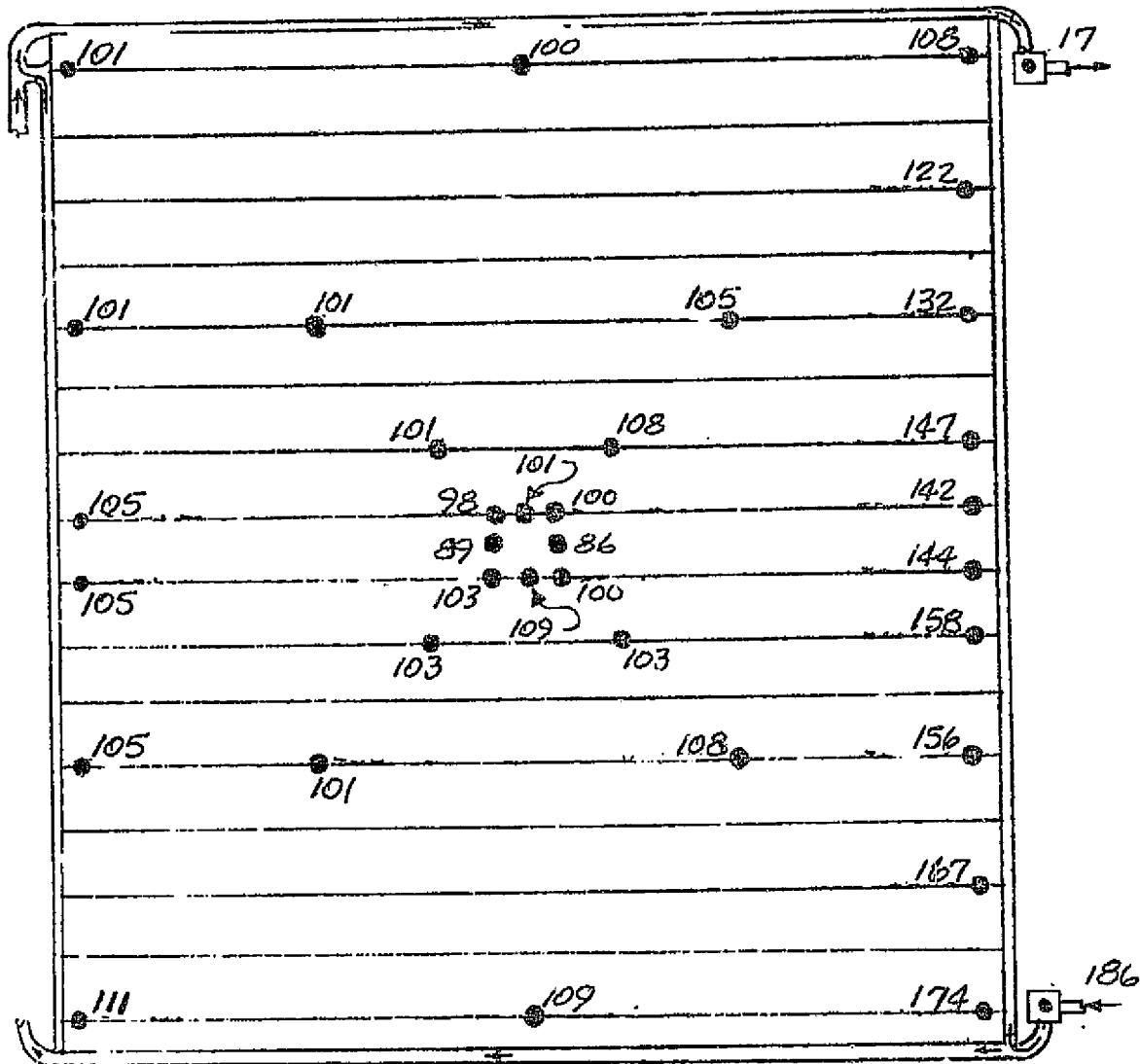
DAY ___295___

TIME ___14:45:05___

Fe_{12} Return

PANEL NO. 2

FIGURE A23 (CONT'D)

TEST POINT __18__

DAY ____295____

TIME ____14:45:05____

Fe$_{12}$ Return

68   105   109   43

113

66   105   105   128

90   89

70   134

105   105

140

105   108   153   194

Fe$_{12}$ Supply

PANEL NO. 3

FIGURE A23 (CONT'D)

TEST POINT ___18___

DAY ___295___

TIME ___14:45:05___
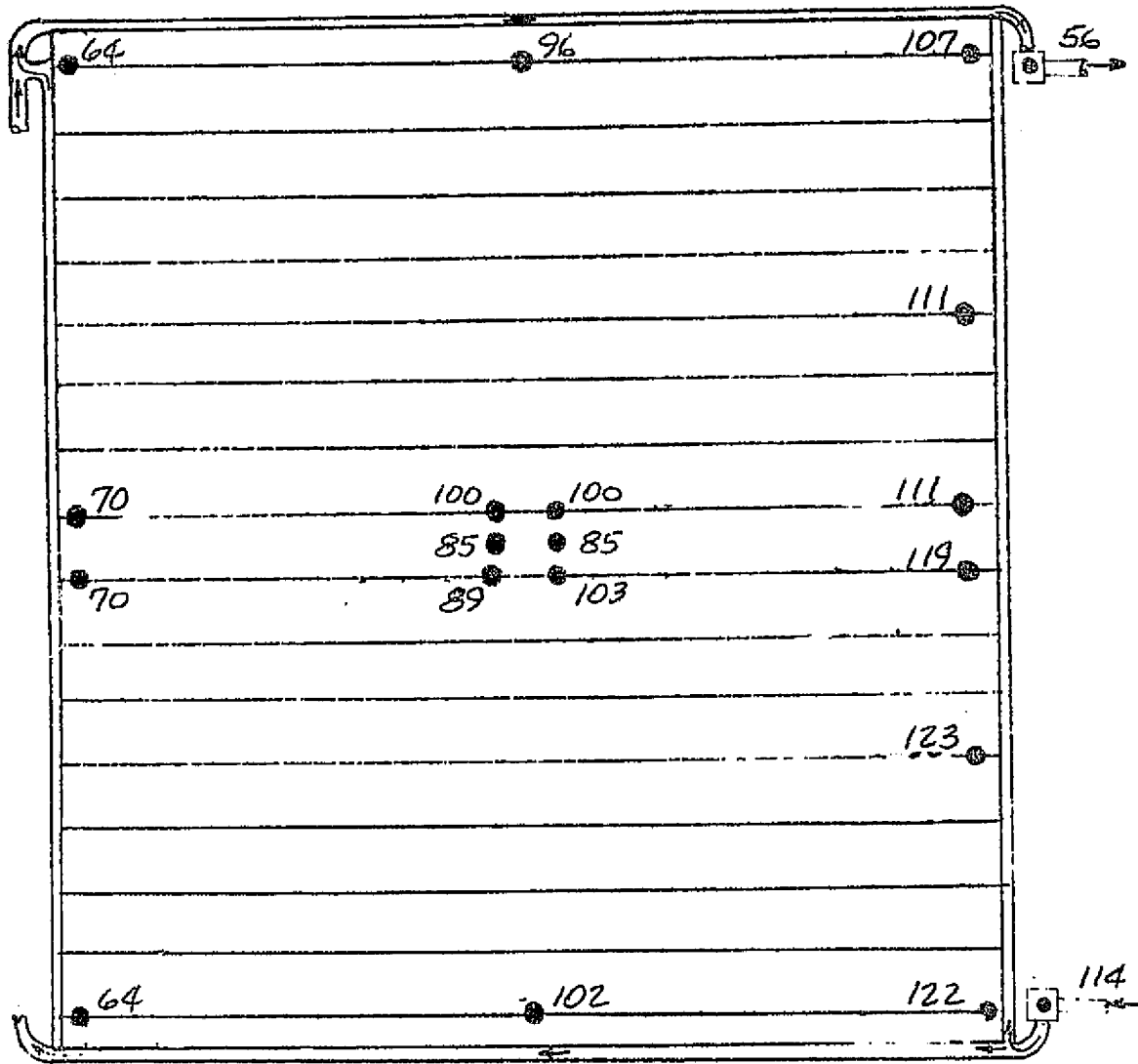
Fe_{12} Return

PANEL NO. 4

FIGURE A23 (CONT'D)

Fe_{12} Supply

Fe$_{12}$ Return

109   109   134 97

108   126 149

106 106 108 113 113 158

109   114 165

108 114 113 113 168

116 111 175

111

109   109 111 175

101 109 178

95 94

109 108   116 186

106 105 109 113 114 181

108 111 108 197

109 109 113

108 111 111 113 197

108 123 200

108 105 111 114 140

108 164

108

123 135
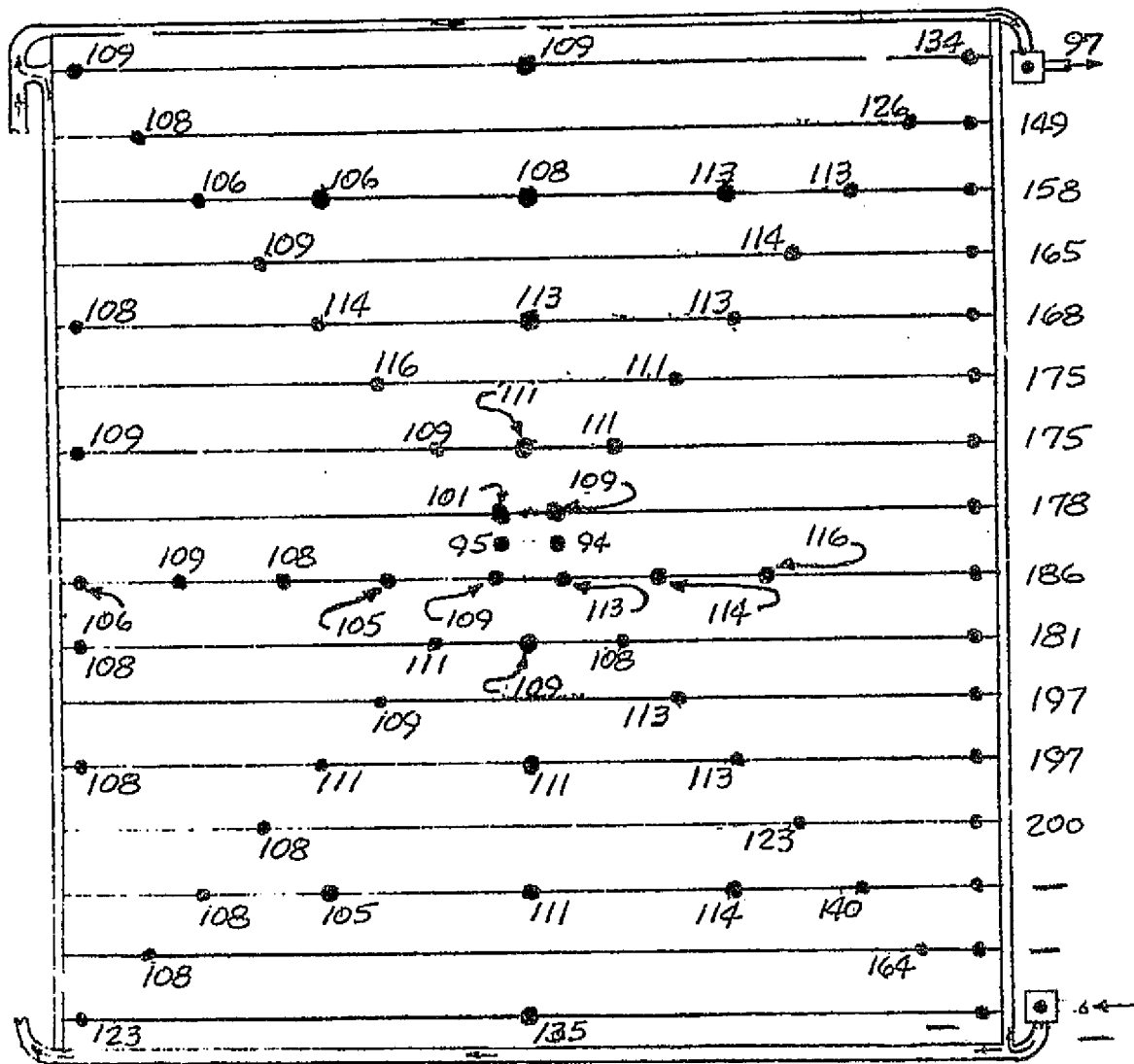
Fe$_{12}$ Supply

PANEL NO. 1

FIGURE A24

STEADY STATE VAPOR COMPRESSION OPERATION PANEL TEMPERATURE MAPS

TEST POINT ___19___

DAY ___295___
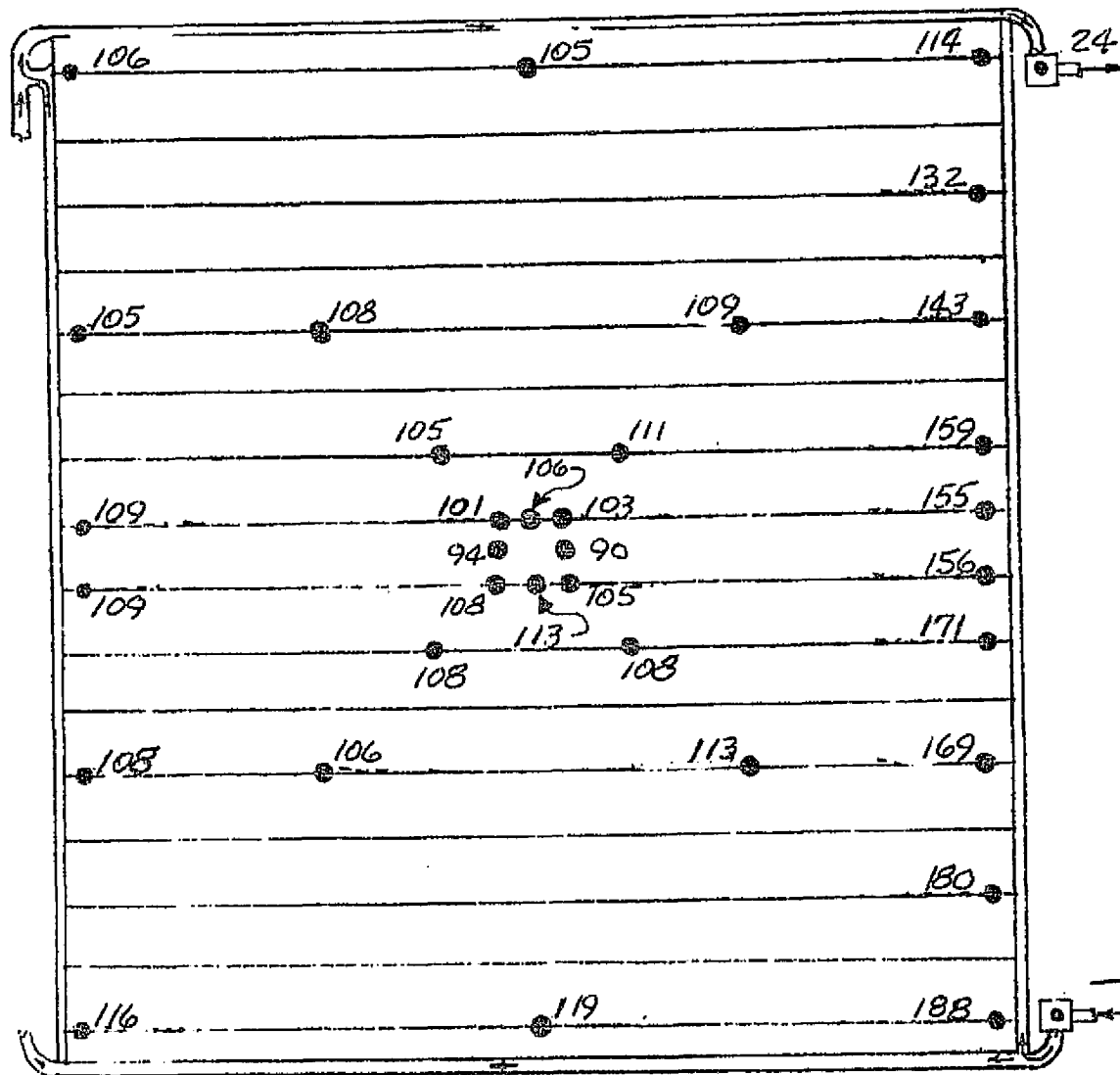
TIME ___16:30:05___

Fe_{12} Return

PANEL NO. 2

FIGURE A24 (CONT'D)

Fe_{12} Supply

TEST POINT _19_

DAY _295_

TIME _16:30:05_

Fe$_{12}$ Return

PANEL NO. 3

FIGURE A24 (CONT'D)

TEST POINT ___19___
DAY ___295___
TIME ___16:30:05___
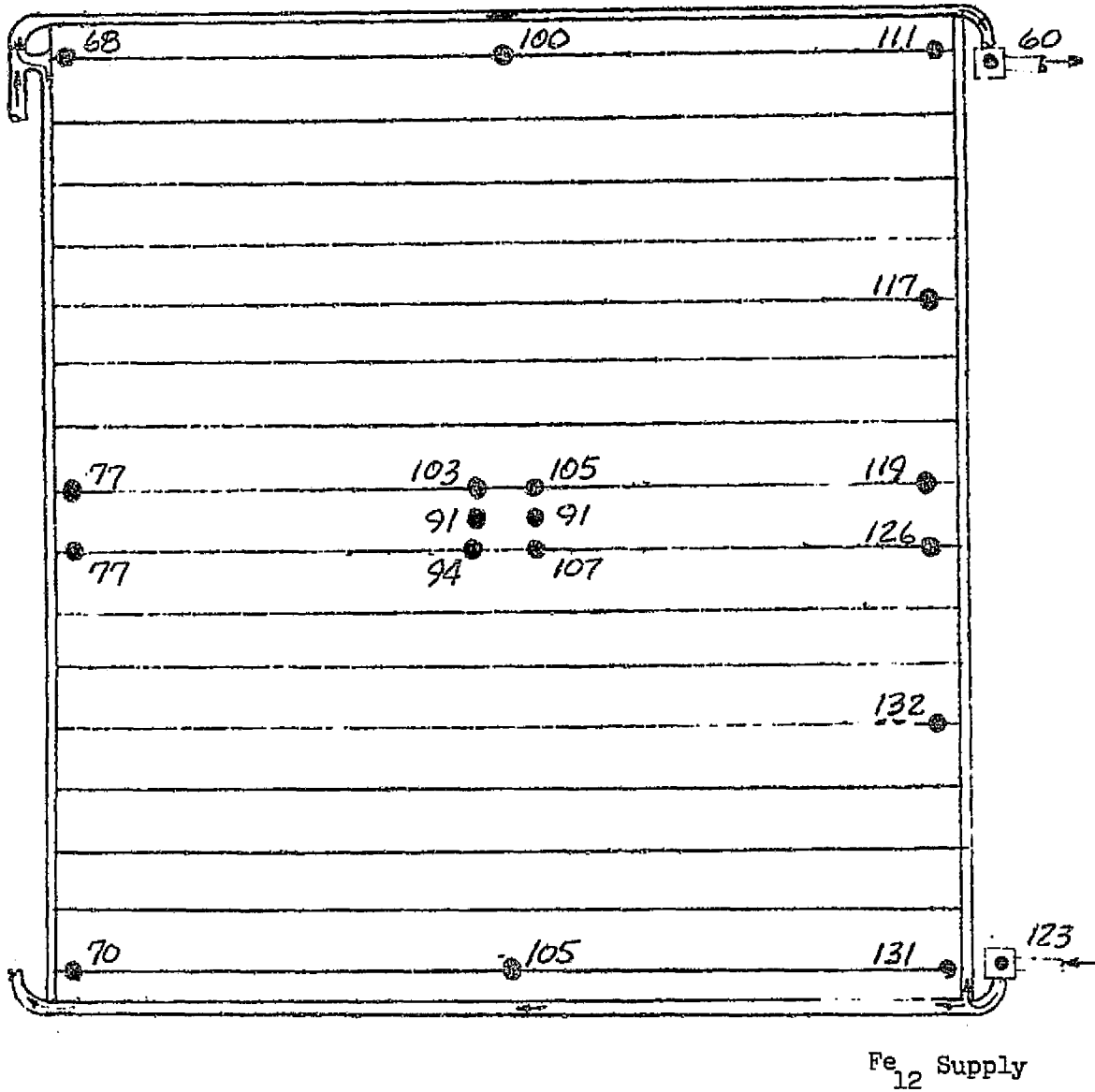
Fe$_{12}$ Return

PANEL NO. 4

FIGURE A24 (CONT'D)

Fe$_{12}$ Supply

TEST POINT ___19A___
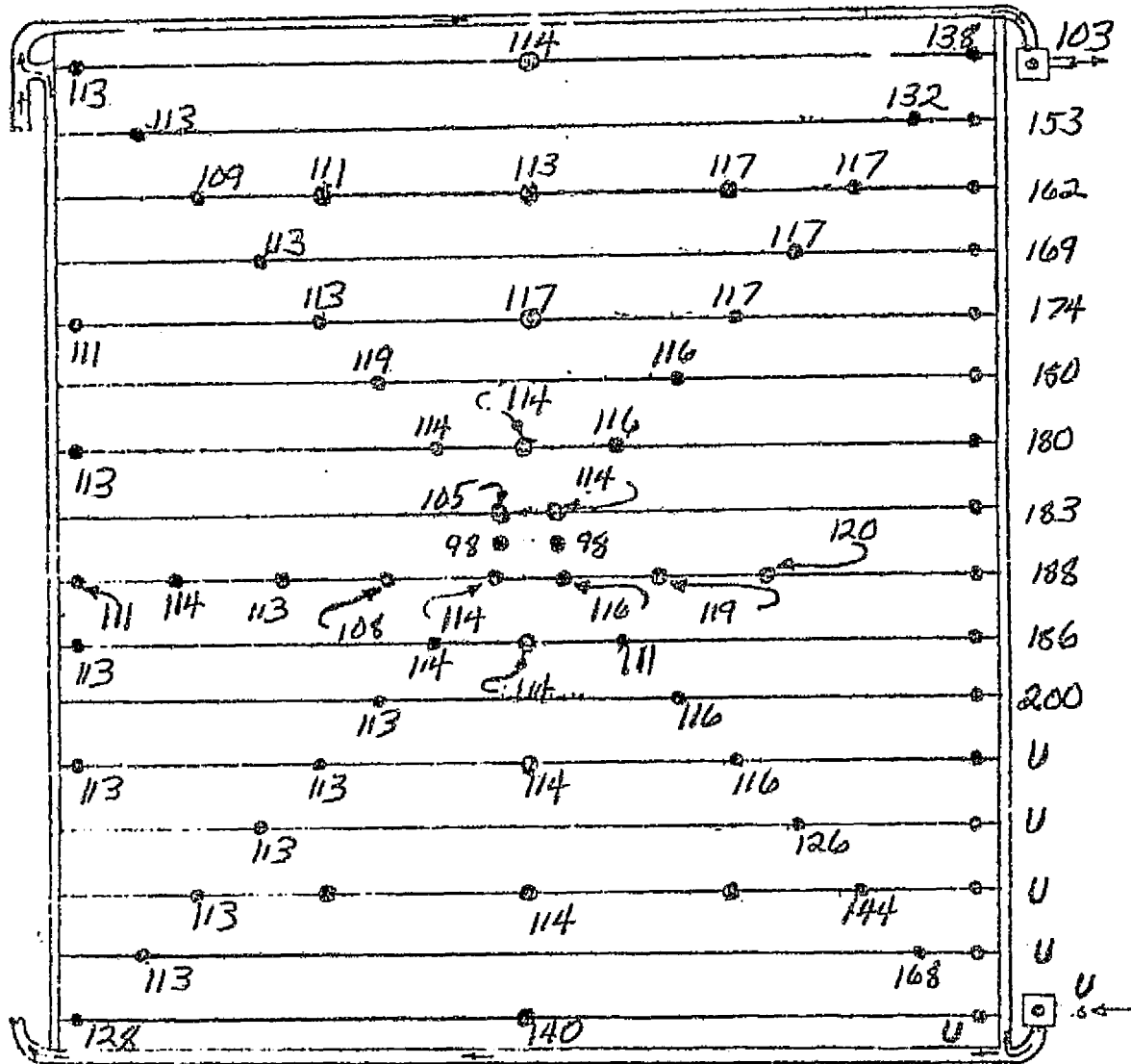
DAY ___296___

TIME ___11:30:00___

Fe$_{12}$ Return

PANEL NO. 1

FIGURE A25

STEADY STATE VAPOR COMPRESSION OPERATION PANEL TEMPERATURE MAPS

TEST POINT __174__

DAY __2·16__

TIME __11:30:00__

Fe$_{12}$ Return
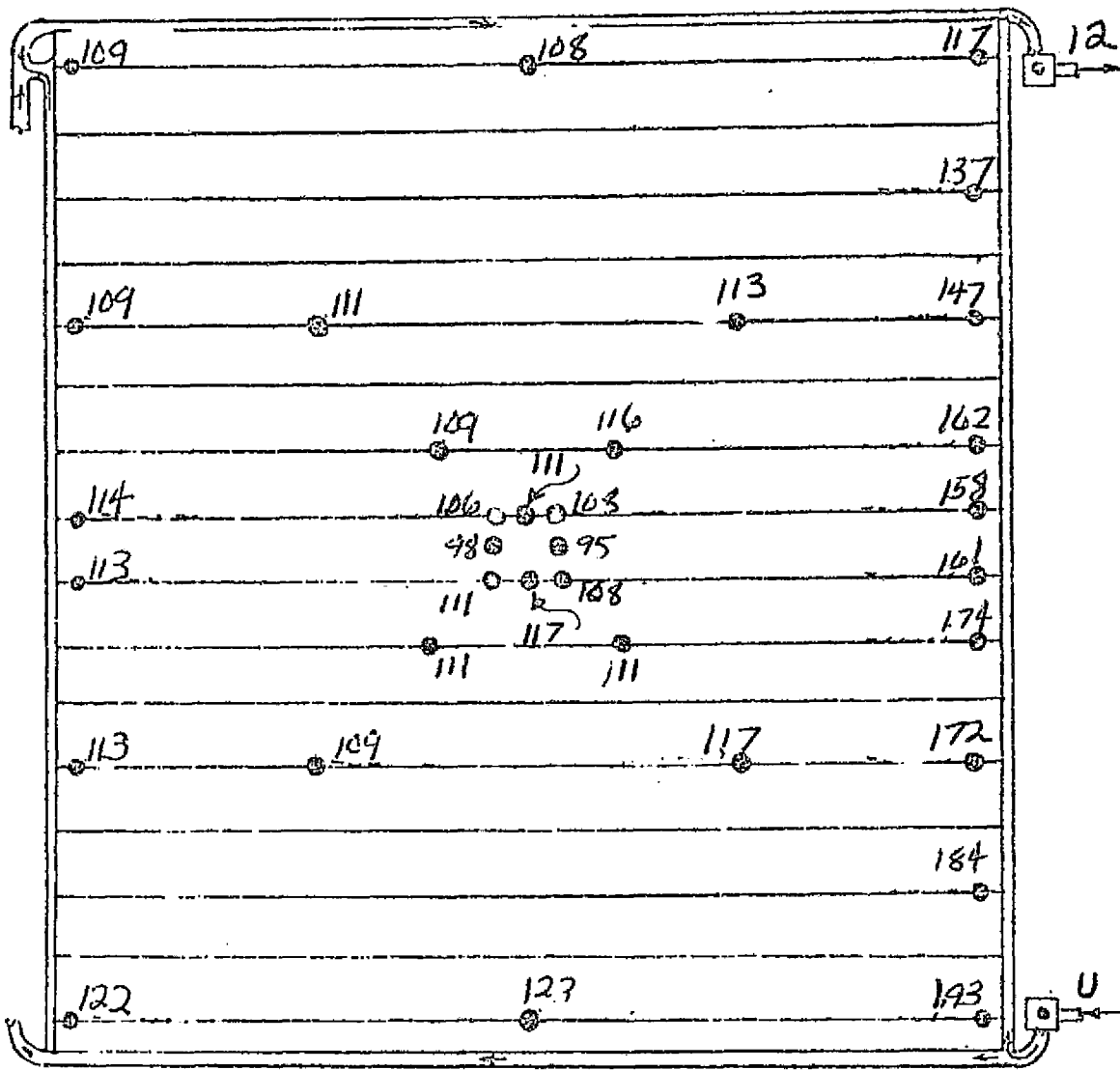
PANEL NO. 2

FIGURE A25 (CONT'D)

TEST POINT ___19A___

DAY ___296___

TIME ___11:30:04___

Fe$_{12}$ Return
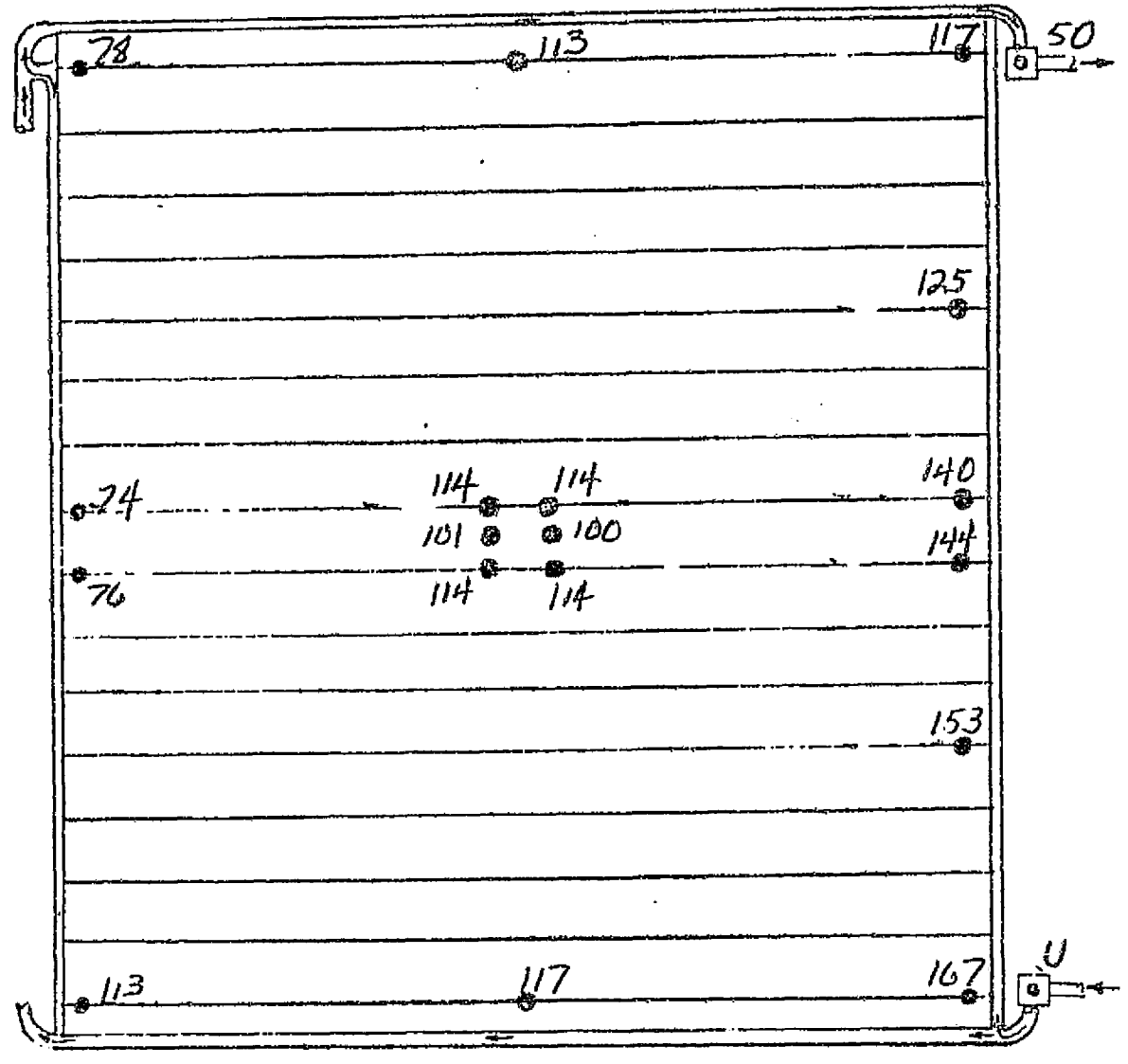
PANEL NO. 3

FIGURE A25 (CONT'D)

TEST POINT _____ 19A

DAY _____ 296

TIME _____ 11:30:00
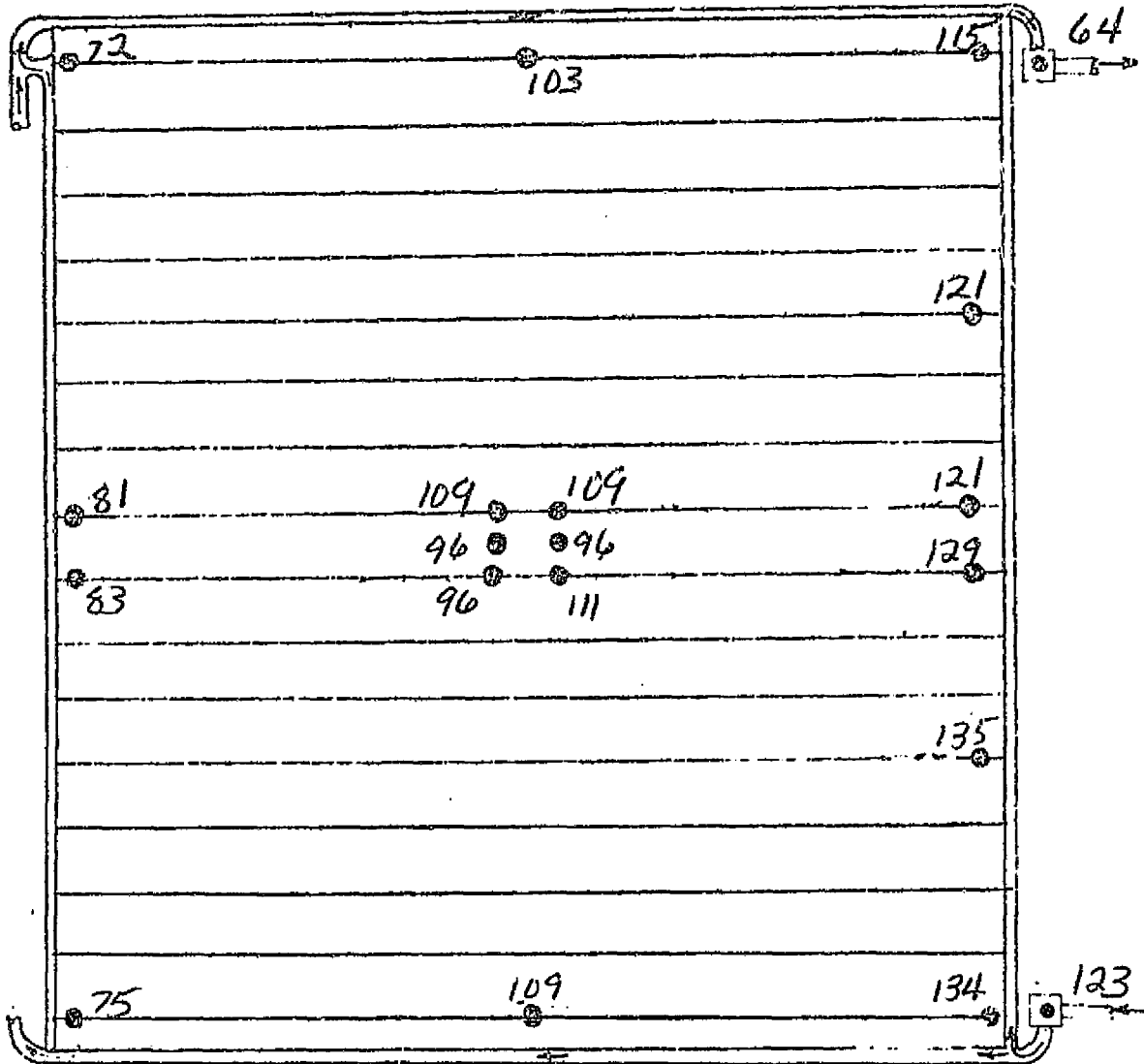
Fe_{12} Return

PANEL NO. 4

FIGURE A25 (CONT'D)

Fe_{12} Supply

A-101

TEST POINT _14A_
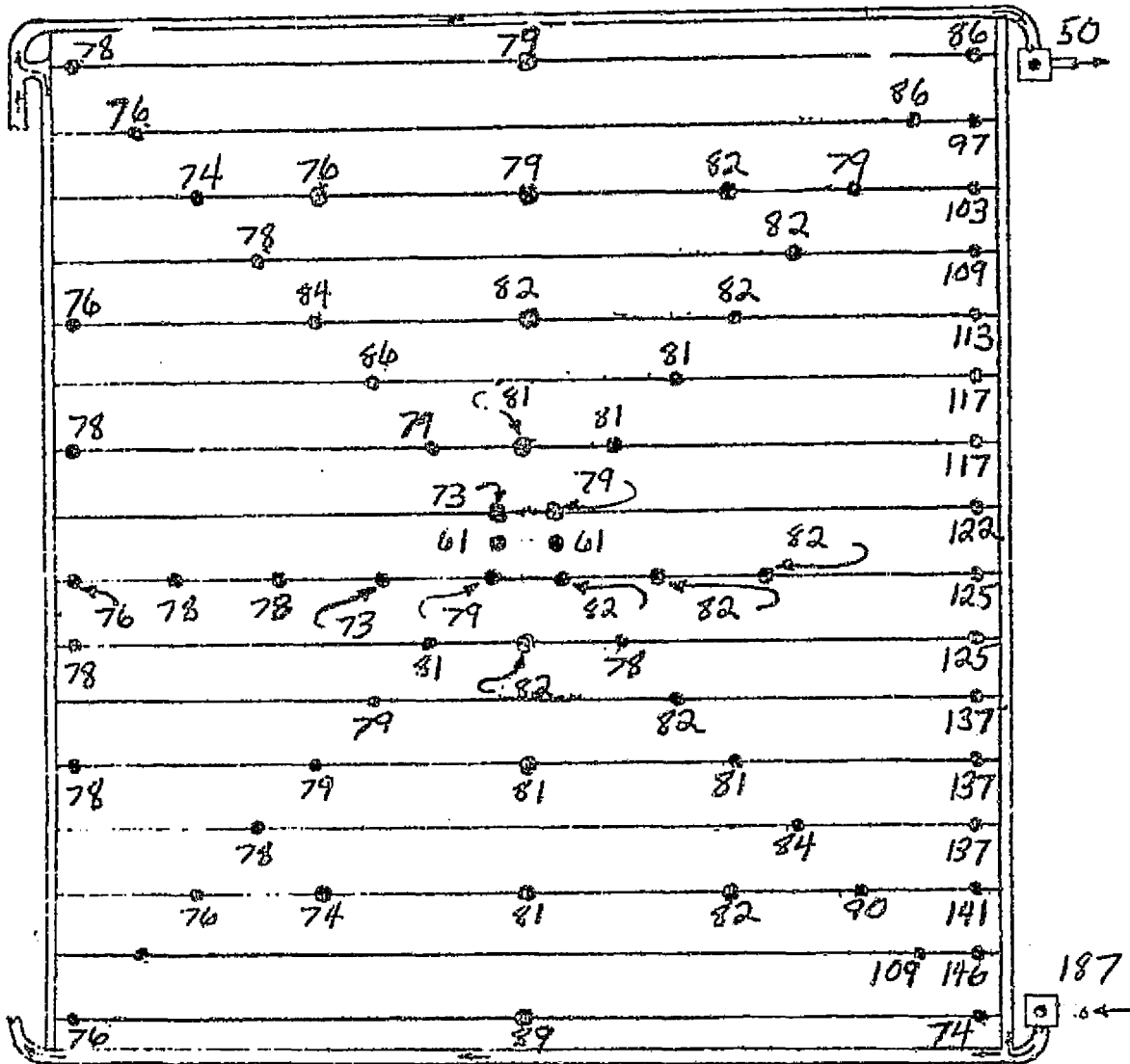
DAY _297_

TIME _04:30:00_

Fe$_{12}$ Return

PANEL NO. 1

FIGURE A26

STEADY STATE VAPOR COMPRESSION OPERATION PANEL TEMPERATURE MAPS

Fe$_{12}$ Supply

A-102

TEST POINT ___14A___
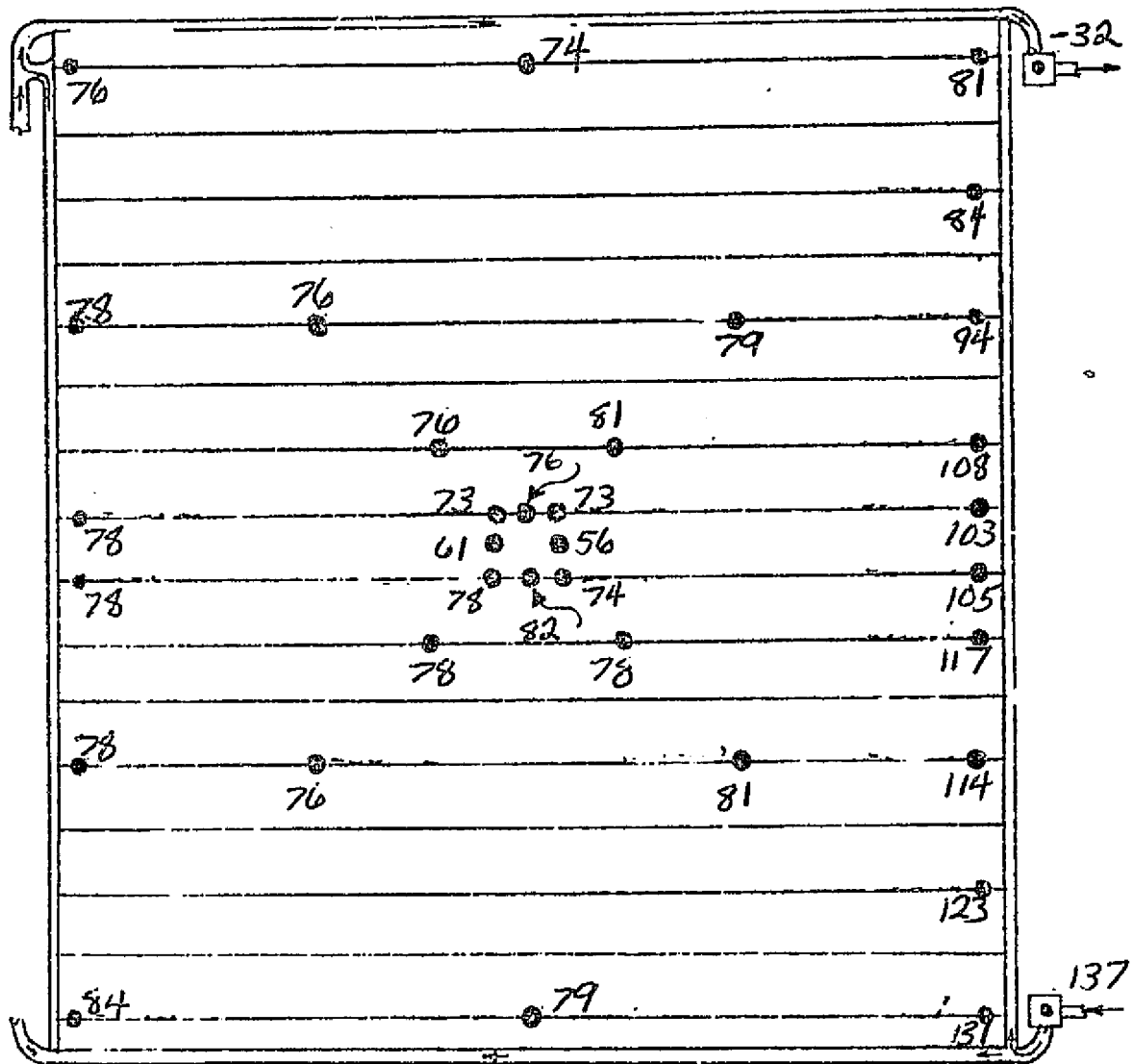
DAY ___297___

TIME ___04:30:00___

Fe$_{12}$ Return

PANEL NO. 2

FIGURE A26 (CONT'D)

Fe$_{12}$ Supply

TEST POINT _14A_

DAY _297_

TIME _04:30:00_

Fe$_{12}$ Return

36   78   84

82

36   78   79   92

61   60

38   78   78   98

101

76   79   149

116

Fe$_{12}$ Supply

PANEL NO. 3

FIGURE A26 (CONT'D)

TEST POINT __14A__

DAY __297__

TIME __04:30:00__
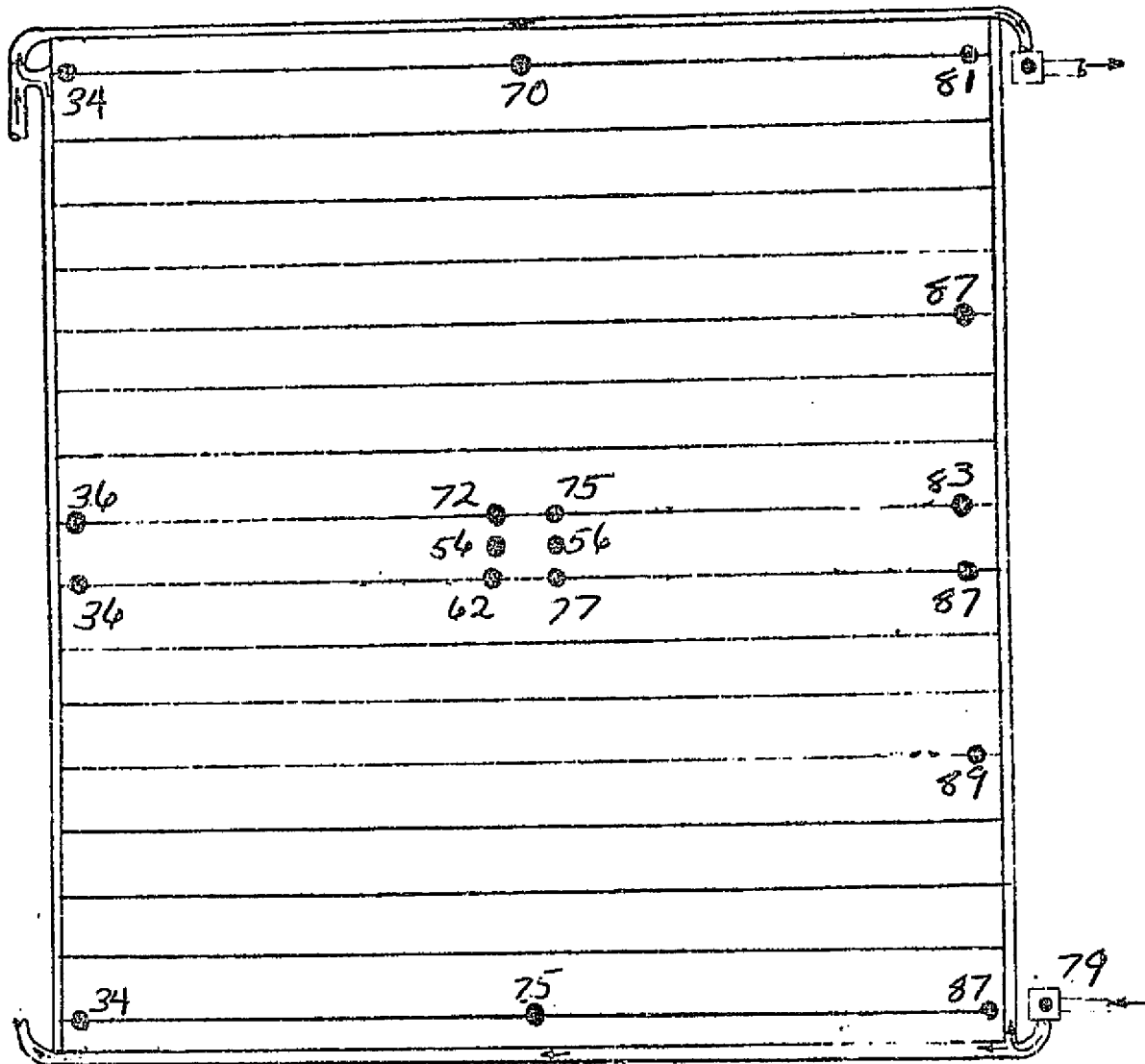
Fe$_{12}$ Return

PANEL NO. 4

FIGURE A26 (CONT'D)

Fe$_{12}$ Supply

TEST POINT _17A_

DAY _297_

TIME _06:00:00_

Fe$_{12}$ Return

PANEL NO. 1

FIGURE A27

STEADY STATE VAPOR COMPRESSION OPERATION PANEL TEMPERATURE MAPS

Fe$_{12}$ Supply

A-106

TEST POINT __17A__
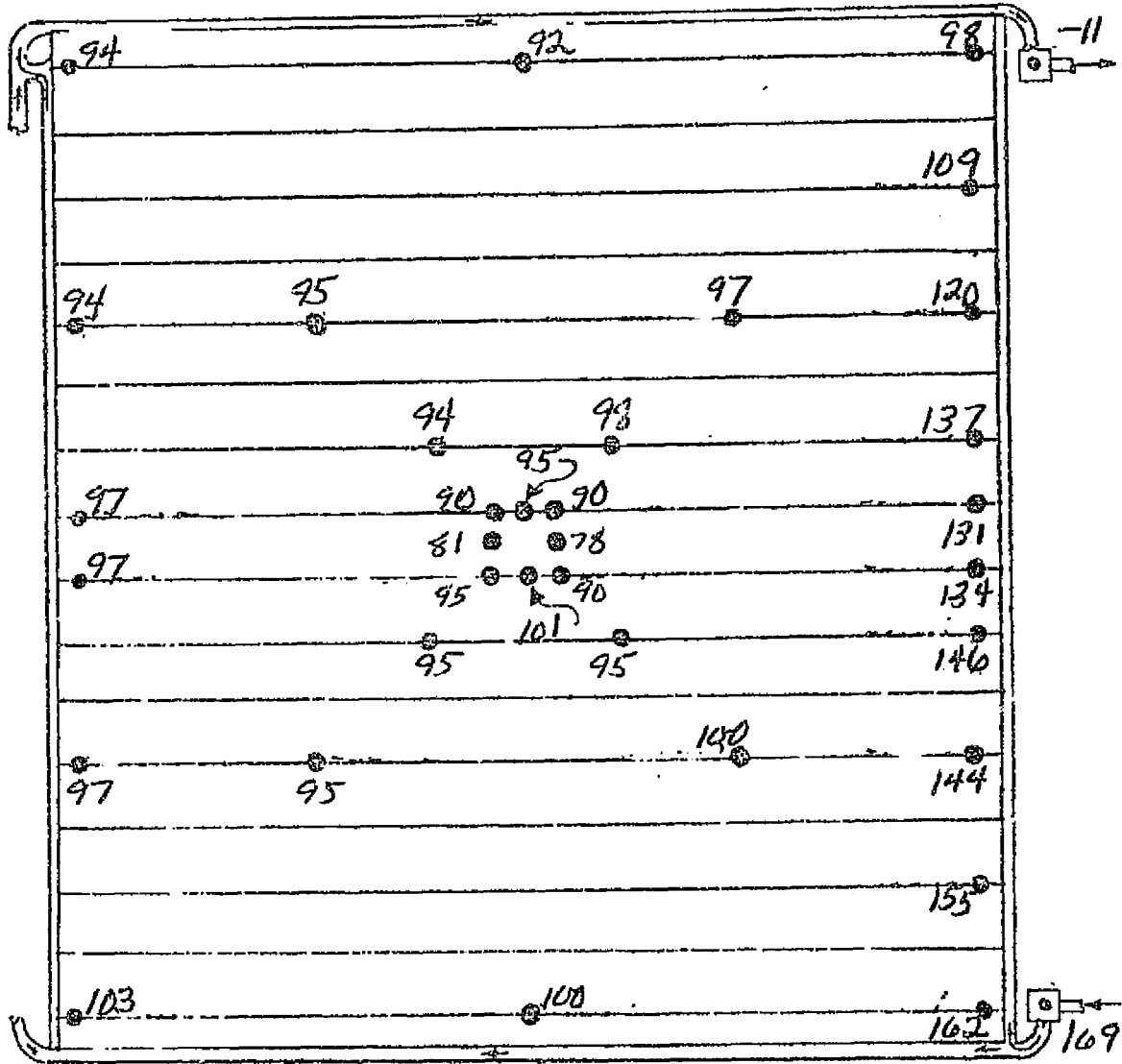
DAY ___297___

TIME ___06:00:00___

Fe_{12} Return

PANEL NO. 2

FIGURE A27 (CONT'D)

Fe_{12} Supply

A-107

TEST POINT ___17A___

DAY ___297___

TIME ___06:00:00___

Fe_{12} Return

Fe_{12} Supply

PANEL NO. 3

FIGURE A27 (CONT'D)

TEST POINT ___17A___

DAY ___297___

TIME ___06:00:00___
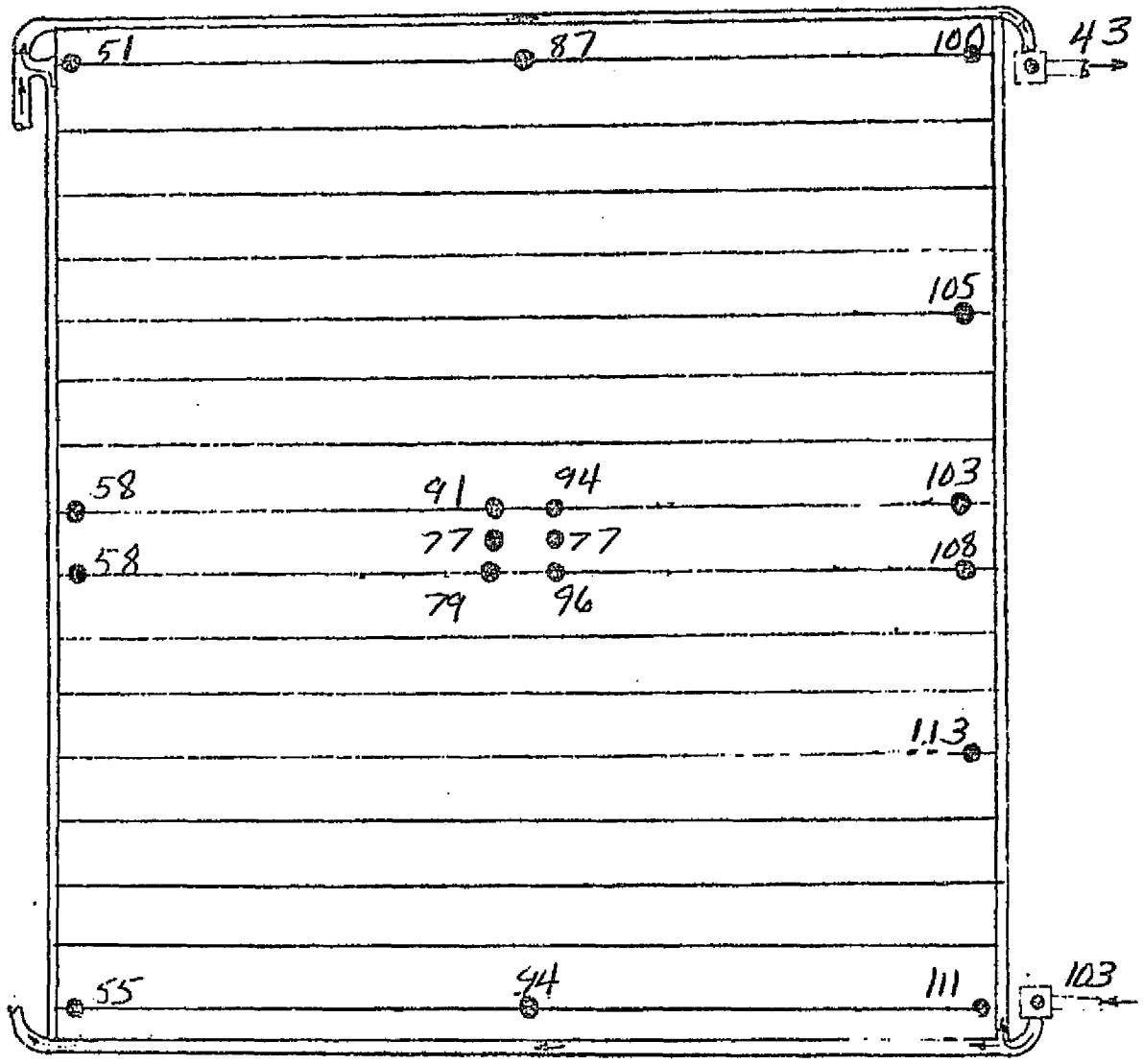
Fe$_{12}$ Return

PANEL NO. 4

FIGURE A27 (CONT'D)

Fe$_{12}$ Supply

TEST POINT _107_
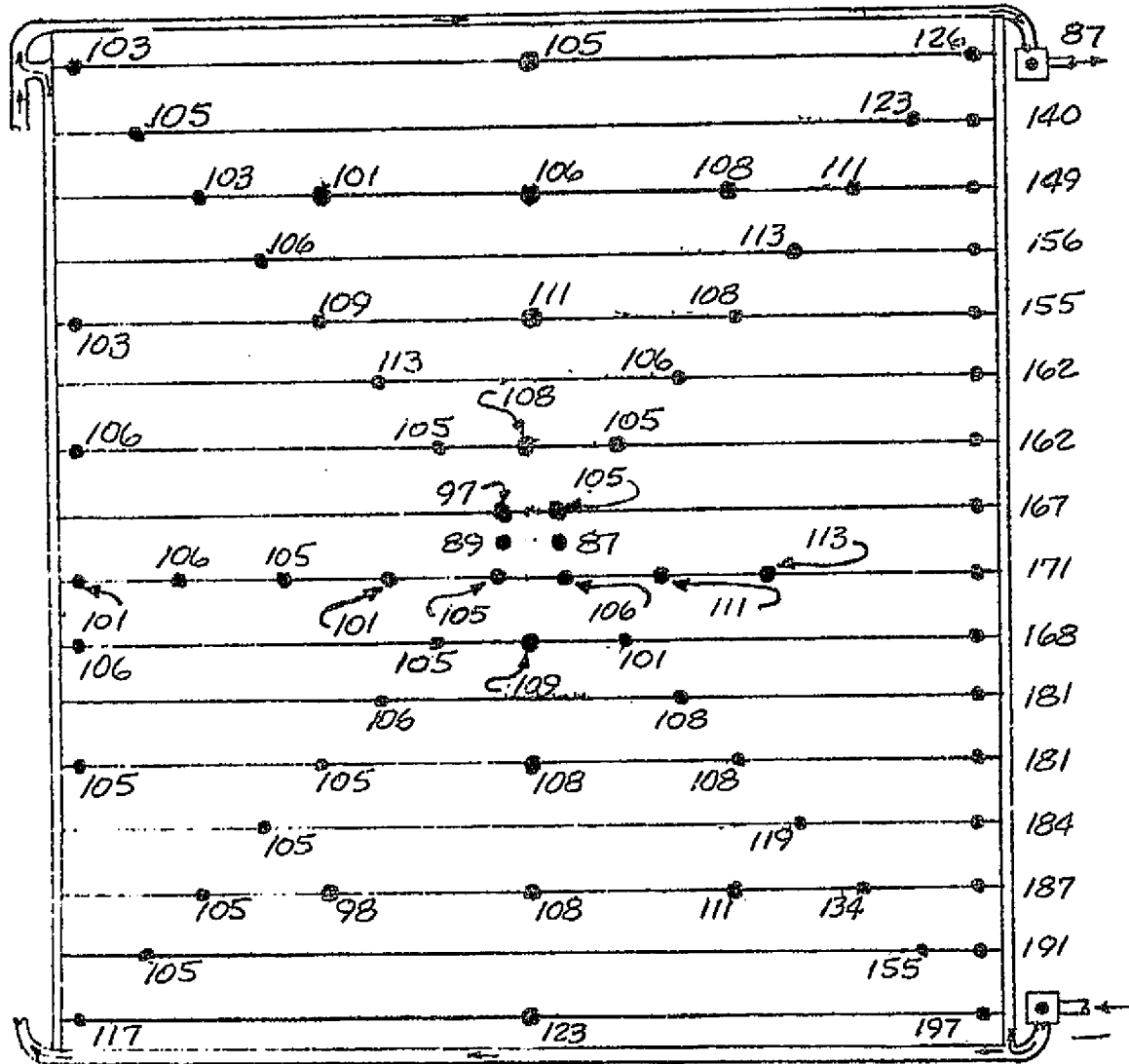
DAY _309_

TIME _7:04:29_

Fe$_{12}$ Return

PANEL NO. 1

FIGURE A28

STEADY STATE VAPOR COMPRESSION OPERATION PANEL TEMPERATURE MAPS

Fe$_{12}$ Supply

A-110

TEST POINT _107_

DAY _309_

TIME _7:04:29_

Fe$_{12}$ Return

101 101 109 89

125

95 101 105 140

100 105 149

101

105 97 101 146

90 87 149

103 105 101 158

108

101 103

108 159

105 101

165

190

111 111 175
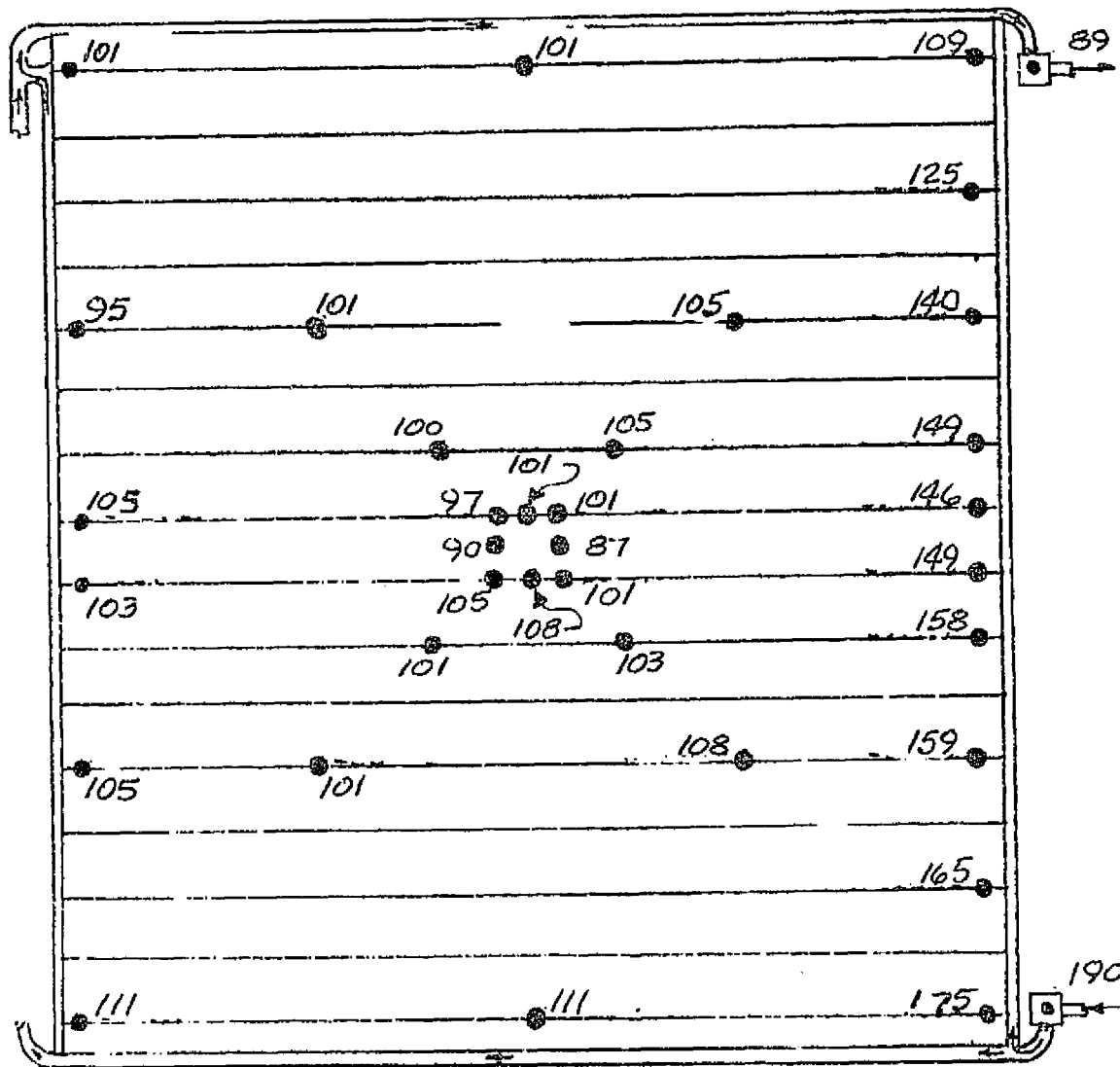
Fe$_{12}$ Supply

PANEL NO. 2

FIGURE A28 (CONT'D)

TEST POINT __107__

DAY __309__

TIME __7:04:29__

Fe$_{12}$ Return

61

103

108

70

114

63

103

105

126

89

89

131

65

103

103

138

103

106

150

193
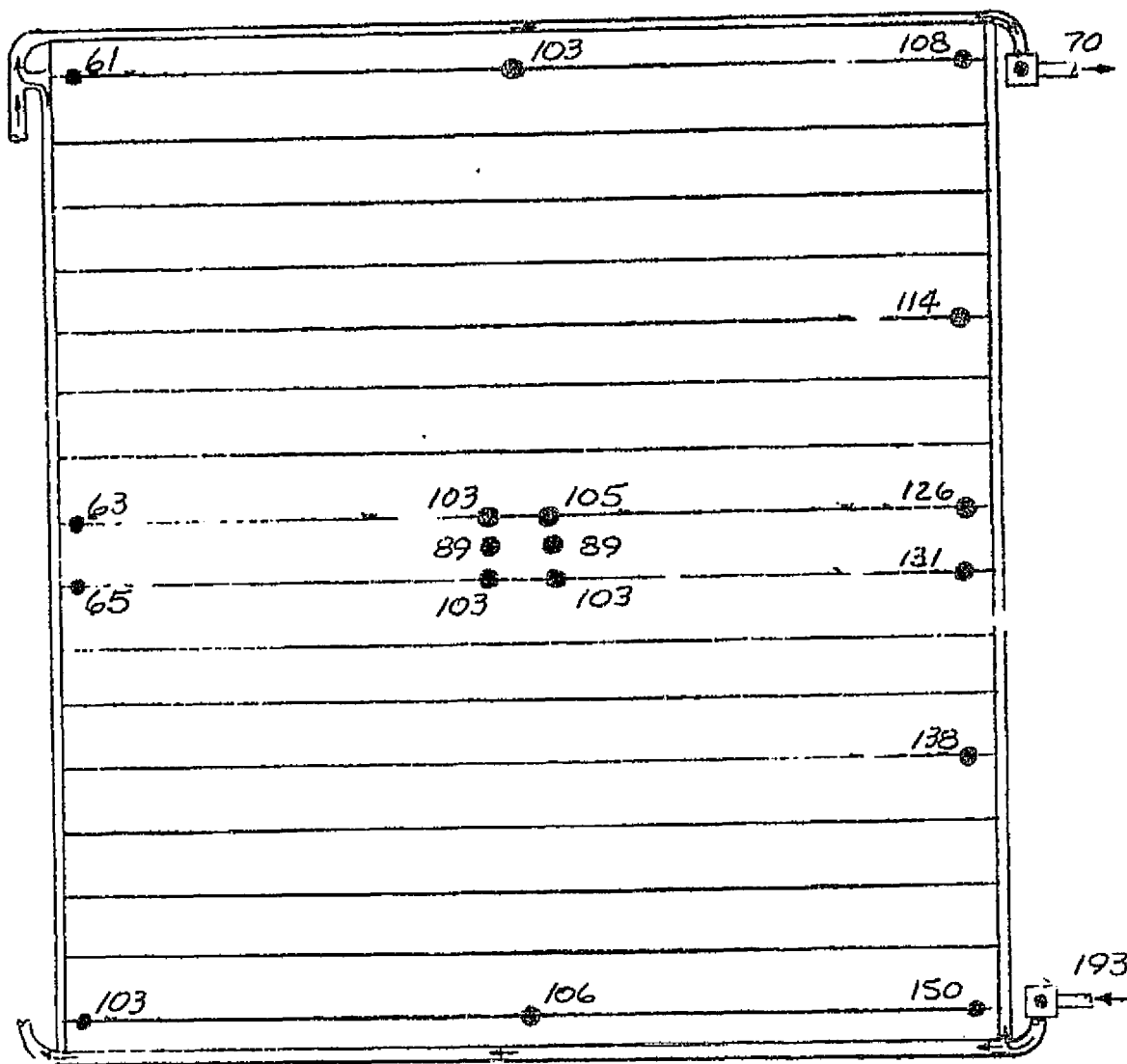
Fe$_{12}$ Supply

PANEL NO. 3

FIGURE A28 (CONT'D)

TEST POINT ___107___

DAY ___309___

TIME ___7:04:29___

Fe$_{12}$ Return

41   89   103   36

109

58   96   96   107

79   79

62   83   98   117

123

60   96   172   108
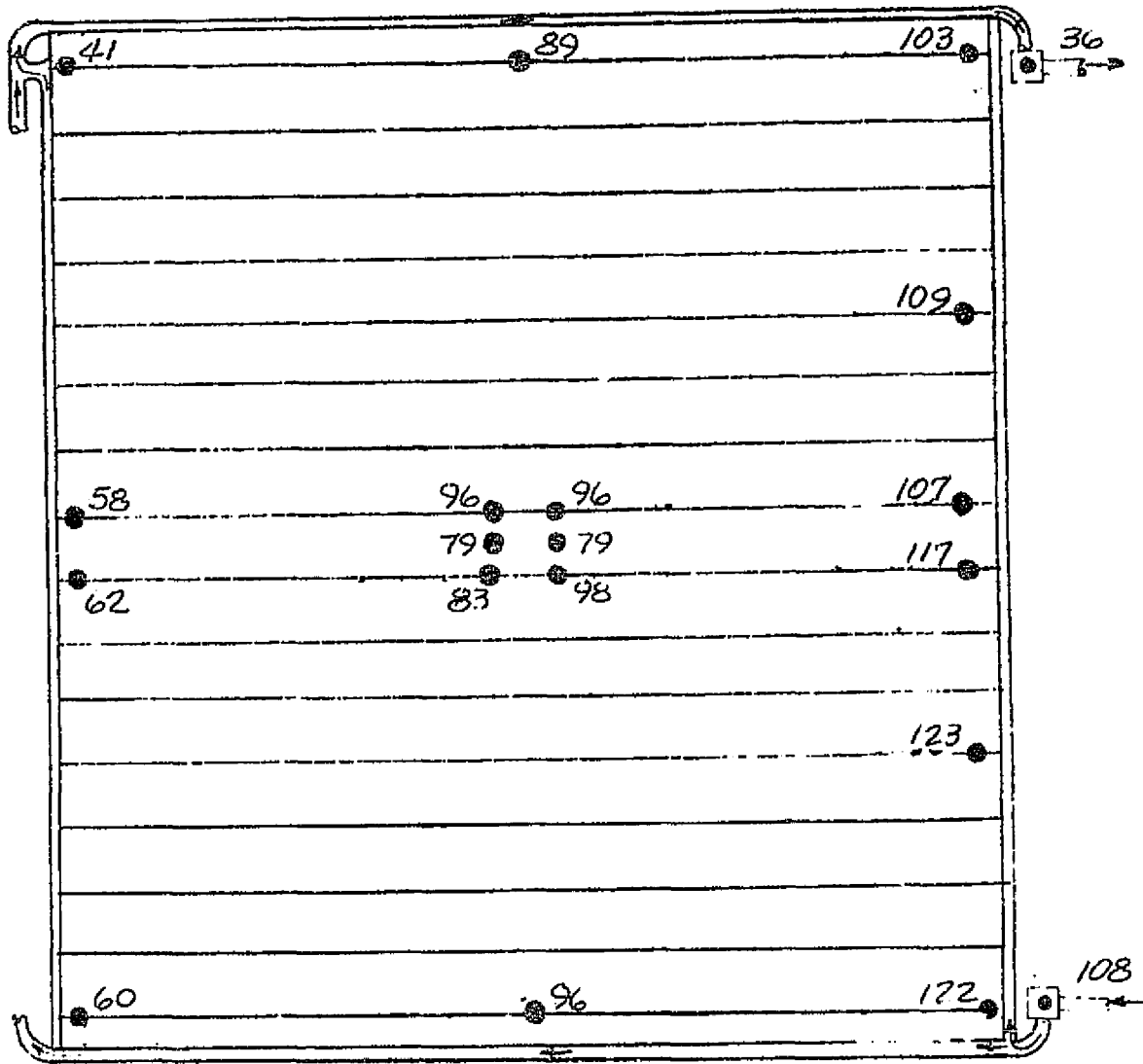
Fe$_{12}$ Supply

PANEL NO. 4

FIGURE A28 (CONT'D)

TEST POINT ___111___
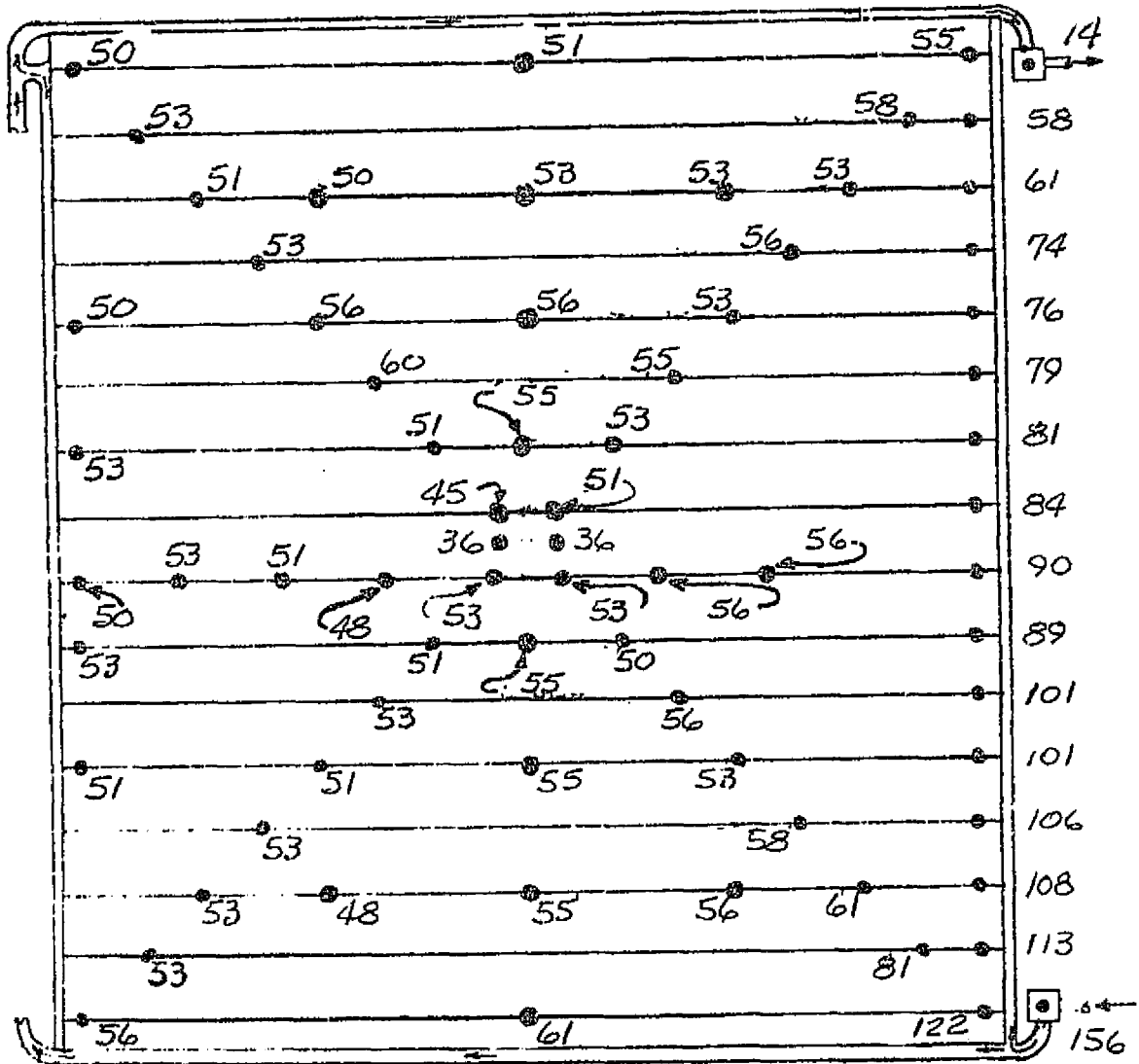
DAY ___309___

TIME ___16:15:06___

Fe$_{12}$ Return

PANEL NO. 1

FIGURE A29

STEADY STATE VAPOR COMPRESSION OPERATION PANEL TEMPERATURE MAPS

Fe$_{12}$ Supply

TEST POINT ___111___
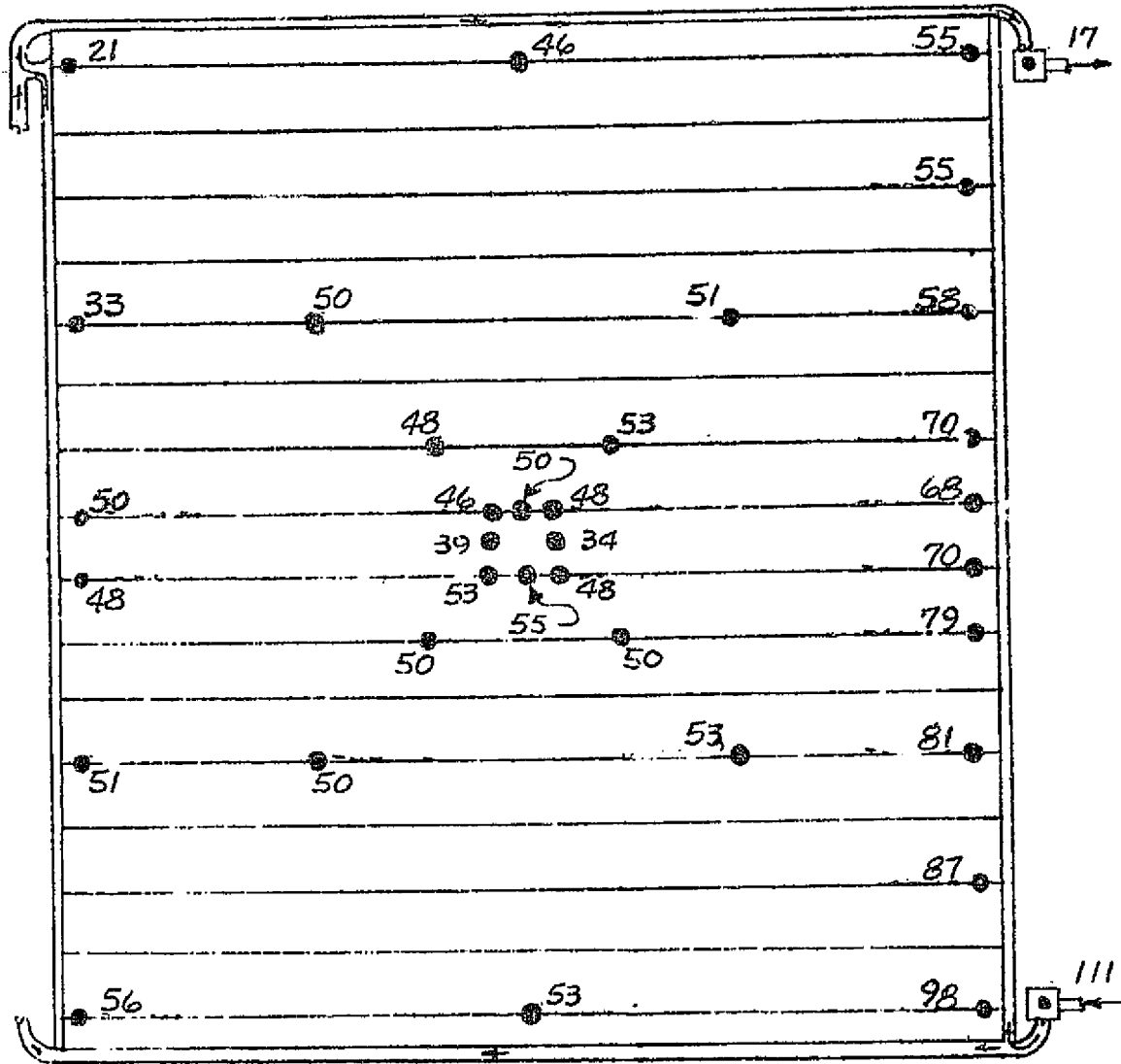
DAY ___309___

TIME ___16:15:06___

Fe_{12} Return

PANEL NO. 2

FIGURE A29 (CONT'D)

Fe_{12} Supply

TEST POINT ___111___

DAY ___309___

TIME ___16:15:06___

PANEL NO. 3

FIGURE A29 (CONT'D)

TEST POINT ___*111*___

DAY ___*309*___

TIME ___*16:15:06*___
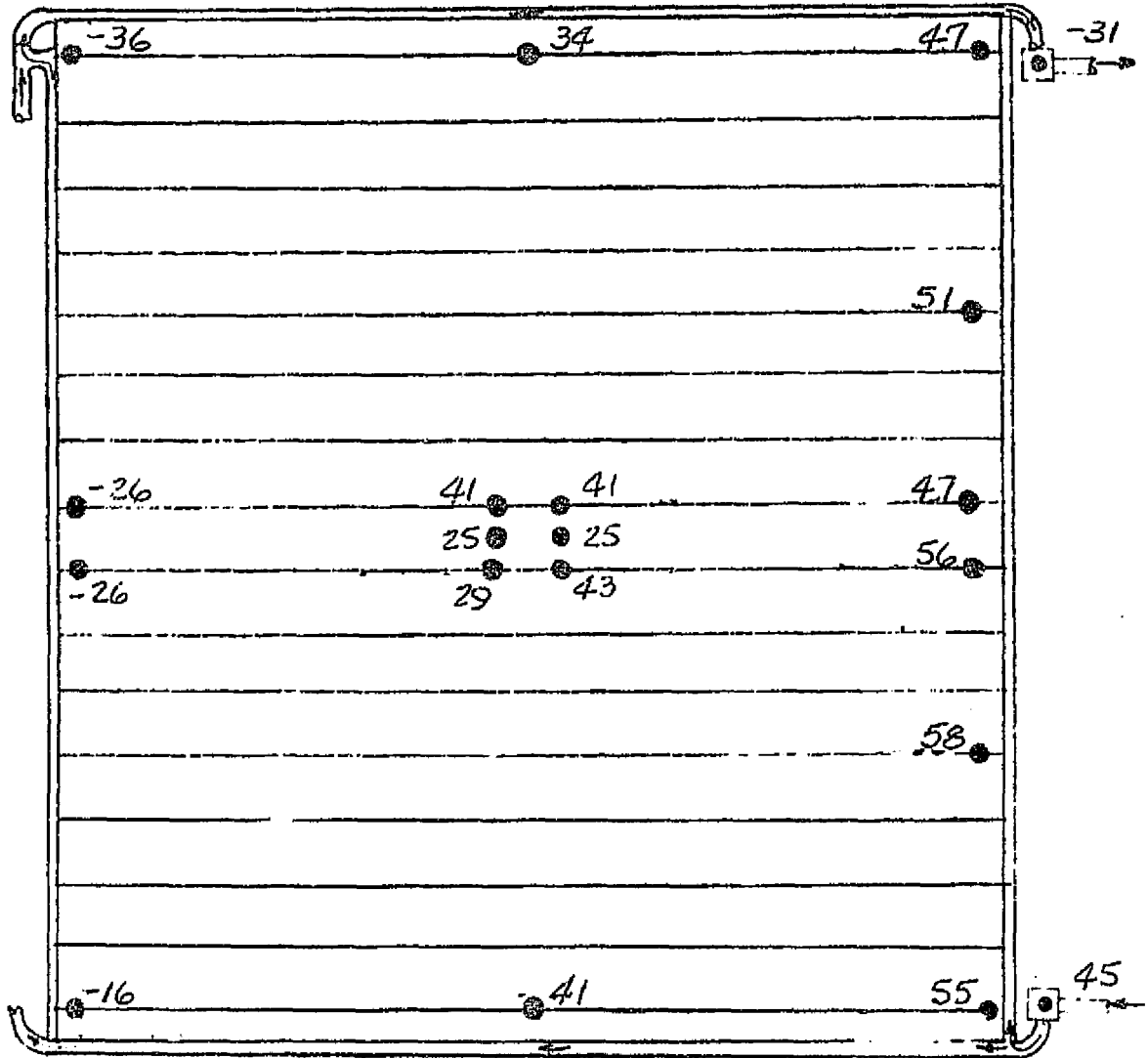
Fe_{12} Return

PANEL NO. 4

FIGURE A29 (CONT'D)

Fe_{12} Supply

TEST POINT __112__
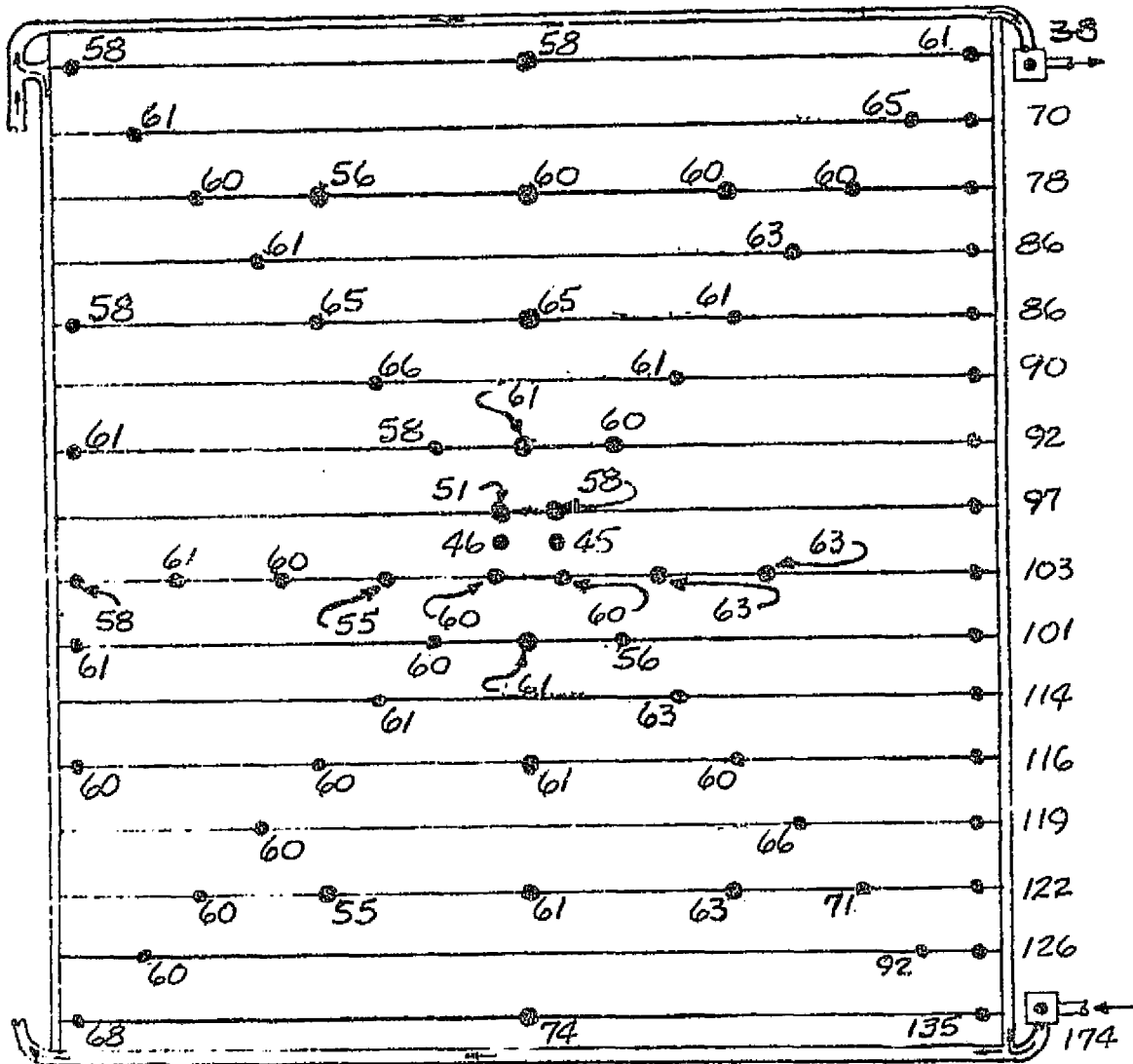
DAY __309__

TIME __18:00:06__

Fe_{12} Return

PANEL NO. 1

FIGURE A30

STEADY STATE VAPOR COMPRESSION OPERATION PANEL TEMPERATURE MAPS

TEST POINT _112_

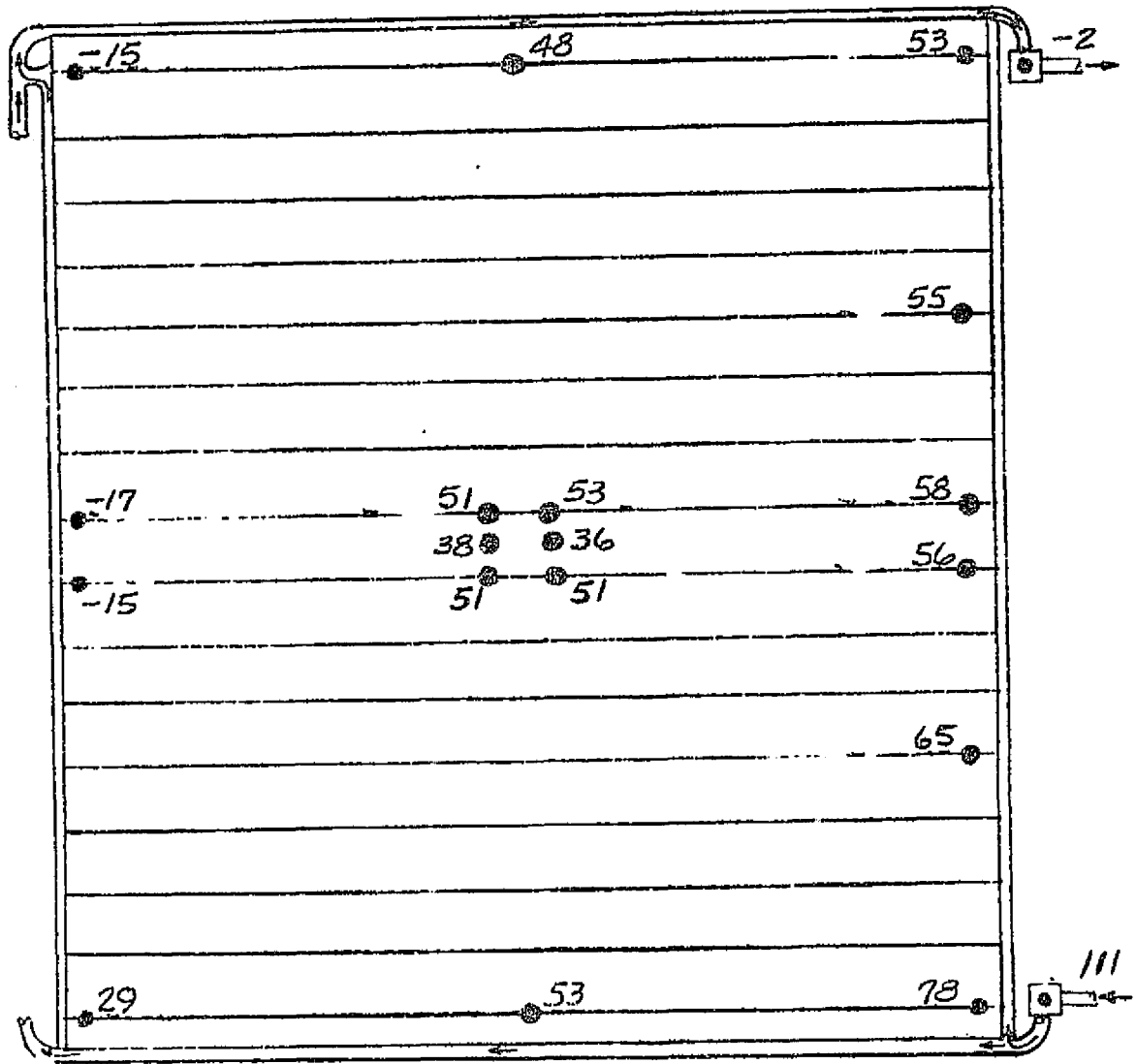DAY _309_
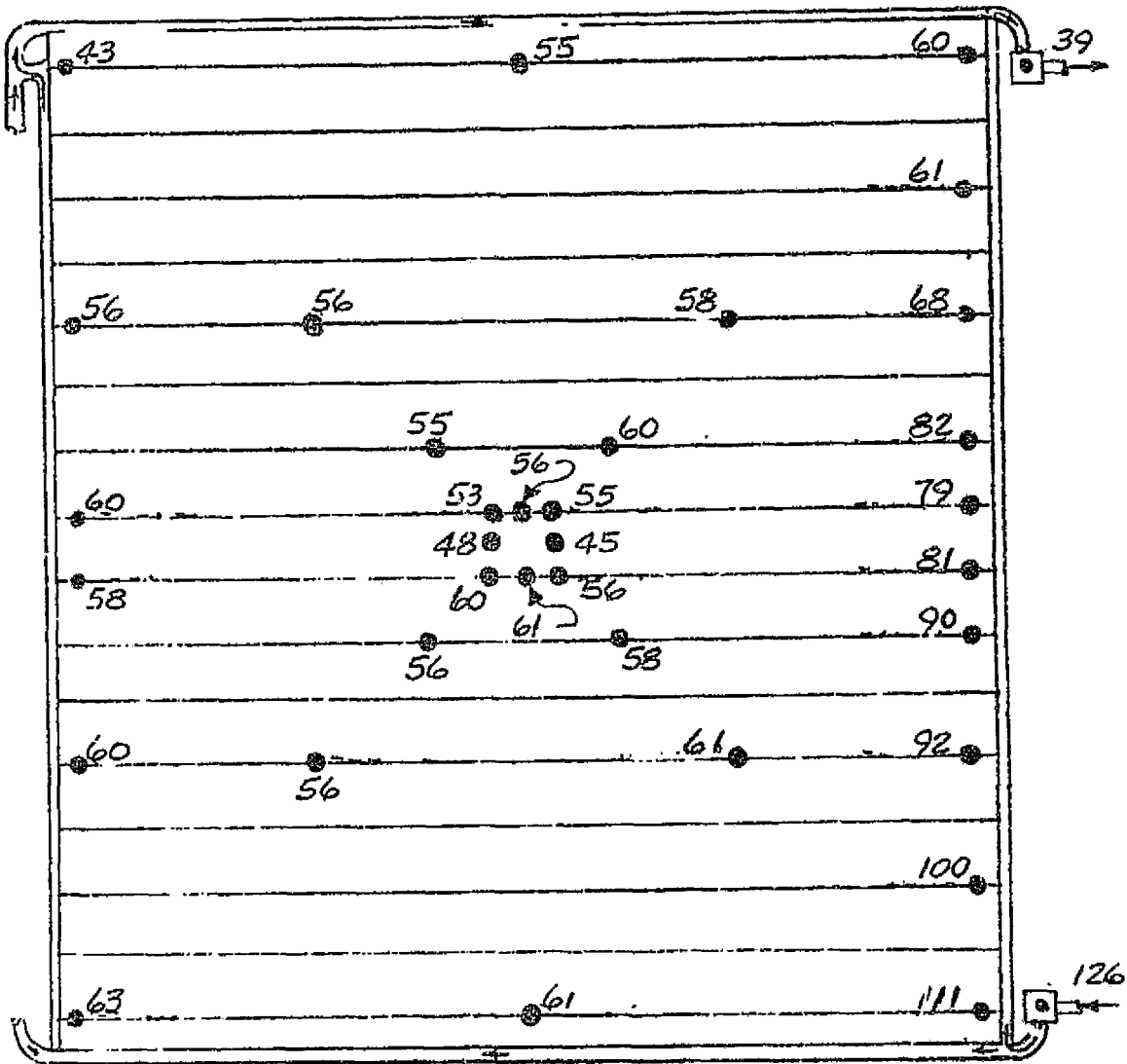
TIME _18:00:06_

Fe$_{12}$ Return

PANEL NO. 2

FIGURE A30 (CONT'D)

Fe$_{12}$ Supply

A-119

TEST POINT _112_
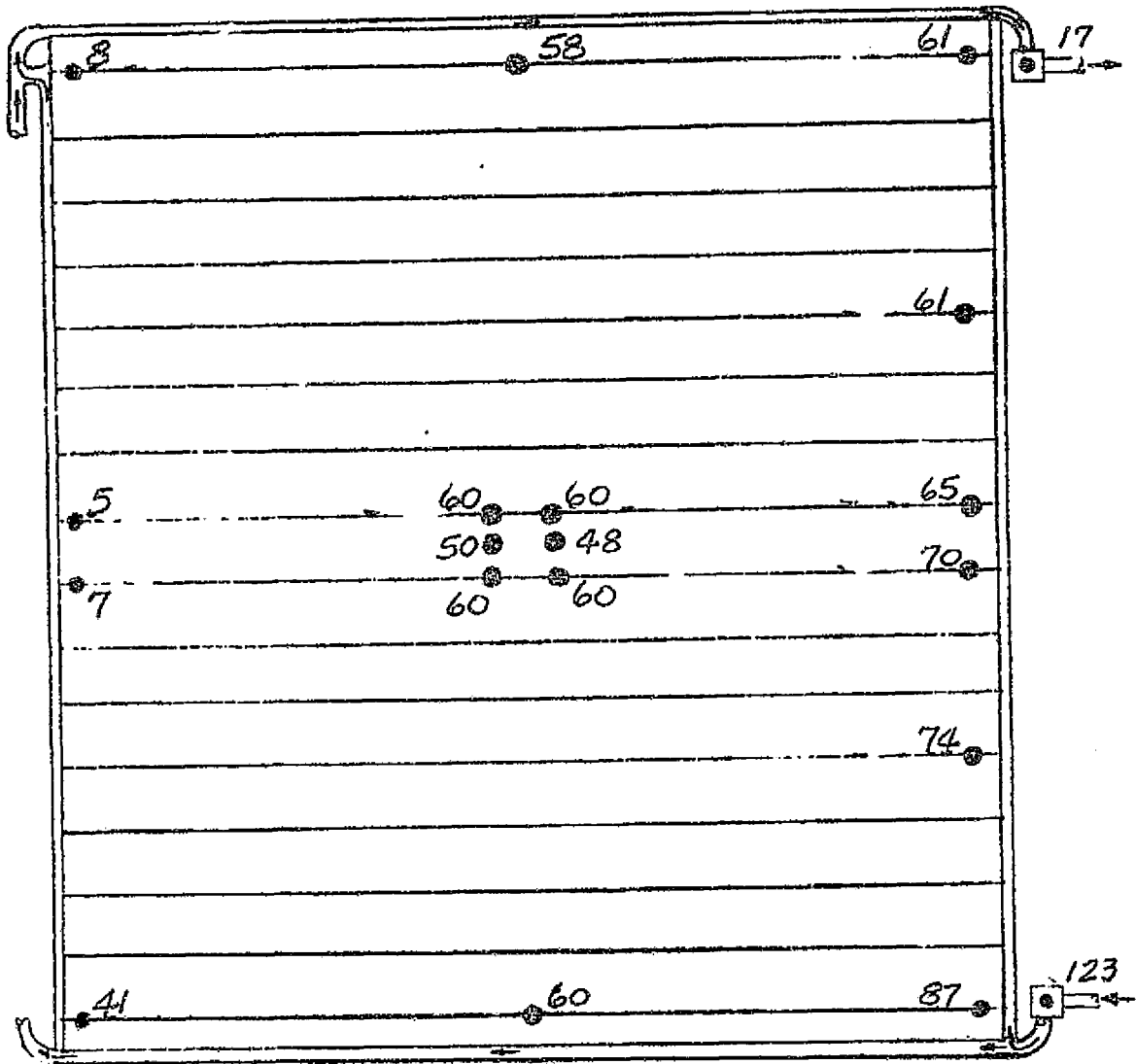
DAY _309_

TIME _18:00:06_

Fe$_{12}$ Return

PANEL NO. 3

FIGURE A30 (CONT'D)

Fe$_{12}$ Supply

A-120

TEST POINT _112_

DAY _309_

TIME _18:00:06_
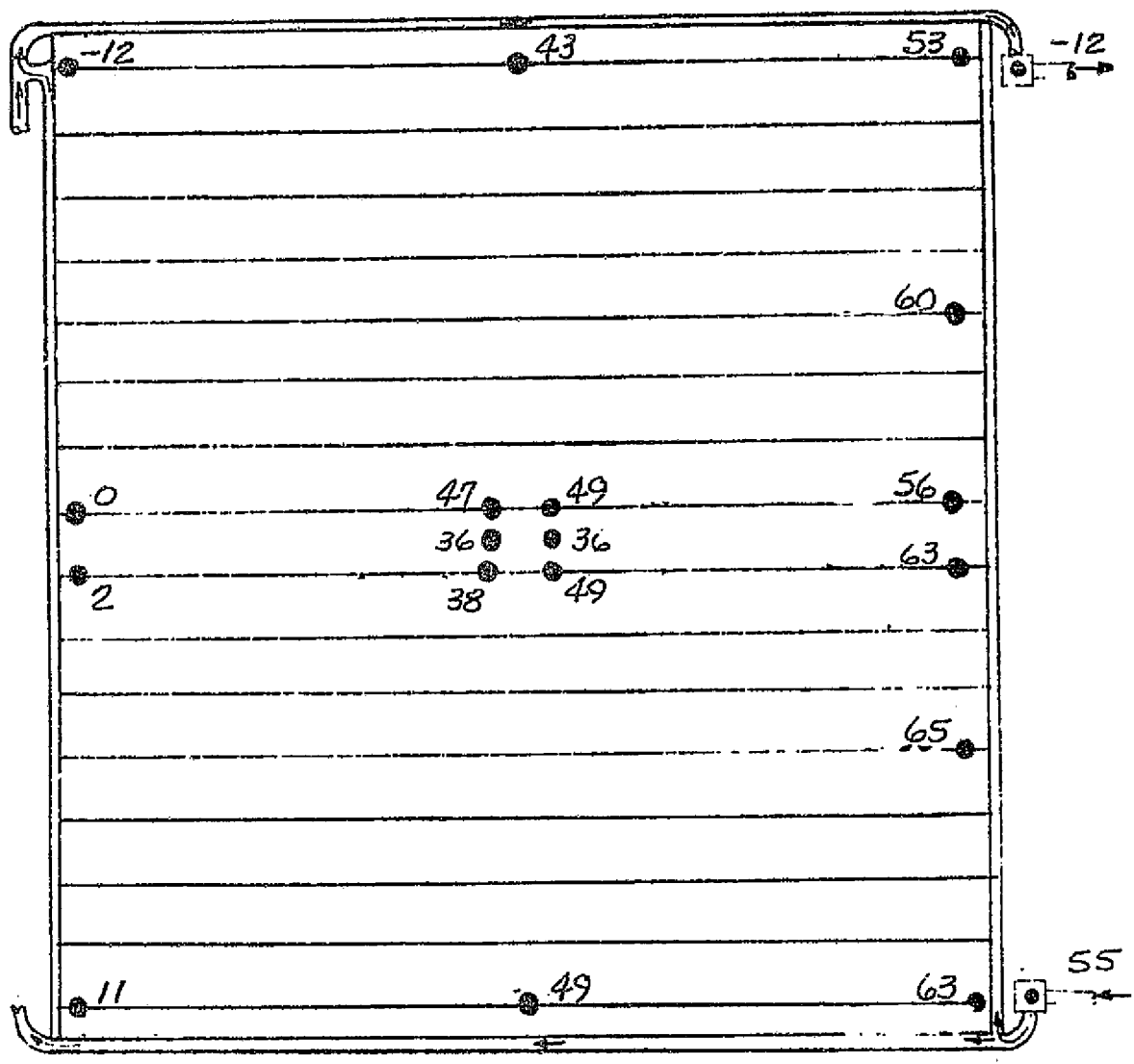
Fe$_{12}$ Return

PANEL NO. 4

FIGURE A30 (CONT'D)

A-121

TEST POINT _113_

DAY _309_

TIME _21:00:06_
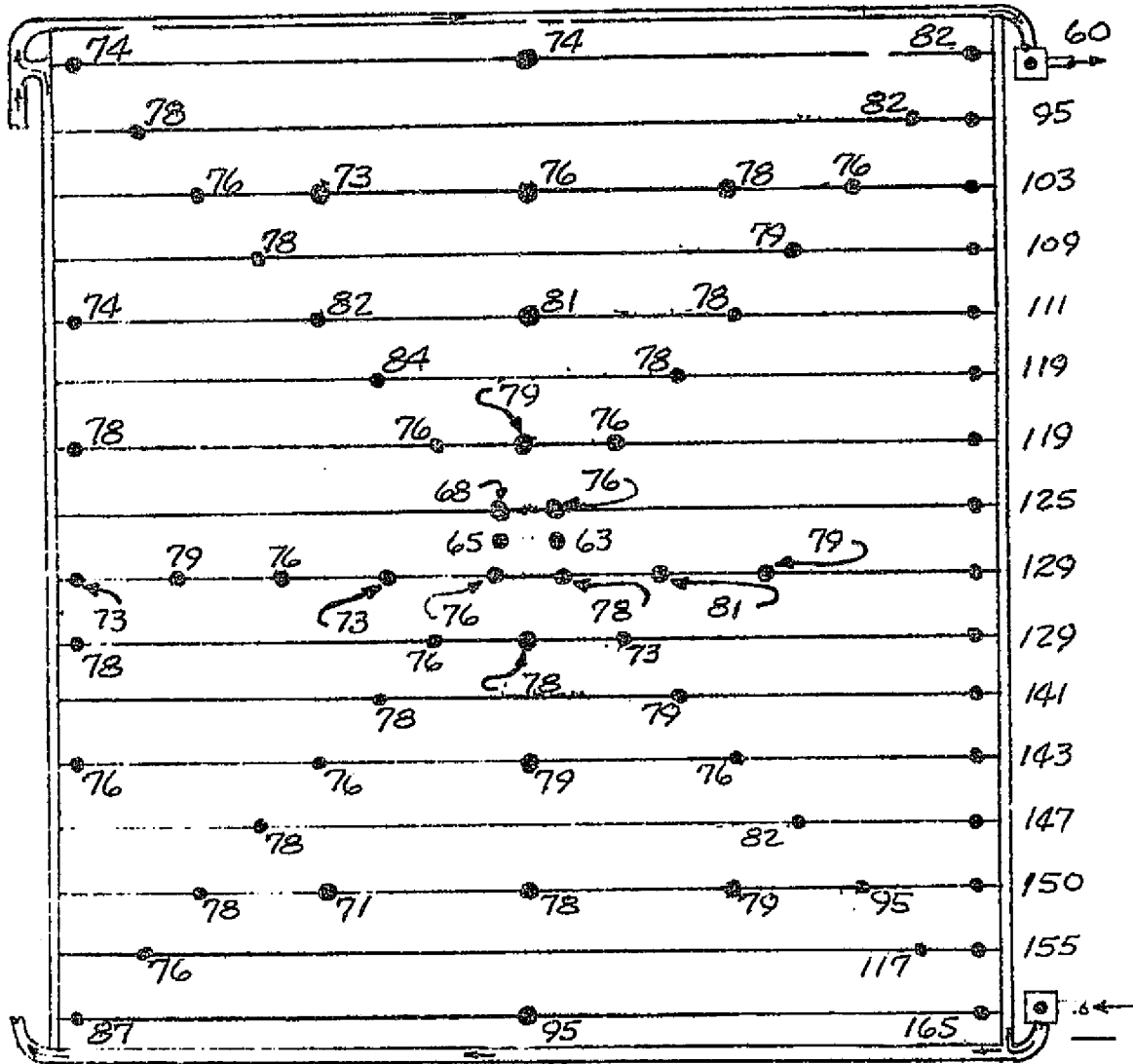
Fe$_{12}$ Return

Fe$_{12}$ Supply

PANEL NO. 1

FIGURE A31

STEADY STATE VAPOR COMPRESSION OPERATION PANEL TEMPERATURE MAPS

A-122

TEST POINT __113__
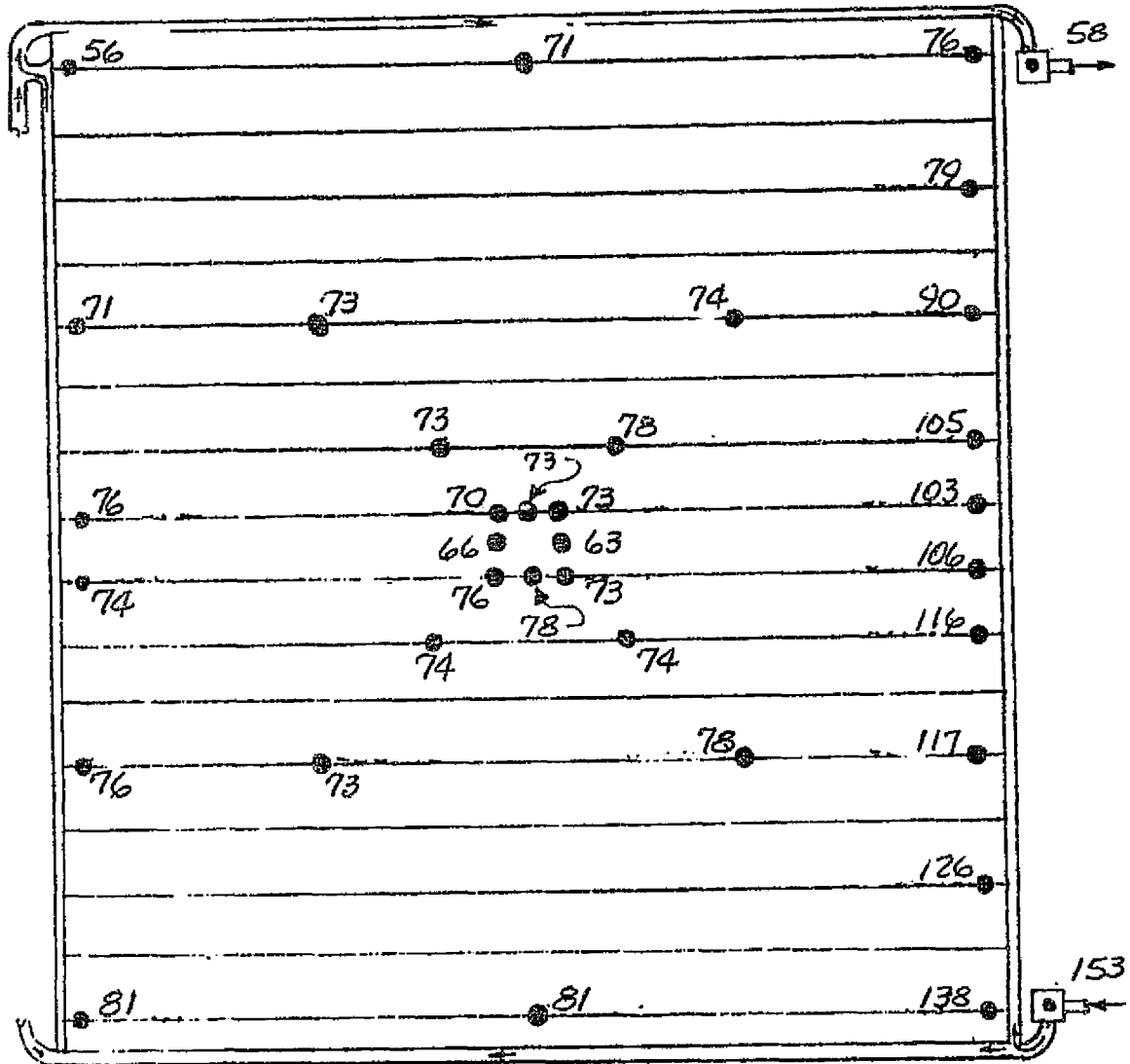
DAY __309__

TIME __21:00:06__ Fe_{12} Return

PANEL NO. 2

FIGURE A31 (CONT'D)

TEST POINT __113__

DAY _____309_____

TIME ____21:00:06____

Fe$_{12}$ Return

26   73   78   36

76

24   76   76   79

66   65   87

28   76   76

94

150

53   76   108
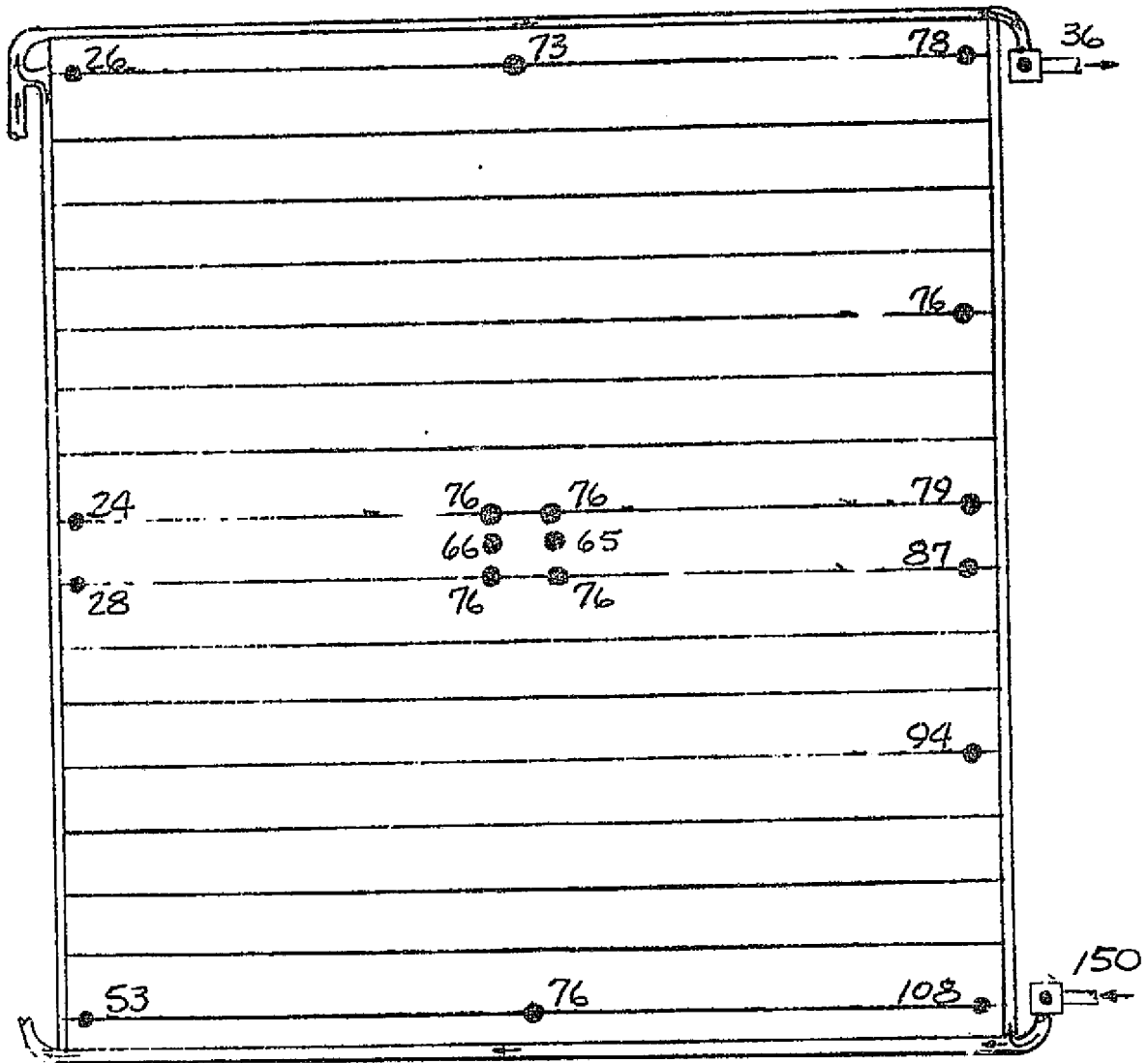
Fe$_{12}$ Supply

PANEL NO. 3

FIGURE A31 (CONT'D)

A-124

TEST POINT ___113___

DAY ___309___

TIME ___21:00:06___
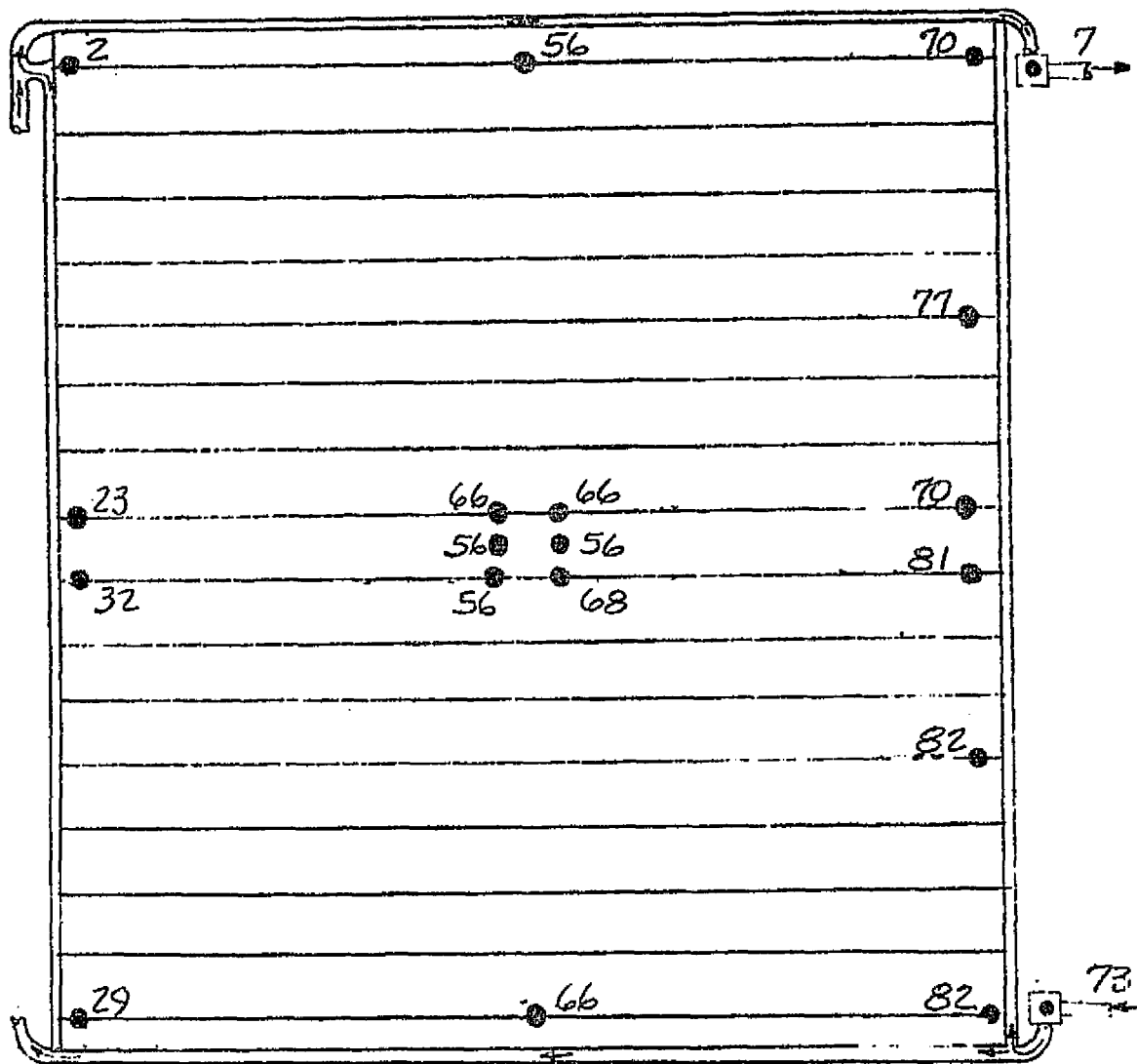
Fe$_{12}$ Return

PANEL NO. 4

FIGURE A31 (CONT'D)

Fe$_{12}$ Supply

A-125

TEST POINT _111A_
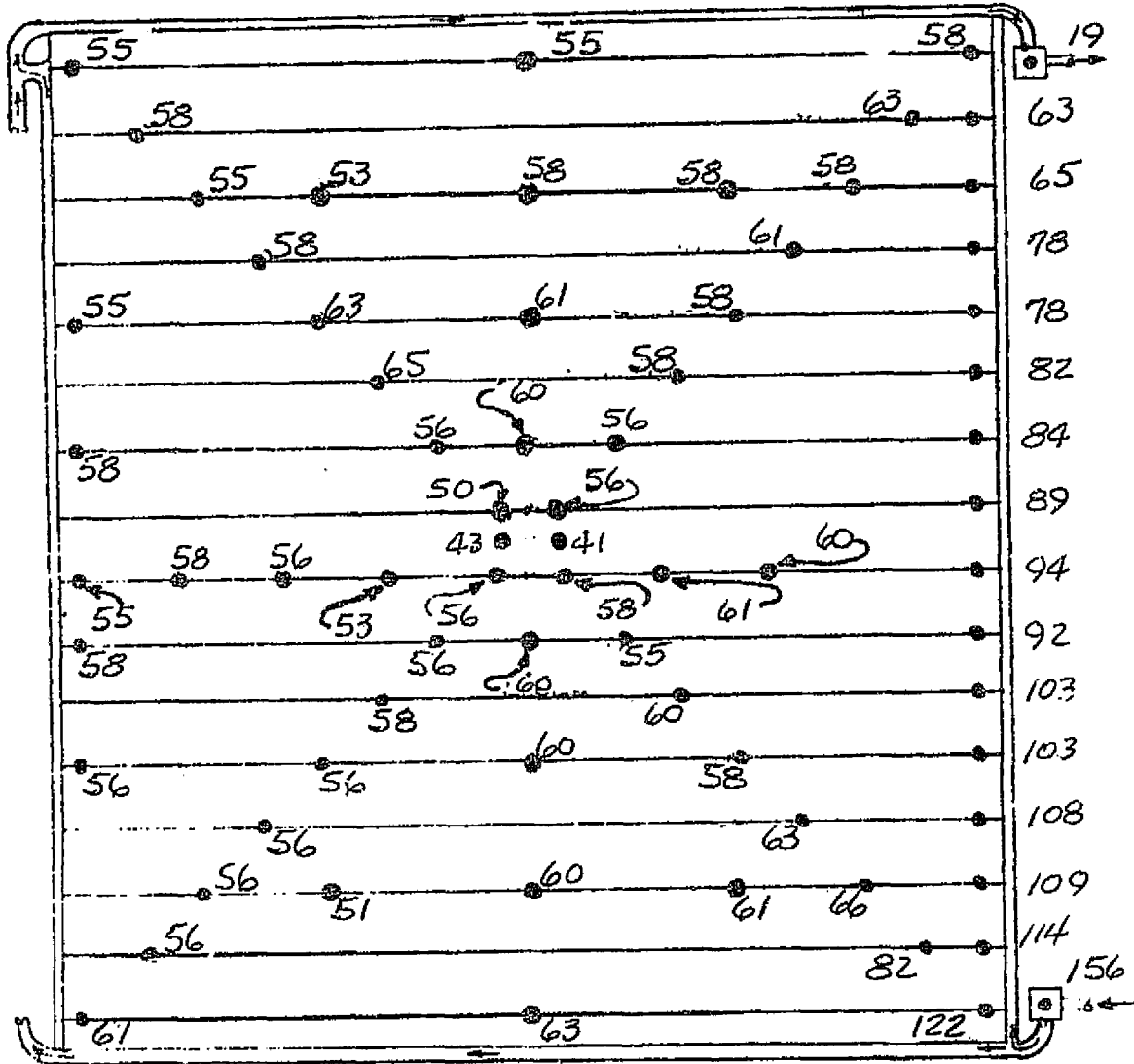
DAY _309_

TIME _22:30:06_

Fe$_{12}$ Return

PANEL NO. 1

FIGURE A32

STEADY STATE VAPOR COMPRESSION OPERATION PANEL TEMPERATURE MAPS

Fe$_{12}$ Supply

A-126

TEST POINT _111A_

DAY _309_

TIME _22:30:06_

Fe$_{12}$ Return

PANEL NO. 2

FIGURE A32 (CONT'D)

Fe$_{12}$ Supply

A-127

TEST POINT ___111A___

DAY ___309___

TIME ___22:30:06___

Fe$_{12}$ Return

-10   53   58   3→

                                        58

-10   56   56   61
           43   41
-8   56   55   61

                                    68

29   56   79   113←
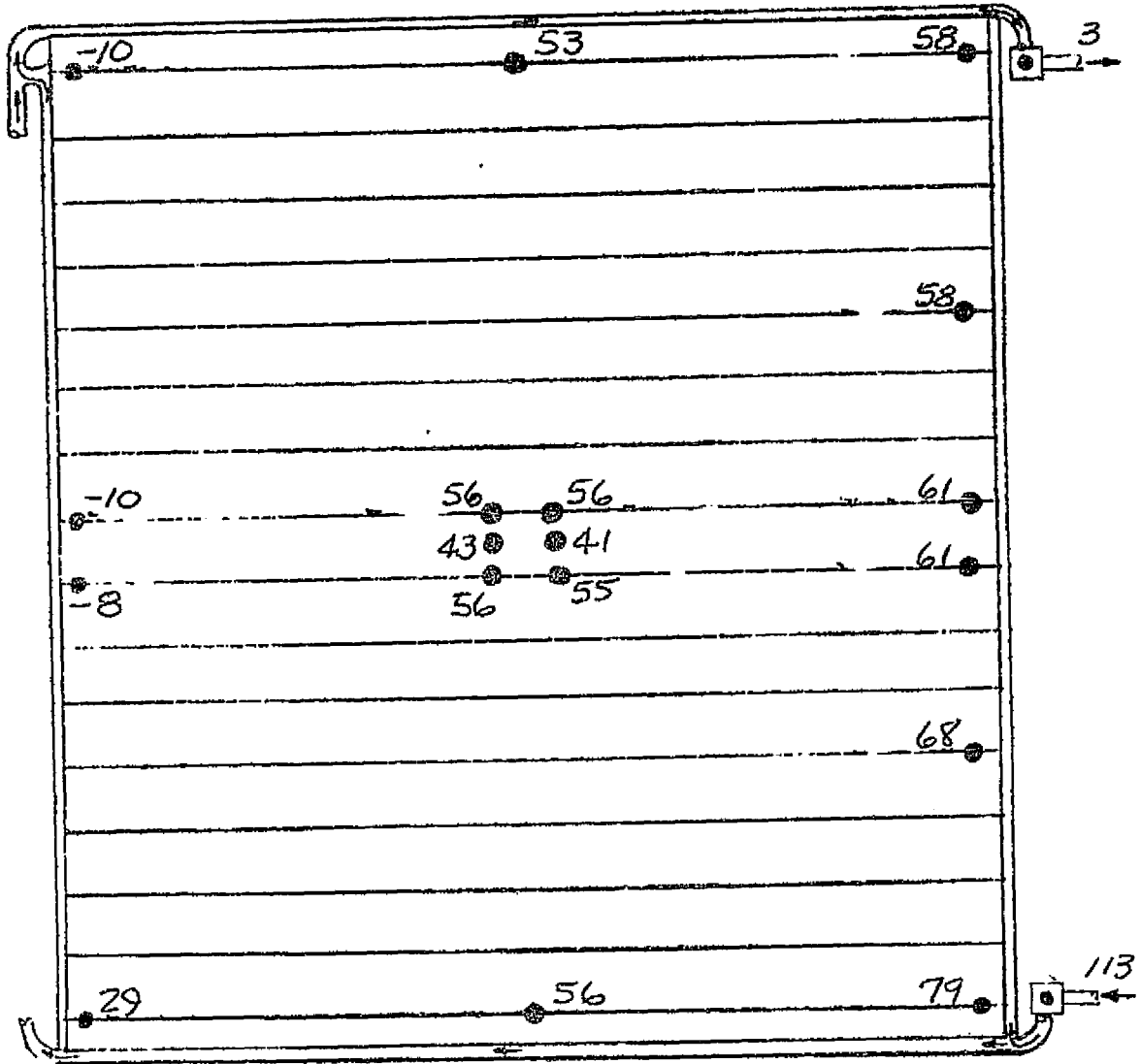
Fe$_{12}$ Supply

PANEL NO. 3

FIGURE A32 (CONT'D)

TEST POINT _____ *111A* _____

DAY _____ *309* _____

TIME _____ *22:30:06* _____

Fe_{12} Return
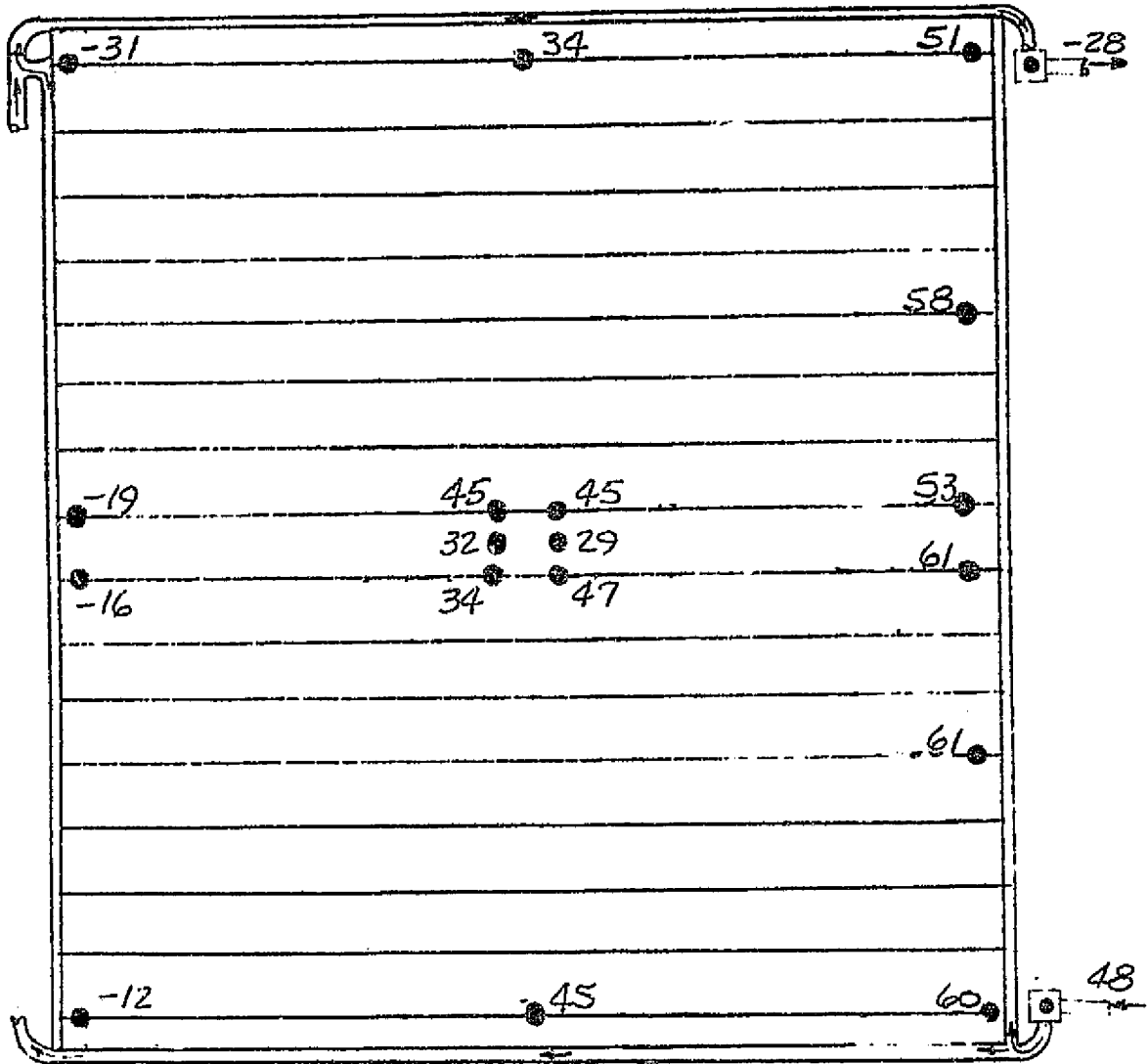
PANEL NO. 4

FIGURE A32 (CONT'D)

Fe_{12} Supply

A-129

TEST POINT ___13___

EVAPORATOR TEMPERATURE(°F) ___35___ ENVIRONMENT(BTU/HR-FT^2 ___83.0___

FLOWRATE(LBm/HR) ___730___
POWER(WATTS) ___4620___
COOLING(BTU/HR)
FROM $\dot{m}C_p \Delta T$ OF R-21 ___37,600___
FROM $\dot{m}\Delta h$ OF R-21 ___37,230___

COEFFICIENT OF PERFORMANCE - COP

FROM POWER AND COOLING MEASUREMENTS ___2.38___
FROM P-h DIAGRAM ___2.04___

FIGURE A33 REFRIGERATION SYSTEM STEADY STATE CYCLIC PERFORMANCE

TEST POINT ____16A____

EVAPORATOR TEMPERATURE(°F) __35__ ENVIRONMENT(BTU/HR-FT^2) __89.3__

FLOWRATE (LBm/HR) ____716____
POWER (WATTS) ____4980____
COOLING (BTU/HR)
  FROM $\dot{m}C_p \Delta T$ OF R-21 __38,820__
  FROM $\dot{m}\Delta h$ OF R-12 __41,170__

COEFFICIENT OF PERFORMANCE - COP

  FROM POWER AND COOLING MEASUREMENTS __2.28__
  FROM P-h DIAGRAM __2.35__

FIGURE A34   REFRIGERATION SYSTEM STEADY STATE CYCLIC PERFORMANCE

TEST POINT ___21___

EVAPORATOR TEMPERATURE(°F) ___-16___   ENVIRONMENT(BTU/HR-FT^2) ___82.0___

FLOWRATE (LBm/HR) ___216___
POWER (WATTS) ___1850___
COOLING (BTU/HR)
 FROM ṁCp ΔT OF R-21 ___13,040___
 FROM ṁΔh OF R-12 ___15,552___

COEFFICIENT OF PERFORMANCE - COP
 FROM POWER AND COOLING MEASUREMENTS ___2.07___
 FROM P-h DIAGRAM ___2.77___

FIGURE A35   REFRIGERATION SYSTEM STEADY STATE CYCLIC PERFORMANCE

A-132

TEST POINT ___22___

EVAPORATOR TEMPERATURE(°F) ___-10___   ENVIRONMENT(BTU/HR-FT^2) ___82___

FLOWRATE (LBm/HR) ___249___
POWER (WATTS) ___1370___
COOLING (BTU/HR)
 FROM $\dot{m}C_p \Delta T$ OF R-21 ___13,370___
 FROM $\dot{m}\Delta h$ OF R-12 ___16,807___

COEFFICIENT OF PERFORMANCE - COP
 FROM POWER AND COOLING MEASUREMENTS ___2.26___
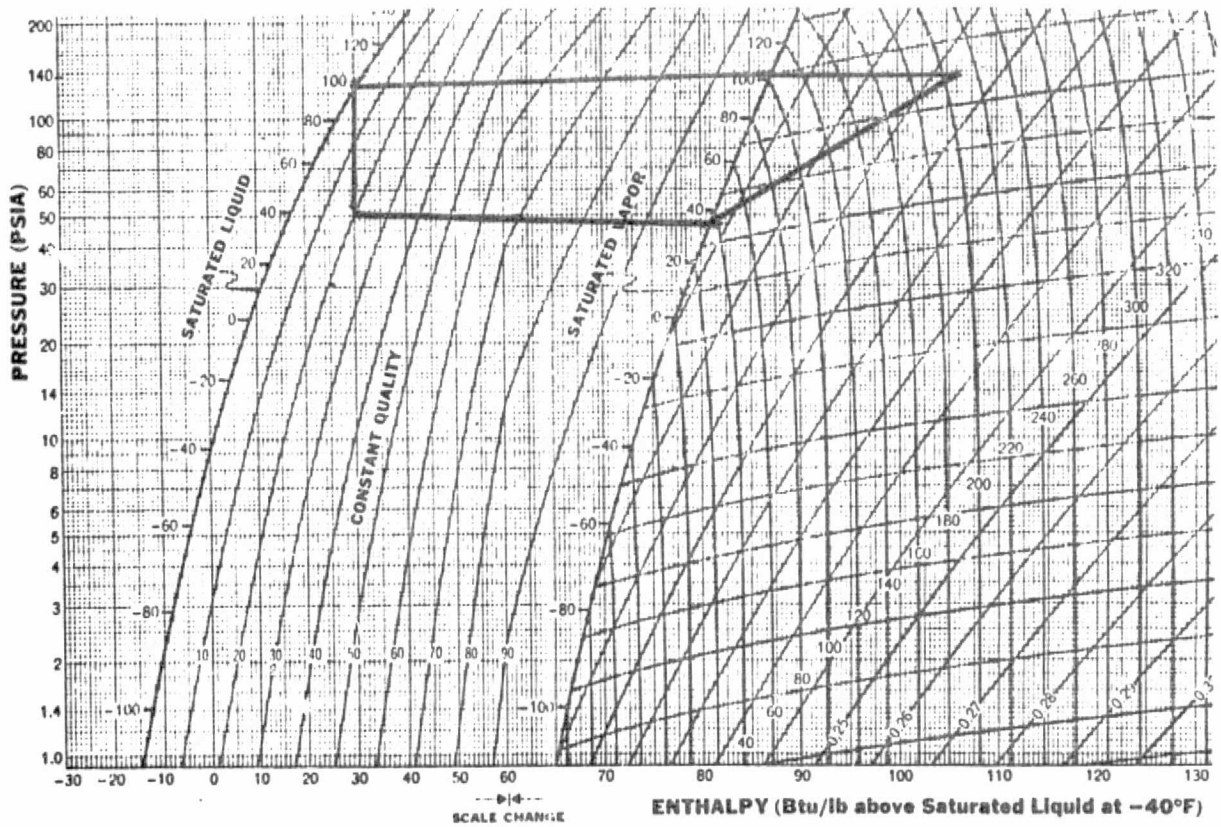 FROM P-h DIAGRAM ___2.70___

FIGURE A36   REFRIGERATION SYSTEM STEADY STATE CYCLIC PERFORMANCE

A-133

TEST POINT ____14____

EVAPORATOR TEMPERATURE(°F) __35__   ENVIRONMENT(BTU/HR-FT^2) __39.3__

FLOWRATE (LBm/HR) ____NA____
POWER (WATTS) ____3,680____
COOLING (BTU/HR)
  FROM ṁCp ΔT OF R-21 ____35,960____
  FROM ṁΔh OF R-12 ____NA____

COEFFICIENT OF PERFORMANCE – COP
  FROM POWER AND COOLING MEASUREMENTS ____2.86____
  FROM P-h DIAGRAM ____4.00____

FIGURE A37   REFRIGERATION SYSTEM STEADY STATE CYCLIC PERFORMANCE

TEST POINT _____17_____

EVAPORATOR TEMPERATURE(°F) __35__   ENVIRONMENT(BTU/HR-FT^2) __104.9__

FLOWRATE (LBm/HR) _____732_____
POWER (WATTS) _____4170_____
COOLING (BTU/HR)
  FROM $\dot{m}C_p \Delta T$ OF R-21 __34,700__
  FROM $\dot{m}\Delta h$ OF R-12 __37,332__

COEFFICIENT OF PERFORMANCE - COP
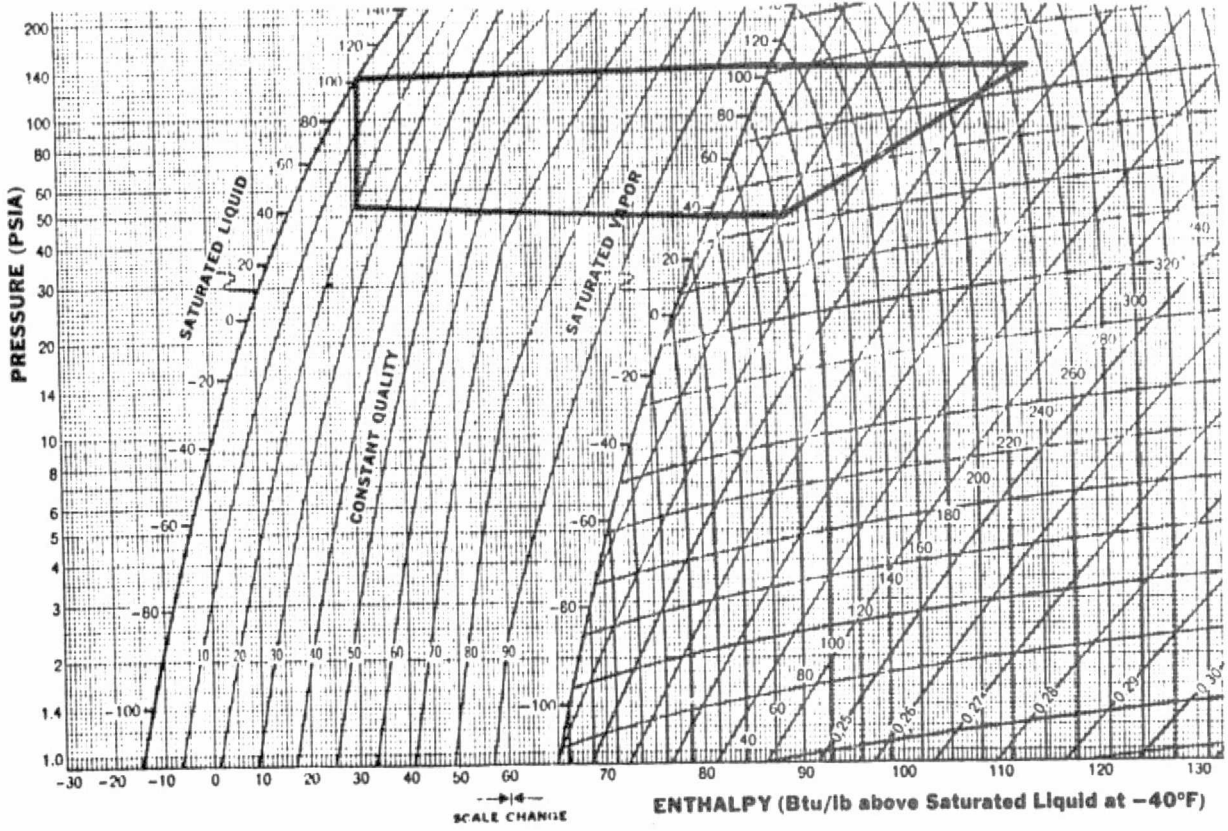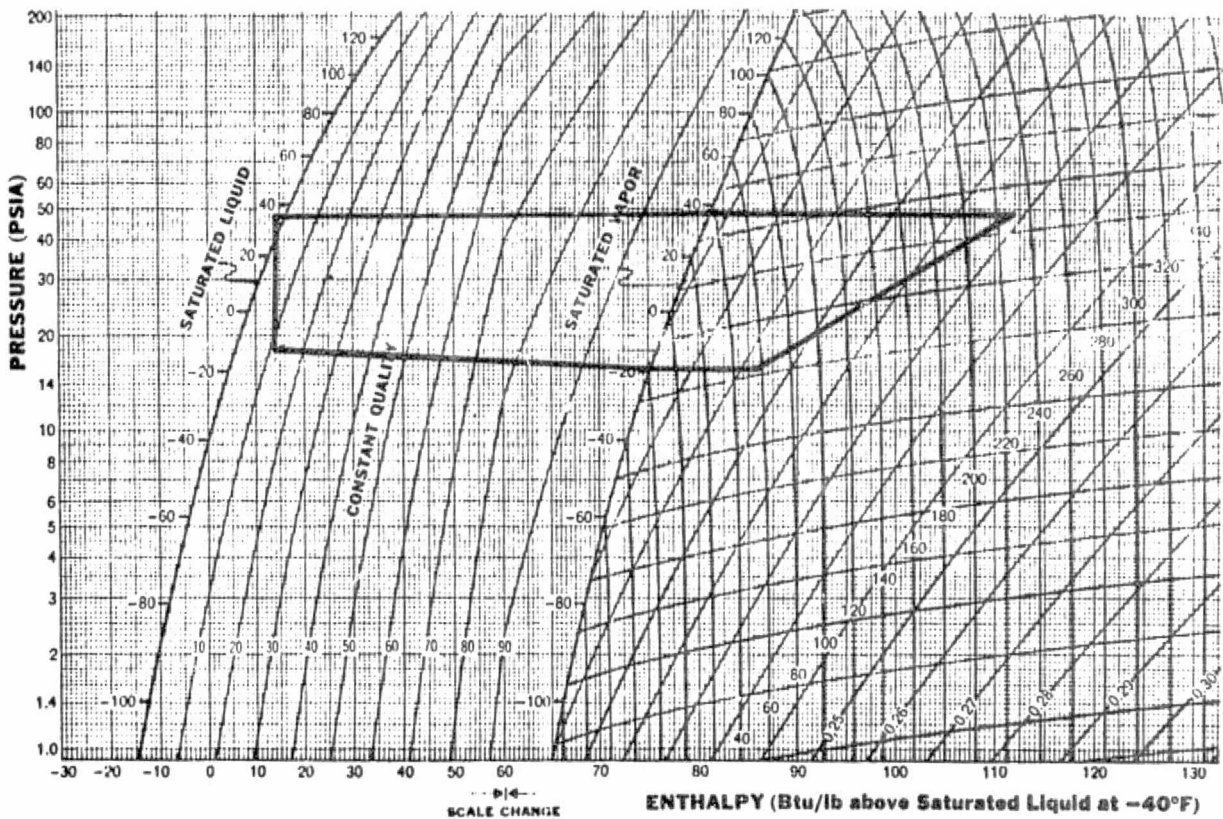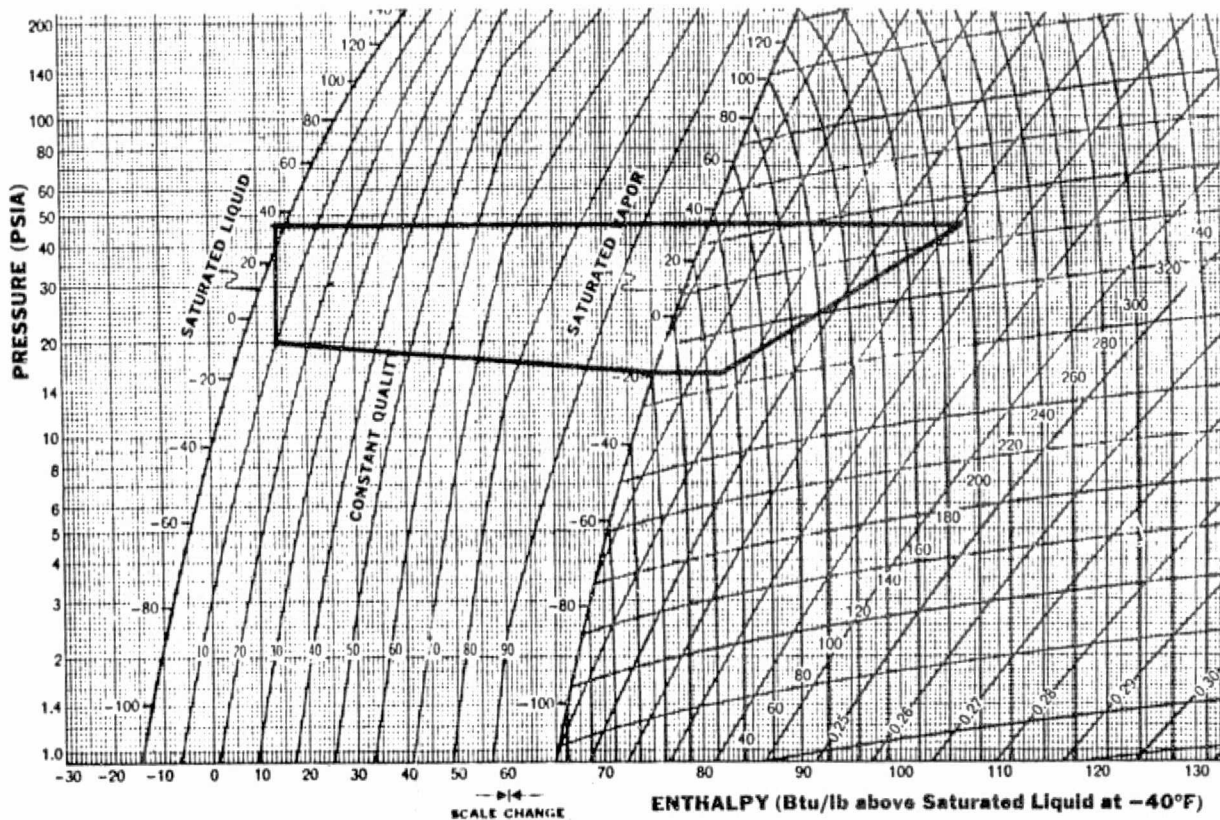 FROM POWER AND COOLING MEASUREMENTS __2.44__
  FROM P-h DIAGRAM _____2.00_____

FIGURE A38   REFRIGERATION SYSTEM STEADY STATE CYCLIC PERFORMANCE

TEST POINT ___18___

EVAPORATOR TEMPERATURE(°F) ___35___   ENVIRONMENT(BTU/HR-FT^2) ___121.7___

FLOWRATE (LBm/HR) ___749___
POWER (WATTS) ___5450___
COOLING (BTU/HR)
  FROM $\dot{m}C_p \Delta T$ OF R-21 ___33,620___
  FROM $\dot{m}\Delta h$ OF R-12 ___38,948___

COEFFICIENT OF PERFORMANCE - COP
  FROM POWER AND COOLING MEASUREMENTS ___1.81___
  FROM P-h DIAGRAM ___1.89___

FIGURE A39   REFRIGERATION SYSTEM STEADY STATE CYCLIC PERFORMANCE

A-136

TEST POINT _____ 19 _____

EVAPORATOR TEMPERATURE(°F) _____ 35 _____   ENVIRONMENT(BTU/HR-FT^2) _____ 141.6 _____

FLOWRATE (LBm/HR) _____ 782 _____
POWER (WATTS) _____ 5570 _____
COOLING (BTU/HR)
  FROM $\dot{m}C_p \Delta T$ OF R-21 _____ 31,070 _____
  FROM $\dot{m}\Delta h$ OF R-12 _____ 41,446 _____

COEFFICIENT OF PERFORMANCE - COP
  FROM POWER AND COOLING MEASUREMENTS _____ 1.63 _____
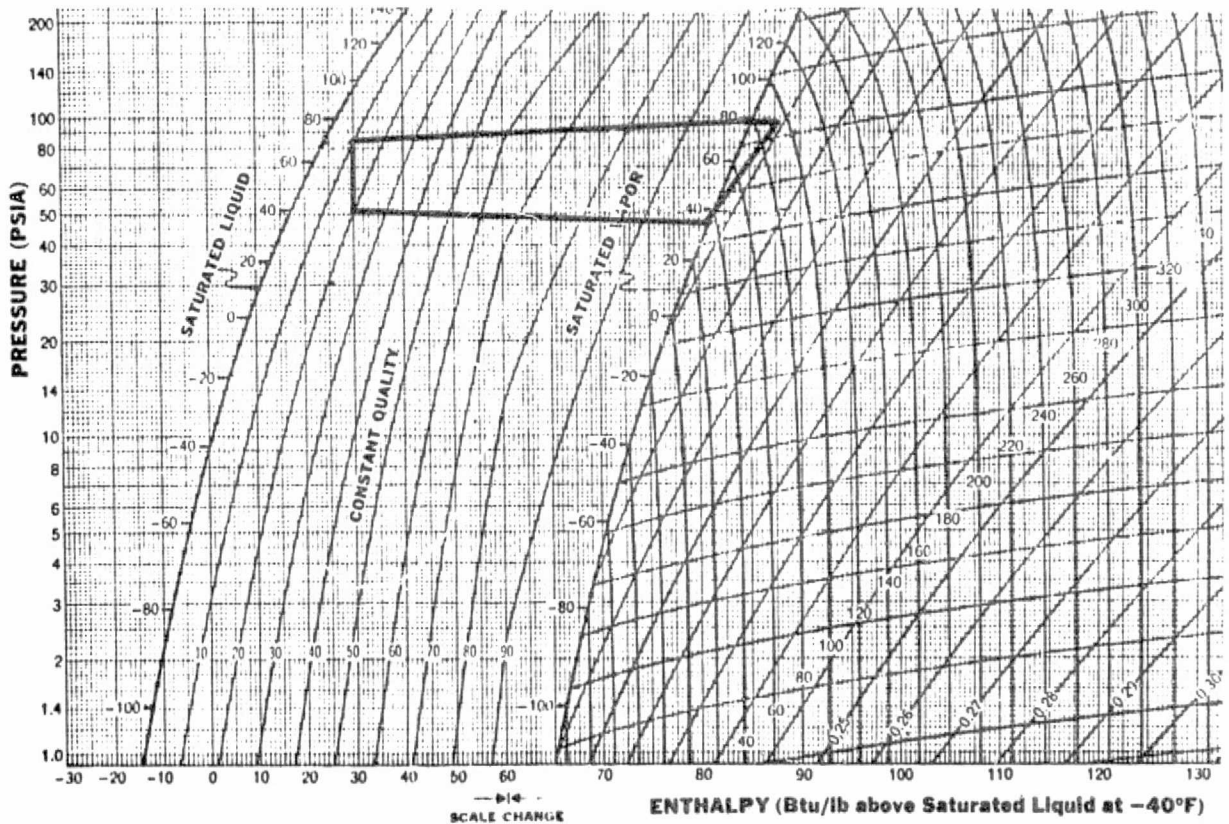 FROM P-h DIAGRAM _____ 1.77 _____

FIGURE A40   REFRIGERATION SYSTEM STEADY STATE CYCLIC PERFORMANCE

TEST POINT ____19A____

EVAPORATOR TEMPERATURE(°F) ____35____ ENVIRONMENT(BTU/HR-FT^2) ____155.4____

FLOWRATE (LBm/HR) ____682____
POWER (WATTS) ____5800____
COOLING (BTU/HR)
  FROM $\dot{m}Cp\ \Delta T$ of R-21 ____32,500____
  FROM $\dot{m}\Delta h$ OF R-12 ____35,464____

COEFFICIENT OF PERFORMANCE - COP
  FROM POWER AND COOLING MEASUREMENTS ____1.64____
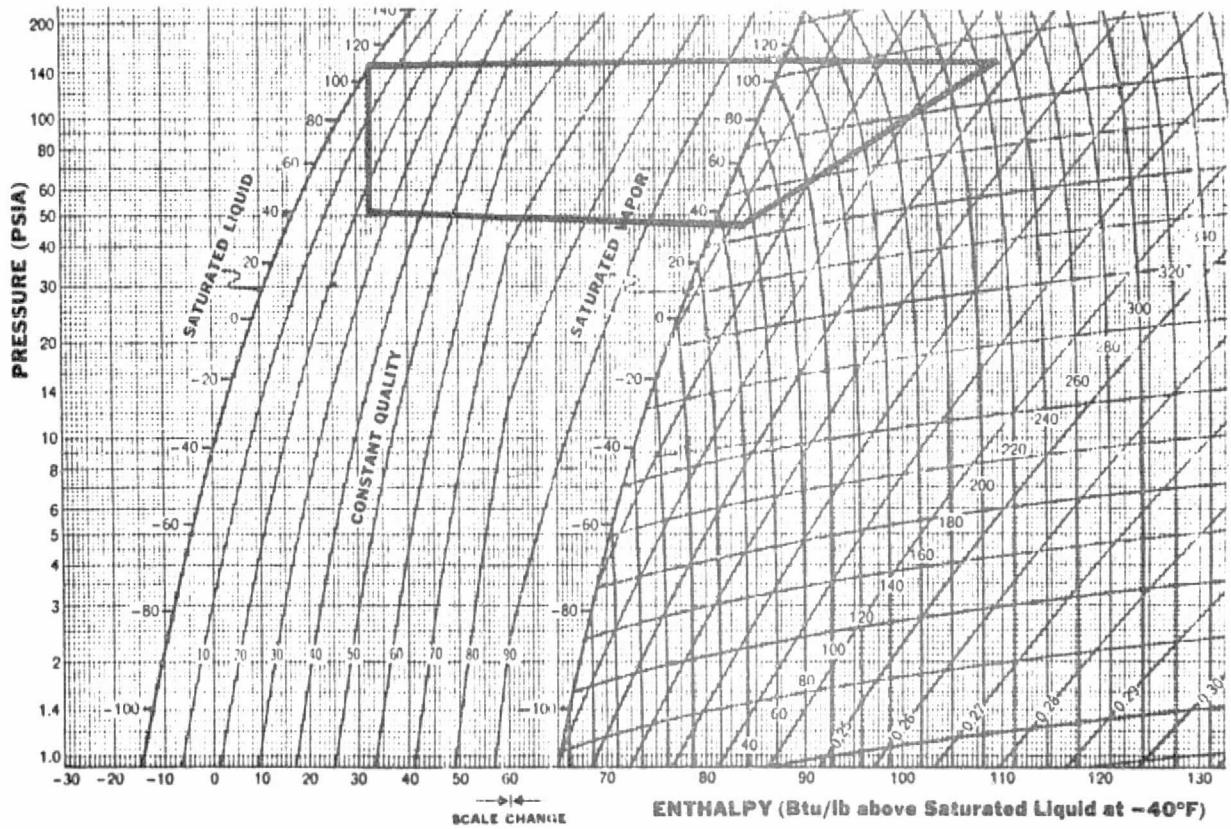 FROM P-h DIAGRAM ____1.65____

FIGURE A41   REFRIGERATION SYSTEM STEADY STATE CYCLIC PERFORMANCE

EVAPORATOR TEMPERATURE(°F) ___35___   ENVIRONMENT(BTU/HR-FT^2) __42.3__

FLOWRATE (LB^m/HR) _____732_____
POWER (WATTS) _____4150_____
COOLING (BTU/HR)
  FROM $\dot{m}Cp\ \Delta T$ OF R-21 ___39,873___
  FROM $\dot{m}\Delta h$ OF R-12 ___43,188___

COEFFICIENT OF PERFORMANCE - COP
  FROM POWER AND COOLING MEASUREMENTS ___2.81___
  FROM P-h DIAGRAM ___3.11___
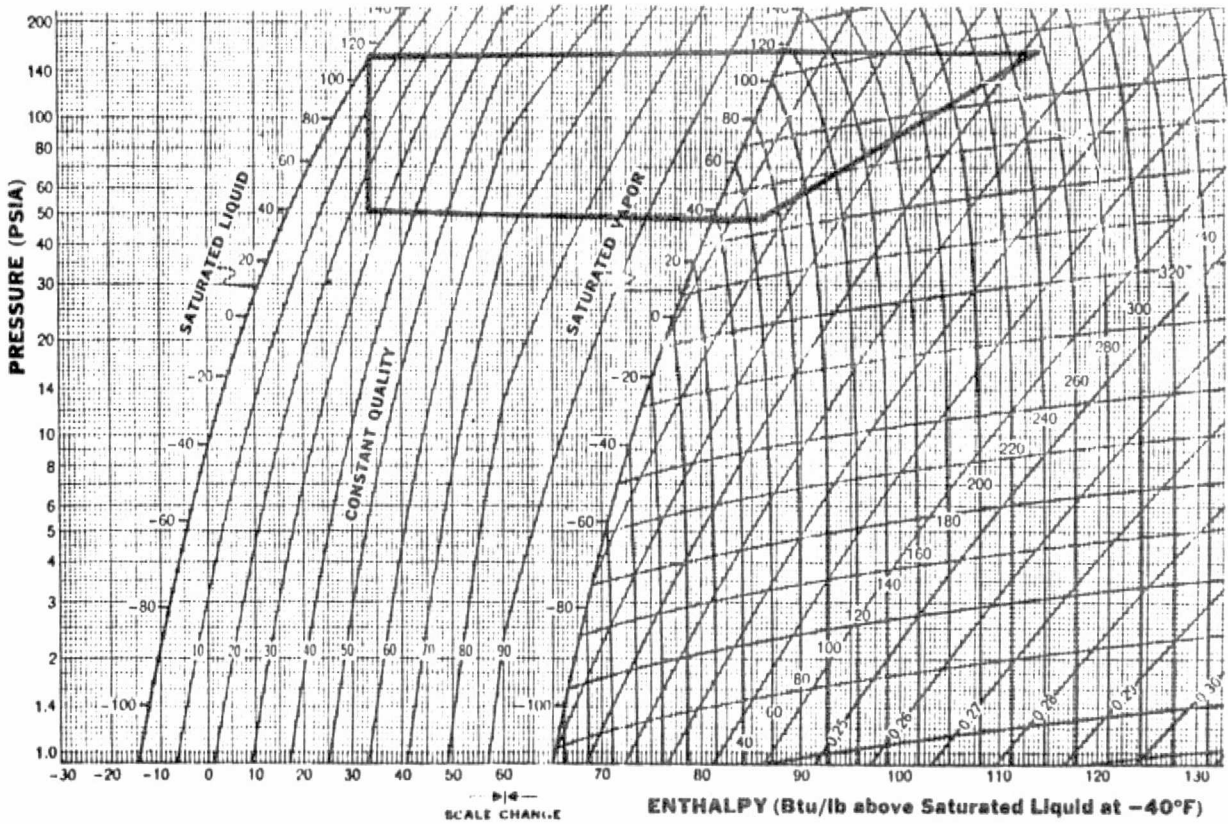

FIGURE A42   REFRIGERATION SYSTEM STEADY STATE CYCLIC PERFORMANCE

TEST POINT ___17A___

EVAPORATOR TEMPERATURE($^\circ$F) ___35___ ENVIRONMENT(BTU/HR-FT^2) ___101.3___

FLOWRATE (LBm/HR) ___682___
POWER (WATTS) ___5000___
COOLING (BTU/HR)
FROM $\dot{m}Cp\,\Delta T$ OF R-21 ___36,190___
FROM $\dot{m}\Delta h$ OF R-12 ___26,487___

COEFFICIENT OF PERFORMANCE - COP
FROM POWER AND COOLING MEASUREMENTS ___2.12___
FROM P-h DIAGRAM ___2.02___
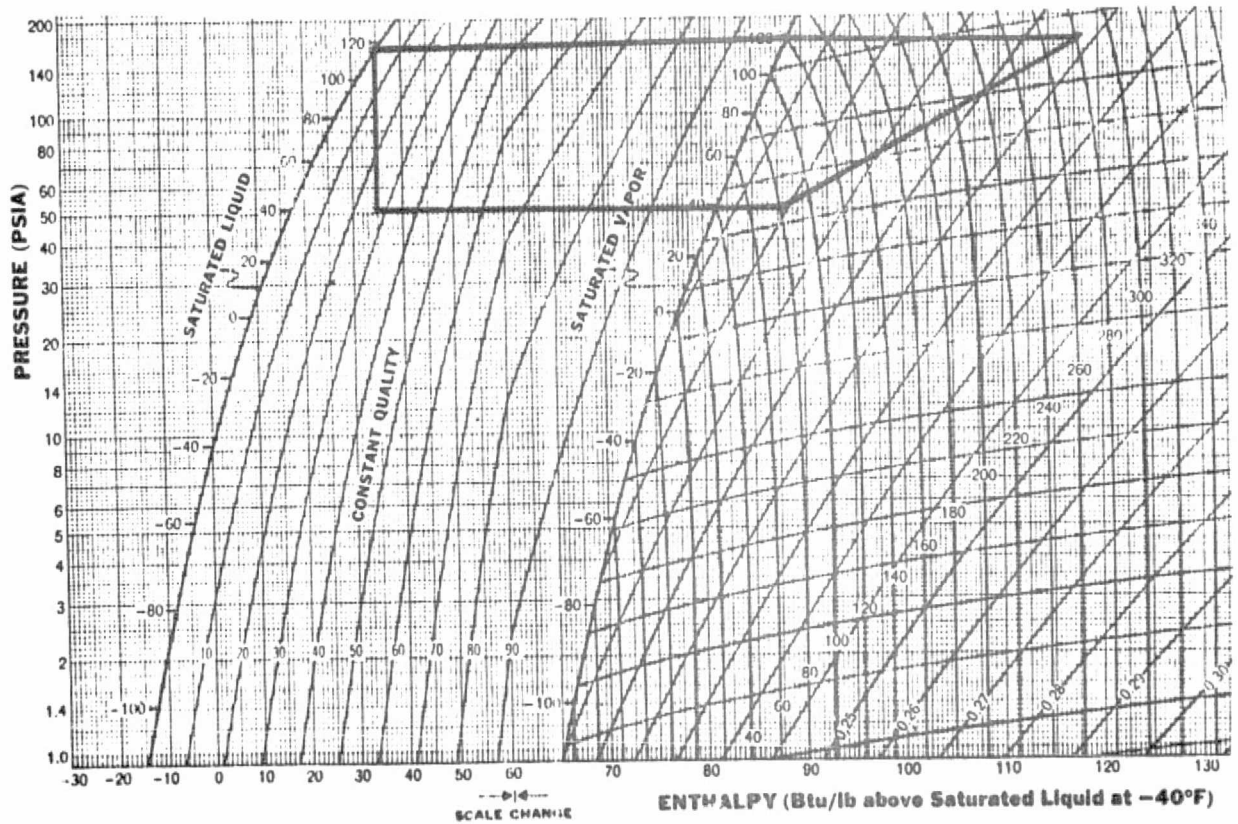

FIGURE A43 REFRIGERATION SYSTEM STEADY STATE CYCLIC PERFORMANCE

TEST POINT ___107___

EVAPORATOR TEMPERATURE(°F) ___35___   ENVIRONMENT(BTU/HR-FT^2) __120.1__

FLOWRATE (LBm/HR) ___682___
POWER (WATTS) ___5220___
COOLING (BTU/HR)
  FROM $\dot{m}C_p \Delta T$ OF R-21 ___36,420___
  FROM $\dot{m}\Delta h$ OF R-12 ___37,169___

COEFFICIENT OF PERFORMANCE - COP
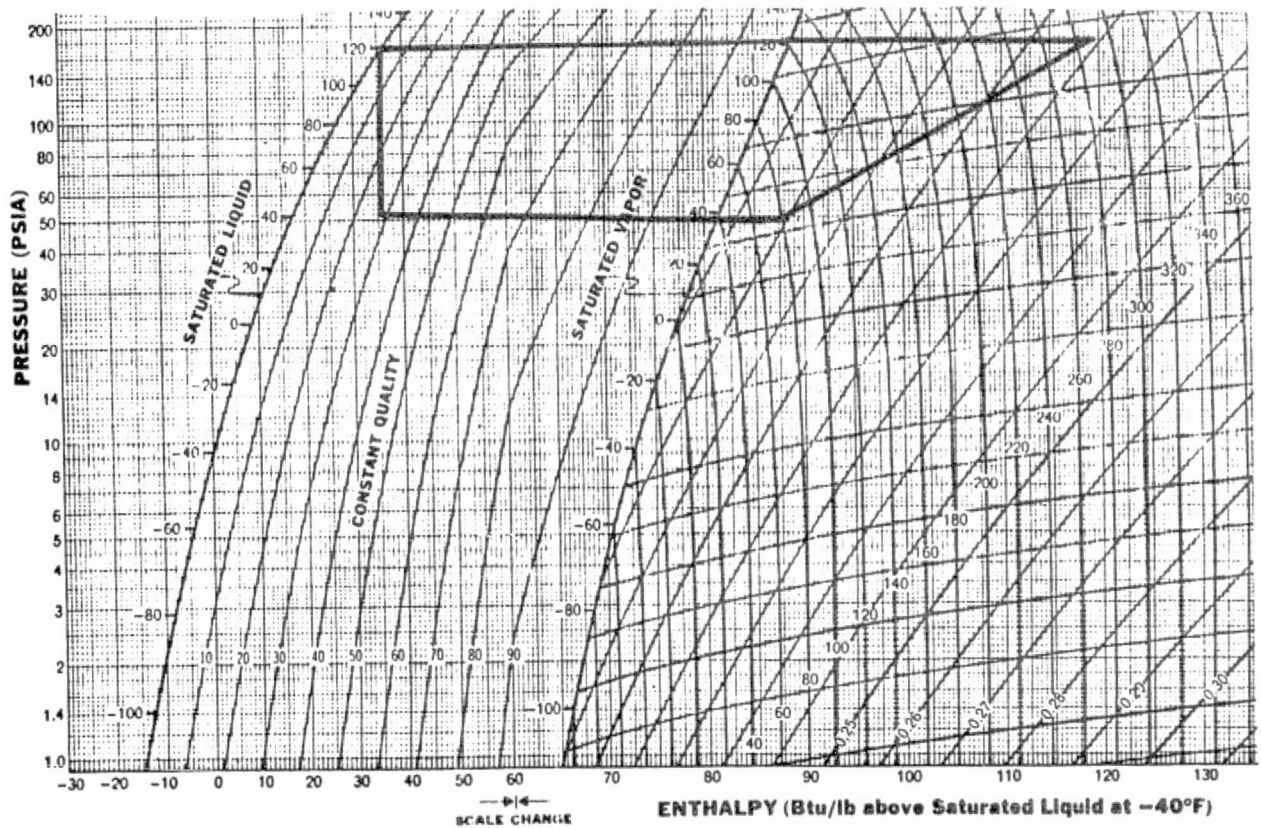 FROM POWER AND COOLING MEASUREMENTS ___2.04___
  FROM P-h DIAGRAM ___2.02___

FIGURE A44   REFRIGERATION SYSTEM STEADY STATE CYCLIC PERFORMANCE

A-141

TEST POINT _____111_____

EVAPORATOR TEMPERATURE(°F) ___15___   ENVIRONMENT(BTU/HR-FT^2) ___42.4___

FLOWRATE (LBm/HR) _____349_____
POWER (WATTS) _____2900_____
COOLING (BTU/HR)
  FROM ṁC$_p$ ΔT OF R-21 ___33,240___
  FROM ṁΔh OF R-12 ___22,685___

COEFFICIENT OF PERFORMANCE - COP
  FROM POWER AND COOLING MEASUREMENTS ___3.36___
  FROM P-h DIAGRAM ___2.82___
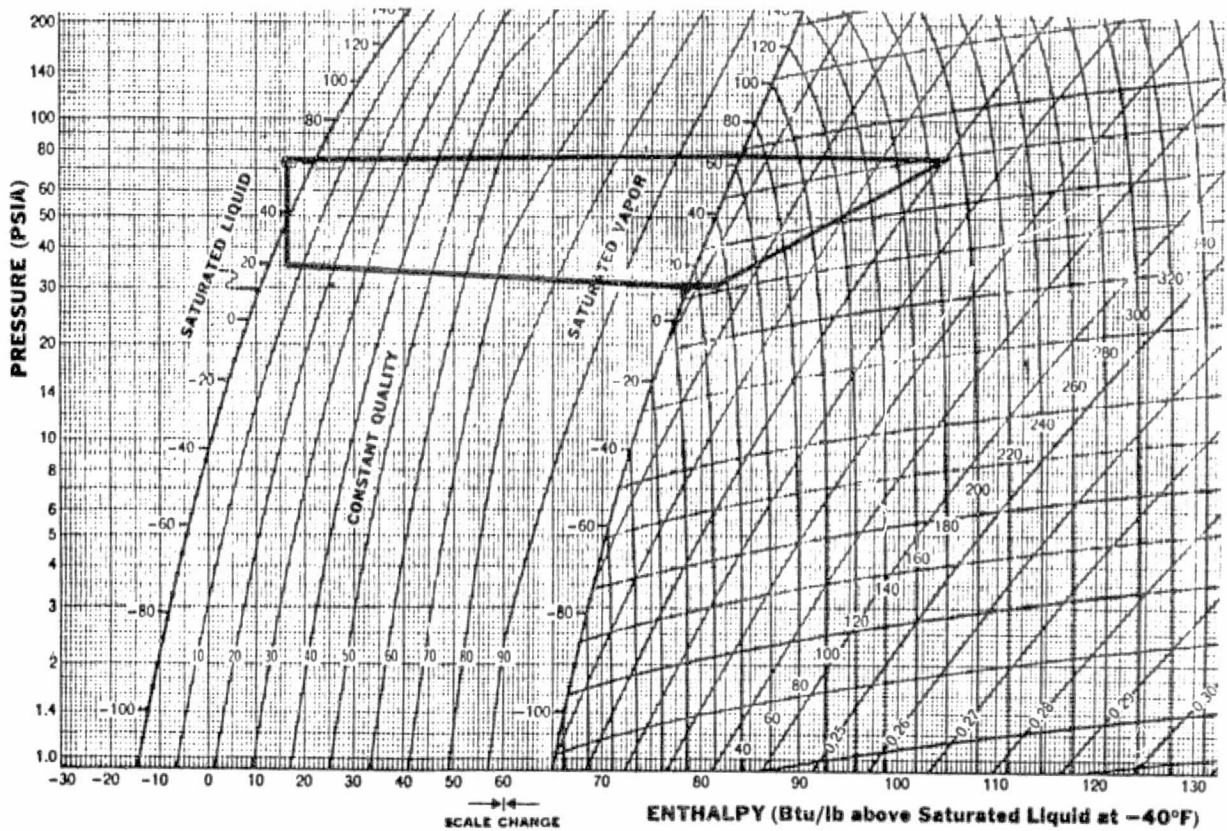
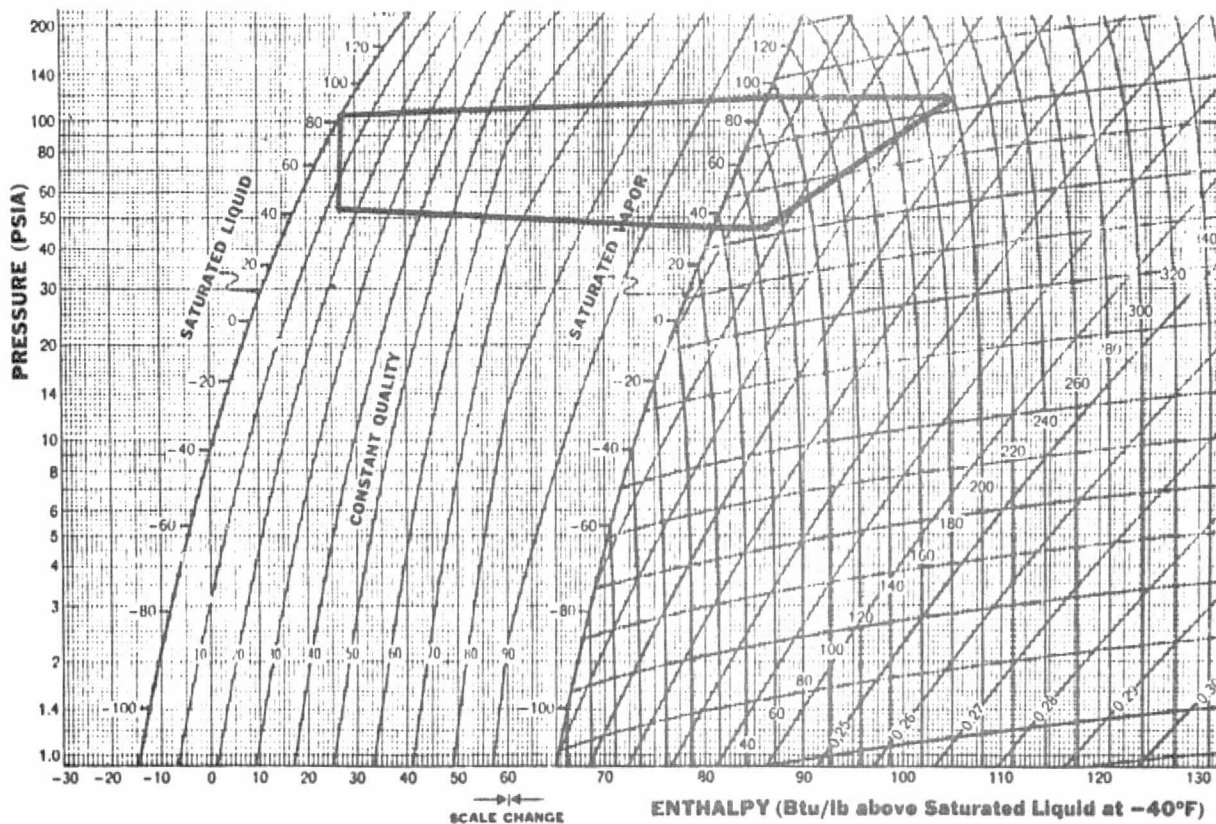

FIGURE A45   REFRIGERATION SYSTEM STEADY STATE CYCLIC PERFORMANCE

TEST POINT ___112___

EVAPORATOR TEMPERATURE(°F) ___15___ ENVIRONMENT(BTU/HR-FT^2) ___81.3___

FLOWRATE (LBm/HR) ___299___
POWER (WATTS) ___2960___
COOLING (BTU/HR)
   FROM $\dot{m}C_p \Delta T$ OF R-21 ___26,920___
   FROM $\dot{m}\Delta h$ OF R-12 ___18,388___

COEFFICIENT OF PERFORMANCE - COP
   FROM POWER AND COOLING MEASUREMENTS ___3.08___
   FROM P-h DIAGRAM ___2.67___
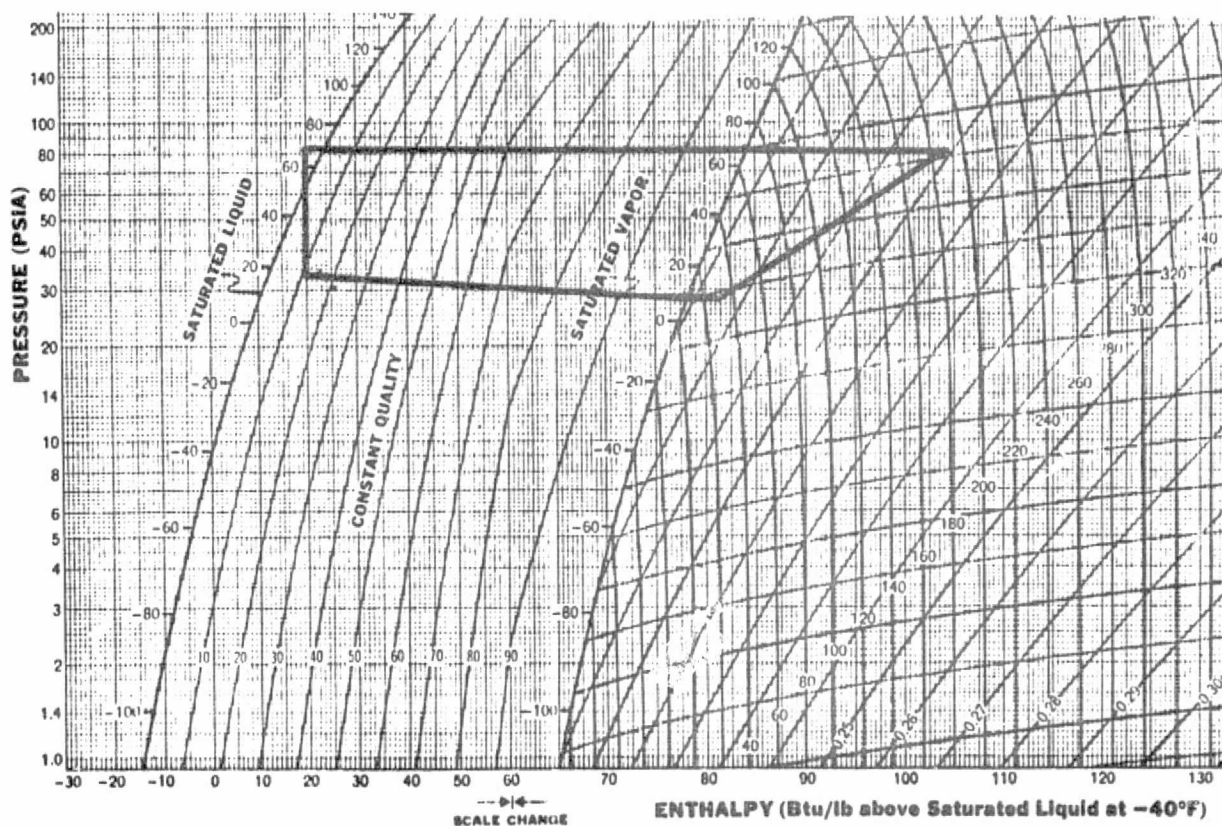
FIGURE A46   REFRIGERATION SYSTEM STEADY STATE CYCLIC PERFORMANCE

TEST POINT   113

EVAPORATOR TEMPERATURE(°F) ___15___   ENVIRONMENT(BTU/HR-FT^2) ___119.4___

FLOWRATE (LBm/HR) ___449___
POWER (WATTS) ___3170___
COOLING (BTU/HR)
  FROM $\dot{m}Cp\ \Delta T$ OF R-21 ___24,450___
  FROM $\dot{m}\Delta h$ OF R-12 ___26,266___

COEFFICIENT OF PERFORMANCE - COP
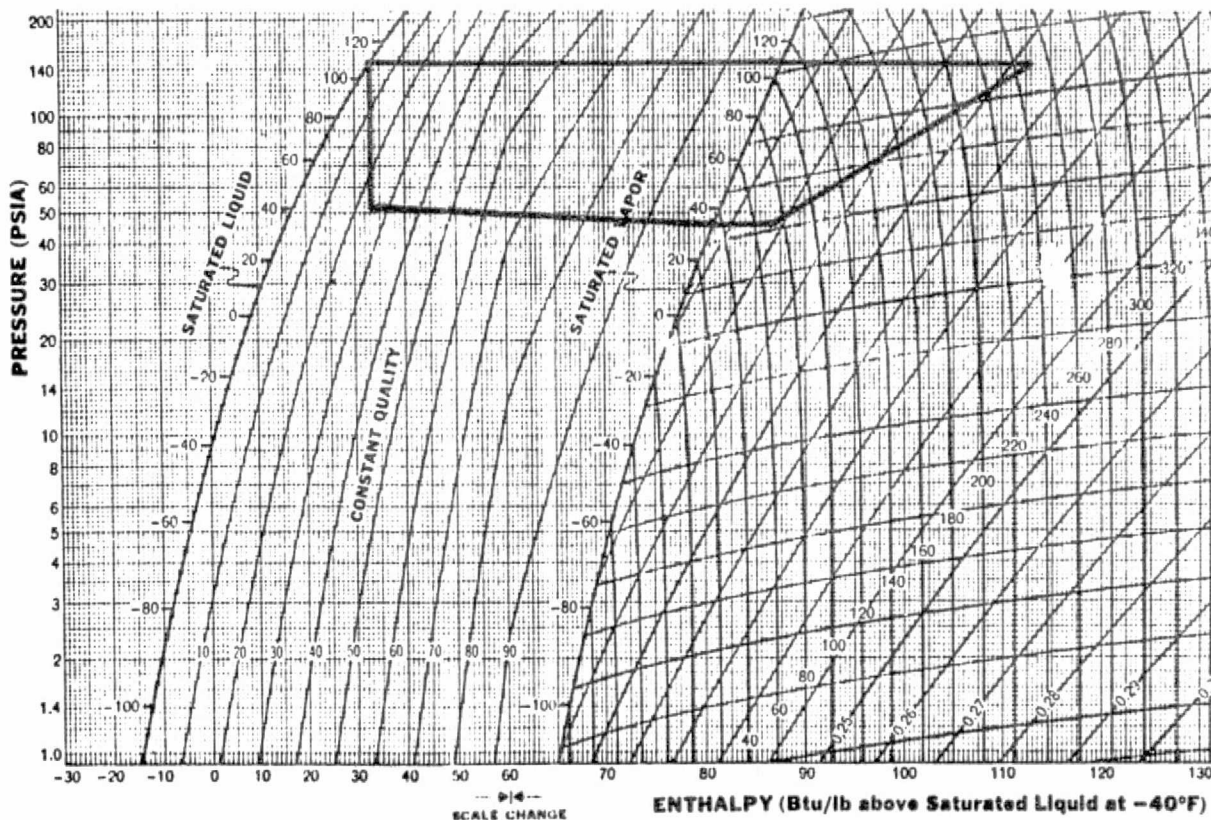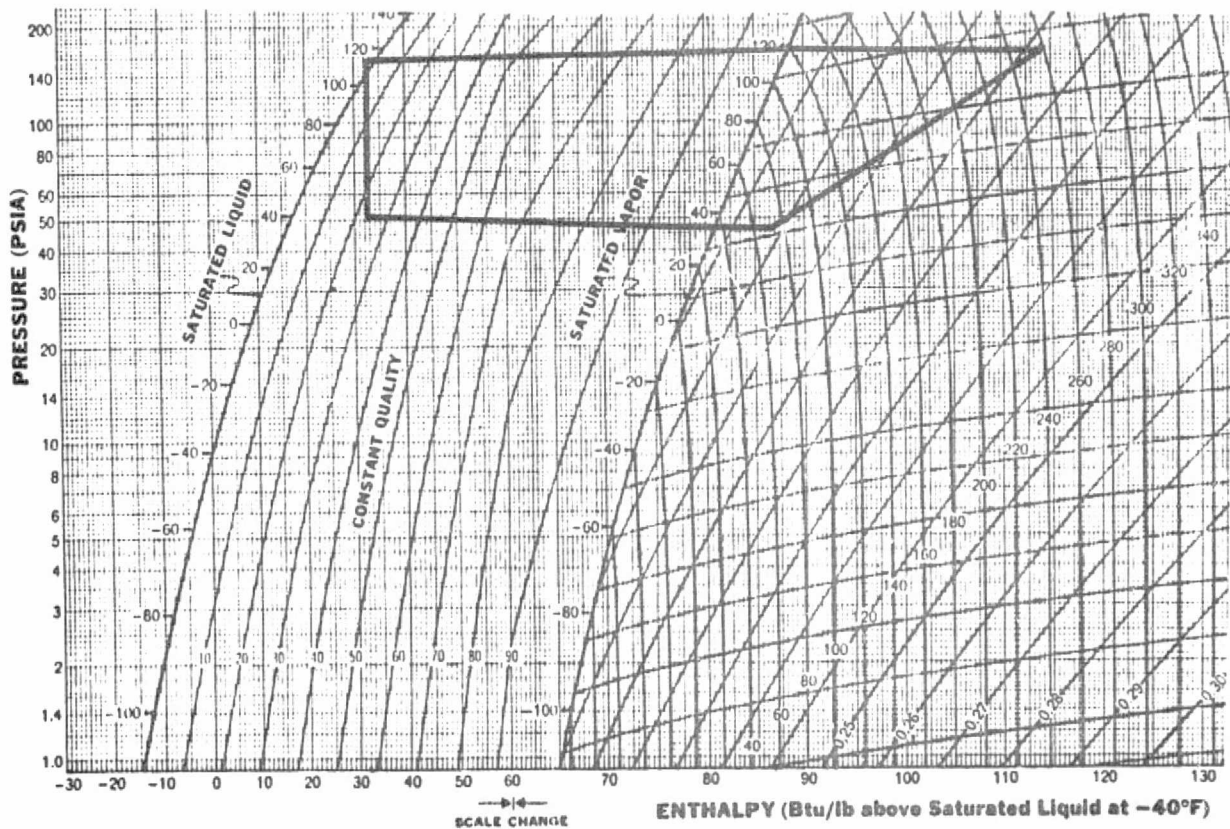 FROM POWER AND COOLING MEASUREMENTS ___2.26___
  FROM P-h DIAGRAM ___2.17___
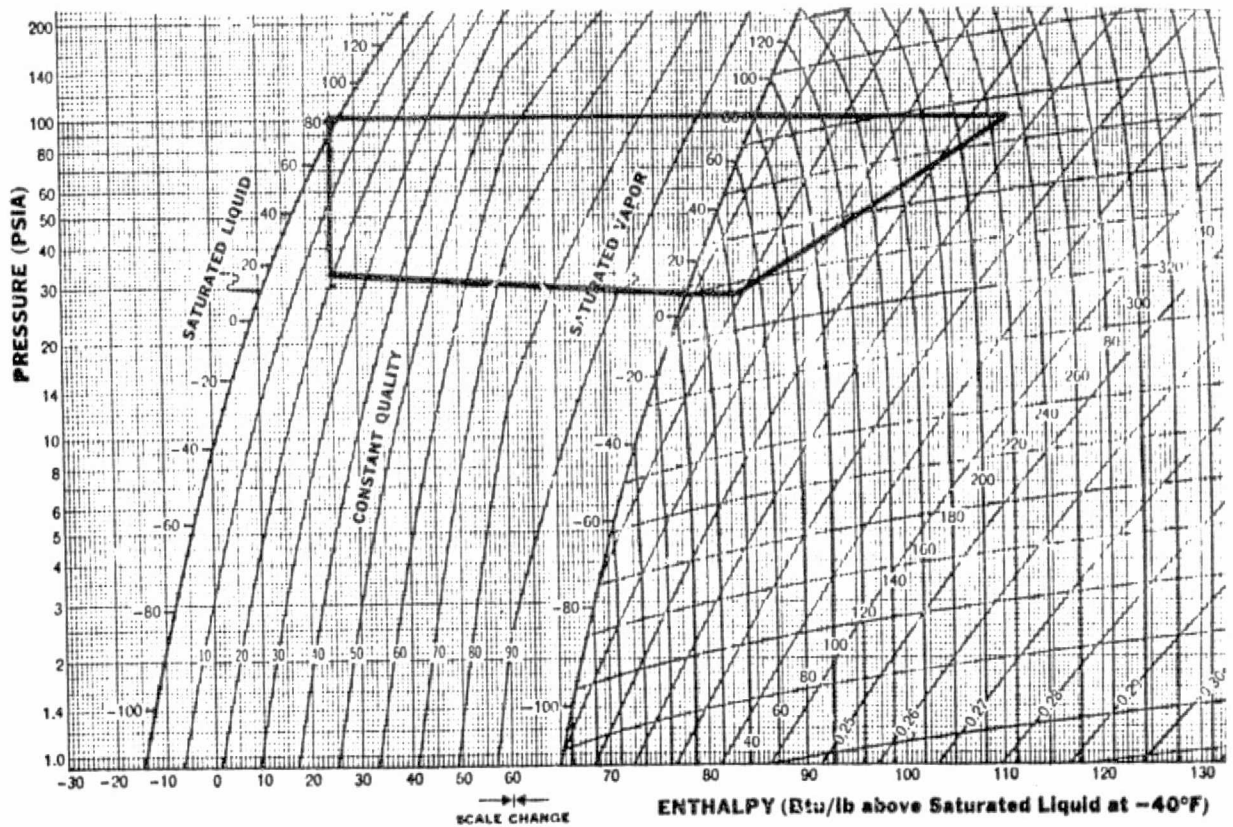
FIGURE A47   REFRIGERATION SYSTEM STEADY STATE CYCLIC PERFORMANCE

TEST POINT ___111A___

EVAPORATOR TEMPERATURE(°F) ___15___ ENVIRONMENT(BTU/HR-FT^2) _____

FLOWRATE (LBm/HR) ___516___
POWER (WATTS) ___3120___
COOLING (BTU/HR)
  FROM $\dot{m}C_p \Delta T$ OF R-21 ___32,590___
  FROM $\dot{m}\Delta h$ OF R-12 ___30,702___

COEFFICIENT OF PERFORMANCE - COP
  FROM POWER AND COOLING MEASUREMENTS ___3.06___
  FROM P-h DIAGRAM ___2.59___
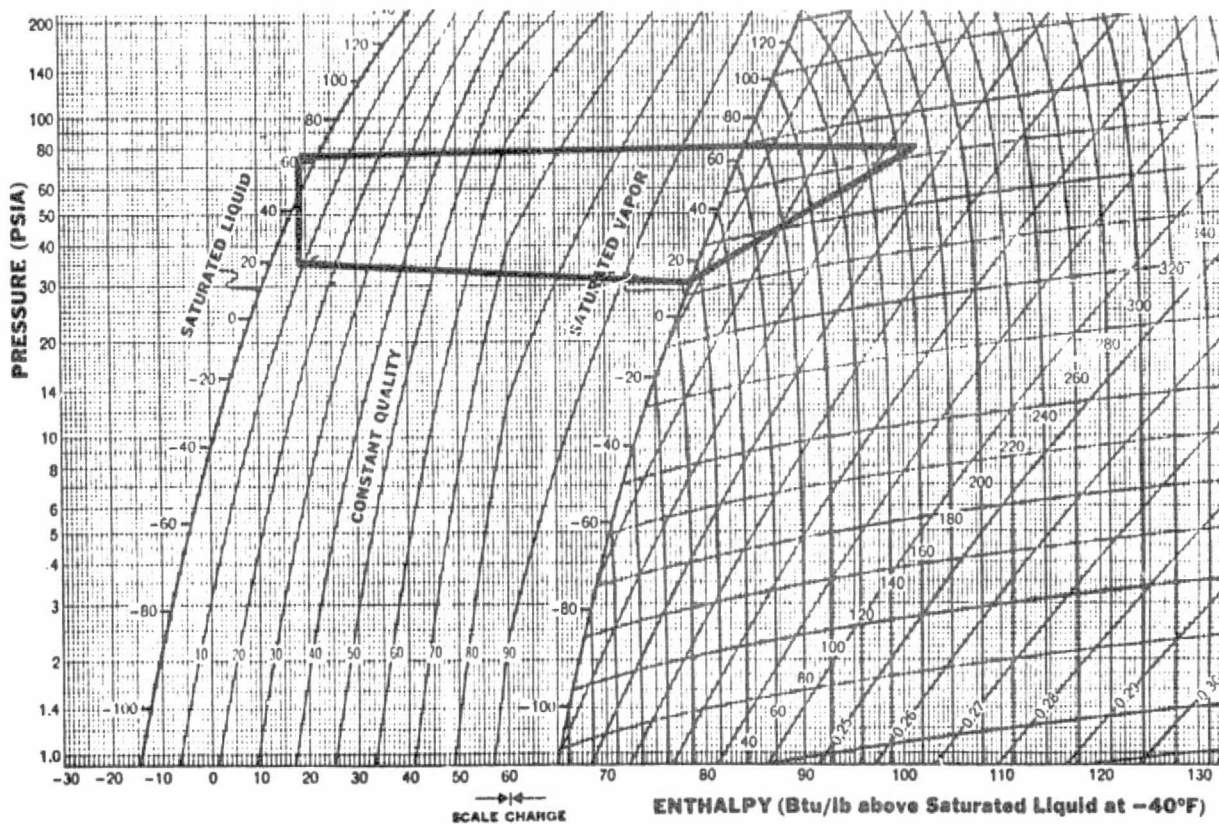
FIGURE A48   REFRIGERATION SYSTEM STEADY STATE CYCLIC PERFORMANCE
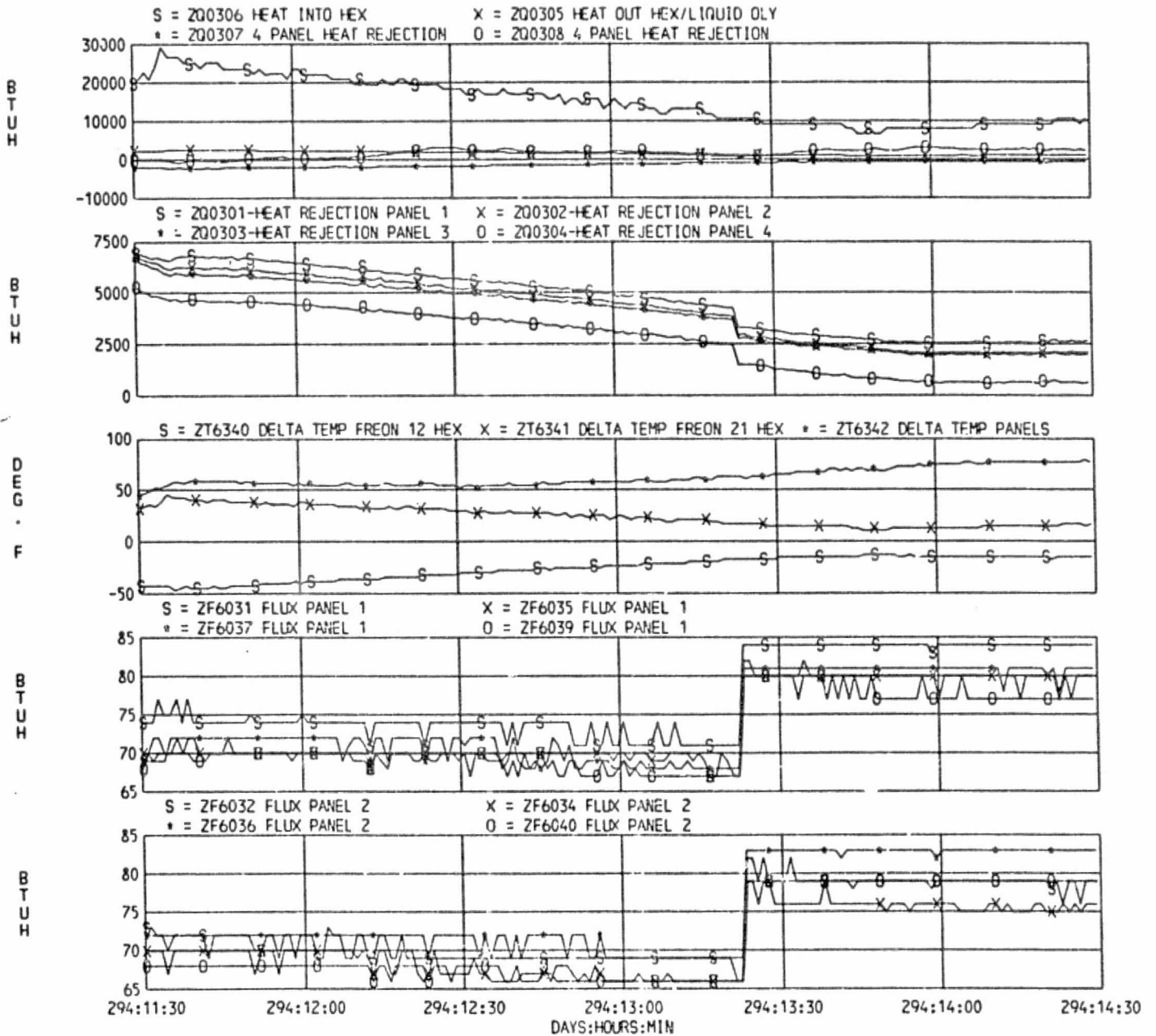
FIGURE A49 RADIATOR MODE SYSTEM TRANSIENT TEST RESULTS

A-146

S FT6314 FREON 21 HEX IN TEMP
* FT6312 FREON 21 HEX OUT TEMP
A FT6300 FREON 12 HEX IN TEMP

X FT6315 FREON 21 HEX IN TEMP
O FT6313 FREON 21 HEX OUT TEMP
+ FT6301 FREON 12 HEX IN TEMP

S FT6302 FREON 12 HEX OUT TEMP
* FT6306 FREON 12 PANEL IN TEMP
A FT6309 FREON 12 PANEL OUT TEMP

X FT6303 FREON 12 HEX OUT TEMP
O FT6307 FREON 12 PANEL IN TEMP
+ FT6308 FREON 12 PANEL OUT TEMP

ELAPSED TIME(HR MIN SEC)

PAGE   2

FIGURE A50   RADIATOR MODE SYSTEM TRANSIENT TEST RESULTS

A-147

SELF CONTAINED HEAT REJECTION MODULE (SHRM)-TEST POINT(S) 5

S = ZQ0306 HEAT INTO HEX   X = ZQ0305 HEAT OUT HEX/LIQUID GLY
* = ZQ0307 4 PANEL HEAT REJECTION   O = ZQ0308 4 PANEL HEAT REJECTION
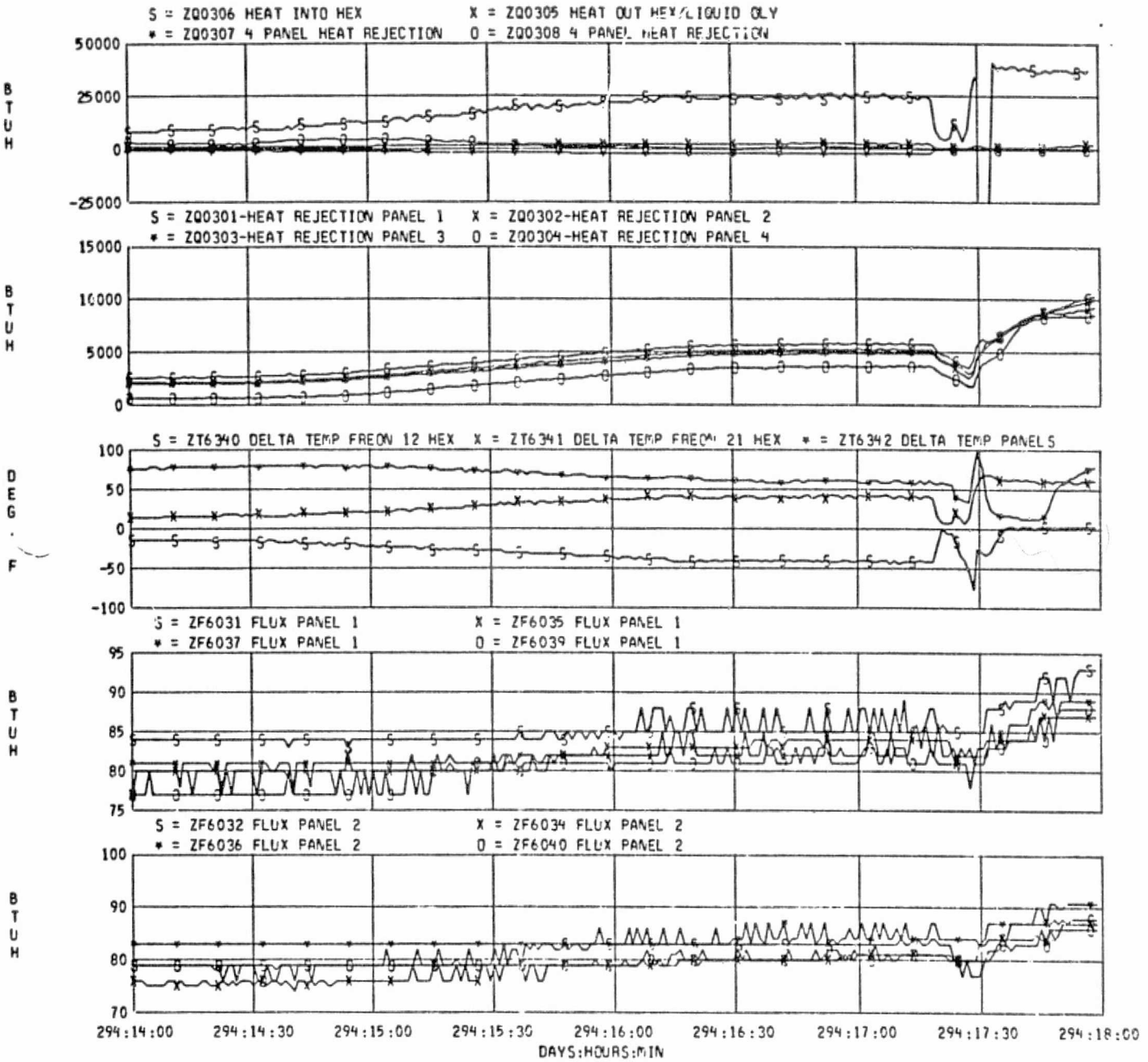
FIGURE A51   RADIATOR MODE SYSTEM TRANSIENT TEST RESULTS

SHRM TEST POINT 5   DAY 299

S FT6314 FREON 21 HEX IN TEMP
* FT6312 FREON 21 HEX OUT TEMP
A FT6300 FREON 12 HEX IN TEMP

X FT6315 FREON 21 HEX IN TEMP
0 FT6313 FREON 21 HEX OUT TEMP
+ FT6301 FREON 12 HEX IN TEMP

S FT6302 FREON 12 HEX OUT TEMP
* FT6306 FREON 12 PANEL IN TEMP
A FT6309 FREON 12 PANEL OUT TEMP

X FT6303 FREON 12 HEX OUT TEMP
J FT6307 FREON 12 PANEL IN TEMP
+ FT6308 FREON 12 PANEL OUT TEMP

ELAPSED TIME(DAY HR MIN SEC)

PAGE   2

FIGURE A52   RADIATOR MODE SYSTEM TRANSIENT TEST RESULTS

A-149

FIGURE A53 RADIATOR MODE SYSTEM TRANSIENT TEST RESULTS

A-150

S FT6314 FREON 21 HEX IN TEMP
* FT6312 FREON 21 HEX OUT TEMP
A FT6300 FREON 12 HEX IN TEMP

X FT6315 FREON 21 HEX IN TEMP
O FT6313 FREON 21 HEX OUT TEMP
+ FT6301 FREON 12 HEX IN TEMP

S FT6302 FREON 12 HEX OUT TEMP
* FT6306 FREON 12 PANEL IN TEMP
A FT6309 FREON 12 PANEL OUT TEMP

X FT6303 FREON 12 HEX OUT TEMP
O FT6307 FREON 12 PANEL IN TEMP
+ FT6308 FREON 12 PANEL OUT TEMP

ELAPSED TIME(HR MIN SEC)

FIGURE A54   RADIATOR MODE SYSTEM TRANSIENT TEST RESULTS

A-151

SELF CONTAINED HEAT REJECTION MODULE (SHRM)-TEST POINT(S) 11

S = ZQ0306 HEAT INTO HEX   X = ZQ0305 HEAT OUT HEX/LIQUID OLY
* = ZQ0307 4 PANEL HEAT REJECTION O = ZQ0308 4 PANEL HEAT REJECTION
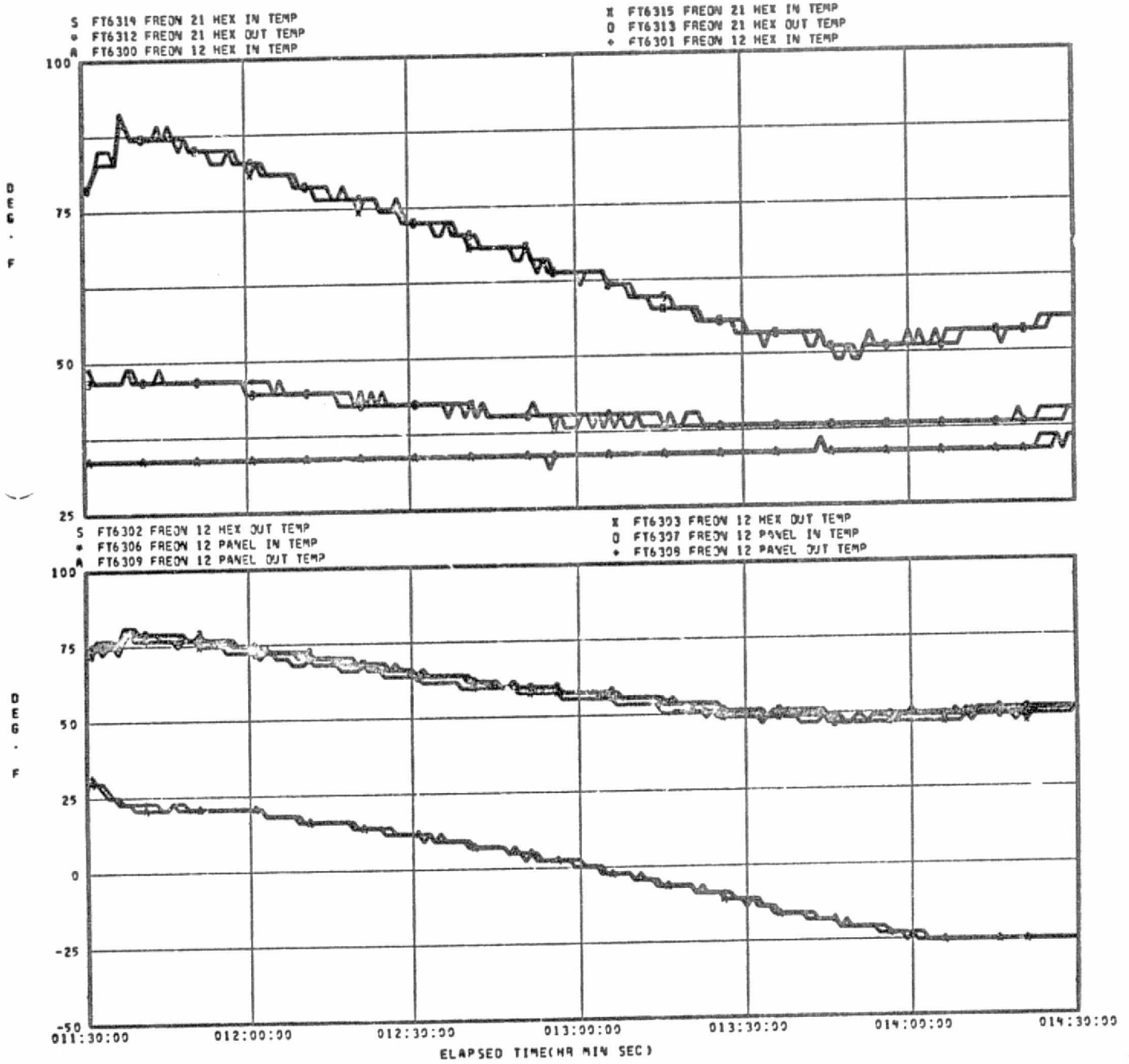
S = ZQ0301-HEAT REJECTION PANEL 1 X = ZQ0302-HEAT REJECTION PANEL 2
* = ZQ0303-HEAT REJECTION PANEL 3 O = ZQ0304-HEAT REJECTION PANEL 4

S = ZT6340 DELTA TEMP FREON 12 HEX X = ZT6341 DELTA TEMP FREON 21 HEX * = ZT6342 DELTA TEMP PANELS

S = ZF6031 FLUX PANEL 1 X = ZF6035 FLUX PANEL 1
* = ZF6037 FLUX PANEL 1 O = ZF6039 FLUX PANEL 1

S = ZF6032 FLUX PANEL 2 X = ZF6034 FLUX PANEL 2
* = ZF6036 FLUX PANEL 2 O = ZF6040 FLUX PANEL 2

DAYS:HOURS:MIN

FIGURE A55 RADIATOR MODE SYSTEM TRANSIENT TEST RESULTS

SHRM TEST POINT 11 DAY 296

S FT6314 FREON 21 HEX IN TEMP
• FT6312 FREON 21 HEX OUT TEMP
A FT6300 FREON 12 HEX IN TEMP

X FT6315 FREON 21 HEX IN TEMP
O FT6313 FREON 21 HEX OUT TEMP
• FT6301 FREON 12 HEX IN TEMP

S FT6302 FREON 12 HEX OUT TEMP
• FT6306 FREON 12 PANEL IN TEMP
A FT6309 FREON 12 PANEL OUT TEMP

X FT6303 FREON 12 HEX OUT TEMP
O FT6307 FREON 12 PANEL IN TEMP
• FT6308 FREON 12 PANEL OUT TEMP

ELAPSED TIME(HR MIN SEC)

PAGE   2

FIGURE A56   RADIATOR MODE SYSTEM TRANSIENT TEST RESULTS

A-153

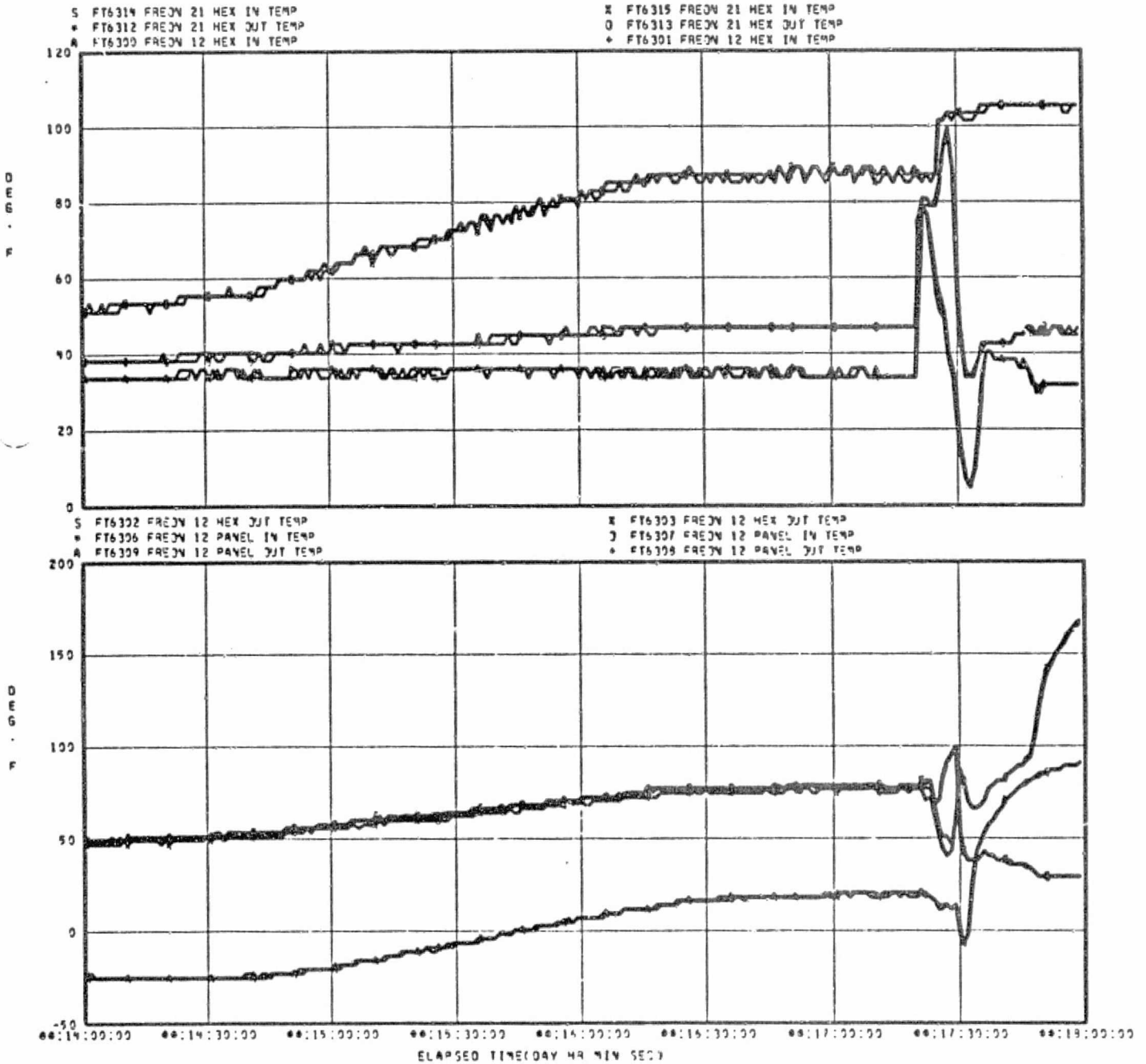SELF CONTAINED HEAT REJECTION MODULE (SHRM)-TEST POINT(S) 16
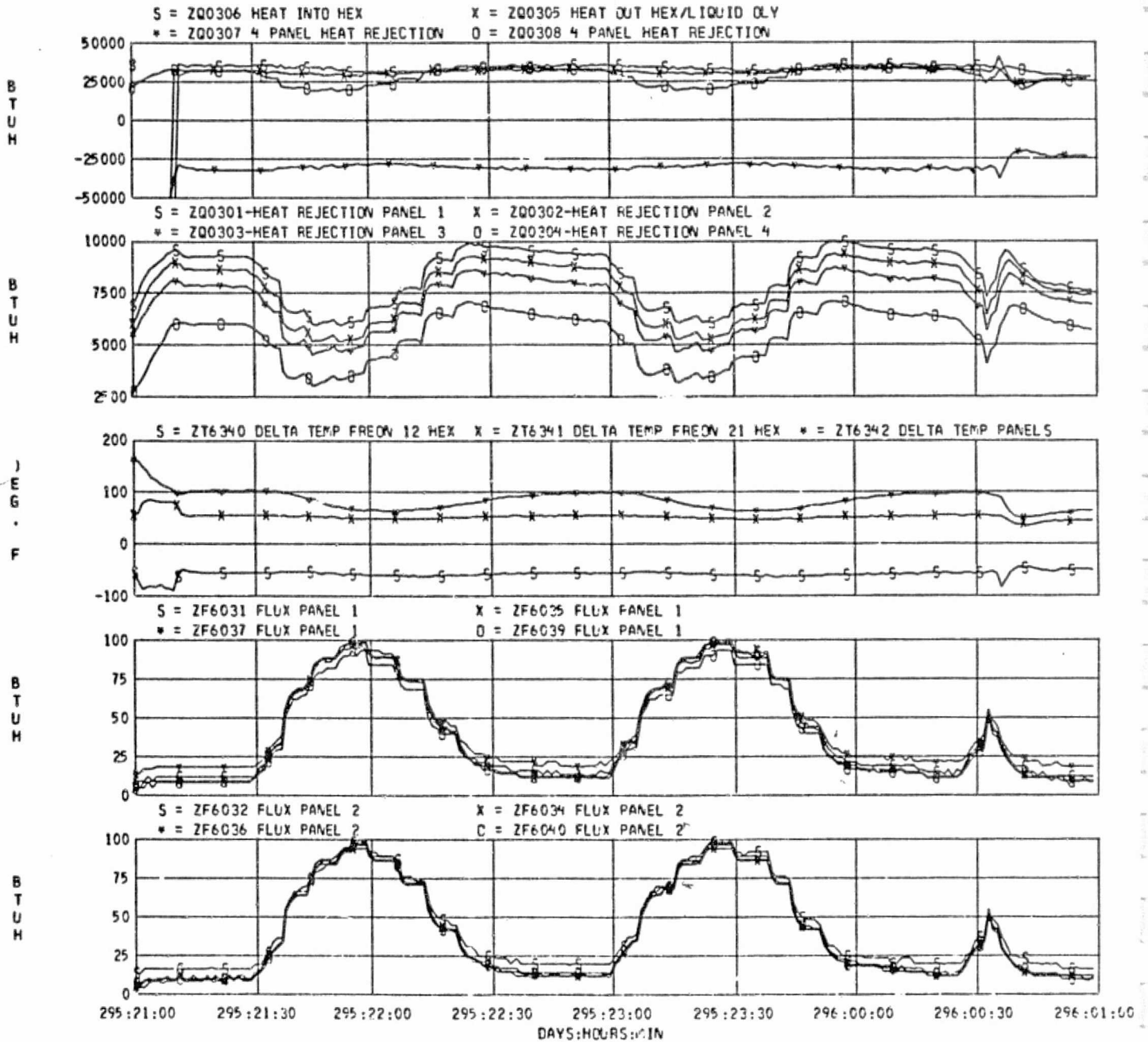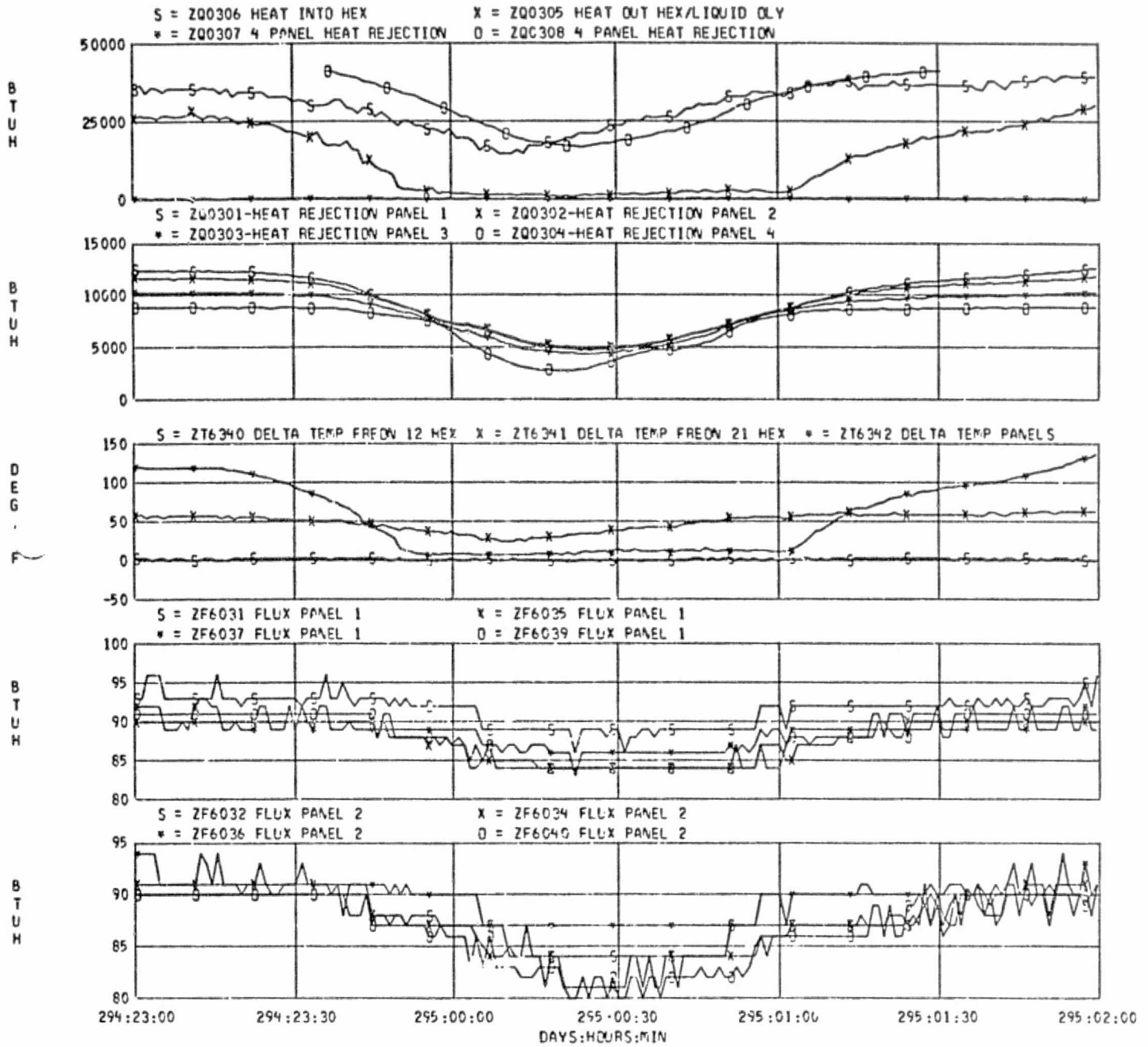

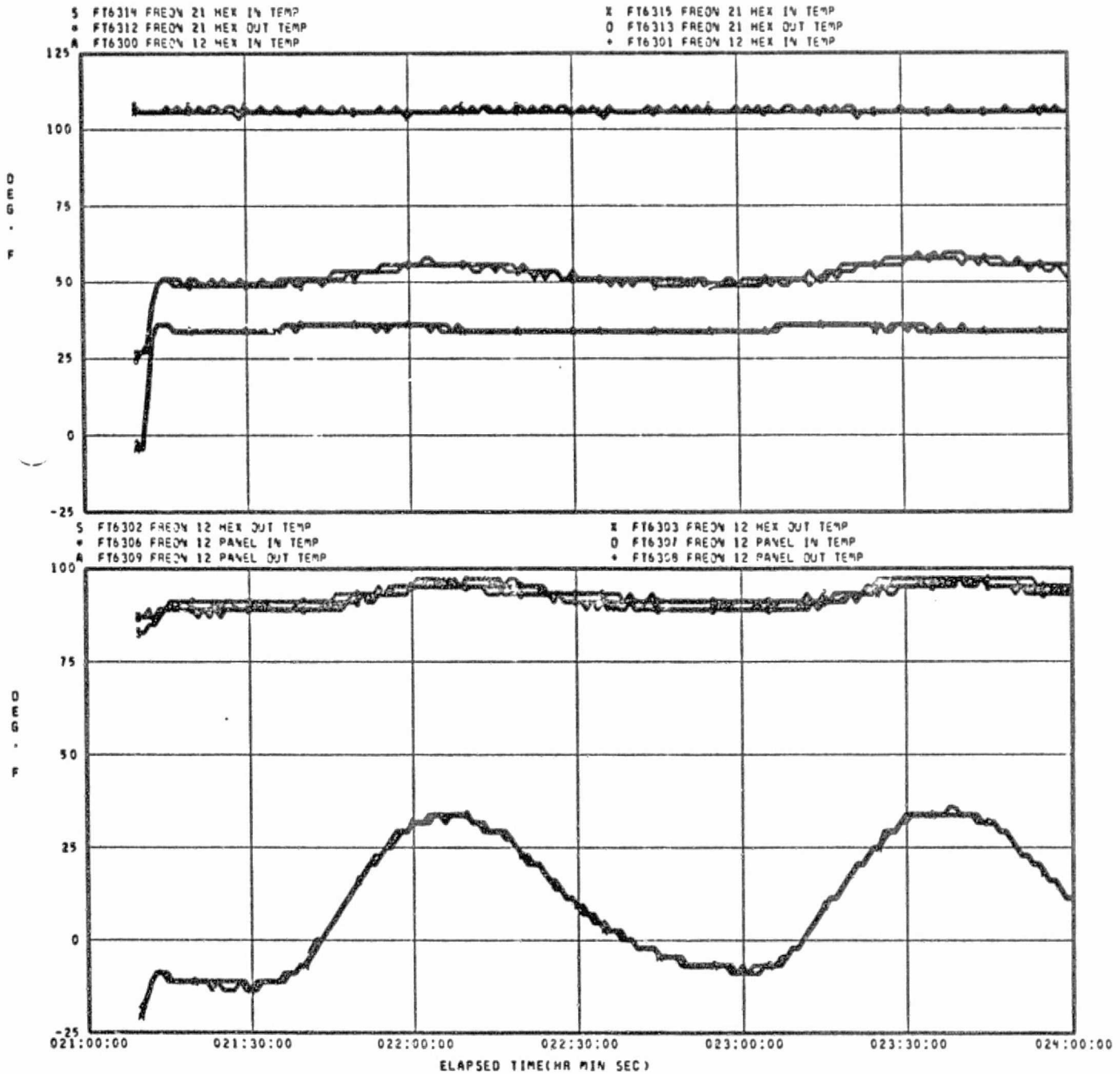FIGURE A57   RADIATOR MODE SYSTEM TRANSIENT TEST RESULTS

SHRM TEST POINT 16 DAY 294

S FT6314 FREON 21 HEX IN TEMP   X FT6315 FREON 21 HEX IN TEMP
* FT6312 FREON 21 HEX OUT TEMP   O FT6313 FREON 21 HEX OUT TEMP
A FT6300 FREON 12 HEX IN TEMP   + FT6301 FREON 12 HEX IN TEMP

D
E
G
.
F

125

100

75

50

25

S FT6302 FREON 12 HEX OUT TEMP   X FT6303 FREON 12 HEX OUT TEMP
* FT6306 FREON 12 PANEL IN TEMP   O FT6307 FREON 12 PANEL IN TEMP
A FT6309 FREON 12 PANEL OUT TEMP   + FT6308 FREON 12 PANEL OUT TEMP

D
E
G
.
F

250

200

150

100

50

0
023:00:00   023:30:00   024:00:00   024:30:00   025:00:00   025:30:00   026:00:00
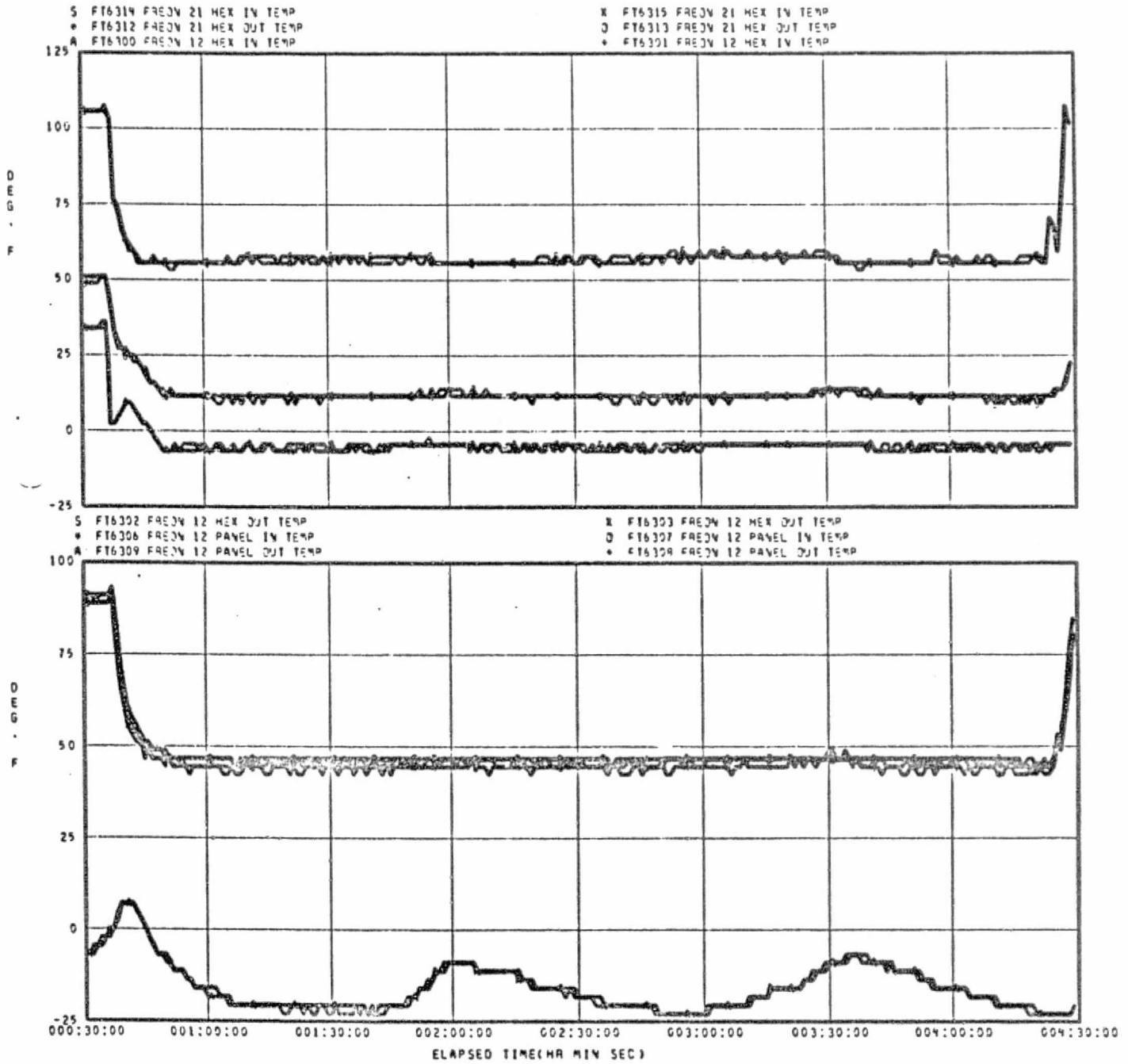
ELAPSED TIME(HR MIN SEC)

PAGE   2
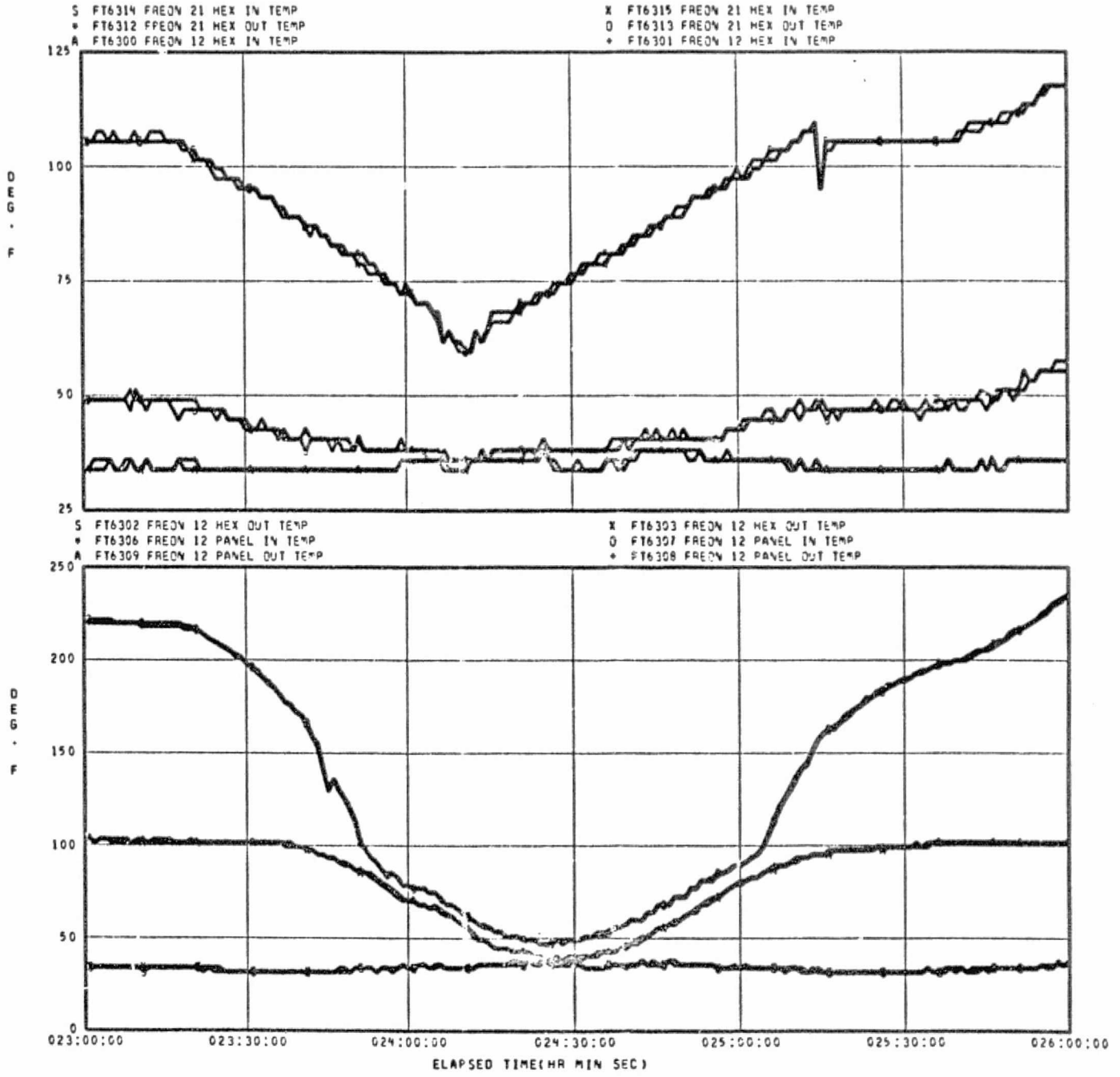
FIGURE A58   RADIATOR MODE SYSTEM TRANSIENT TEST RESULTS

A-155

FIGURE A59   RADIATOR MODE SYSTEM TRANSIENT TEST RESULTS

APPENDIX B

SHRM OPERATING INSTRUCTIONS

APPENDIX B

SHRM OPERATING INSTRUCTIONS

The Self Contained Heat Rejection Module fluid system is serviced
and operated from the flow module and the control console. A schematic
of the flow module is shown in Figure B-1. The various equipment identified
in this figure will be referred to in the following servicing and operating
instructions. The control consoles are shown in Figure B-2. The various
switches and indicators necessary to operate the system are located on
this console and will also be referred to in the following instructions.

1.0 FLUID SERVICING OF THE SHRM SYSTEM AT AMBIENT CONDITIONS

Step A.

Open the system remotely operated valves SV3, SV4, SV7, SV8, SV9
and BV3. Vent the top of the accumulator by opening SV6 and vent-
ing through the pressure regulator PR1 to ambient. Open the valve
to the auxiliary accumulator.

Step B.

Evacuate the system through FV1 or FV3 or both. Charge with
R12 gas.

Step C.

Close SV4 and the valve to the auxiliary accumulator. Fill the
auxiliary accumulator with liquid R12 to a level visible in the
top sight glass. Fill the accumulator through FV3 until a level
near full is indicated by the electrical quantity readout. (4.48
is empty, 3.14 is full, a value of approximately 3.40 is suggested.)
Weigh and record the total weight of R12 used.

Step D.

Determine the quantity of oil necessary by taking 4% of the total
R12 weight. Add 1/3 this amount of oil to the system through
FV1 and 2/3 to the R12 in the auxiliary accumulator. The oil can
be inserted by use of a commercial refrigerant oil charging pump
of the type available in refrigeration supply stores.

Step E.

        Set the control console mode selection to REF, compressor switch
to OFF and ST.PT. to 38°.

Step F.

        Pressurize the accumulator to 150 psig using PR1. Open SV4 and
allow R12 to flow from the accumulator into the system until the
accumulator indicates nearly empty (about 3.30). Close SV4, vent
and refill accumulator to about 3.40. Repressurize to 150 psig.

Step G.

        Place a heat load on CHX by flowing R21 through CHX B at 2440 lbm/hr
at a temperature of 110°F.

Step H.

        Start the compressor by switching the compressor control switch to
AUTO. Set compressor power to 400 Hz. Allow the refrigeration
system operation to stabilize. Monitor SG2 to insure adequate oil
supply. If oil is not visible add more oil through FV1 as in
Step D until oil is visible in SG2.

Step I.

        Monitor SG3 and SG4. If SG3 and 4 are not clear add more Freon
by opening SV4 until SG4 clears continue to add until SG3 is clear
then remove R12 by venting the accumulator pressure by adjusting
PR1 to a pressure below system pressure (P4) and opening SV4. Re-
move R12 until SG3 just indicates frothy flow. If SG1 was clear
at the outset remove R12 as just described. When proper quantity
is obtained close SV4. Set compressor switch to OFF.

Step J.

        The system now has the proper charge for vapor compression operation.
Record the accumulator quantity and verify level of R12 in the
auxiliary accumulator as visible in the top sight glass.

Step K.

        To operate system in the refrigeration mode select set point
(0° 138°) and switch compressor to AUTO.

2.0 SYSTEM STARTUP IN RADIATOR MODE

To initiate operation in the radiator mode at any time after completing servicing of 1.0 perform the following:

Step A.

Set pump switch to OFF; Set mode selection to RAD

Step B.

Heat auxiliary accumulator to achieve 150 psi (valve to aux accumulator open). Maintain until system pressures (P1, P2, P4, and P) equalize with accumulator pressure.

Step C.

Close valve to auxiliary accumulator

Step D.

Set reg. GN2 at 150 psi

Step E.

Command SV4 open

Step F.

Select and set radiator control valve set point (0°/38°F)

Step G.

Command pump "automatic"

Step H.

Command pump "automatic"

Step I.

Chill auxiliary accumulator to achieve 50 psi prior to anticipated mode switch.

3.0   RETURN TEMPERATURE CONTROL

        With mode selection on AUTO or RAD the system controller automatically controls the return temperature in the radiator mode to the selected value. With selection on AUTO when control is not possible due to severe environments, the controller automatically initiates switch to refrigeration mode. If the required heat rejection is less than system capacity in the refrigeration mode the evaporator will no longer evaporate all the R12 flow. This will be evidenced by a saturation temperature at T3 and T4 corresponding to the pressure at P1. Adjustments in system capacity are made by varying the input power frequency between 400 and 150 Hz to control compressor speed. This is done from the console "Compressor Input Frequency Control". Frequency should be adjusted until 15°F superheat if obtained at T4 (T4 temperature reads 15°F higher than the saturation temperature at P1). Excessive superheats (30°F or more) when the compressor is operating full speed (400 Hz) indicate heat loads in excess of system capacity. Shut down or heat load reduction is in order.

4.0 MODE SWITCHES

To switch modes either prior to or during or after testing use the following procedures.

RADIATOR TO REFRIGERATION MODE SWITCH – MANUAL

Step A.

Command pump "OFF"

Step B.

Command SV4 CLOSED

Step C.

Open BV2

Step D.

Set inverter at minimum speed (200 Hz)

Step E.

Command compressor "OFF"

Step F.

Command controller to "REFRIGERATION"

Step G.

Verify valve status check list

Step H.

Command compressor "AUTOMATIC"

Step I.

Monitor aux accumulator when liquid level reaches upper right glass, close BV2

Step J.

Prior to anticipated switchover raise temperature of aux accumulator to achieve 200 psi vapor pressure

Step K.

Command SV5 and SV6 "AUTOMATIC"

RADIATOR TO REFRIGERATION - AUTOMATIC

When the system is set for automatic operation (all switches in "AUTOMATIC"), Freon 12 system must be monitored at the console at all times. When it begins to switch over to refrigeration mode, Steps B, C, D, I and J above must be carried out.

REFRIGERATION TO RADIATOR - MANUAL

Step A.

Set mode control switch to "RADIATOR'

Step B.

Open BV2, maintain until Freon 12 system pressure and aux compressor pressure equalize

Step C.

Command SV4 "OPEN"

Step D.

Set reg. N2 pressure at 150 psi

Step E.

Verify valve status check list

Step F.

Close BV2

Step G.

Monitor accumulator quantity level. If quantity in accumulator goes below 5 percent, command SV4 closed, and shut down system.

Step H.

Prior to next anticipated switchover to refrigeration mode, chill aux accumulator to achieve vapor pressure of 50 psi.

SHRM FLOW SCHEMATIC

NOMENCLATURE

BV – BALL VALVE
CV – CHECK VALVE
CHX – CONTACT HEAT EXCHANGER
DP – DELTA PRESSURE
EXPV – EXPANSION VALVE
FD – FILTER DRYER
FM – FLOW METER
FV – FILL VALVE
P – PRESSURE TRANDUCER
PR – PRESSURE REGULATOR
RCV – RADIATOR CONTROL VALVE
RV – RELIEF VALVE
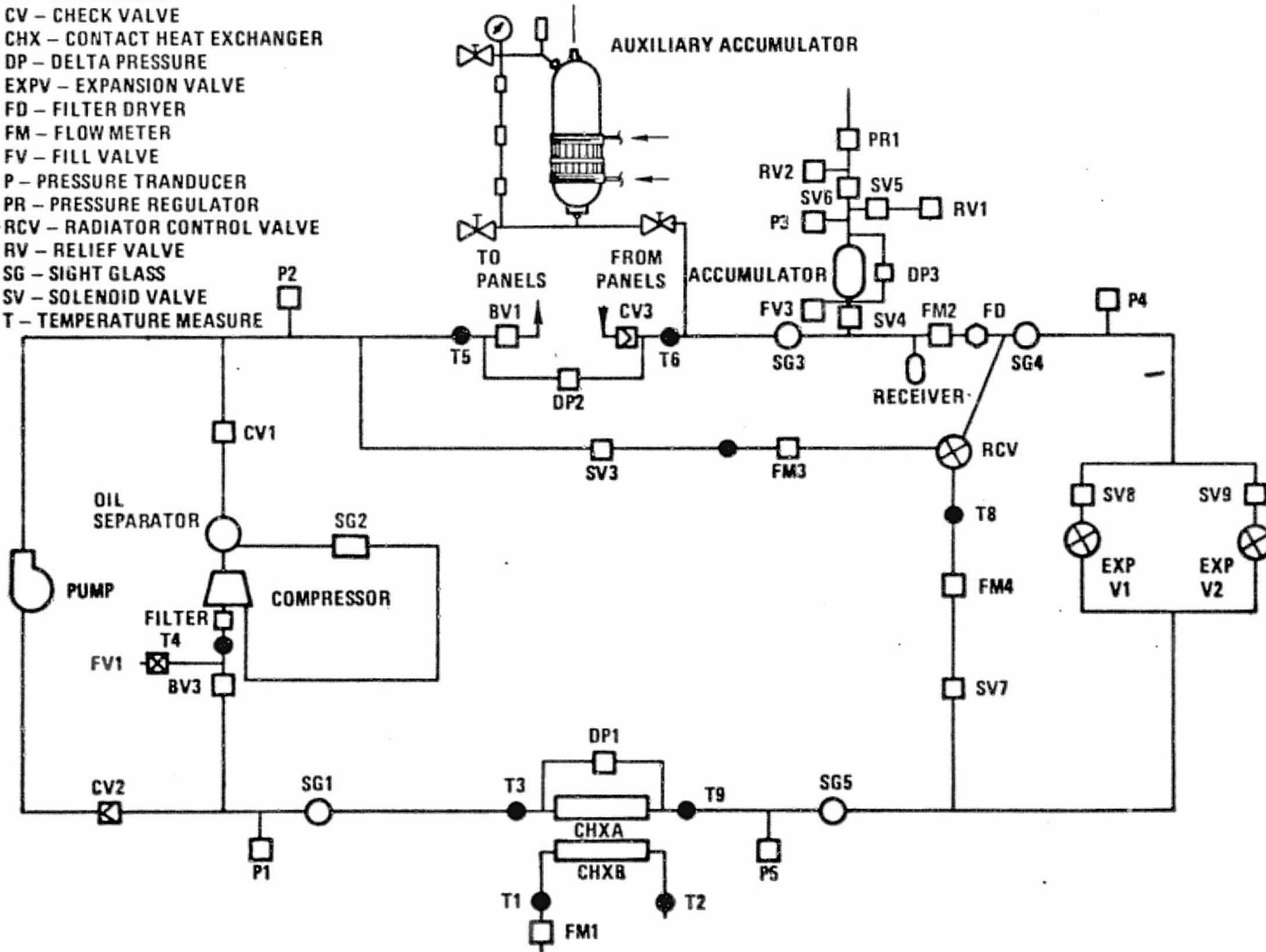SG – SIGHT GLASS
SV – SOLENOID VALVE
T – TEMPERATURE MEASURE

AUXILIARY ACCUMULATOR
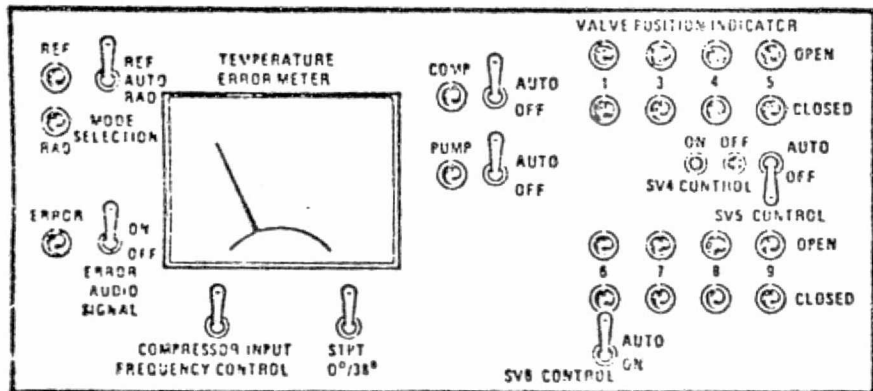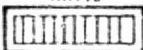
FIGURE B1   FLOW MODULE SCHEMATIC

COMPRESSOR
POWER
WATTS

VALVE POSITION INDICATOR

REF
REF
AUTO
RAO
MODE
SELECTION
RAO
ERROR
ON
OFF
ERROR
AUDIO
SIGNAL

TEMPERATURE
ERROR METER

COMP
AUTO
OFF

PUMP
AUTO
OFF

1   3   4   5   OPEN

CLOSED

ON OFF
SV4 CONTROL
AUTO
OFF

SVS CONTROL

6   7   8   9   OPEN

CLOSED

AUTO
ON
SV8 CONTROL

COMPRESSOR INPUT
FREQUENCY CONTROL

STPT
0°/38°

SHRM CONTROL CONSOLE

COMPRESSOR
POWER
FREQ.

PUMP POWER
CIRCUIT
BREAKER

AMPS
0   50

VOLTS
0   300

PHASE
A

AMPS
0   50

VOLTS
0   300

PHASE
B

AMPS
0   50

VOLTS
0   300

PHASE
C

COMPRESSOR ELECTRICAL MEASUREMENTS

TEMPERATURE °F
0   100

TEMP ERROR °F
−5°F TO +5°F
50   0   50

VALVE POSITION
−0.05 TO +0.05 IN.
50   0   50

AUTO   35°F

MAN   −5°F

OPERATION   TEMP.
MODE   CONTROL

FAST   +

SLOW   −

PULSE   DIREC.
RATE

SINGLE STEP

NORMAL   SINGLE
OPERATION   STEP

── SINGLE PULSE ──

AUTO MODE ──────── MANUAL MODE ──────

FLOW VALVE CONTROL CONSOLE

FIGURE B2   SHRM CONTROLLER CONSOLES